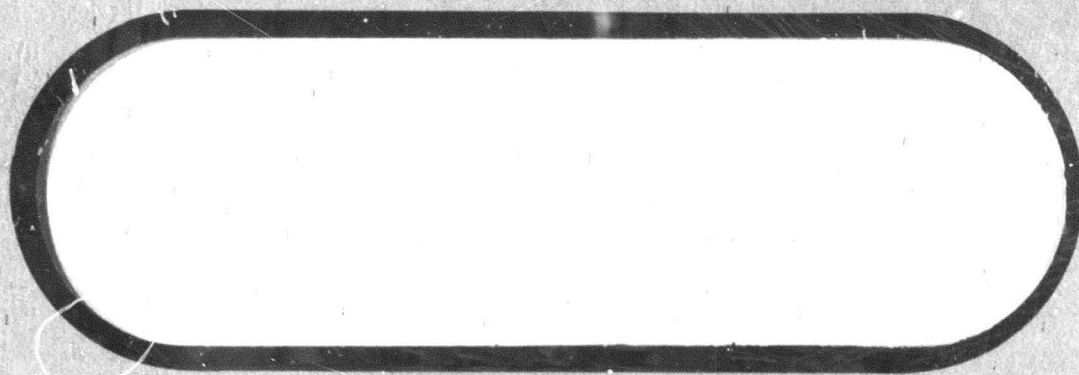


# ***BOEING***

AD 734237



Reproduced by  
**NATIONAL TECHNICAL  
INFORMATION SERVICE**  
Springfield, Va. 22151

**D D C**  
**RECEIVED**  
**DEC 29 1971**  
**RECEIVED**  
**D**

Unclassified

Security Classification

DOCUMENT CONTROL DATA - R & D

(Security classification of title, body of abstract and indexing annotation must be entered when the overall report is classified)

1. ORIGINATING ACTIVITY (Corporate author) Vertol Division The Boeing Company P. O. Box 16858, Philadelphia, PA 19142		2a. REPORT SECURITY CLASSIFICATION Unclassified	
		2b. GROUP N/A	
3. REPORT TITLE 1/3 Scale V/STOL Cyclic Pitch Propellers: Results of Wind Tunnel Tests			
4. DESCRIPTIVE NOTES (Type of report and inclusive dates) Contractor Test Report (November-December 1970)			
5. AUTHOR(S) (First name, middle initial, last name) Widmayer, Edward and Tomassoni, J			
6. REPORT DATE February 1971		7a. TOTAL NO. OF PAGES 152	7b. NO. OF REFS 5
8a. CONTRACT OR GRANT NO. F33615-70-C-1000		8a. ORIGINATOR'S REPORT NUMBER(S) Boeing Vertol Document D170-10040-1	
b. PROJECT NO. 698BT			
c. Task Area Number: 02		9b. OTHER REPORT NO(S) (Any other numbers that may be assigned this report)	
d. Work Unit Number: 005		AFFDL TR 71-91, Reference 5	
10. DISTRIBUTION STATEMENT Approved for public release; distribution unlimited.			
11. SUPPLEMENTARY NOTES		12. SPONSORING MILITARY ACTIVITY Air Force Flight Dynamics Laboratory Wright-Patterson AFB, Ohio 45433	
13. ABSTRACT This report presents the results of a wind tunnel test performed in the Boeing-Vertol wind tunnel on a 1/3 scale V/STOL 4-bladed cyclic pitch propeller, having a total Activity Factor of 640. The propeller was tested as both an isolated propeller and as an installed propeller. The primary objectives of the test were to determine: (1) the effectiveness of cyclic pitch control for longitudinal control during hover and transition, (2) the change in power required for cyclic pitch control and (3) blade and hub loads for use in design and for verification of analytical methods.			

DD FORM 1 NOV 65 1473

Unclassified

Security Classification

**Security Classification**

**Security Classification**

THE **BOEING** COMPANY  
VERTOL DIVISION • PHILADELPHIA, PENNSYLVANIA

CODE IDENT. NO. 77272

NUMBER D170-10040-1TITLE 1/3 SCALE V/STOL CYCLIC PITCH PROPELLERS:RESULTS OF WIND TUNNEL TESTS

ORIGINAL RELEASE DATE \_\_\_\_\_. FOR THE RELEASE DATE OF  
SUBSEQUENT REVISIONS, SEE THE REVISION SHEET. FOR LIMITATIONS  
IMPOSED ON THE DISTRIBUTION AND USE OF INFORMATION CONTAINED  
IN THIS DOCUMENT, SEE THE LIMITATIONS SHEET.

MODEL 170 CONTRACT D33615-70-C-1000

ISSUE NO. \_\_\_\_\_ ISSUED TO: \_\_\_\_\_

PREPARED BY	<u>E. Widmayer</u> <u>J. Tomassoni</u>	DATE	<u>2/3/71</u>
	<u>E. Widmayer/J. Tomassoni</u>		
APPROVED BY	<u>E. Widmayer</u>	DATE	<u>2/3/71</u>
	<u>E. Widmayer</u>		
APPROVED BY	<u>W. I. Lapinski</u>	DATE	<u>2/3/71</u>
	<u>W. I. Lapinski</u>		
APPROVED BY	<u>K. B. Gillmore</u>	DATE	<u>2/3/71</u>
	<u>K. B. Gillmore</u>		

## DISTRIBUTION STATEMENT A

Approved for public release;  
Distribution Unlimited

DDC  
RECEIVED  
DEC 29 1971



LIMITATIONS

This document is controlled by V/STOL Technology, Org. 7420

All revisions to this document shall be approved by the  
above noted organization prior to release.

ACTIVE SHEET RECORD											
SHEET NUMBER	REV LTR	ADDED SHEETS				SHEET NUMBER	REV LTR	ADDED SHEETS			
		SHEET NUMBER	REV LTR	SHEET NUMBER	REV LTR			SHEET NUMBER	REV LTR	SHEET NUMBER	REV LTR
i						36					
ii						37					
iii						38					
iv						39					
v						40					
1						41					
2						42					
3						43					
4						44					
5						45					
6						46					
7						47					
8						48					
9						49					
10						50					
11						51					
12						52					
13						53					
14						54					
15						55					
16						56					
17						57					
18						58					
19						59					
20						60					
21						61					
22						62					
23						63					
24						64					
25						65					
26						66					
27						67					
28						68					
29						69					
30						70					
31						71					
32						72					
33						73					
34						74					
35						75					

ACTIVE SHEET RECORD											
SHEET NUMBER	REV LTR	ADDED SHEETS				SHEET NUMBER	REV LTR	ADDED SHEETS			
		SHEET NUMBER	REV LTR	SHEET NUMBER	REV LTR			SHEET NUMBER	REV LTR	SHEET NUMBER	REV LTR
76						116					
77						117					
78						118					
79						119					
80						120					
81						121					
82						122					
83						123					
84						124					
85						125					
86						126					
87						127					
88						128					
89						129					
90						130					
91						131					
92						132					
93						133					
94						134					
95						135					
96						136					
97						137					
98						138					
99						139					
100						140					
101						141					
102						142					
103						143					
104						144					
105						145					
106						146					
107						147					
108											
109											
110											
111											
112											
113											
114											
115											



**ABSTRACT**

This report presents the results of a wind tunnel test performed in the Boeing-Vertol wind tunnel on a 1/3 scale V/STOL 4-bladed cyclic pitch propeller, having a total Activity Factor of 640. The propeller was tested as both an isolated propeller and as an installed propeller. The primary objectives of the test were to determine: (1) the effectiveness of cyclic pitch control for longitudinal control during hover and transition, (2) the change in power required for cyclic pitch control and (3) blade and hub loads for use in design and for verification of analytical methods.

**KEY WORDS**

Cyclic Pitch Propeller

Isolated Propeller

Installed Propeller

Hover

Transition

TABLE OF CONTENTS

<u>SECTION</u>		<u>PAGE</u>
1.0	INTRODUCTION	4
2.0	MODEL DESCRIPTION	5
2.1	BLADES	5
2.2	WING	5
3.0	TEST INSTALLATION	9
4.0	MODEL INSTRUMENTATION, DATA ACQUISITION AND DATA REDUCTION	9
5.0	SIGN CONVENTION AND NOMENCLATURE	11
5.1	POSITIVE SIGN CONVENTION	11
5.2	NOMENCLATURE	12
6.0	TEST PROCEDURE	12
7.0	RUN LOG	14
7.1	HOVER	14
7.2	TRANSITION	14
7.3	CRUISE	14
7.4	HUB AND SPINNER TARES	15
8.0	RESULTS AND DISCUSSION	16
8.1	INTRODUCTION	16
8.2	PROPELLER PERFORMANCE CHARACTERISTICS	17
8.3	EFFECT OF CYCLIC PITCH ON PITCHING MOMENT	27
8.4	EFFECT OF CYCLIC PITCH ON THRUST AND POWER	27

TABLE OF CONTENTS (CONT.)

<u>SECTION</u>		<u>PAGE</u>
8.5	EFFECT OF CYCLIC PITCH ON NORMAL FORCE	28
8.6	BLADE LOADS	28
8.7	EFFECT OF $C_T$ ON PITCHING MOMENT	30
8.8	BLADE FREQUENCIES	30
8.9	TRANSITION	51
8.10	NOMINAL TRANSITION	51
8.11	THE EFFECT OF SHAFT ANGLE	52
8.12	EFFECT OF $\theta_2$	52
8.13	EFFECT OF CYCLIC ON BLADE LOADS	53
8.14	PROPELLER WITH WING	53
8.15	EFFECT OF $\theta_2$ ON CONTROL POWER	54
9.0	CONCLUSIONS AND RECOMMENDATIONS	83
10.0	REFERENCES	86
	APPENDIX A - BLADE DESIGN	87
	APPENDIX B - MODEL INSTRUMENTATION AND DATA ACQUISITION SYSTEM	107
	APPENDIX C - TEST PROCEDURE	117
	APPENDIX D - DETAILED RUN LOG	129
	APPENDIX E - SPINNER AND HUB TARES	140



## 1.0 INTRODUCTION

The Boeing Company, Vertol Div., under Cont. F33615-70-C-1000, designed, fabricated and tested a 1/3 scale model of a cyclic pitch propeller of the type which would be used on a proposed tilt wing transport aircraft. The tests were conducted in the Boeing-Vertol 20 X 20 foot V/STOL Wind Tunnel (See Figure 2.1) with flow conditions representative of full-scale flight in hover, transition and cruise.

The general objectives of the test program were to:

- ° assess the effectiveness of cyclic pitch for longitudinal control during hover and transition
- ° measure change in power required for cyclic pitch control
- ° obtain loads test data for use in design and as a basis for verification of analytical methods.

Specifically, it is intended to:

- ° measure the forces and moments in the fixed system and the control and blade loads for hover, transit and cruise.
- ° determine the influences of scaling on rotor performance comparing the test results of the 1/3 scale model to the 1/12 scale performance propeller model.
- ° determine the effect of wing-propeller interference.

The blade data has been processed such that the magnitude and phase of harmonics has been determined with and without the presence of the wing. Primary quantities obtained are the sensitivities of pitching moment, blade bending moments and power due to cyclic pitch.

## 2.0 MODEL DESCRIPTION

The model assembly shown in Figures 2.1a & 2.1b consisted of four major components. These are the blades, the hub and control, the spinner and wing, and the balance and DRTS\*. These components are shown in exploded view in Figure 2.2. The wing (not shown) was attached to the DRTS such that the wing and fairing loads are carried directly to the ground. Thus, the balance senses the blade and spinner loads only.

\*Dynamic Rotor Test Stand

### 2.1 BLADES

The four-bladed propeller used in this test is Froude scaled (See Table 2.1) from a design suitable for full-scale tilt wing application. The full-scale propeller represents a compromise to achieve required figure of merit and good cruise efficiency and is a design that evolved through many iterations. The full-scale propeller was designed for a hover tip speed of 900 ft/sec at 650 RPM and for cruise at 630 ft/sec at 455 RPM. The propeller has activity factor per blade of 164, a solidity of .272 and full-scale diameter of 26.4 ft.

The 1/3 scale blade design characteristics are given in App.A. Full-scale blade mass, stiffness, and geometrical properties are presented. Because of differences in construction between the full-scale and the 1/3 scale blades, the 1/3 scale blade has some slight differences from the full-scale. These differences are also shown in Appendix A. The airfoils are modified NACA 64 series with no cusp in the trailing edge.

The test blades have a fiberglass spar, compressed balsa core, woven glass skins and titanium root ends. The blades were assembled in a master mold and cured in an autoclave to form a unit. Root retention was achieved by filament winding. The cuff was attached in a secondary operation. This method of construction gave good repeatability in dynamic properties and aerodynamic shape, particularly in twist.

### 2.2 WING

The wing has a span of 120 inches and a chord of 45 inches. The airfoil was a modified NACA 63<sub>3</sub>418. A leading edge slat and a single slotted flap extended from the wing tips to the wing junction with the DRTS. The wing leading edge was located 37% of chord aft of the center of rotation, and

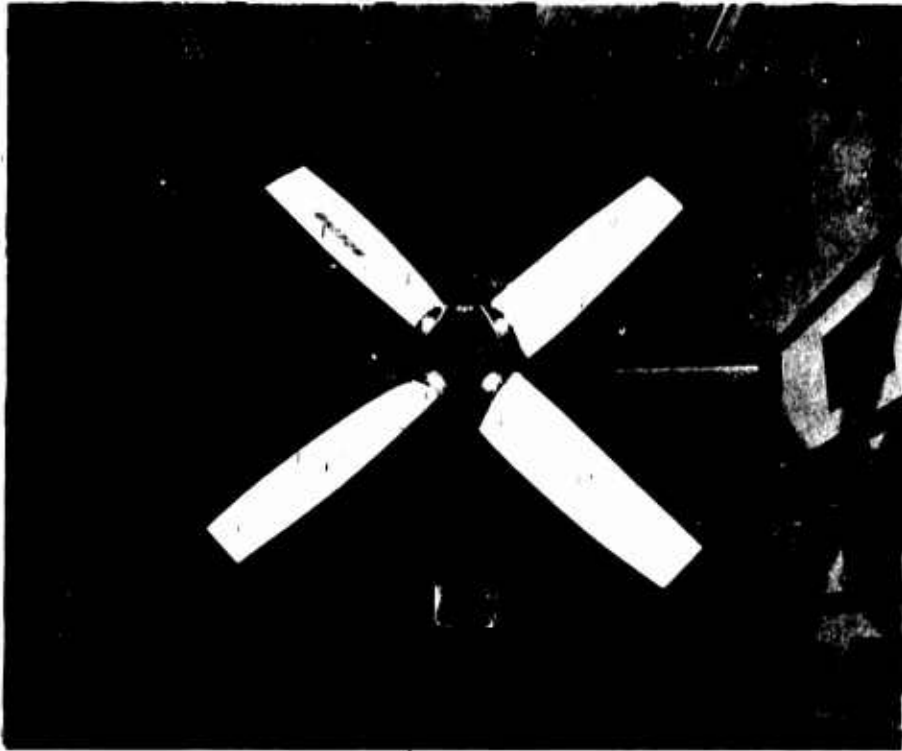
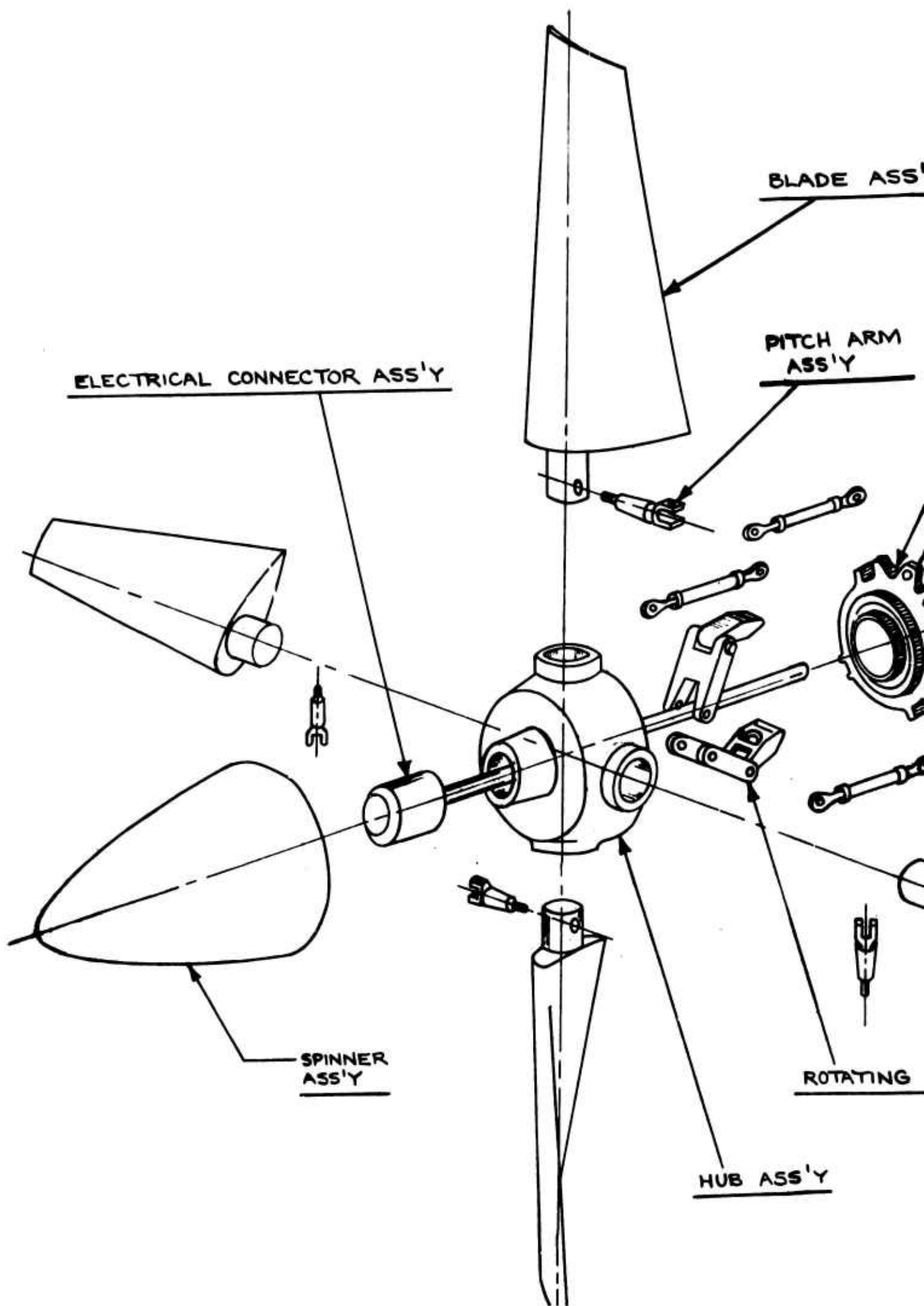


Figure 2.1a  
INSTALLED PROPELLER IN WIND TUNNEL LOOKING AFT



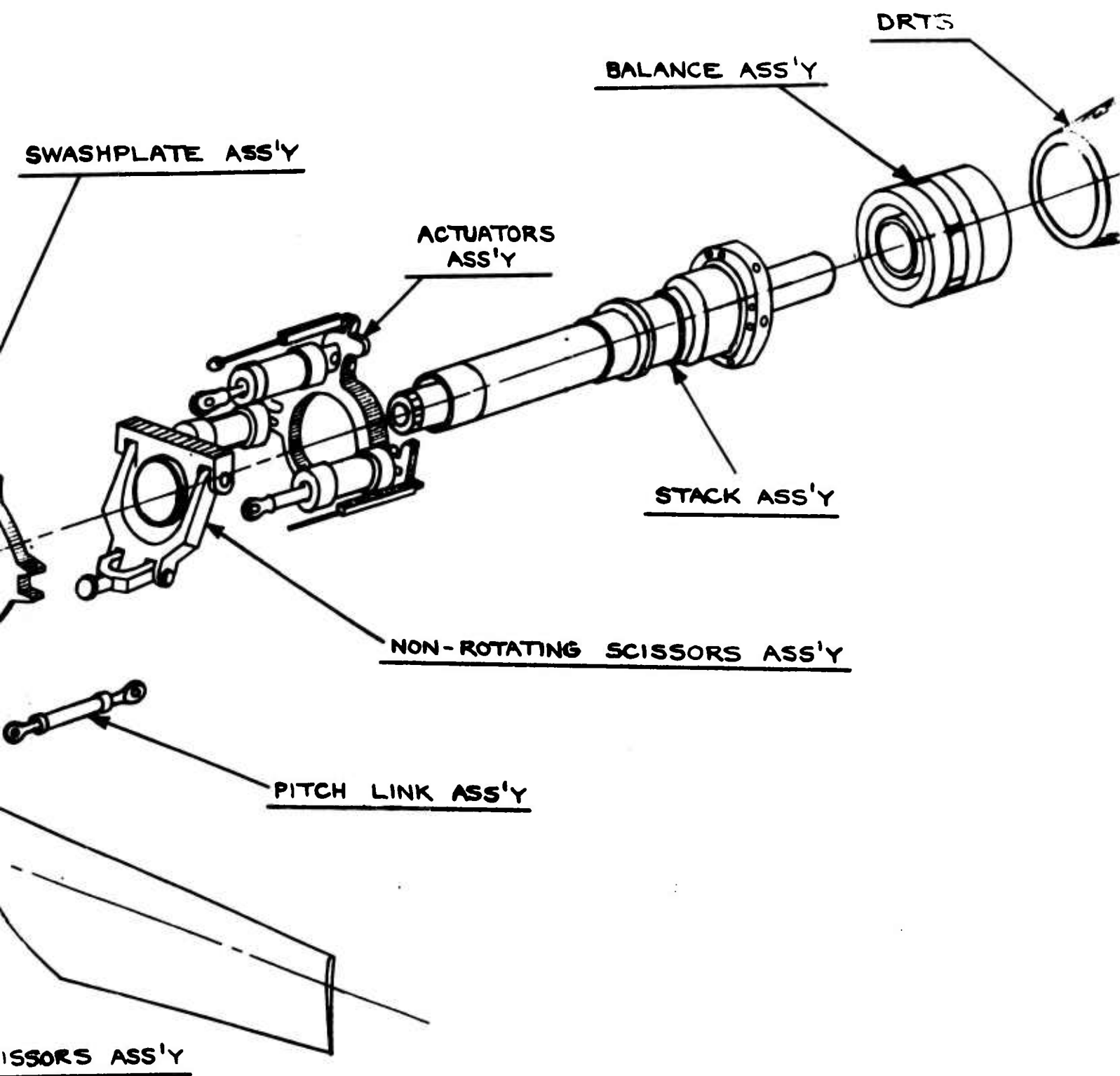
Figure 2.1b  
INSTALLED PROPELLER IN WIND TUNNEL LOOKING FORWARD

A



1 B

D170-10040-  
Figure 2.2



1/3 SCALE M-170 HUB & CONTROLS

TABLE 2.1SCALE FACTORS

PARAMETER		SCALE FACTOR (MODEL/FULL-SCALE)
LENGTH	$L$	$1/3$
FROUDE NO.	$F_N$	$1.0$
DENSITY	$\rho$	$1.0$
TIME	$T = L^{1/2}$	$\sqrt{1/3}$
VELOCITY	$V = L^{1/2}$	$\sqrt{1/3}$
FREQUENCY	$f = L^{-1/2}$	$\sqrt{3}$
MASS	$W = L^3$	$1/27$
MASS/UNIT LENGTH	$w = L^2$	$1/9$
INERTIA	$I = L^5$	$1/243$
INERTIA/UNIT LENGTH	$i = L^4$	$1/81$
FORCE	$F = L^3$	$1/27$
MOMENT	$M = L^4$	$1/81$
PRESSURE	$q = L$	$1/3$
STIFFNESS (EI & GJ)	$K = L^5$	$1/243$
POWER	$P = L^{7/2}$	$0.0214$

approximately 15% of chord above the thrust axis. The wing mean chord line was inclined  $2^\circ$  nose up to the thrust axis. End plates with a width of approximately 1 chord were mounted at each wing tip. Flow fences were mounted on the wing, 17.5" from the thrust centerline.

The flaps were tested in two positions, extended to  $45^\circ$  and in the fully retracted position. The leading edge slats were tested in an extended position and in the fully retracted position. These settings have been tested previously on a semispan wing model at the University of Maryland Wind Tunnel in Boeing-Vertol Test 040.

### 3.0 TEST INSTALLATION

The test was conducted in the Boeing-Vertol V/STOL Wind Tunnel. See Figure 3.1 for a schematic drawing of the tunnel.

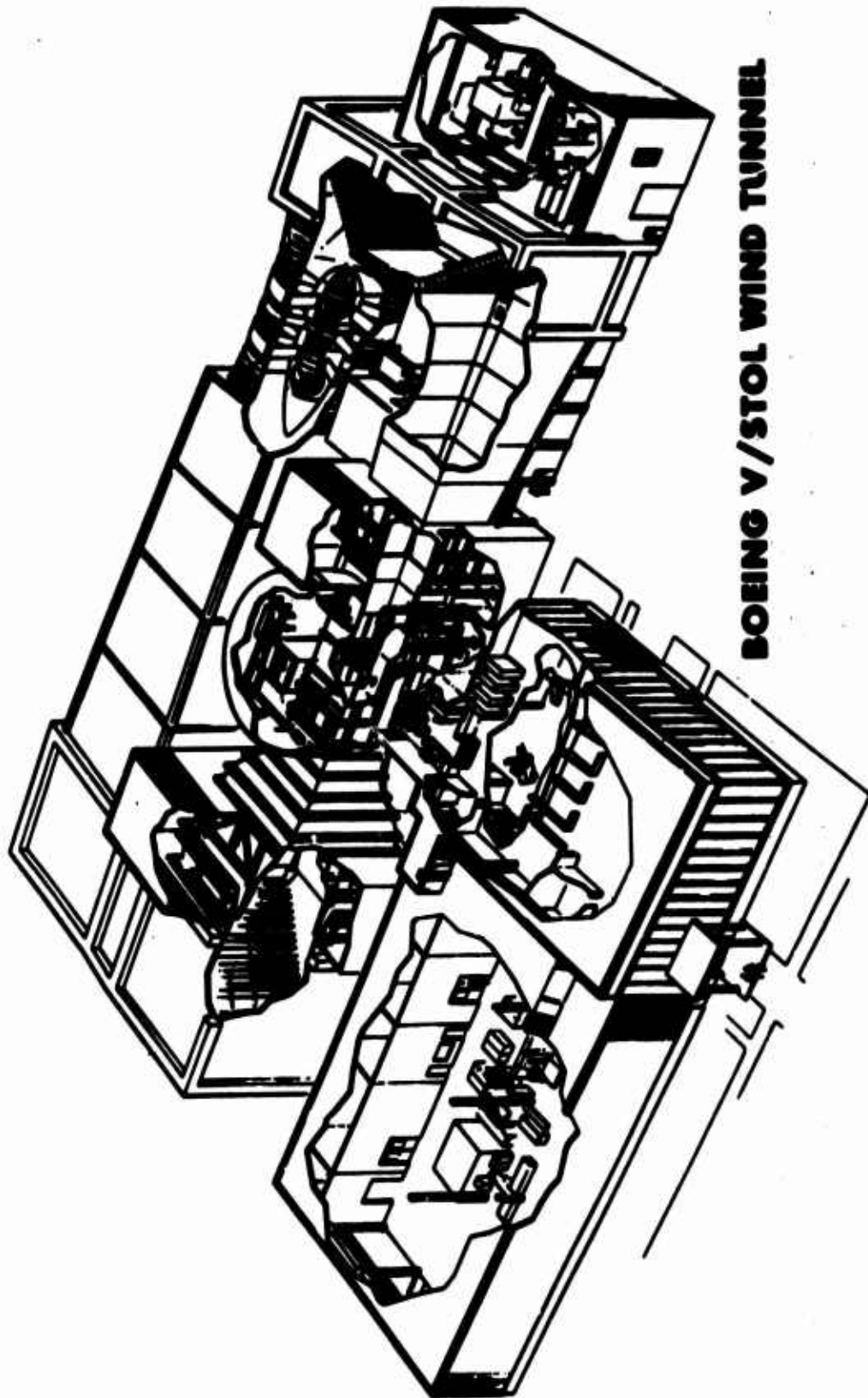
Three test section configurations are available, two of which were used for this test. These are open throat and slotted throat. For hover testing the open throat was used with the model thrust axis normal to the tunnel free stream wind axis. The test section is located inside a Plenum which has a circular cross section with a diameter of 65 feet. In the hover mode the Plenum floor is 30 feet below the propeller disk plane and the roof is 30 feet above the propeller disk plane. In this configuration the model is thought to be essentially in free air out of ground effect. For cruise and transition testing the model was located in the 20 X 20 foot test section with walls, floor and ceiling in the slotted configuration at 10% porosity. The spinner and hub tares were obtained with the test section walls and ceiling removed.

### 4.0 MODEL INSTRUMENTATION, DATA ACQUISITION SYSTEM AND DATA REDUCTION

The model was instrumented to measure blade flap and chord bending moments at .22 radius and at .45 radius. Blade torsion was measured at .22 radius. The pitch links were instrumented to give axial control loads in the links.

Shaft torque was measured by strain gages on the drive shaft. The 5-component balance measured three orthogonal forces and two moments. The balance measurements are referenced to the propeller disk plane. The 1/rev signal was provided.





These data were converted from analog to digital signals stored on tape for further processing and processed "on-line". A more detailed description is contained in Appendix B.

## 5.0 SIGN CONVENTION AND NOMENCLATURE

The positive sign convention and the force and moment nomenclature are provided in Figure 5.1

### 5.1 Positive Sign Convention

- a) Collective Pitch - Blade L/E rotated nose-up
- b) Longitudinal            - Positive cyclic produces a  
Cyclic Pitch               positive pitching moment
- c) Pitch Link              - Compression
- d) Shaft Angle of        - Nose-up from cruise configuration  
Attack
- e) Blade Flapwise        - Compression in upper surface  
Bending
- f) Blade Chordwise       - Compression in L/E  
Bending
- g) Blade Torsional       - Blade L/E rotated nose-up  
Moment
- h) Delta Shaft            - Nose-up from the horizontal  
Angle

## 5.2 Nomenclature

### a) Control Deflection

- f - Flap deflection--positive trailing edge down
- L - Leading edge slat deflection--positive leading edge down
- $\theta_{75}$  - Collective pitch - positive leading edge up
- B<sub>1</sub> - Longitudinal cyclic - Positive cyclic produces a positive hub pitching moment

### b) Configuration Symbols

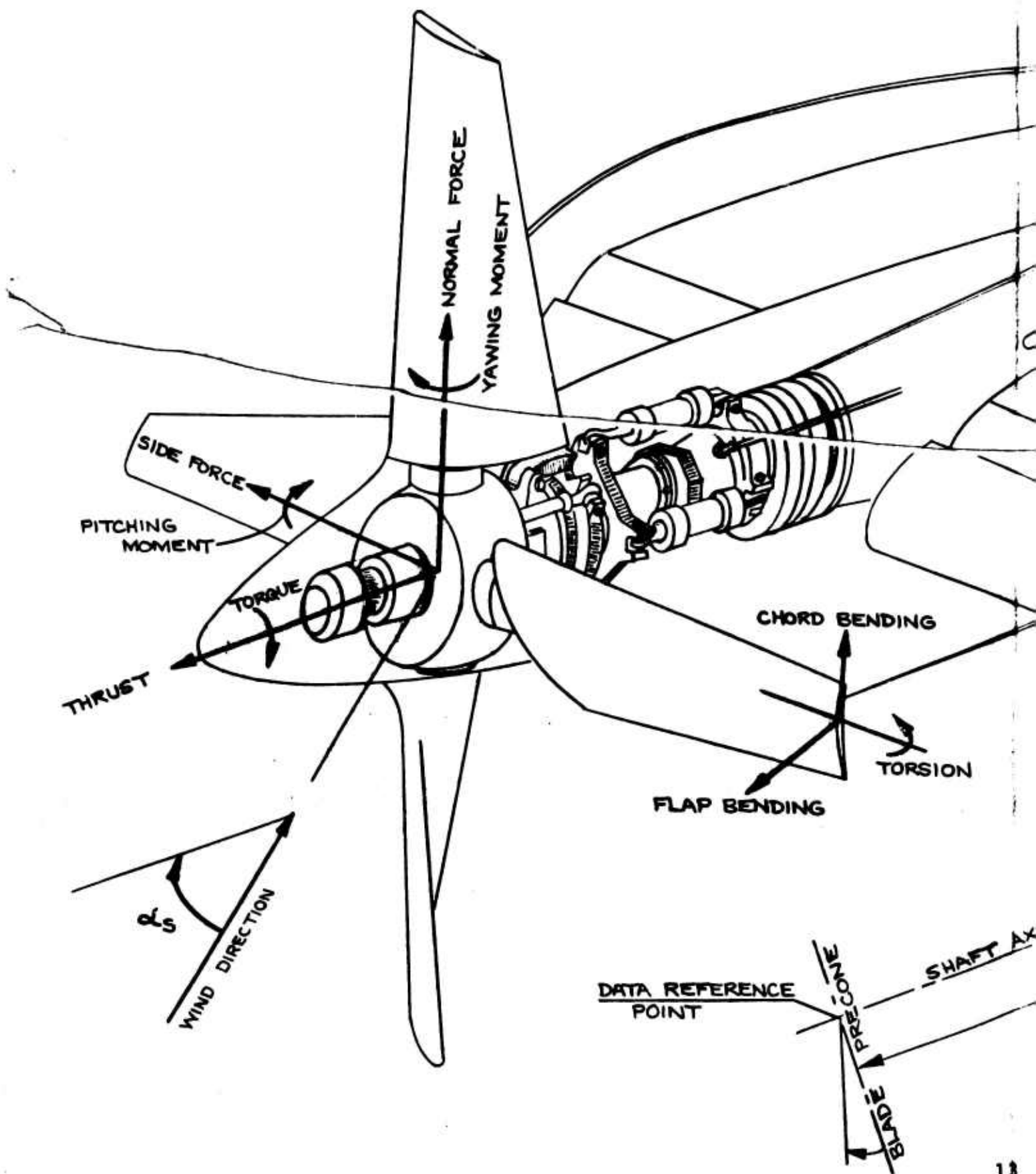
- W - Wing
- L - Wing with leading edge slat
- F - Wing with trailing edge flap
- P - Propeller
- H - Hub
- S - Propeller Spinner

## 6.0 TEST PROCEDURE

The test procedure is given in detail in Appendix C. The remote operation of the collective pitch, cyclic pitch, shaft angle, propeller RPM, and tunnel speed afford the opportunity to conduct the test runs in the manner best suited to obtain the desired data for a given run. Any of the above parameters could be varied in any run with the remaining variables held constant. The test conditions were only limited by the "allowable" blade loads and by the power available to drive the propeller.

R

# MODEL AND BALANCE AND POSITIVE



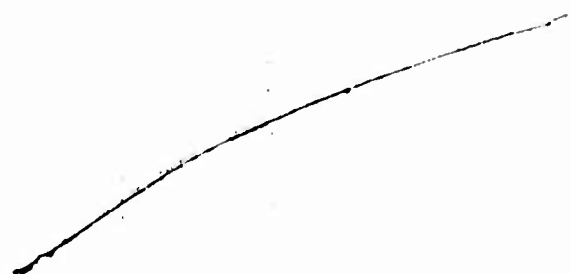
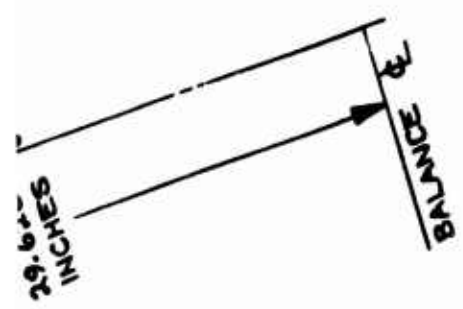
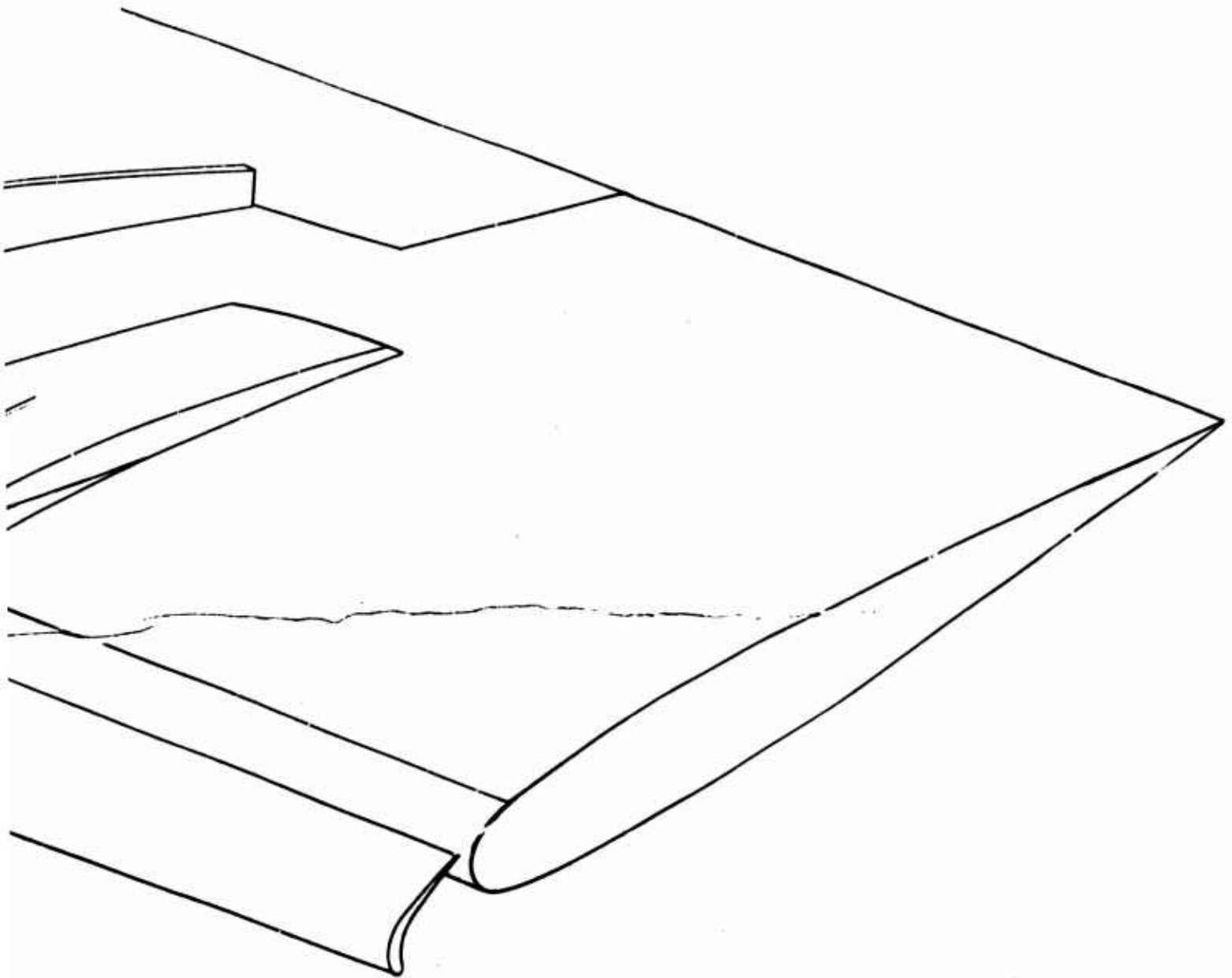
B

FORCE AND MOMENT NOMENCLATURE

D170-10040-1

Figure 5.1

SIGN CONVENTION



## 7.0 RUN LOG

The run log is presented in Appendix D.

### 7.1 HOVER

Runs 1-12 were familiarization and checkout runs. Isolated propeller hover data was taken in runs 13-18, 26, 77-86. Runs 13-18 and runs 80 and 81 have variations in  $C_T$ ,  $\Theta_2$ , and RPM. Runs 12, 17, 77 and 78 provide performance data. Run 26 is a shaft angle sweep with walls, roof, and floor installed. Runs 85 and 86 are shaft angle sweeps with open test section.

The installed propeller was tested in hover in runs 19-25. Runs 19 and 20 provide clean wing performance and cyclic data. Run 21 has the slats and flaps extended for performance. Runs 22, 23 and 24 provide data on cyclic pitch for various  $C_T$ . Run 25 provides data at two RPM's with  $\Theta_2 = 2^\circ$  with the walls, floor and roof installed.

### 7.2 TRANSITION

Transition data was taken in runs 27-44, 70-76, and 87 at hover RPM. The isolated propeller was tested in runs 27-33 for shaft angle sweeps with no cyclic pitch for a range of J. Runs 34-39 include the effects of cyclic pitch. The installed propeller data was taken in runs 40-44. Run 87 is for a typical transition.

### 7.3 CRUISE

Cruise data was taken in runs 45-69 at cruise RPM for a range of J from 0 to 2.6. The isolated propeller data is given in runs 58-69. In run 58-65  $\Theta_{75}$  was held constant for a given run. In run 66 the shaft angle was  $+5^\circ$  and  $\Theta_{75}$  was varied to representative collective angles. Run 67 gives data at  $C_p = .20$  with the shaft angle at  $+5^\circ$ .

The installed propeller with clean wing data is given in runs 45-57. Runs 45-53 give the cruise performance data. Runs 54-56 give data for shaft angles of 5, 10 and  $15^\circ$  for blade loads.

7.4 HUB AND SPINNER TARES

Hub and spinner tare data was taken in runs 89-92 for two values of dynamic pressure and for two values of RPM.



## 8.0 RESULTS AND DISCUSSION

### 8.1 INTRODUCTION

The results of the tests are presented in this section. The data are presented in graphical form. The range of the test variables covers the whole operating spectrum for the tilt wing aircraft and was extended beyond to the design allowables of the propeller blades.

The data exhibited excellent repeatability. When early runs conducted for familiarization and model checkout were repeated, the data showed no serious scatter. Because of the wide range of weight tares due to changing shaft angle, the hub force and moment data are within  $\pm 3\%$  of the applied loads.

An implicit objective of the test program was the development of a reliable hub and controls for the testing of cyclic propellers. The hardware performed well throughout the test period. The only shutdown experienced in the program was for the purpose of repairing blade strain gages. The ability to remotely vary cyclic and/or collective pitch while the propeller was running permitted an efficient gathering of large quantities of data.

It should be noted that the aerodynamic design of the propeller is non-optimal. The aerodynamic parameters for the blade were originally selected for a three-bladed propeller. The design was being changed to a four-bladed propeller at the initiation of the work but the aerodynamic parameters had not yet been worked. The result was to use four-blades having the three-bladed aerodynamic properties for the propeller. The aerodynamic effect on cyclic loads could be adjusted primarily on the basis of solidity so the test propeller is suitable for loads. However, the aerodynamic performance of the propeller might be expected to depart from the "best design practices".

This section is divided into three parts: propeller performance, hover and transition. In each part the isolated propeller data and the installed propeller data are presented and compared. The effects of cyclic pitch are given in the second and third parts. These data form an excellent basis

for the comparison of analytical results. The generation of analytical results and the comparison with the test data should be done in the next phase.

## 8.2 PROPELLER PERFORMANCE CHARACTERISTICS

The hover performance characteristics of the propeller were measured for the case of the isolated propeller, the propeller with clean wing, and for the propeller with the flaps and slats extended. The cruise performance was measured for the isolated propeller and for the propeller with clean wing.

The hover performance results are shown in Figures 8.1 to 8.8. In Figure 8.1 the variation of  $C_T$  with  $C_p$  may be seen for RPM of 1100. For the isolated propeller the analytically predicted  $C_T$  vs  $C_p$  curve is shown. It may be seen that at the lower  $C_p$  the predicted values and the measured values are in agreement while for the higher  $C_p$  the measured values exceed the analytical values. The addition of the wing causes an increase in power for a given thrust. The deflection of the flaps causes a further increase in power. The effect of tip speed on  $C_T$  vs  $C_p$  is shown in Figure 8.2. It may be seen that the influence of tip speed shows small but consistent influence on  $C_T$  vs  $C_p$ .

The influence of the wing on  $C_T$  vs  $\Theta_{75}$  and for  $C_p$  vs  $\Theta_{75}$  is shown in Figures 8.3 and 8.4 for 1100 RPM. Comparing the isolated propeller to the propeller with wing, to maintain the constant  $C_T$  or  $C_p$ , an increase in collective is required. As the high lift devices are deployed, additional collective is required to maintain  $C_T$  and  $C_p$ .

Figure of Merit as a function of  $C_T$  is shown in Figures 8.5 and 8.6. The Figure of Merit remains nearly constant at a high value over a wide range of values of  $C_T$ . In Figure 8.5 it may be seen that the presence of the wing costs approximately 5 points of Figure of Merit. There does not appear to be a significant difference between the effect of the clean wing as compared to the wing with slats and flaps extended. The effect of tip speed on Figure of Merit for the isolated propeller is shown in Figure 8.6. The increase in Figure of Merit of 5 points is obtained in going from 850 RPM to 1050 RPM. Going from 1050 RPM to 1100 RPM results in no change or a slight decrease in Figure of Merit. The reduction in Figure of Merit with lower RPM is probably associated with the lower  $N_R$ .

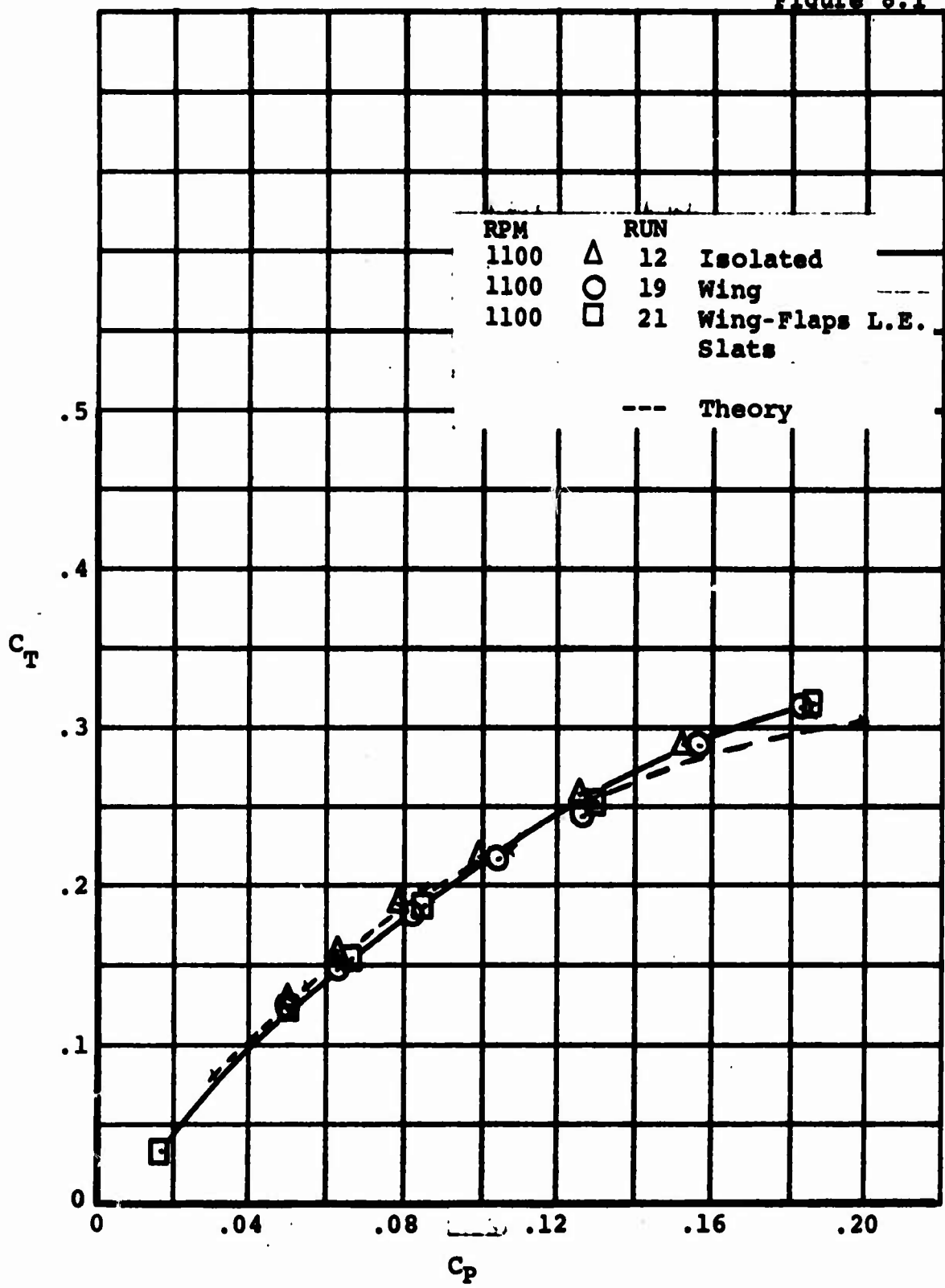
Evan at the highest tip speed no appreciable Mach number effect is apparent or predicted.

The maximum Figure of Merit predicted analytically for the full-scale propeller is 0.76. The measured Figure of Merit for the isolated propeller is 0.82. This difference caused considerable concern and led to an extensive investigation of the balance. The interactions matrix was established through extensive calibration. There remains the possibility of a systematic error in the test configuration and measurements. There is also the possibility of some ground effect from the flat top of the Dynamic Rotor Test Stand and a possibility of some recirculation despite the large size of the plenum.

The measured cruise performance is summarized in terms of  $C_p$  vs  $J$  in Figures 8.7 and 8.8. Also shown in Figures 8.7 and 8.8 are lines of constant collective and constant cruise efficiency. At high values of  $J$ , the measured cruise efficiency is less than the predicted values by almost ten points. Possible causes for this include the high drag of the round blade roots, the effect of supervelocities due to spinner, spinner tares and live twist. These causes require further investigation before drawing any conclusions from the cruise efficiency data.

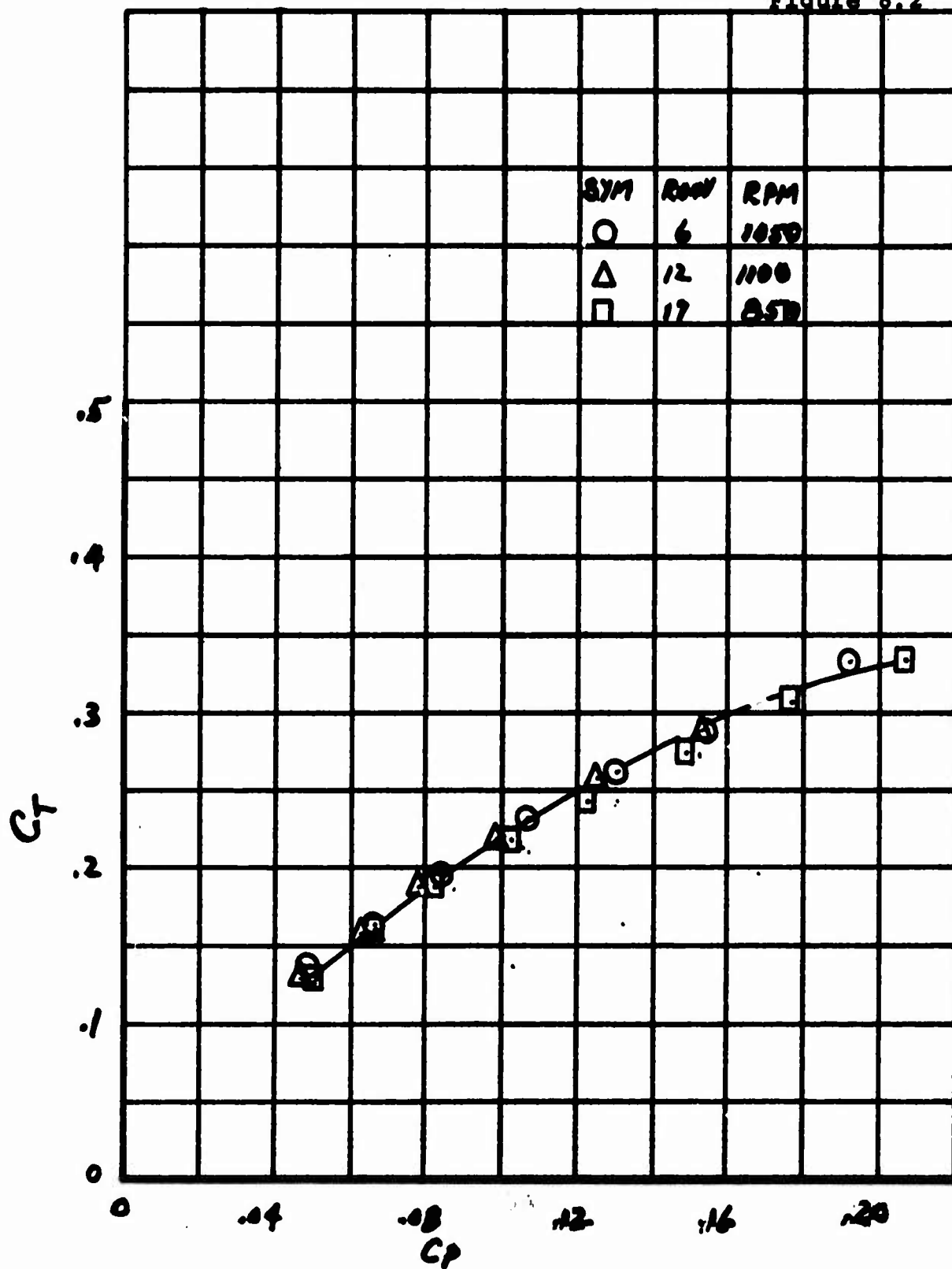
Comparing the cruise performance of the isolated propeller, Figures 8.7, to that for the propeller with wing, Figure 8.7 shows that the cruise efficiency is degraded by the presence of the wing. For conditions likely to be encountered in cruise, (i.e.,  $C_p = .16$ ) the loss in efficiency is approximately 5 points. It should be noted that the shape of the constant efficiency curves has been affected by the influence of the wing.

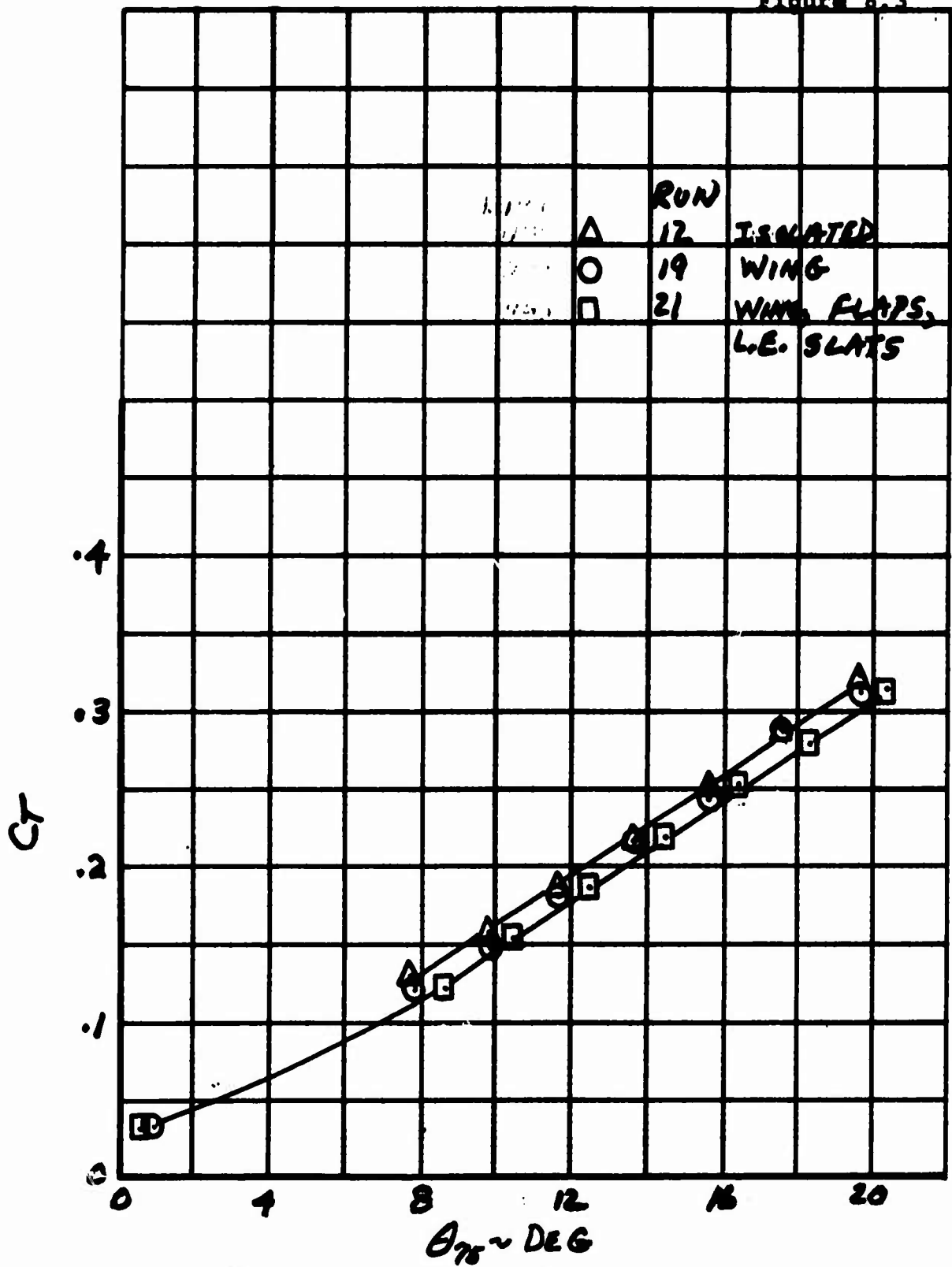
In computing the cruise efficiency and the Figure of Merit, no account has been taken for the effect of "live" twist. Aeroelastic blade load calculations show the "live" twist at 1100 RPM and  $\phi_{75} = 13^\circ$  to be approximately  $1.7^\circ$  from tip to pitch link tending to untwist the blade. The effect of "live" twist would be to increase the Figure of Merit and to decrease the cruise efficiency.



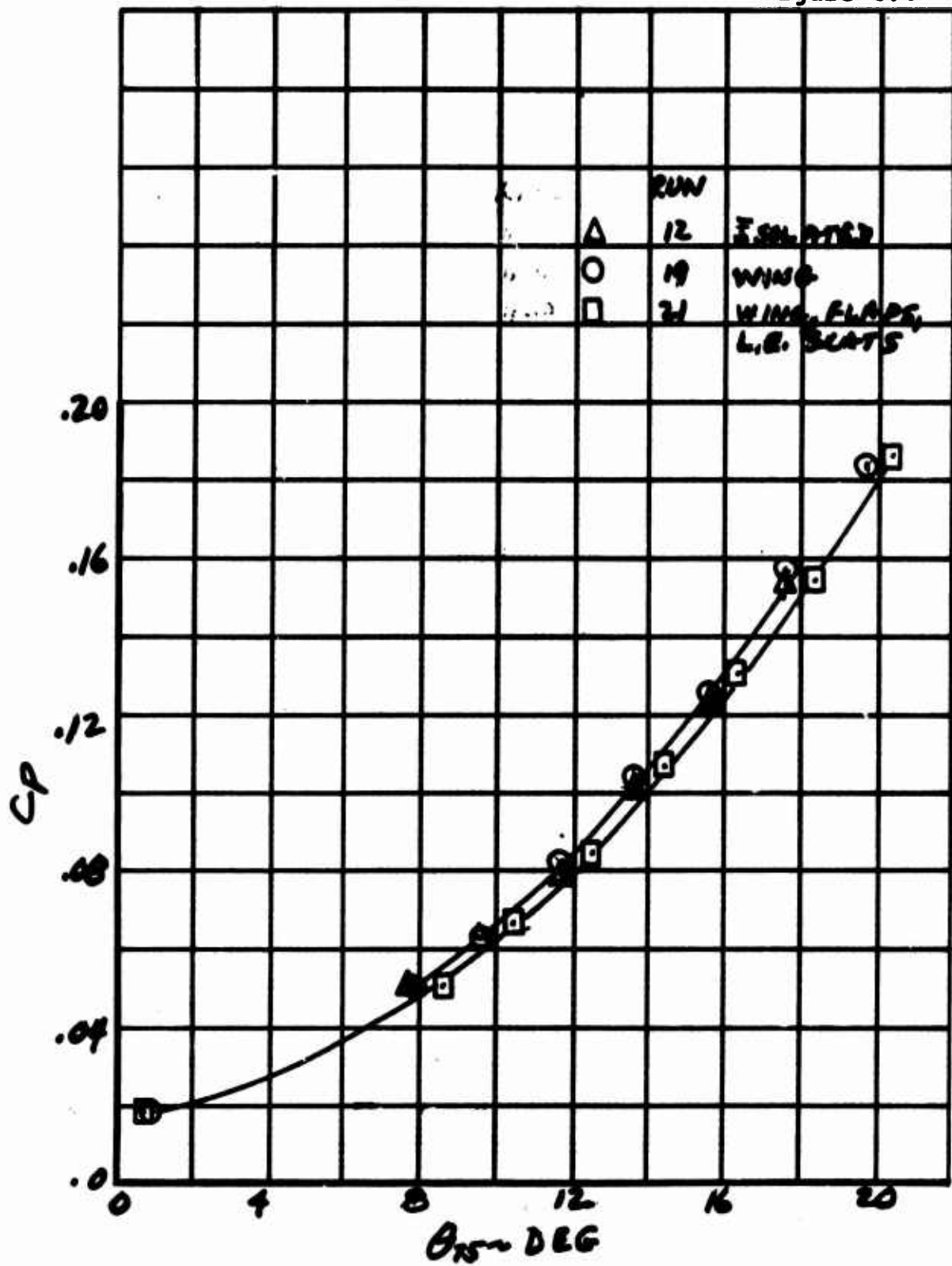
EFFECT OF WING, FLAPS AND SLATS ON  
HOVER PERFORMANCE

Figure 8.2

EFFECT OF TIP SPEED ON HOVER PERFORMANCE  
ISOLATED PROPELLER

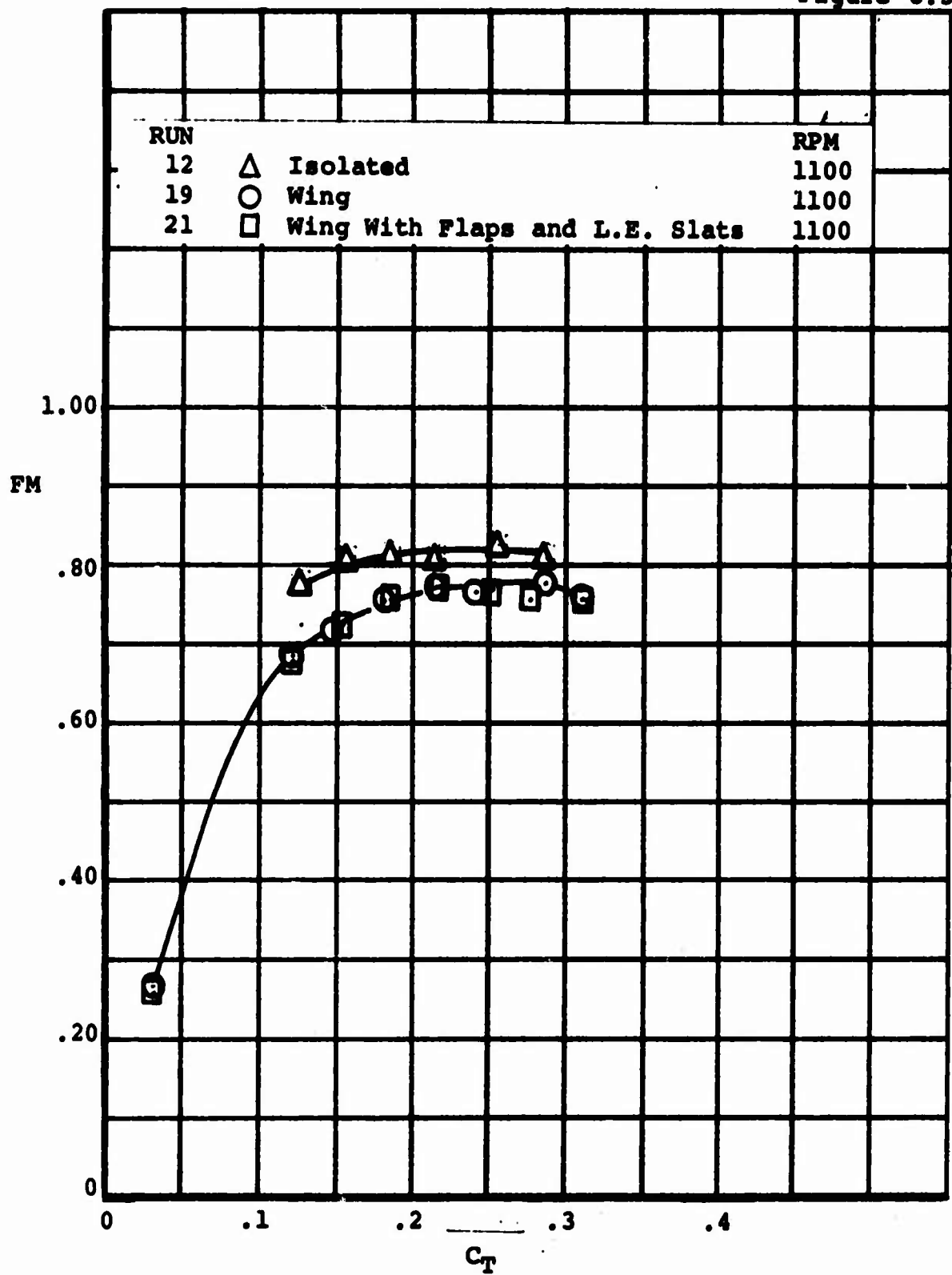


$C_T$  VS  $\theta_{75}$  FOR THE ISOLATED AND INSTALLED PROPELLER  
 $N = 1100$  RPM

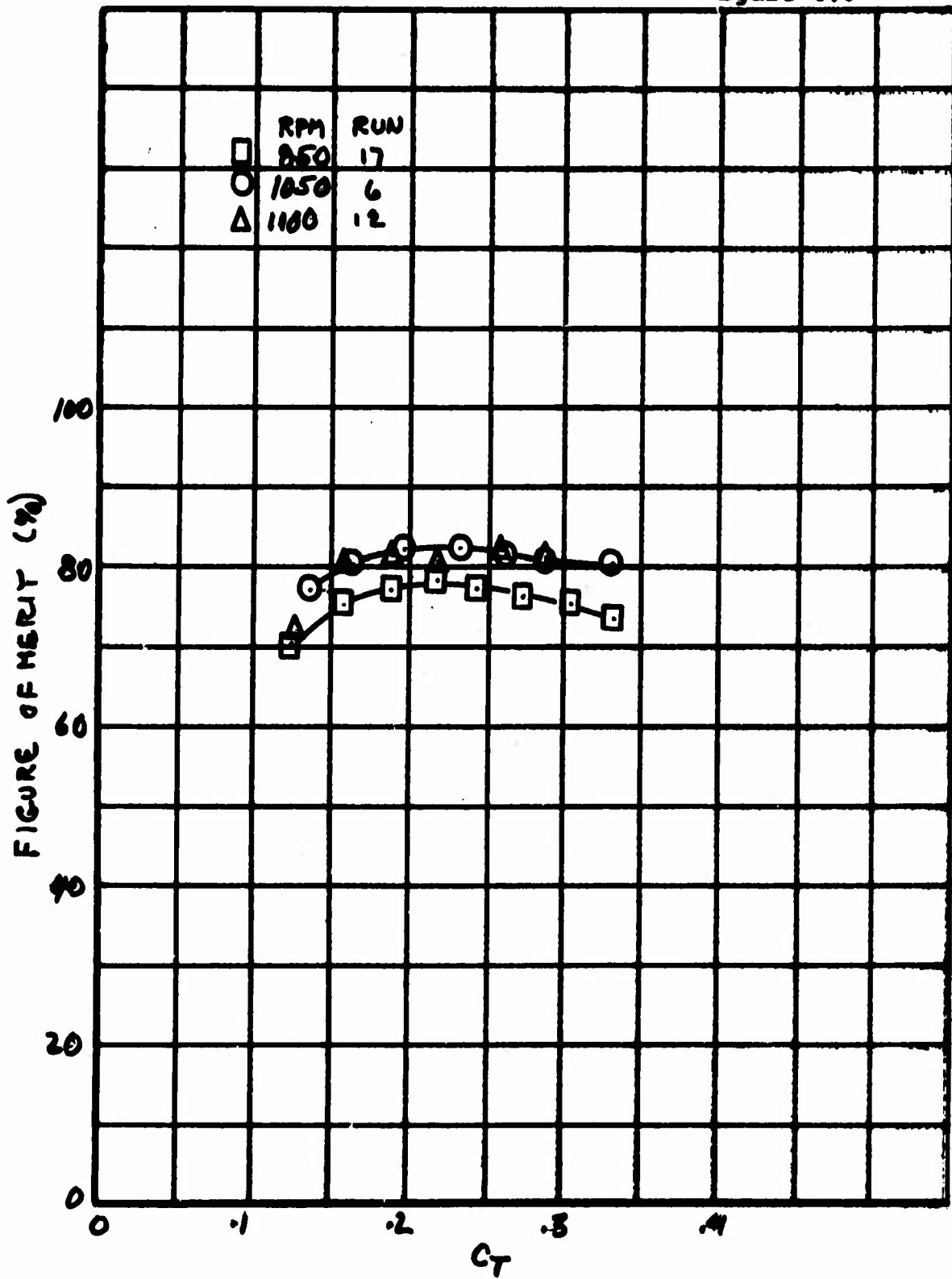


$C_p$  VS  $\theta_{75}$  FOR THE ISOLATED AND INSTALLED PROPELLER  
 $\Omega = 1400$  RPM

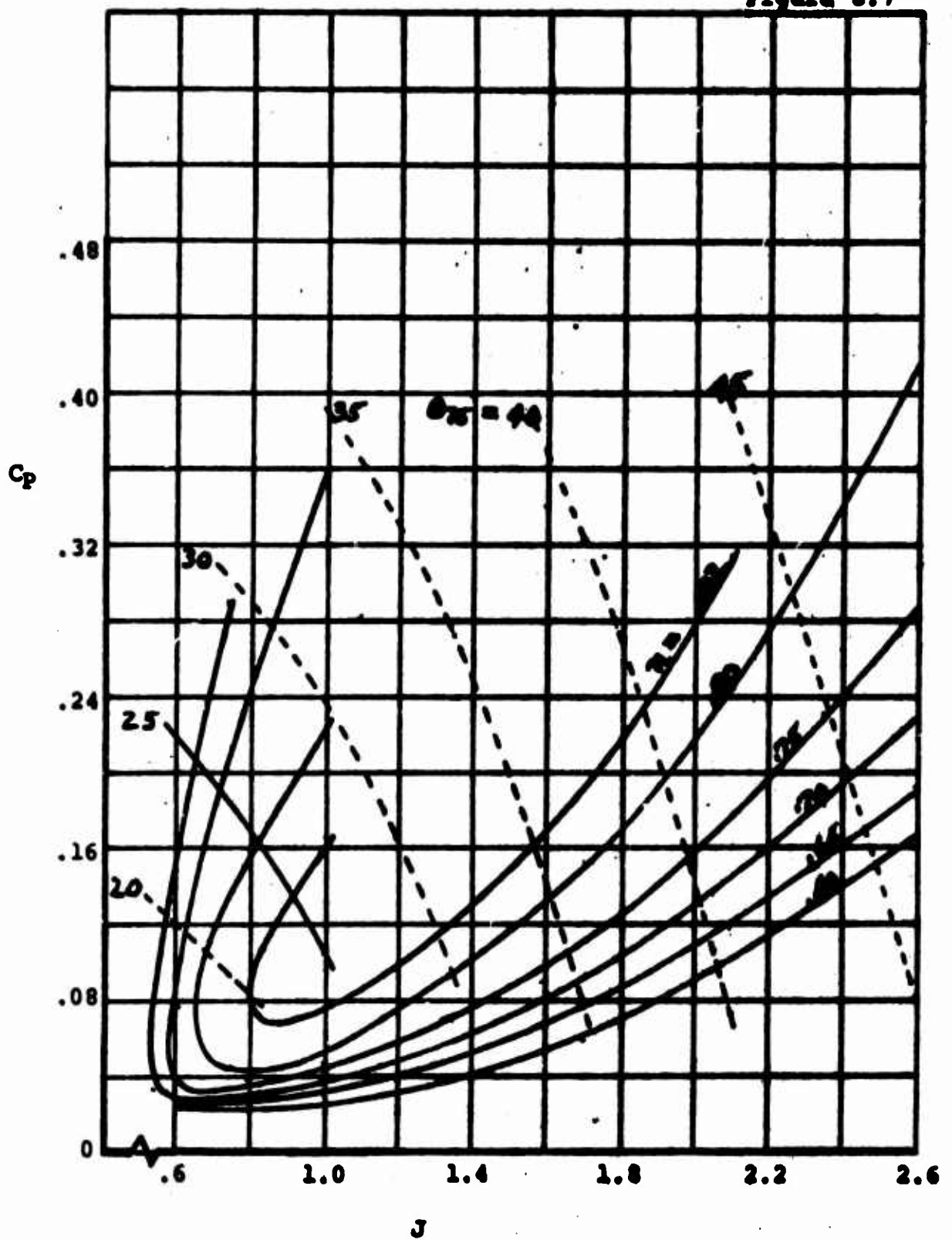




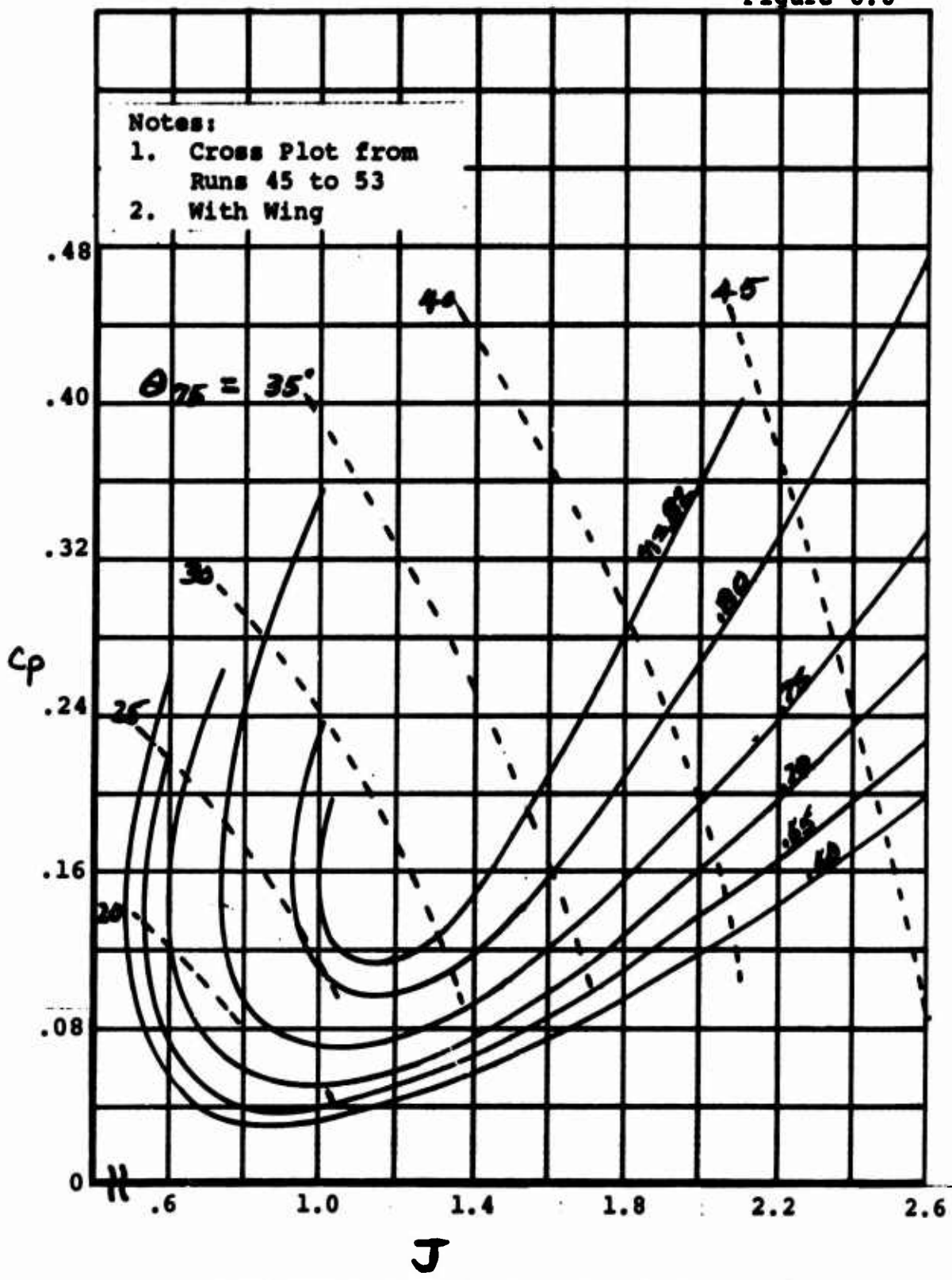
EFFECT OF WING, FLAPS AND SLATS ON  
FIGURE OF MERIT



ISOLATED PROPELLER FIGURE OF MERIT



CRUISE EFFICIENCY, ISOLATED PROPELLER



CRUISE EFFICIENCY PROPELLER WITH WING

### 8.3 EFFECT OF CYCLIC PITCH ON PITCHING MOMENT

The effect of cyclic pitch on pitching moment is shown in Figures 8.9 and 8.11. In Figure 8.9 is shown the variation of  $C_M$  with  $\theta_2$  for conditions approximating hover ( $C_T = .21$ ). It is seen that  $C_M$  vs  $\theta_2$  is linear for  $\theta_2 = \pm 10^\circ$  and that for  $\theta_2$  greater than  $10^\circ$  the non-linearity is not serious. At hover rpm (1100), approximately  $\pm 7^\circ$  of  $\theta_2$  provides .6 radian/sec<sup>2</sup> pitch acceleration to the V/STOL aircraft for which the propeller was designed. In Figure 8.11 a comparison of data for 850 RPM with data taken at 1100 RPM indicates that the effect of tip speed on  $C_M$  is negligible.

It should be noted that there appears to be about  $0.8^\circ$  of negative cyclic bias in the data. This bias may arise from interference due to the slipstream impinging with the structure of the DRTS. This would tend to give a negative pitching moment.

The phase of the pitching moment with respect to the cyclic pitch is shown in Figure 8.10. The phase is seen to be independent of  $\theta_2$  from  $\pm 15^\circ$  of cyclic pitch. The shift in phase from positive to negative cyclic pitch is  $180^\circ$ . The predicted phase shift of the moment was approximately  $10^\circ$ . To allow for this the cyclic pitch axis was advanced  $10^\circ$ . The measured phase relative to the cyclic pitch axis was a lag of  $25^\circ$ . It was not deemed necessary to reset the advance of the pitch axis (a major model change).

The thrust offset in terms of  $X/R$  vs  $\theta_2$  is shown in Figure 8.11. These data are another way of expressing the results shown in Figure 8.9. The comments on Figure 8.9 are also applicable to the thrust offset.

### 8.4 EFFECT OF CYCLIC PITCH ON THRUST AND POWER

The effect of  $\theta_2$  on  $C_T$  is shown in Figure 8.12.  $C_T$  is seen to be independent of  $\theta_2$ . These results differ from the results obtained by other investigators (See References 1 and 2), where  $C_T$  experiences a slight symmetrical drop off at  $\theta_2$  is increased. In the present tests, the RPM was held constant within  $\pm 2$  RPM over the cyclic range which might account for the lack of variation.

The effect of  $\Theta_2$  on  $C_p$  for the isolated propeller is shown in Figure 8.13. The variation of  $C_p$  with  $\Theta_2$  is seen to be an approximately parabolic curve.  $C_p$  as measured in this test includes the mechanical friction of the swashplate, pitch links, bearings, etc. forward of the strain gage on the drive shaft. The hub was designed to flight hardware quality and should give a reasonable representation of the mechanical friction present in a full-scale hub. Since the control requirements for a typical V/STOL transport may be met with  $\pm 7^\circ$  of cyclic pitch or an incremental  $C_M$  of .02, the power penalty of cyclic pitch control in hover is approximately 12% of the hover power.

The induced effects of the wing are shown in Figure 8.14. The ratio  $C_p/C_{p0}$ , where  $C_{p0}$  is  $C_p$  at  $\Theta_2 = -0.8^\circ$  is shown as a function of  $C_{mp}$  for both the isolated propeller and for the propeller with wing. Comparison of these data shows that the presence of the wing reduces the power requirements for control to approximately 7.5% of the hover power.

Examination of the effect of cyclic pitch on the isolated propeller Figure of Merit, Figure 8.15, gives the combined effect of the variation of  $C_T$  and  $C_p$  with  $\Theta_2$ . The principle variation does lie in  $C_p$ . However, the variation in Figure of Merit does show a drop off as the amplitude of  $\Theta_2$  is increased. This drop off reflects the performance penalty shown in the  $C_p$  curves.

#### 8.5 EFFECT OF CYCLIC PITCH ON NORMAL FORCE

The effect of cyclic pitch on normal force is shown in Figure 8.16. The slope of  $C_{Nf}$  curve is positive as would be expected. The apparent bias in  $\Theta_2$  is -2.5. Little variation is observed in going from 850 RPM to 1100 RPM. The effect of the wing is to reduce the bias, see Figure 8.17.

#### 8.6 BLADE LOADS

Blade loads for hover are shown in Figures 8.18 to 8.24. Figures 8.18 and 8.19 compare the steady flap and chord bending moments to the alternating flap and chord bending moments for changes in collective pitch at  $\Theta_2 = 0^\circ$ . The steady moments are seen to vary approximately linearly with collective up to  $18^\circ$ . The alternating moments remain essentially independent of  $\Theta_{75}$  until  $\Theta_{75} = 18^\circ$  above which the alternating loads show a marked increase. The behavior

in slope above  $\Theta_{75} = 18^\circ$  is attributed to the onset of blade stall.

The effect of RPM on the steady loads is seen to be proportional to  $(\Omega_1/\Omega_2)^2$  as might be expected. The alternating loads are essentially independent of RPM.

In Figure 8.19 are shown the effects of the wing on the flap bending moments as a function of  $\Theta_{75}$  for  $\Theta_2 = 0$ . The steady moments exhibit no influence from the presence of the wing. The alternating loads are influenced by the presence of the wing, showing a consistent reduction.

The alternating moments due to cyclic for the isolated propeller are given in Figures 8.20 and 8.21. The moments are presented as a total alternating moment and as the first three harmonics. The phase of the harmonics is also shown. The residual cyclic bias is also present in the moments. The total alternating moment and the first harmonic are linear with cyclic. The first harmonic exhibits a  $180^\circ$  phase shift in going from positive to negative cyclic. The second and third harmonics are relatively insensitive to cyclic pitch. Significantly, the ratio of the higher harmonics to the fundamental decreases as the total load increases with cyclic pitch.

A comparison of the blade loads due to cyclic pitch at  $\Theta_{75} = 14^\circ$  for the isolated propeller with the loads for the propeller with wing is shown in Figure 8.22. The alternating flap bending loads are reduced by the presence of the wing. The chord bending moment and the torsional moment are insensitive to the influence of the wing.

In Figure 8.23 the harmonics of the flap bending moment for the propeller with wing at  $\Theta_{75} = 14^\circ$  for a range of  $\Theta_2$  are presented. The moments are shown on a logarithmic scale because of the rapid decrease in the magnitude of the harmonics. Comparison of the total alternating moment with the first harmonic shows that even with the wing the blade loads are principally due to cyclic pitch. The second and higher harmonics are a magnitude less than the first harmonic. As regards hover, it appears that the primary loads experienced are the steady loads and the first harmonic due to cyclic.

The effect of RPM on the blade loads due to cyclic is shown in Figure 8.24. The change in sensitivity of the load with  $\theta_2$  is due primarily to the  $\omega/\omega_N$ , where  $\omega_N$  is the first coupled resonance of the blade. For these blades the first resonance, under rotation, is approximately 2200 CPM. The propeller responds as a simple single degree of freedom system with a cyclic forcing moment. Examination of the amplitude and phase angle of the blade loads confirm the validity of this representation.

### 8.7 EFFECT OF $C_T$ ON PITCHING MOMENT RATE

The pitching moment vs cyclic pitch for  $C_T$  ranging from 0.0085 to 0.30 is shown in Figure 8.25. The slope of the pitching moment curves is seen to increase as  $C_T$  is increased. The variation of slope with  $C_T$  is often attributed to the induced effects of the vorticity (Reference 3). These data indicate that at low  $C_T$ , approaching zero, that substantial loss of control power may be encountered.

Comparison of the results of this test with data from other tests is presented in Figure 8.26. These data are normalized with respect to solidity.

The data from this test are in general agreement with the data from the other tests. It may be seen that the data from reference 4 appears to be consistently higher than the other data. Shown as a dotted line is the analytical moment coefficient using a section lift curve slope of 0.1 per degree. At hover  $C_T$  of .21, the measured slopes are close to the analytical slopes. As  $C_T$  is decreased, the measured slopes decrease, suggesting that the induced wake effects may be significant in some phases of control.

### 8.8 BLADE FREQUENCIES

For blade loads and for proper operating conditions, the frequencies of the scaled test blades must have the same relationship to operating RPM as the full-scale blades. The test blades were designed to meet this condition (See Appendix A). The correlation between the design and the measured frequency data is shown in Figure 8.27.

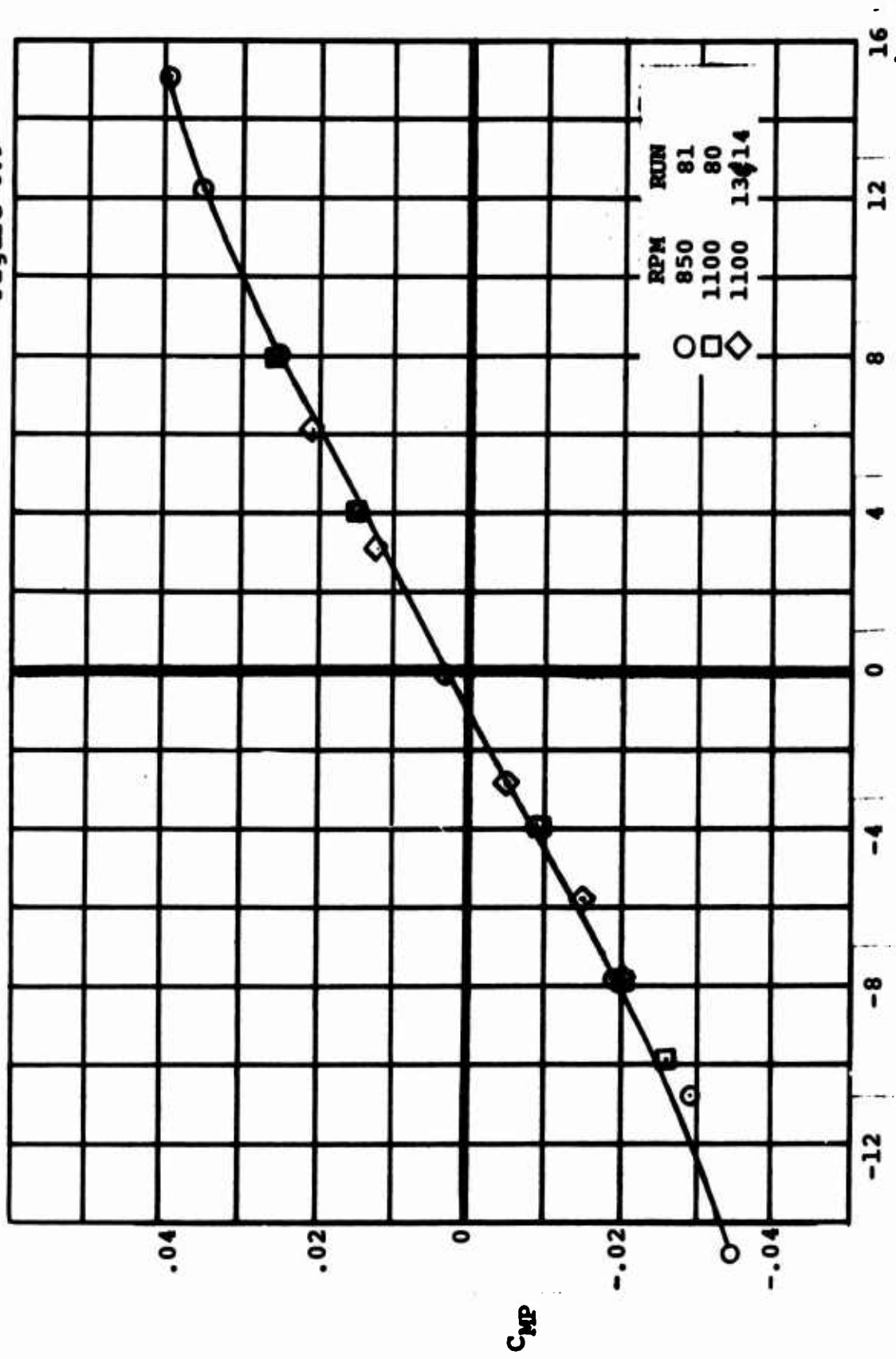


"Hand" analysis of CEC records revealed the existence of blade harmonic responses. Frequencies obtained from two runs are plotted in Figure 8.27 along with predictions (L-21)\*. The correlation of the test with predicted frequencies is good. Data were obtained from two separate runs as indicated. Run 4 with  $\Theta_{75} = 20^\circ$  and the rotor speed decreasing slowly under a shutdown condition and Run 7 with  $\Theta_{75} = 14^\circ$  at various steady rotor speeds. Original calculations indicated collective to have no appreciable effect on blade frequencies.

The data points shown for  $\Omega = 0$  were obtained from electromagnetic shake tests of the total system prior to the tests. Flap bending "tweak" tests were performed during the course of testing (between model changes at  $\Omega = 0$ ). The frequency remained unchanged.

\*L-21    Coupled Flap and Chord Bending Vibration Analysis  
         of a Rotor Blade

DL170-10040-1  
Figure 8.9

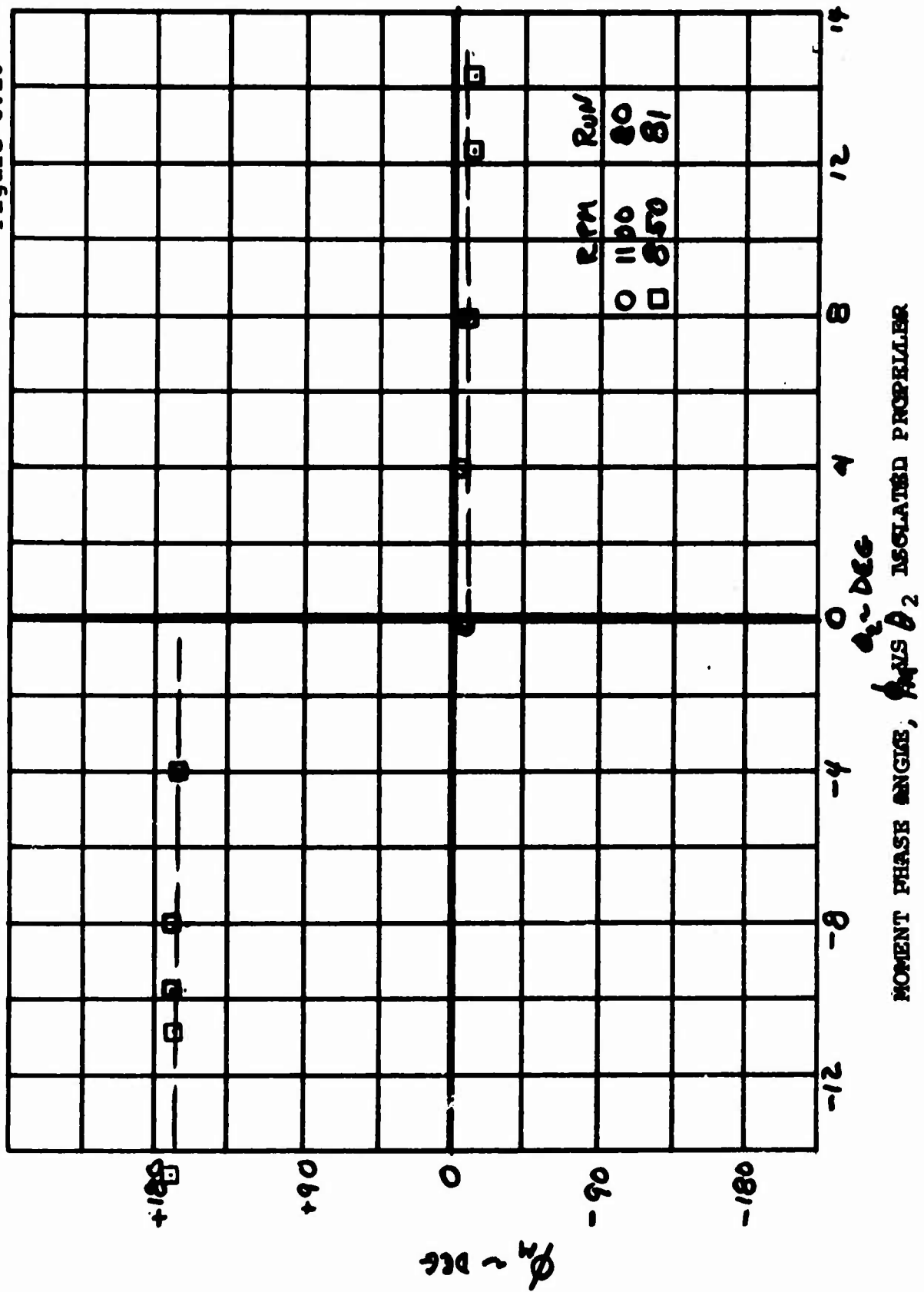


$\theta_2 \sim \text{DEG}$

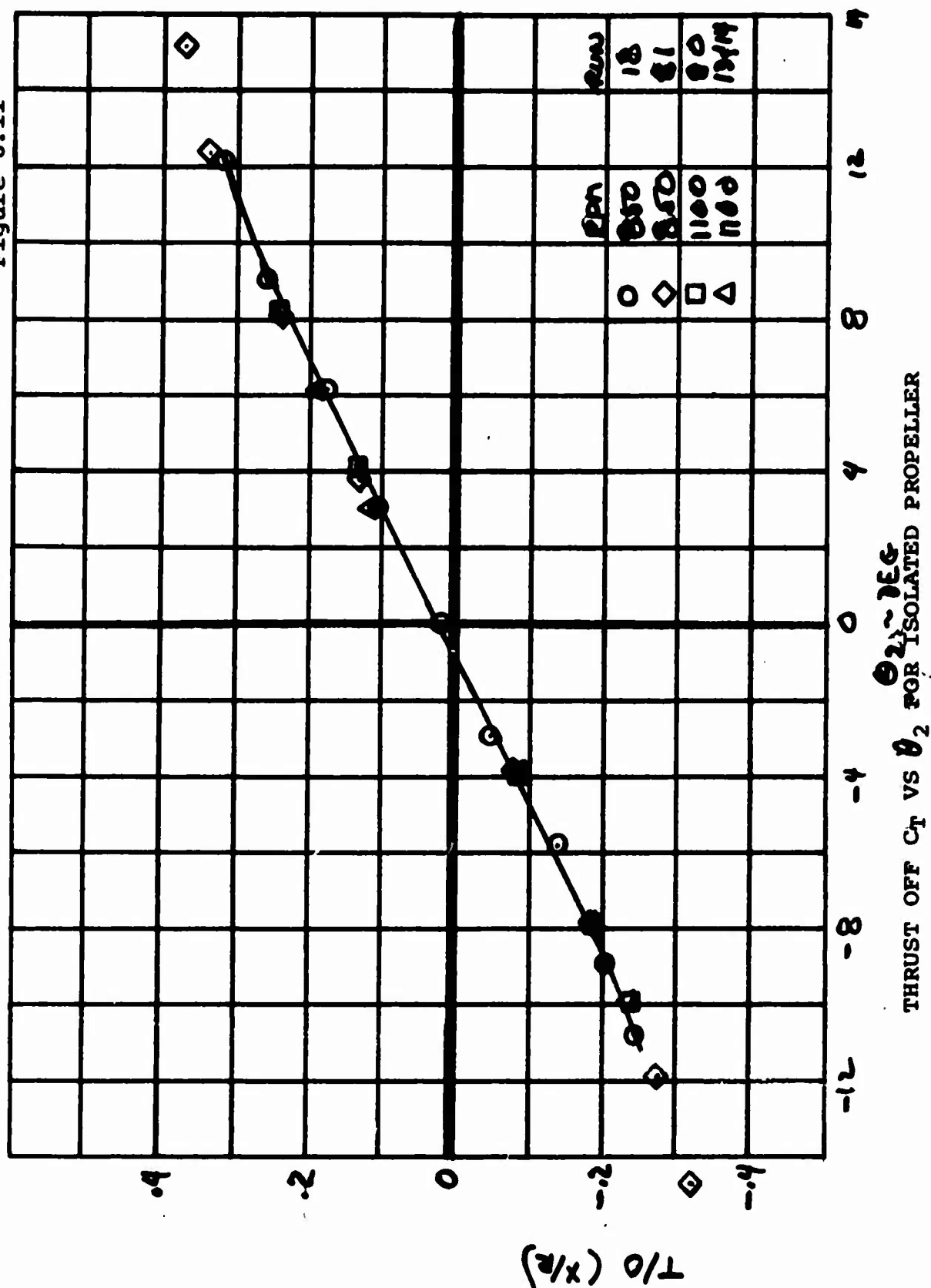
HOVER -  $C_{MP}$  VS.  $\theta_2$

$\theta_{75} = 13.65^\circ$

D170-10040-1  
Figure 8.10

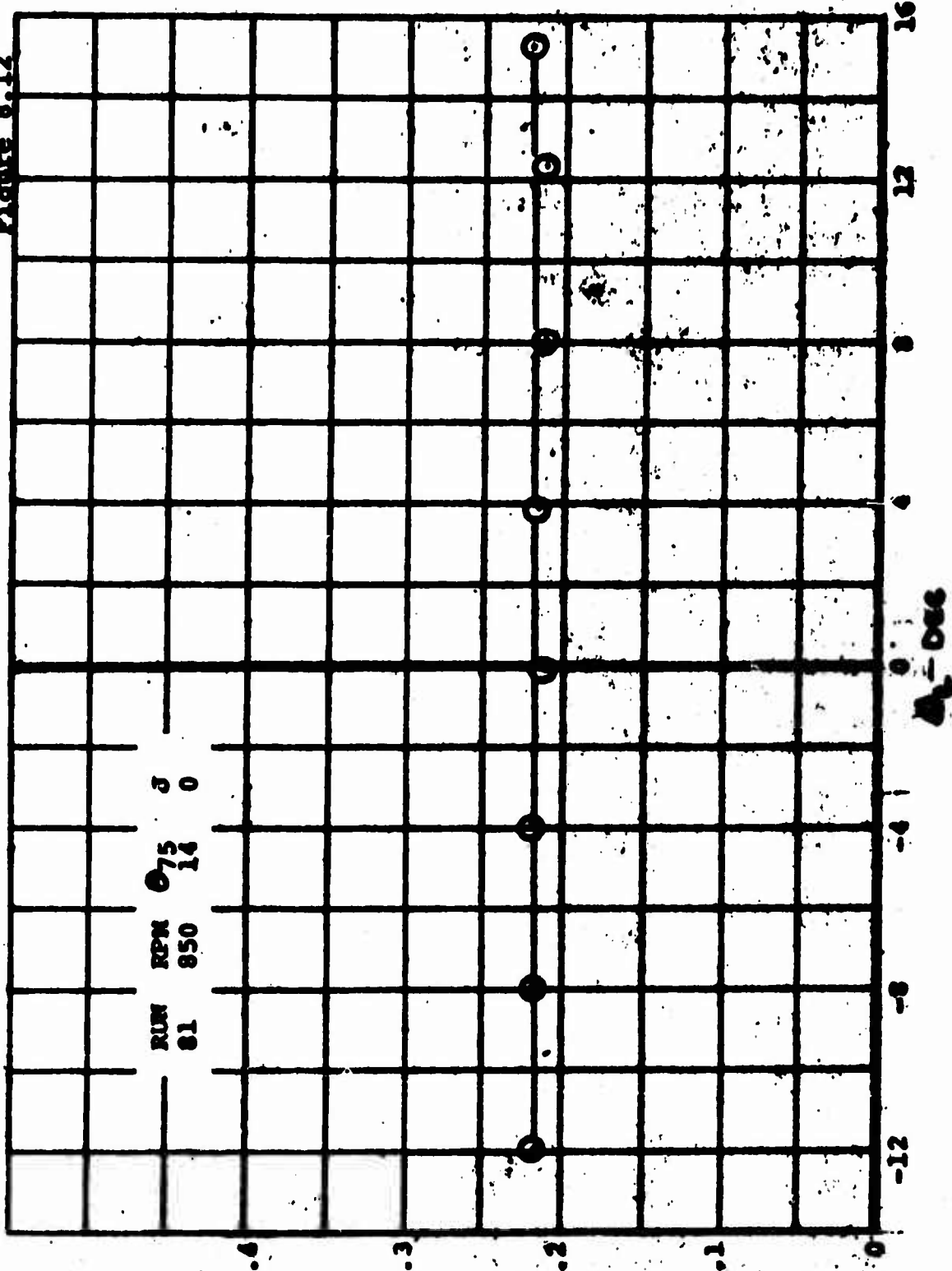


D170-10040-1  
Figure 8.11



D170-10040-1

Figure 8.12

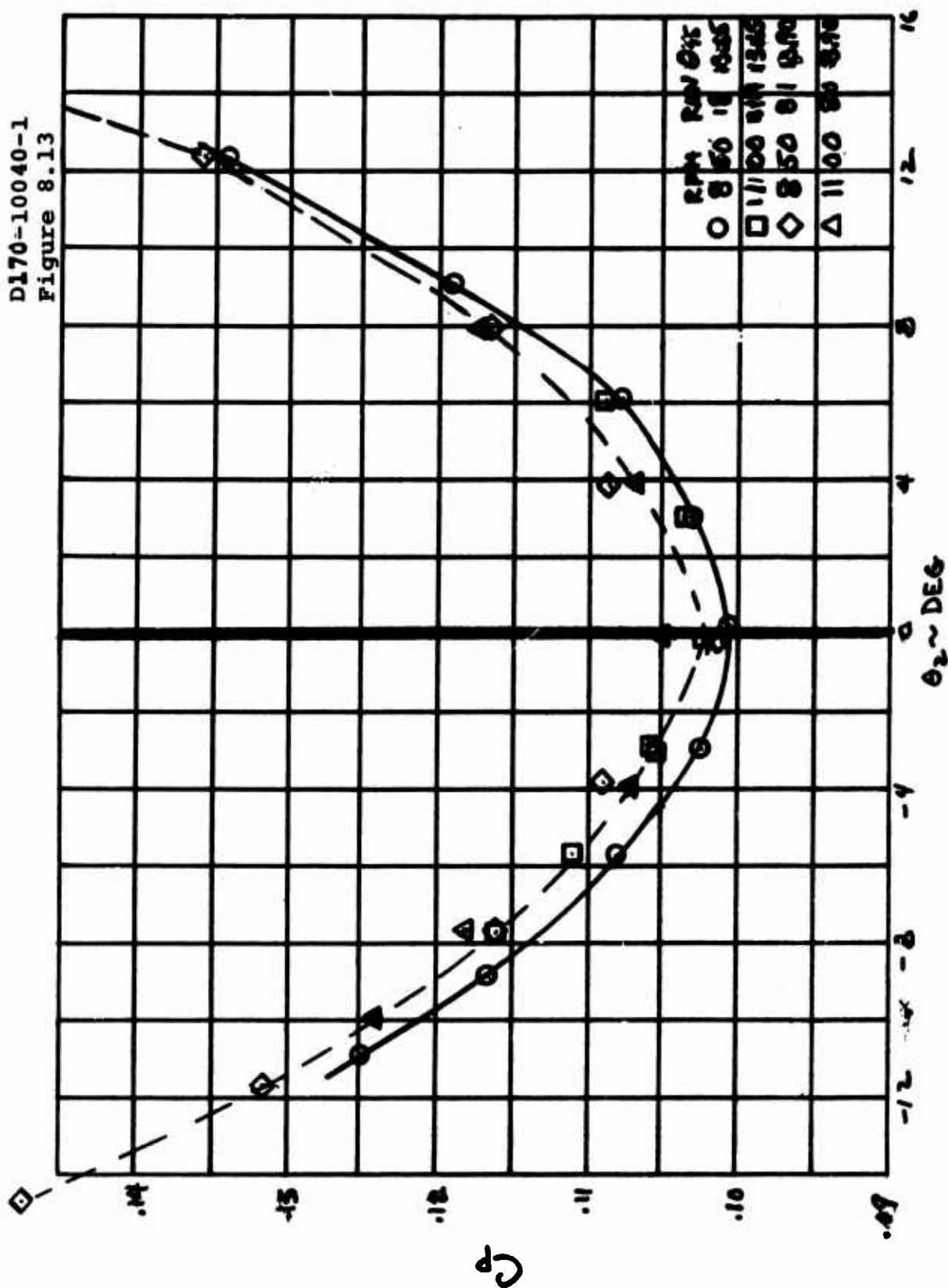


RUN RPM  $\theta_{75}$   $\delta$   
81 950 14 0

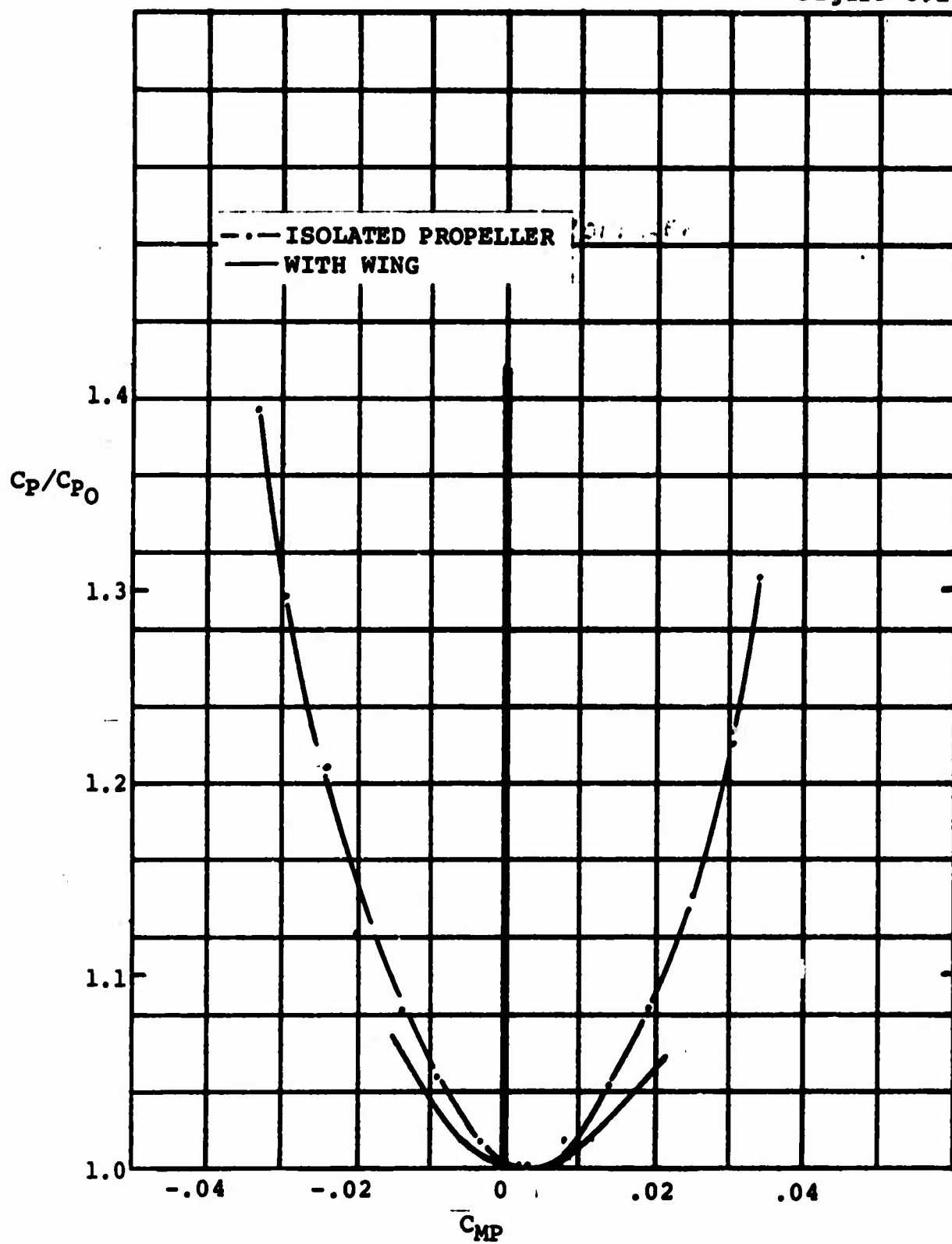
EFFECT OF CYCLIC ON THRUST IN HOVER

$\theta_{75} = 13.65^\circ$   $\Omega = 850$  RPM

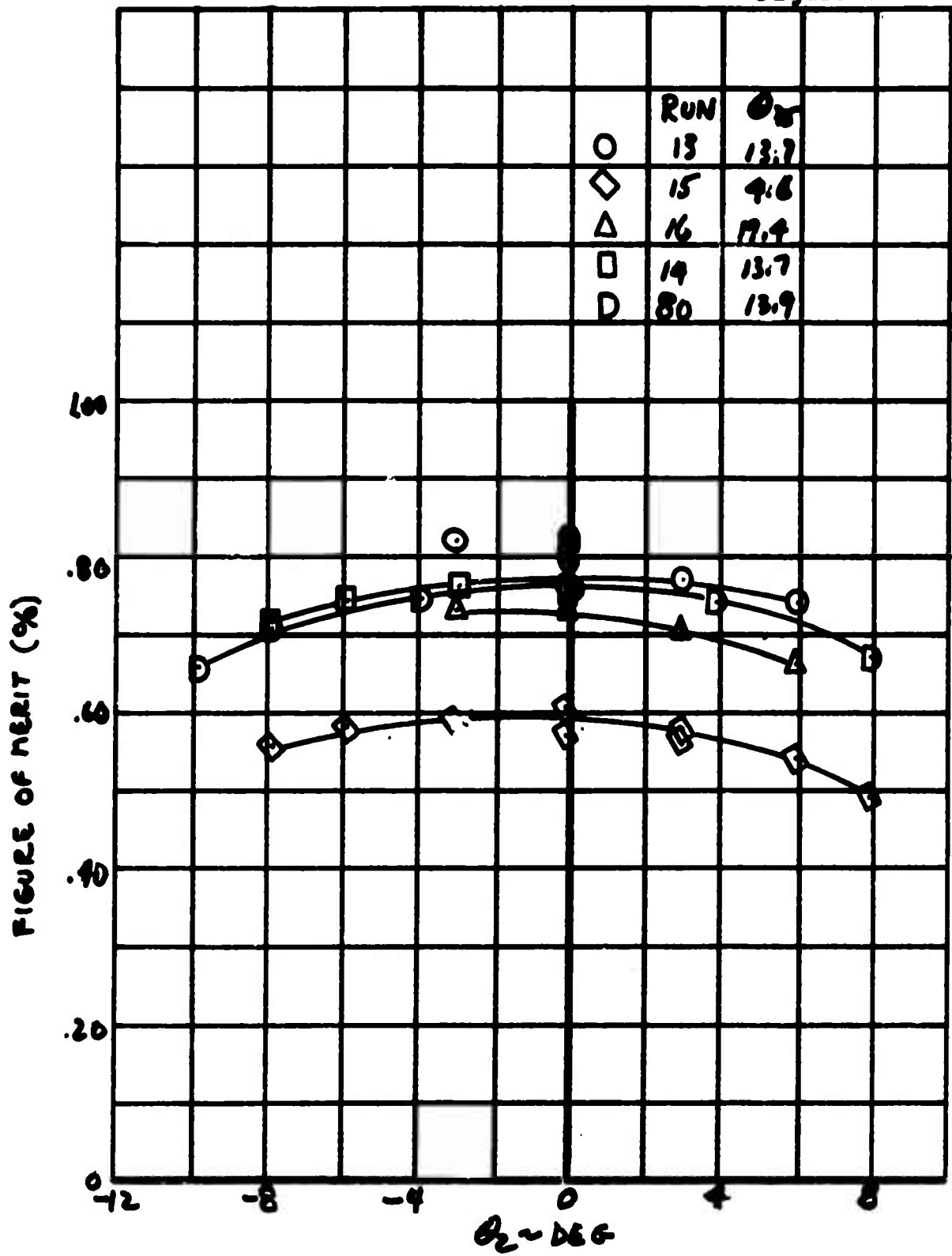
D170-10040-1  
Figure 8.13



POWER REQUIRED FOR CYCLIC PITCH CONTROL ISOLATED PROPELLER



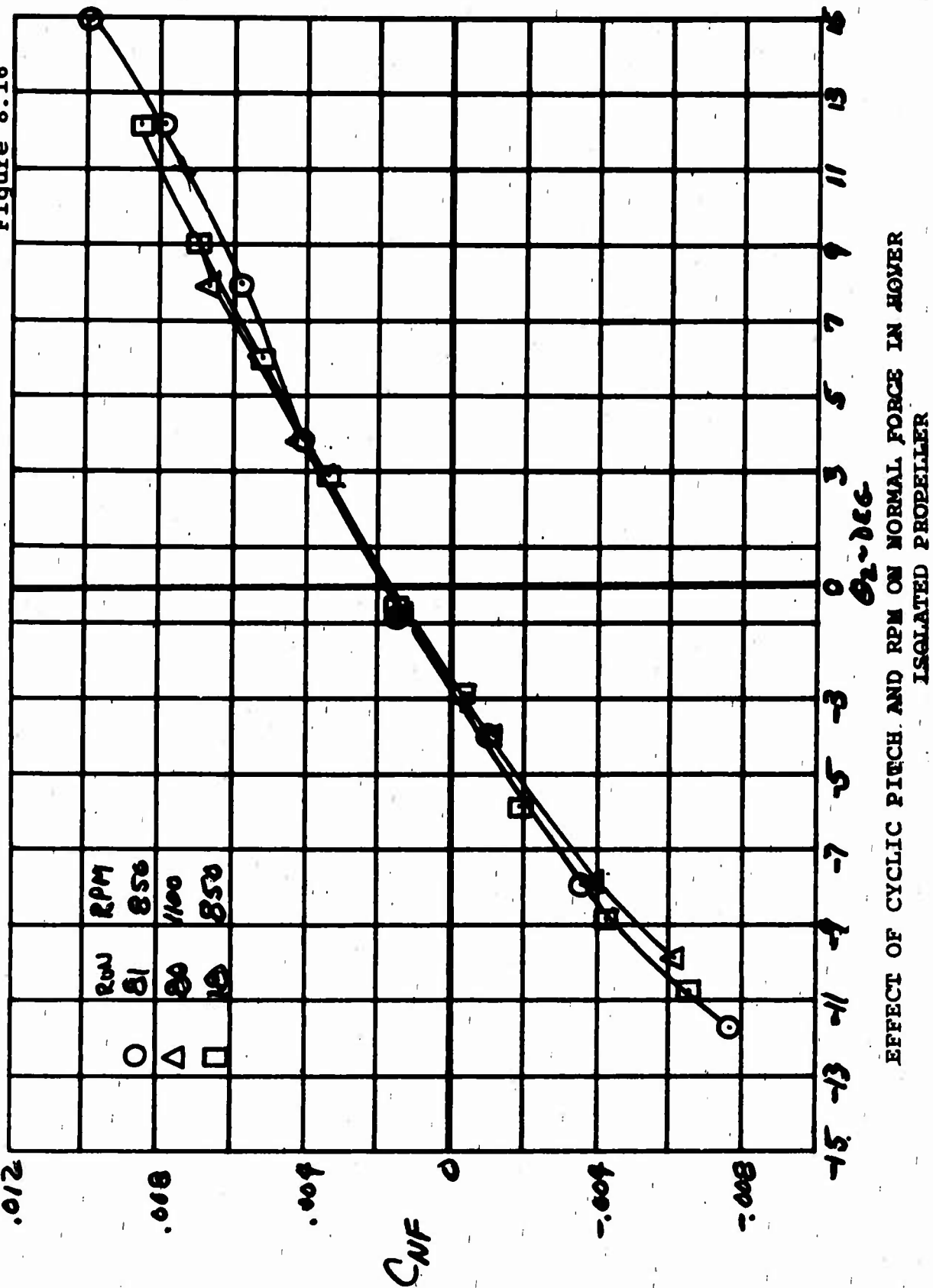
HOVER CONTROL POWER

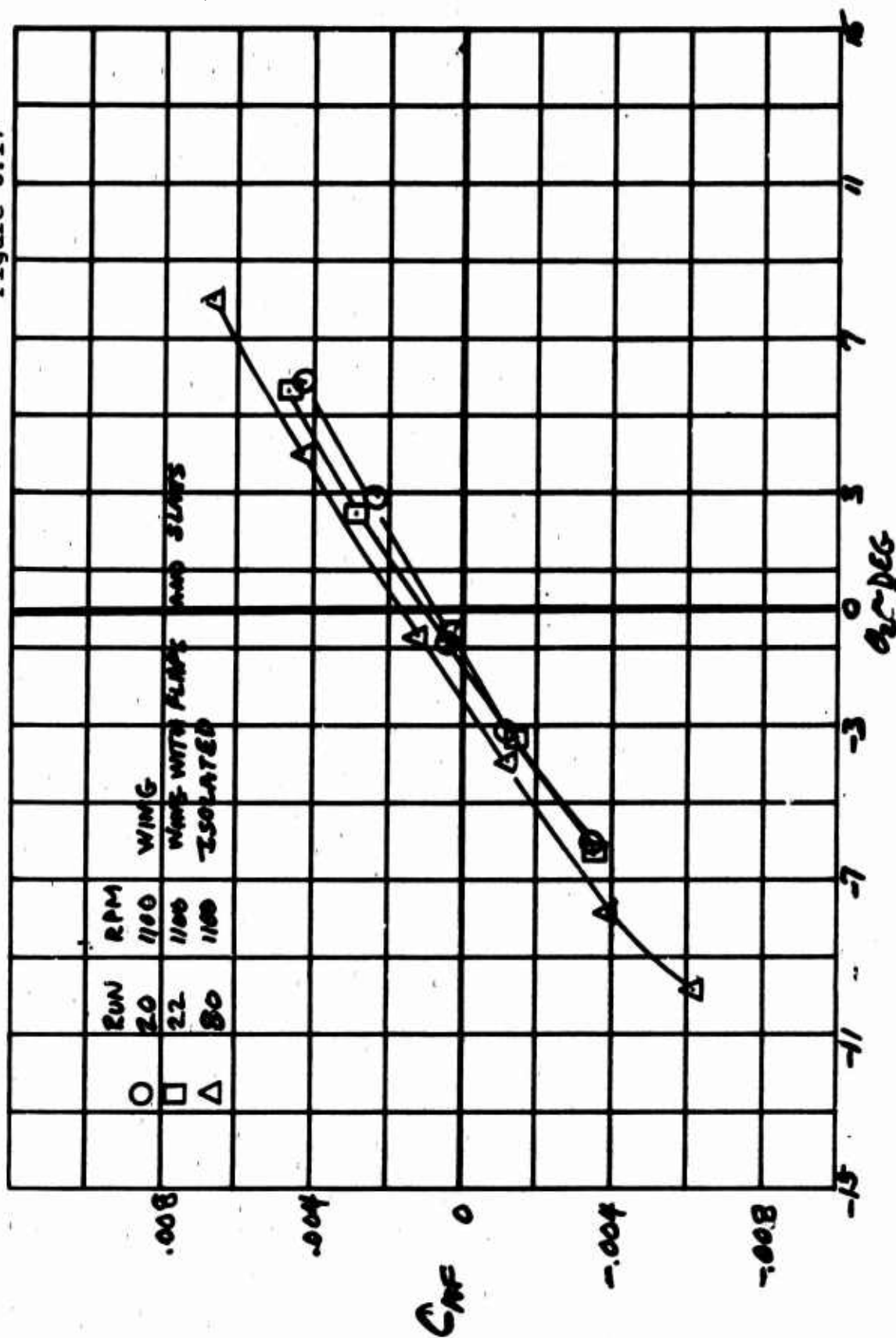


EFFECT OF CYCLIC PITCH ON F.M. IN HOVER - ISOLATED  
PROPELLER  $\Omega=1100 \text{ RPM}$

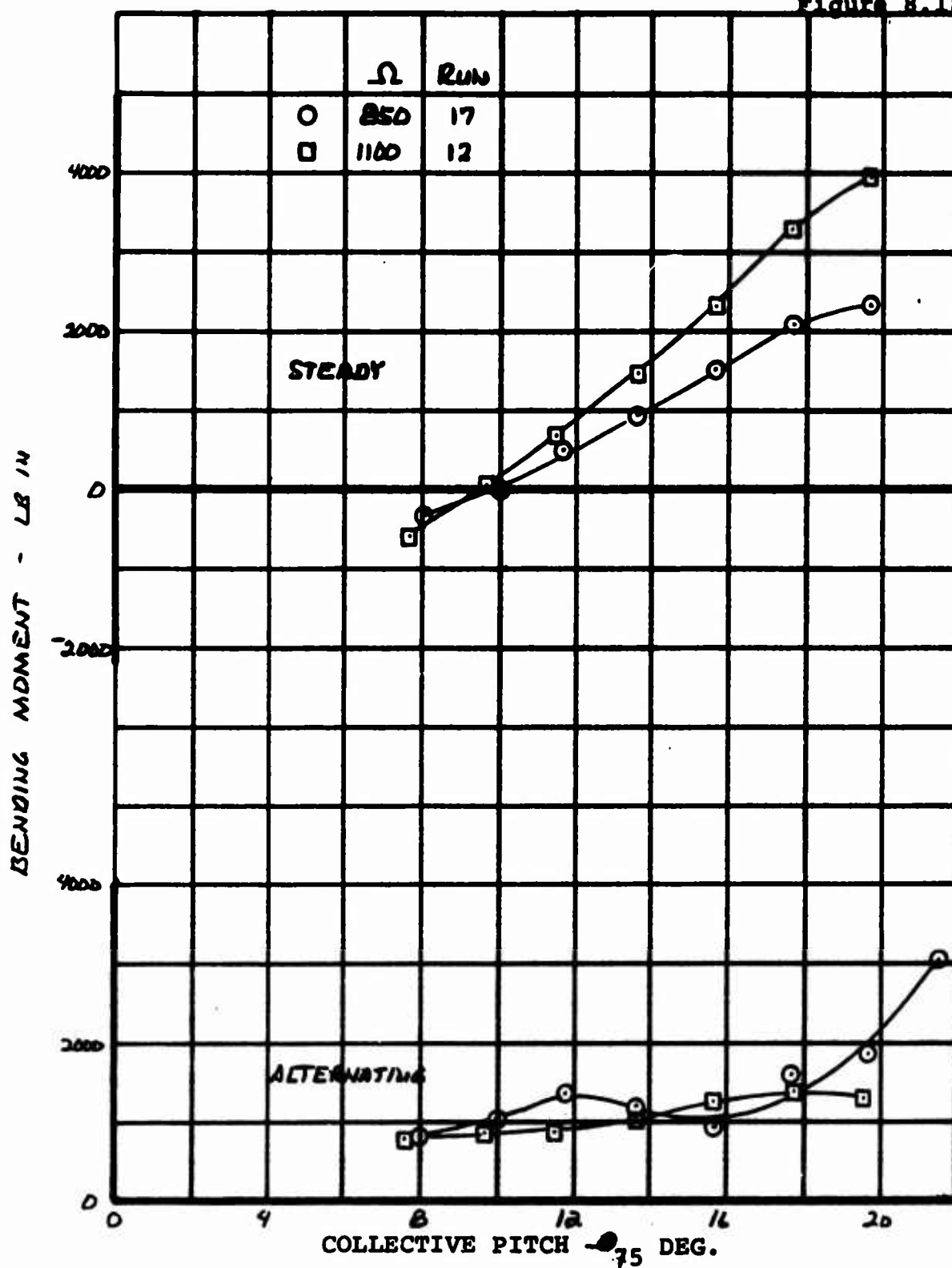


D170-10040-1  
Figure 8.16



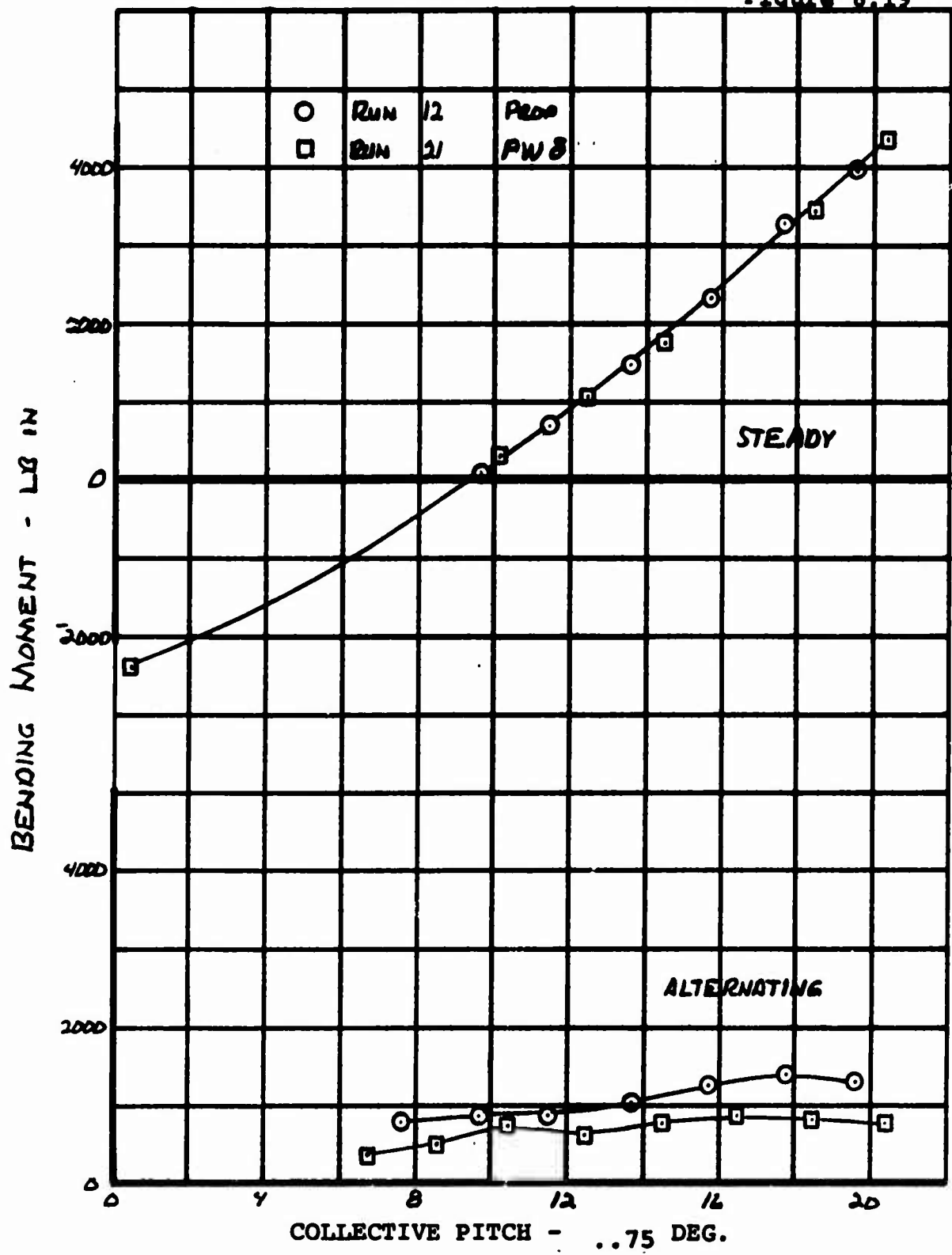


EFFECT OF CYCLIC PITCH AND WING ON NORMAL FORCE IN HOVER

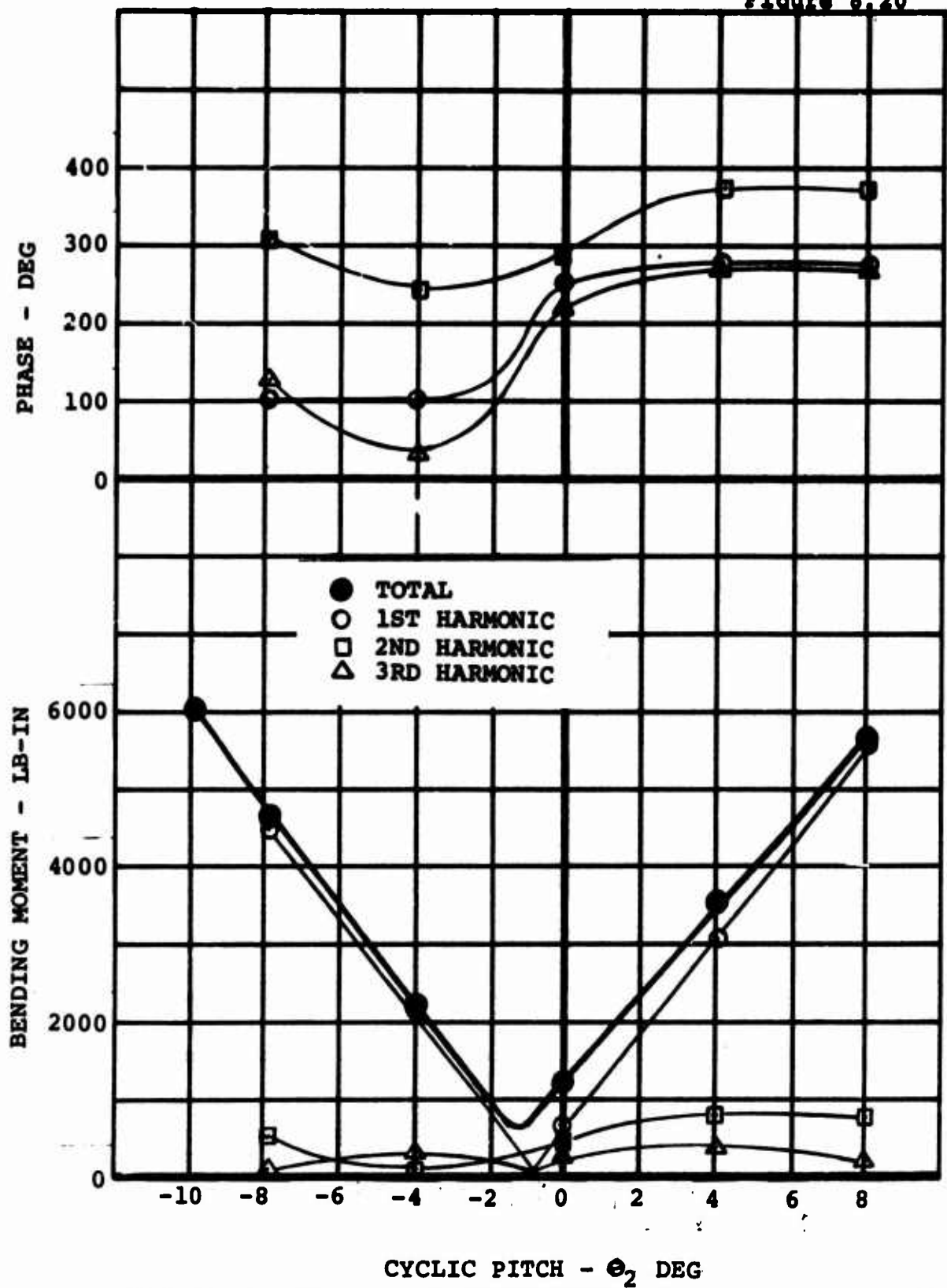


EFFECT OF ROTOR SPEED ON FLAP BENDING LOAD @ .22R PROP

$\Theta_2 = 0^\circ$

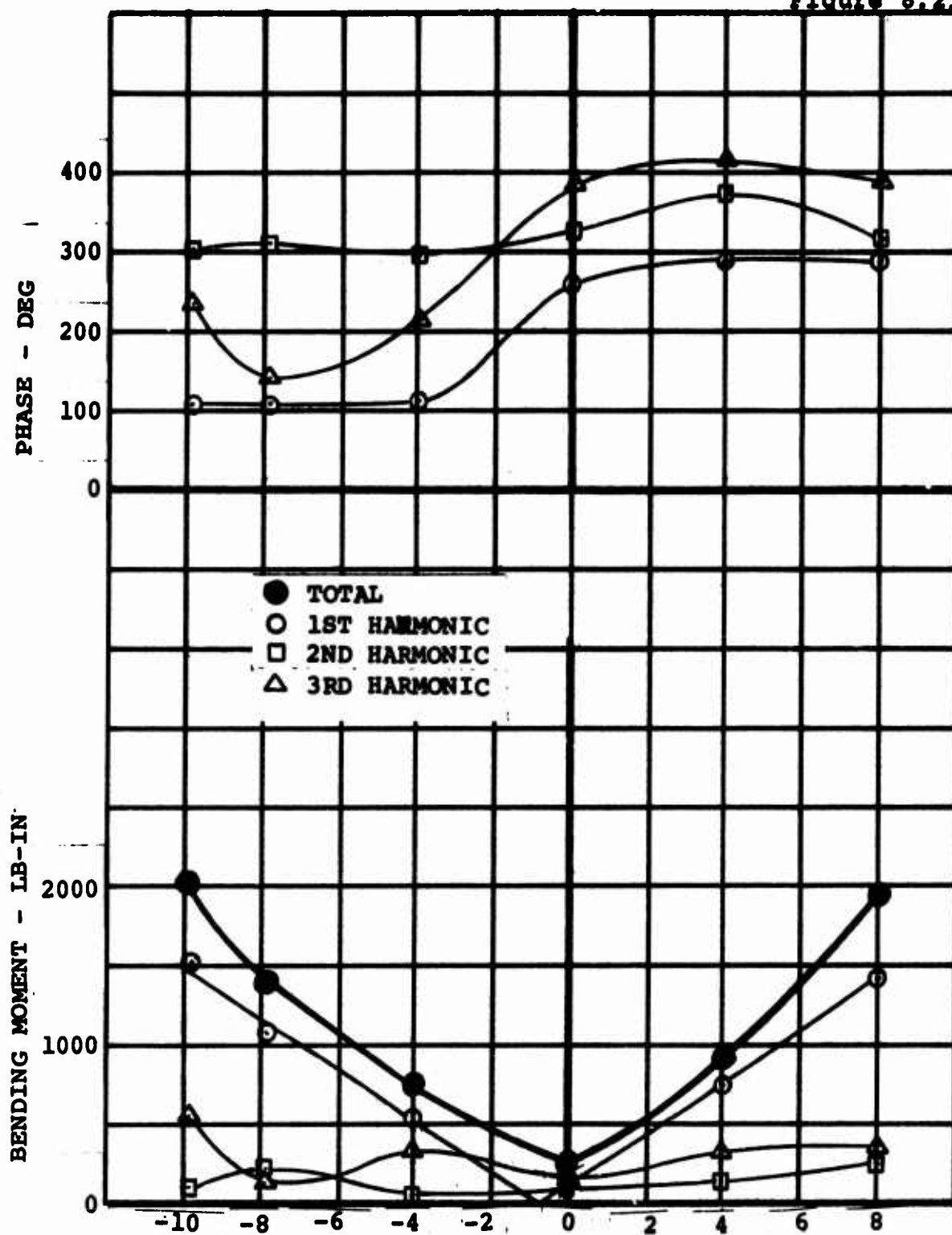


EFFECT OF WING ON FLAP BENDING LOAD @.22R  
 $\Omega = 1100, \Theta_2 = 0^\circ$

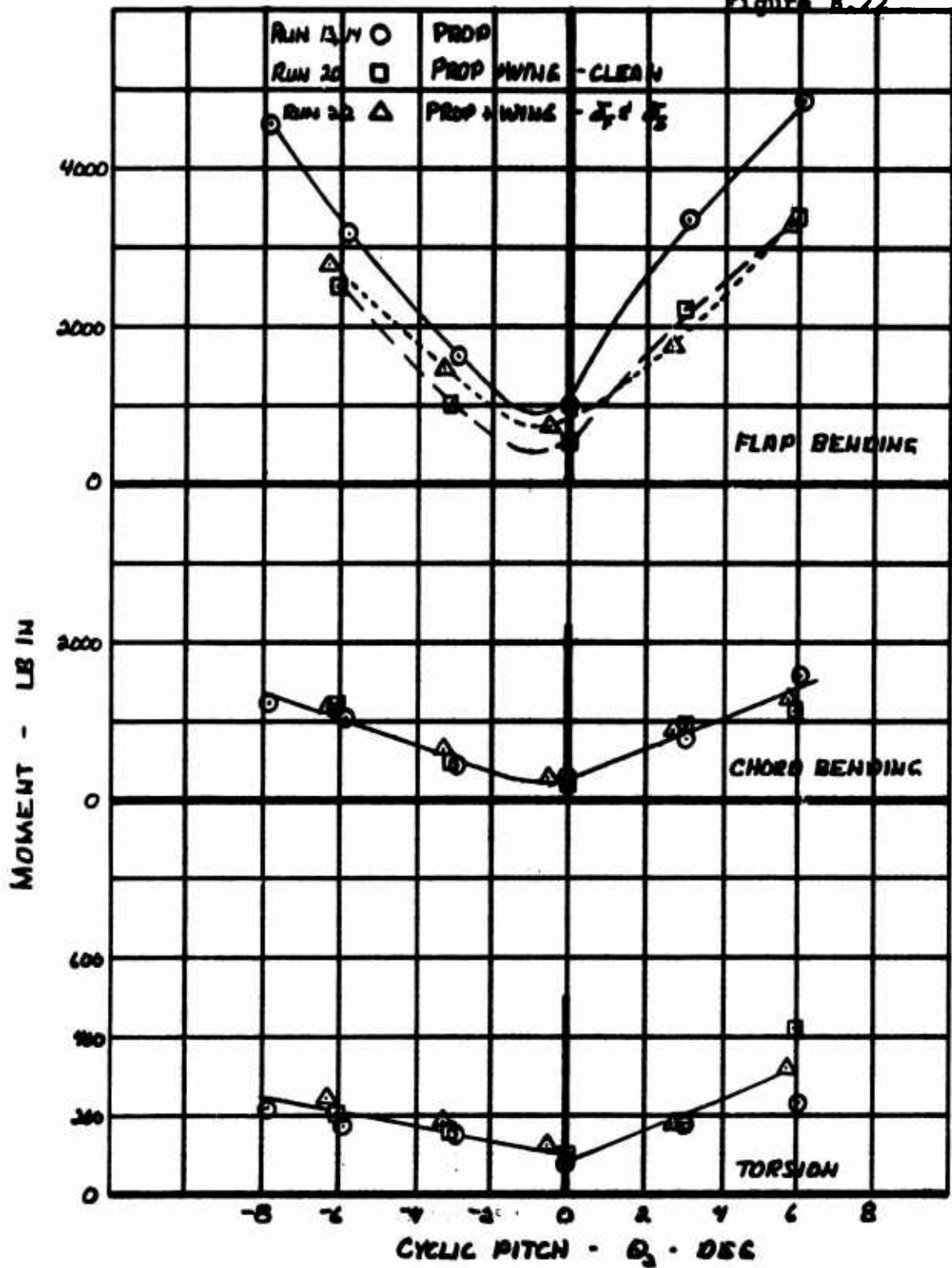


HOVER ALTERNATING FLAP BENDING LOAD DUE TO CYCLIC - .22R  
 $\theta_{cr} = 14^\circ$        $\Omega = 1100$       RUN 80  
 PROP ONLY

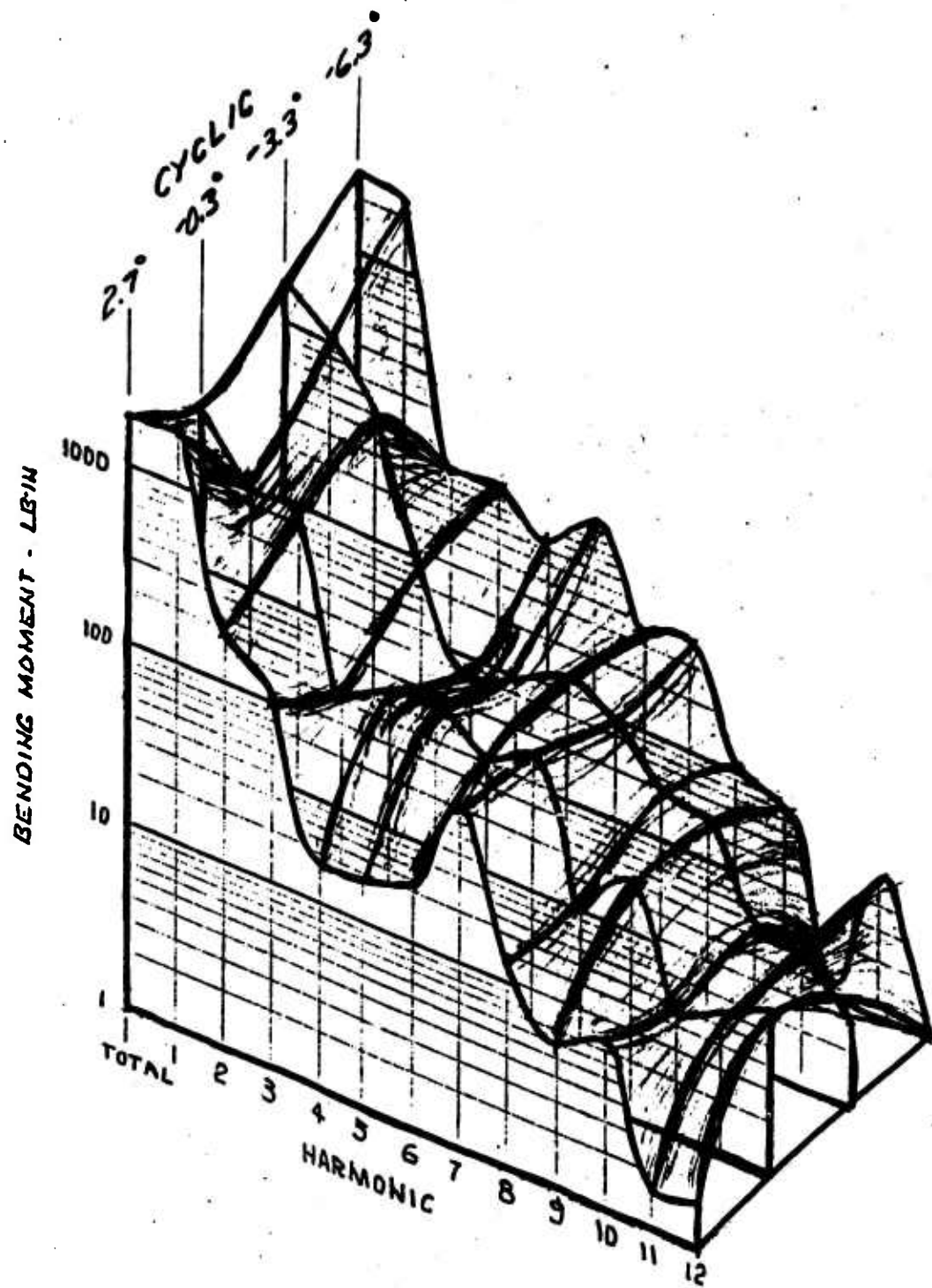
Figure 8.21



ALTERNATING CHORD BENDING LOAD DUE TO CYCLIC  $-.22R$   
 $= 14^\circ$   $\Omega = 1100 \text{ RPM}$  RUN 80  
 PROP ONLY

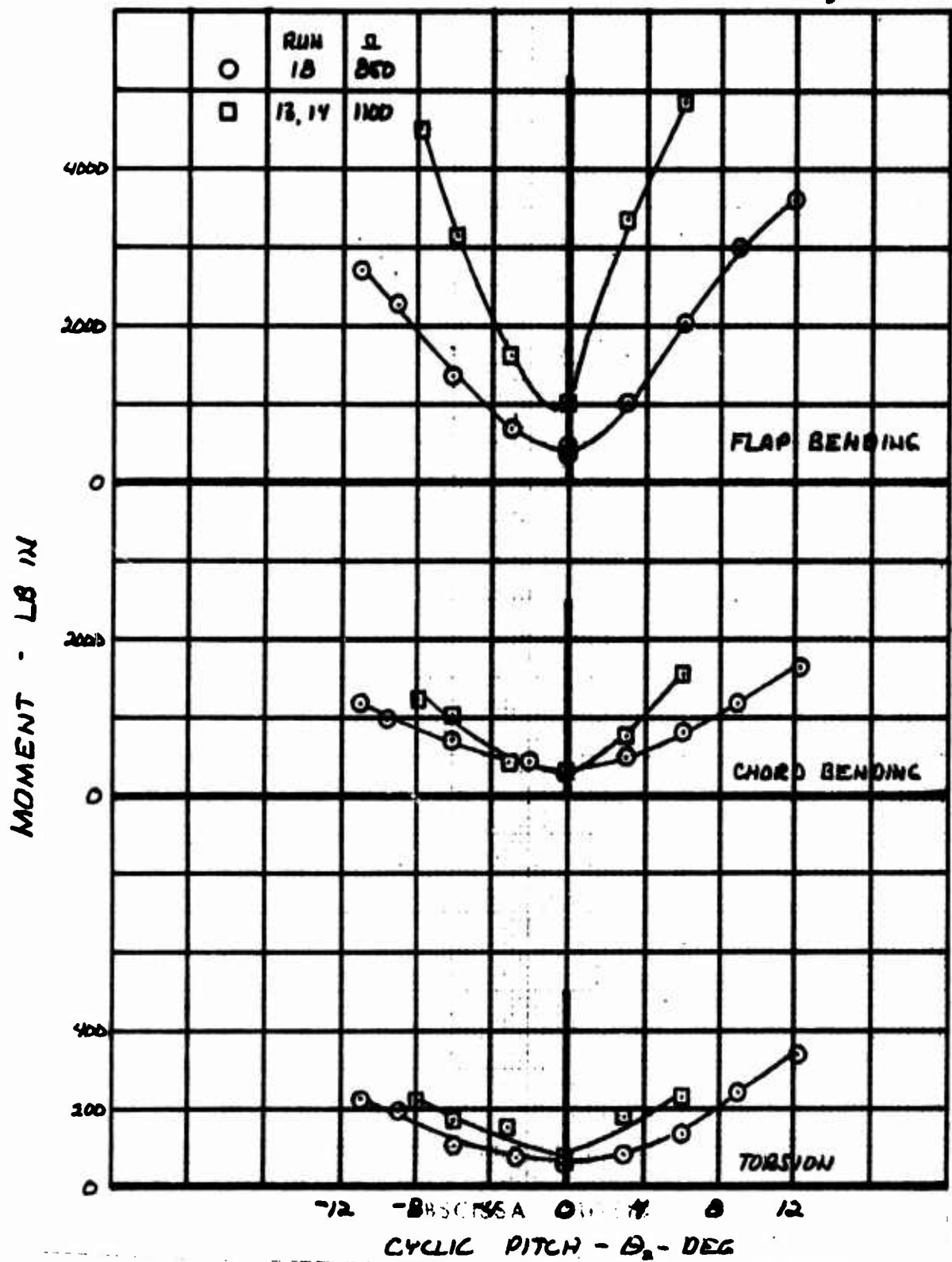


EFFECT OF CYCLIC PITCH ON BLADE ALTERNATING LOADS  
X/R 2.22.

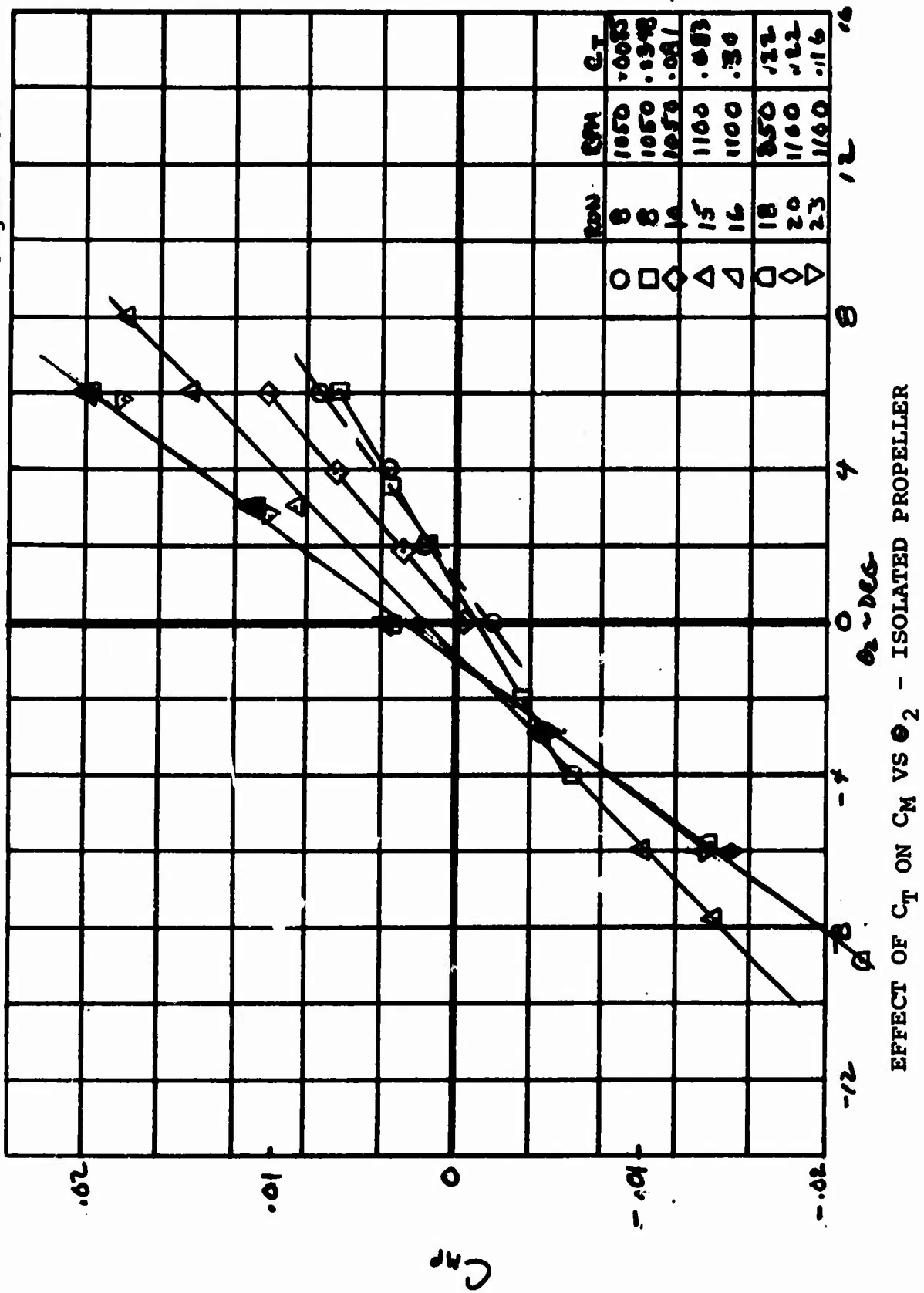


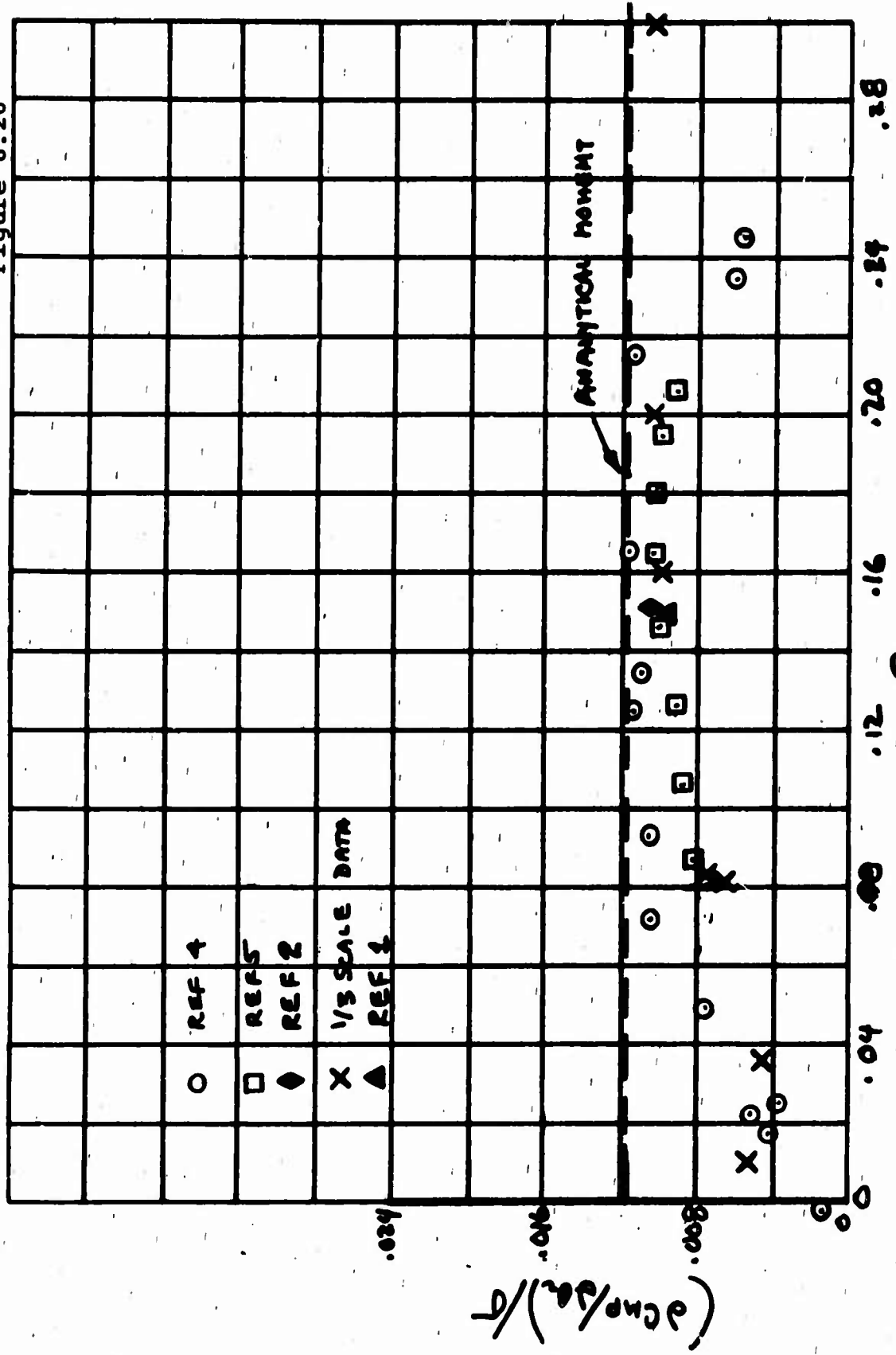
FLAP BENDING HARMONIC LOADS DUE TO CYCLIC  
AT .22R HOVER CONDITION  $\theta, 14^\circ$  RUN 22



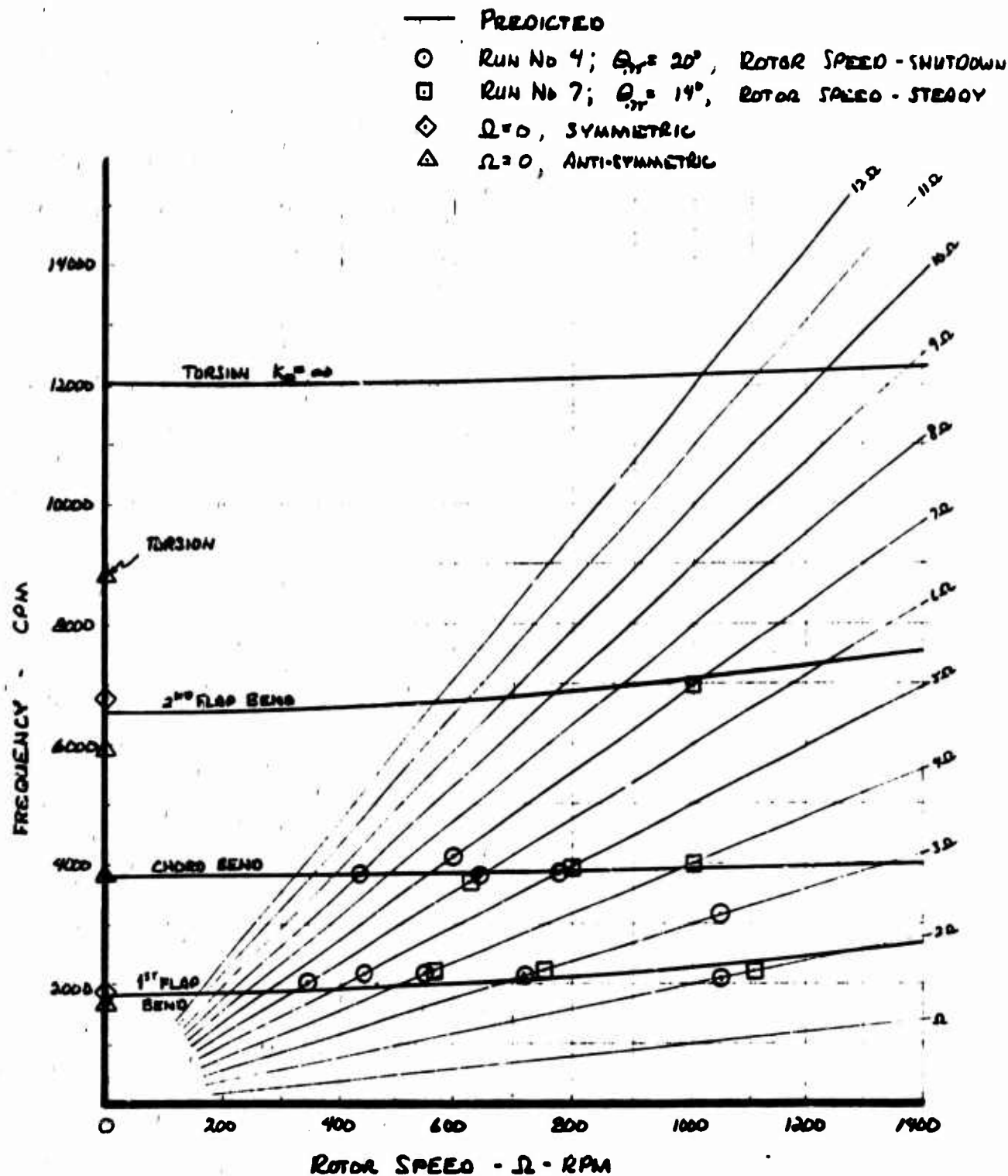


EFFECT OF ROTOR SPEED ON BLADE ALTERNATING  
LOADS IN HOVER  $\theta_{.75} = 14^\circ$ ,  $X/R = .22$





EFFECT OF  $C_T$  ON  $dC_m/dC_t$  WITH COMPARISON WITH OTHER TESTS



BLADE FREQUENCY SPECTRUM - CORRELATION OF TEST  
WITH ANALYSIS

## 8.9 TRANSITION

The presentation of the transition data is divided into three sections. The first section presents data for a nominal schedule for a medium transport (80,000 lbs. gross weight) undergoing an unaccelerated transition with no applied control moments. The configuration tested was the propeller and wing with flaps and slats. The tunnel had an open throat for these tests. The second section presents data for the variation of shaft angle at constant  $J$  for  $\Theta_{75} = 14^\circ$  and  $\Theta_2 = 0$  for both the isolated propeller and for the propeller and wing with flaps and slats. The third section presents the effects of  $\Theta_2$  on the data of the second section.

## 8.10 NOMINAL TRANSITION

The nominal schedule of  $\Theta_{75}$ ,  $J$ ,  $C_T$  and  $C_P$  as a function of shaft angle for model hover RPM of 1100 is presented in Figures 8.28 to 8.31. For these tests  $\alpha_s$  and  $J$  were set, then  $\Theta_{75}$  was adjusted to give the required  $C_T$ .  $C_P$  was the open variable.

In Figure 8.29 is shown  $C_T$  vs  $\alpha_s$ . The conditions for data point a  $\alpha_s = 15^\circ$  were misread from the analytical schedule. This error was not uncovered until after the test program was complete. The data at  $\alpha_s = 15^\circ$ , while not representative of the transition, is correct as presented.

In Figure 8.30  $C_P$  vs  $\alpha_s$  is presented. The predicted  $C_P$  is shown as the dashed line. It can be seen that although the measured  $C_P$  for the transition is generally less than the predicted  $C_P$ , the trends are similar.

The alternating loadings experienced by the blades during this transition are shown in Figures 8.31 to 8.35. The total loading and the first three harmonics are shown as a function of  $J$ . In Figure 8.31 the flap bending moment peaks at  $\alpha_s = 67$  degrees.  $\alpha_s = 67^\circ$  may not represent a true maximum since the vicinity on either side was not explored. The moments for  $\alpha_s = 90^\circ$  are less than  $\alpha_s = 67$  by a factor of 4.

As  $J$  increases and  $\alpha_s$  decreased approaching the end of transition, the flap moments decrease by a factor of 2. Having reached  $15^\circ$ ,  $J$  increases as the aircraft increases speed in

horizontal flight. The blade flap bending moments increase with increasing  $J$ . The phasing of the blade first harmonic flap moments over most of the transition is approximately  $290^\circ$  which produces a positive hub pitching moment. Thus, the  $\alpha_s$  moments would be in adding and subtracting from the control pitching moments.

The higher harmonics do not contribute significantly to the blade loads during the low  $J$  portion of the transition (See Figures 8.32 to 8.35). Only the magnitude of flap bending appears to be affected by the increase in  $J$ . The second harmonic makes an appreciable contribution to flapping moment for  $J$  greater than 0.5. The first 12 harmonics for the flapping bending, chord bending and blade torsion for the transition are shown in Figures 8.36 to 8.38.

### 8.11 THE EFFECT OF SHAFT ANGLE

Data for test runs 27 through 33 for the isolated propeller at constant collective at different shaft angles as a function of  $J$  is presented in Figure 8.39. In Figure 8.39 are shown  $C_T$  and  $C_p$ .  $C_T$  approximately varies linearly with  $\alpha_s$ . For the lower shaft angles  $C_T$  decreases as  $J$  increases due to the reduction in the local angle of attack.  $C_p$  is seen to decrease with  $J$  for the same reason.

In Figure 8.40 are shown the  $C_{YM}$ ,  $C_{MP}$ , and  $C_{NF}$  as a function of shaft angle for constant values of  $J$ . The data are seen to be approximately linear with  $\alpha_s$  for the range of  $\alpha_s$  and  $J$  tested for constant  $J$  with an intercept close to the origin.

### 8.12 EFFECT OF $\Theta_2$

For the isolated propeller in Runs 34 through 38 the effect of  $\Theta_2$  on the  $C_{PM}$ ,  $C_{YM}$ , and  $C_{NF}$  is shown in Figures 8.41 to 8.45 for a range of  $\alpha_s$  for constant  $J$ . The data exhibit a linear relationship between the coefficients and  $\Theta_2$ . In these tests the range of  $\Theta_2$  was limited by the design allowances for the blades. The  $\Theta_2$  to trim the pitching moment for a given  $J$  is seen to be a function of  $\alpha_s$ , becoming increasingly negative as  $J$  is increased and as  $\alpha_s$  goes from  $30^\circ$  to  $90^\circ$ . The sensitivity of the coefficients is essentially independent of  $\alpha_s$ .

### 8.13 EFFECT OF CYCLIC ON BLADE LOADS

The effect of  $\Theta_2$  on the blade loads is shown in Figure 8.46 for the case of  $\alpha_g = 60^\circ$ ,  $J = .32$  and  $\Theta_{75} = 13.83^\circ$ . The shift in the location of the minimum of the first and second harmonics from  $\Theta_2 = 0$  is in agreement with the shift observed for the hub loads. The magnitude of the first harmonic at  $\Theta_2 = 5^\circ$  reflects the effect of the cross flow. It was observed during the test that the waveform of the flap bending signal underwent a drastic change in frequency content as the cyclic angle was varied. This change is reflected by the variation in the relative amounts of the first and second harmonics as  $\Theta_2$  was varied from  $-9^\circ$  to  $0^\circ$ . As can be seen, for the large negative  $\Theta_2$ , the ratio of the first to second harmonic is on the order of 4:3, while for the low negative  $\Theta_2$  the ratio is closer to 3:1.

The phase of the harmonics relative to the 1/rev index is also shown in Figure 8.46. The phase of the first harmonic varies smoothly from  $+76^\circ$  at  $\Theta_2 = -9^\circ$  to  $-63^\circ$  at  $\Theta_2 = 0^\circ$  with the sign change corresponding to the projected minimum in magnitude at  $\Theta_2 = -5^\circ$ . The departure for a  $180^\circ$  phase shift is attributed to the vector addition of the residual moment to the moment due to  $\Theta_2$ . The second harmonic shows a strong phase shift occurring near the projected minimum in the magnitude. The residual second harmonic magnitude is seen to be small. The sharpness of the phase shift indicates that the second harmonic is strongly dependent on  $\Theta_2$ .

### 8.14 PROPELLER WITH WING

In Runs 40 to 44, the transition conditions for the isolated propeller were repeated for the propeller with wing. These data are shown in Figures 8.47 to 8.51.

Most significantly, comparisons of these data with the data for Runs 34 to 39 show essentially no major effect due to the presence of the wing. Examples of these comparisons are shown in Figures 8.52 to 8.54. In Figure 8.52 the effect of the wing is shown.  $C_{MP}/C_{CS}$  is slightly greater for the propeller with wing than for the isolated propeller and the slope of the curve is slightly greater. Projection of the two curves towards the

origin gives an intersection in the vicinity of  $J = 0$ . This result is basically different from the results of previous investigations, where a factor approaching 2.5 exists between the isolated propeller and the propeller with wing for any value of  $J$ .

In Figure 8.53 is shown a comparison of the  $\partial C_{MP} / \partial \theta_2$  as a function of  $J$ . As can be seen, the curves are almost coincident. These data indicate that wing effects are extremely small.

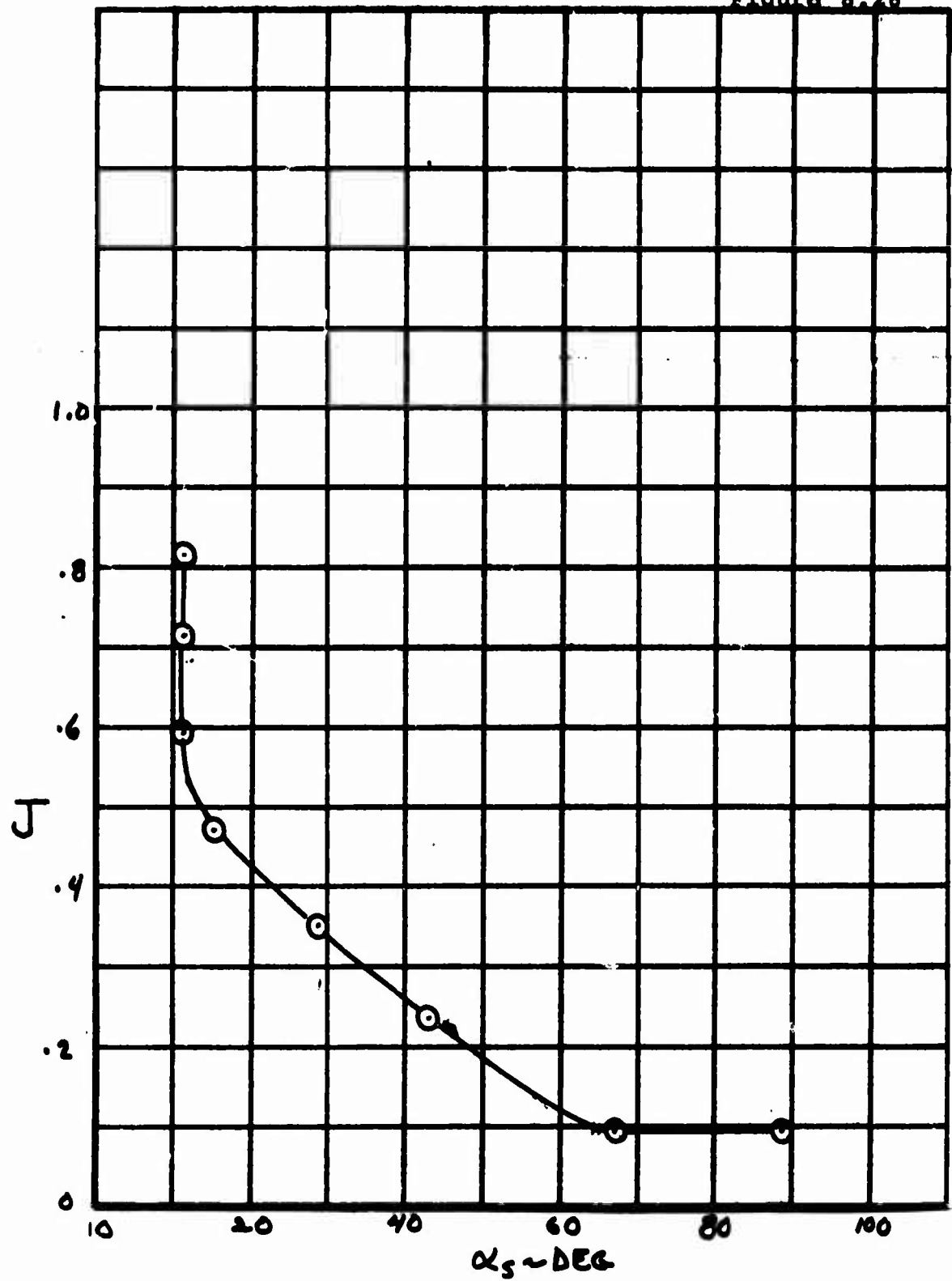
In Figure 8.54 is shown the variation of  $C_{MP}$  with  $\alpha_s$  for a range of  $J$  for both the isolated propeller and the propeller with wing. As can be seen, the effect of the wing is to increase the intercept with the vertical axis while causing only a slight change to the slope as compared to data for the isolated propeller.

#### 8.15 EFFECT OF $\theta_2$ ON CONTROL POWER

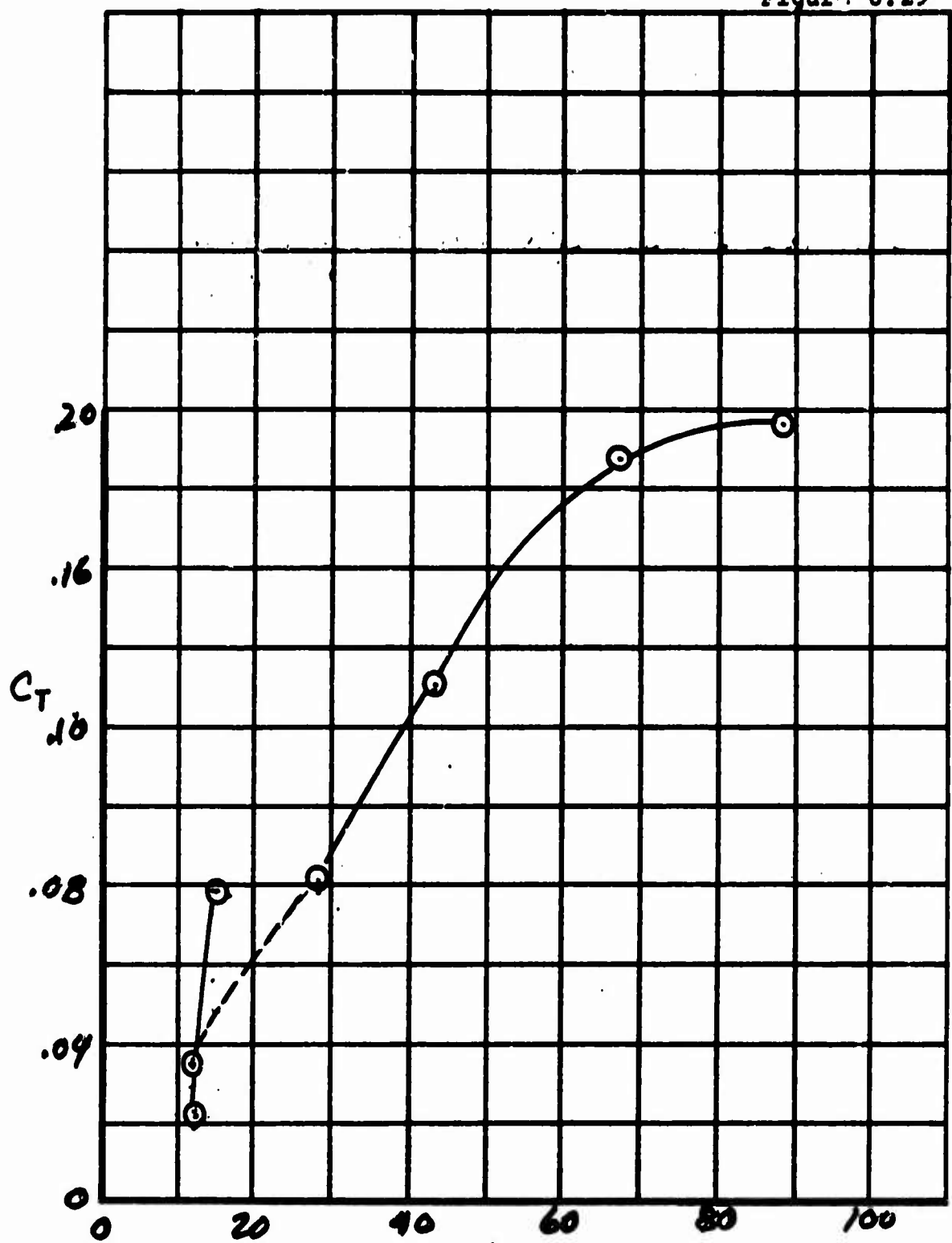
In Figure 8.55 is presented data for the effect of  $\theta_2$  on control power during transition for the case of isolated propeller and for the propeller with wing and flaps at  $\alpha_s = 60^\circ$ . The data appears as a family of curves. As  $J$  is increased, the locus of the minimum  $C_p$  is obtained by the application of negative  $\theta_2$ . The data for the positive  $\theta_2$  was restricted by the combined stress from the steady plus alternating loads. The minimum is shifted further to the negative  $\theta_2$  by the presence of the wing.

For a  $J$  of .2 the influence of the wing is to reduce the required  $C_p$  by approximately 1% for comparable  $C_T$ . As  $J$  is increased, this spread becomes less and tends to vanish. The increase in  $J$  at these shaft angles would cause an increase in the skewness of the propeller wake. As the skewness increased, the wing would exert less effect on the wake. In the extreme case the wake would miss the wing giving rise to a different flow geometry completely.

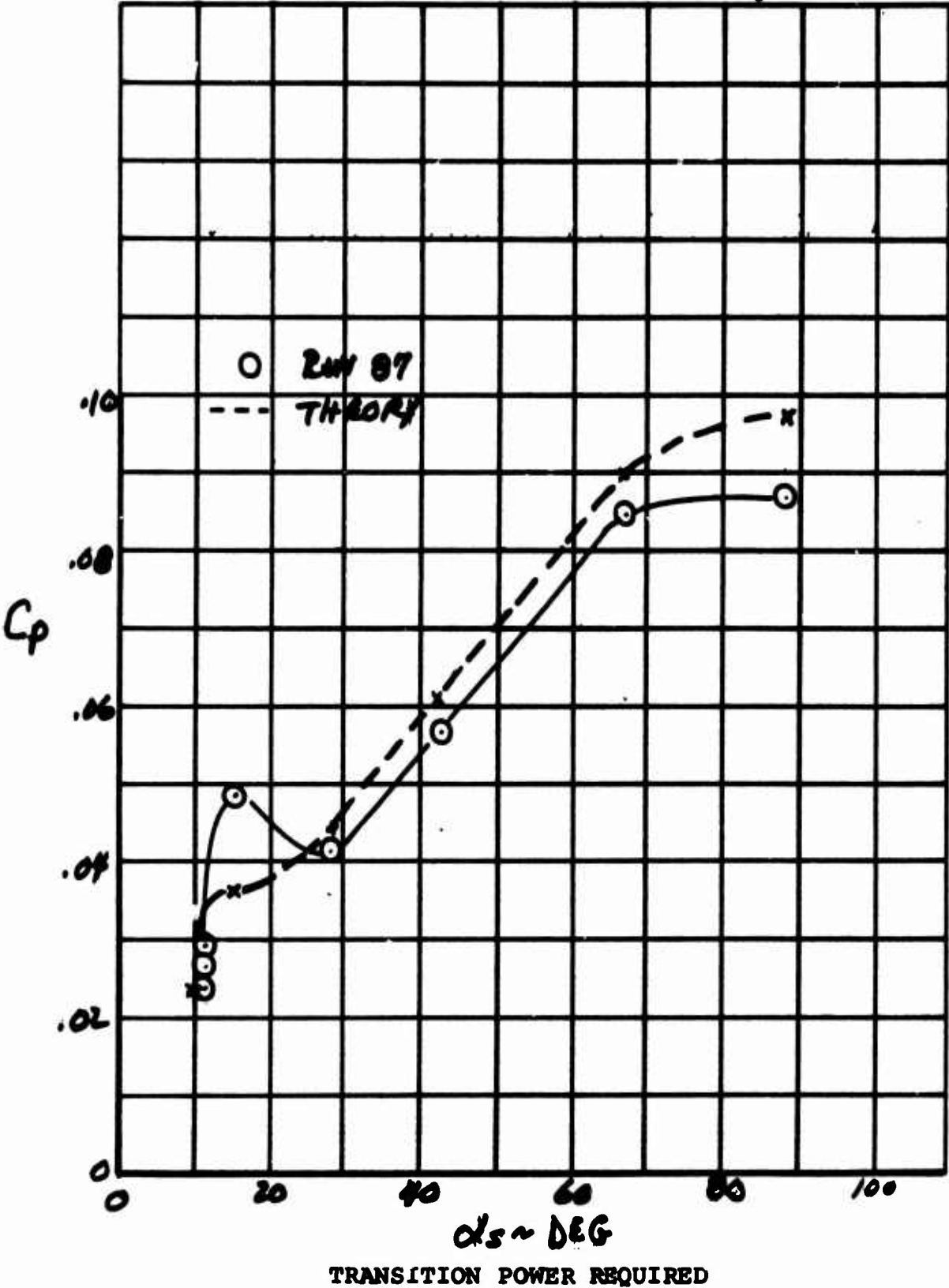


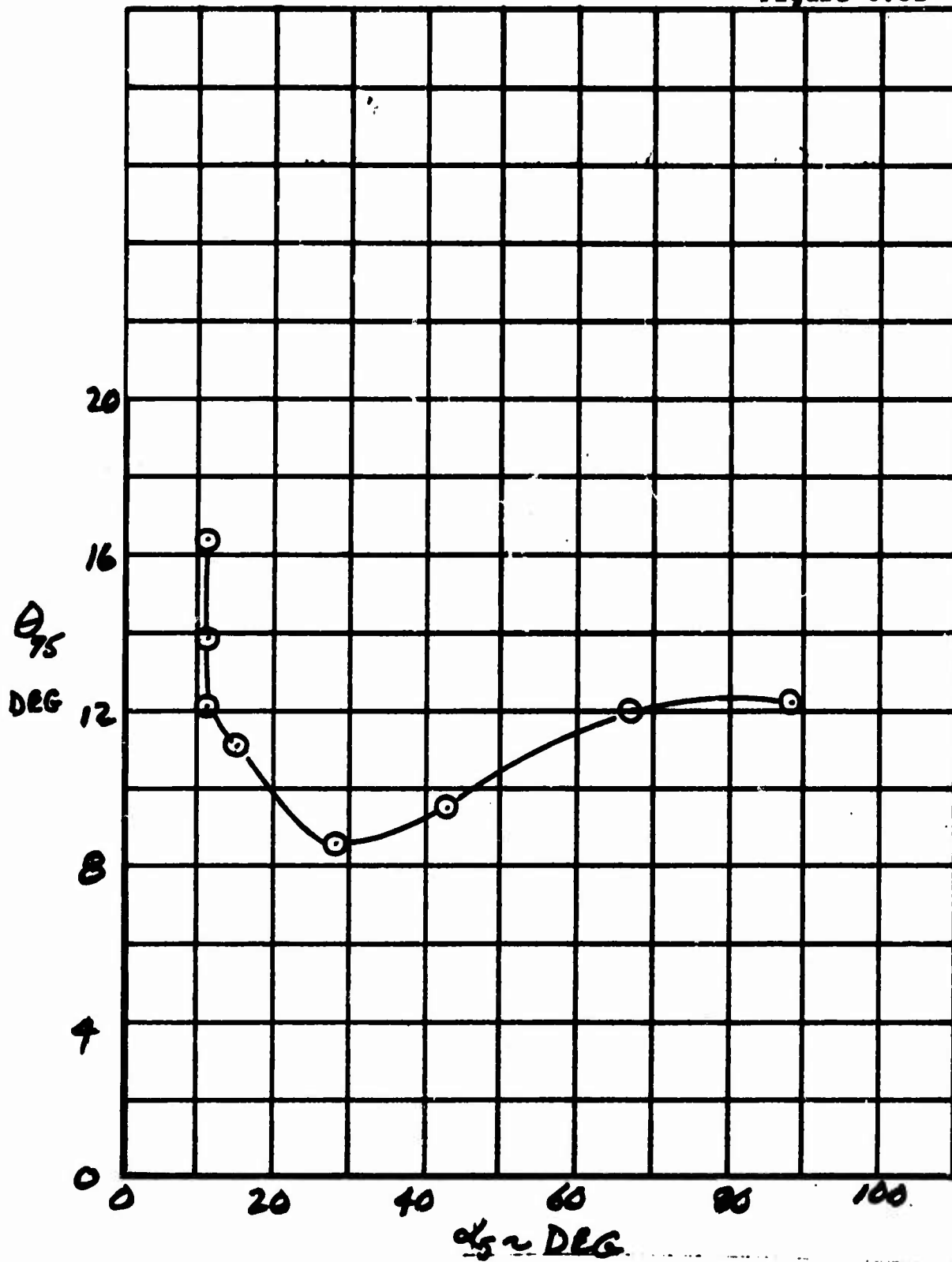


TRANSITION SCHEDULE - UNACCELERATED

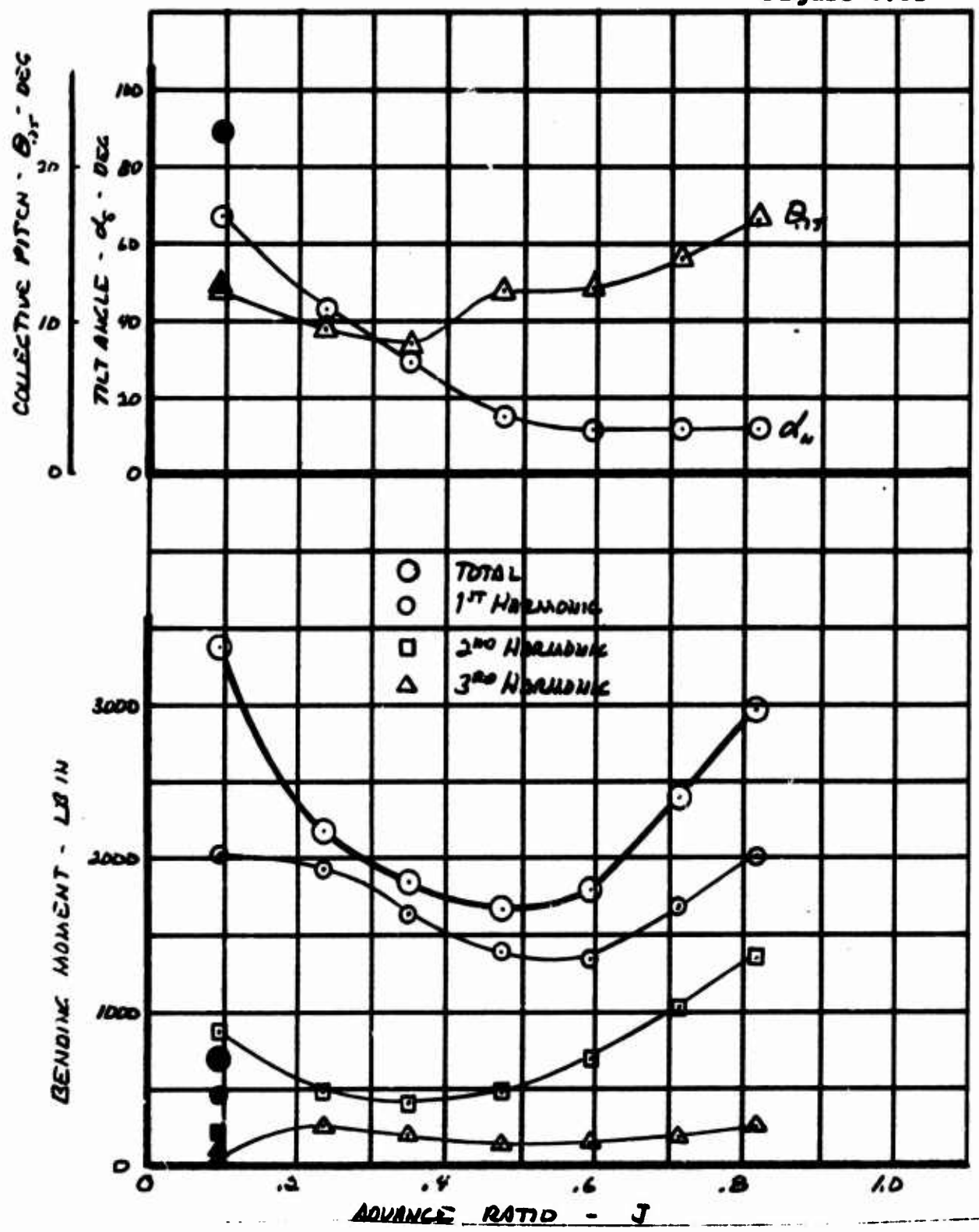


$\alpha_s \sim 22.6^\circ$   
TRANSITION SCHEDULE -  $C_T$  VS  $S$   
RUN 87 INSTALLED PROPELLER, FLAPS AND SLATS

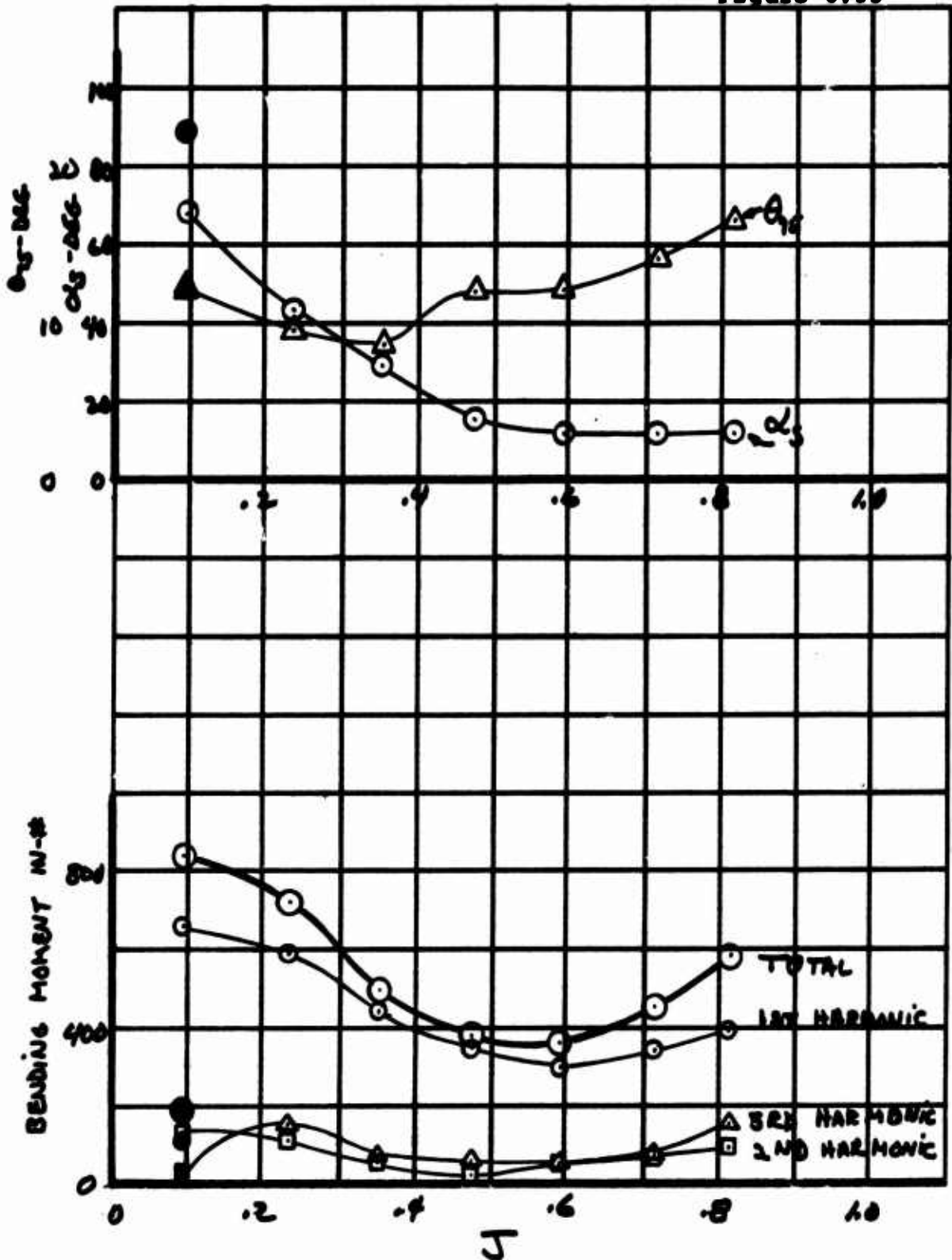




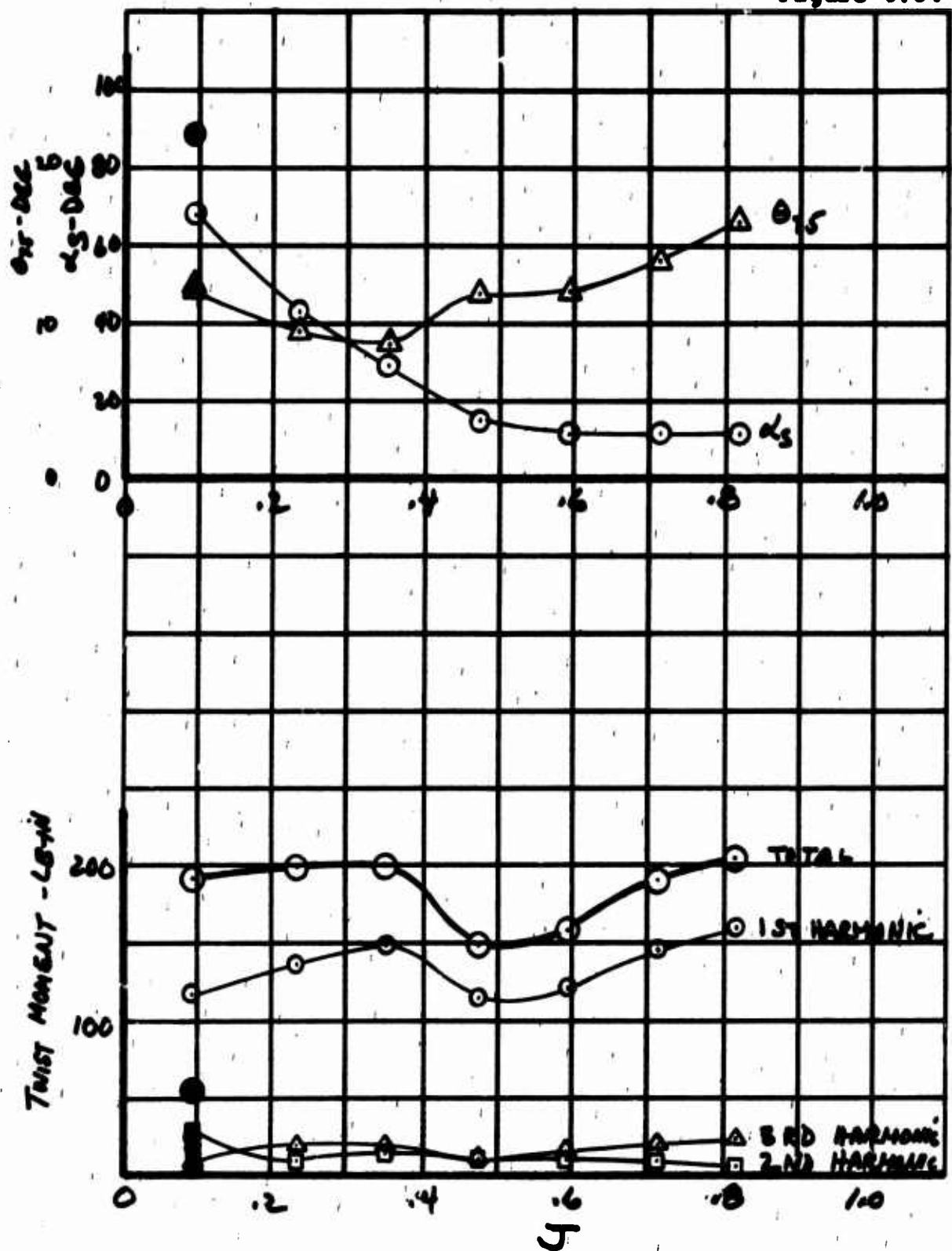
TRANSITION - COLLECTIVE SCHEDULE



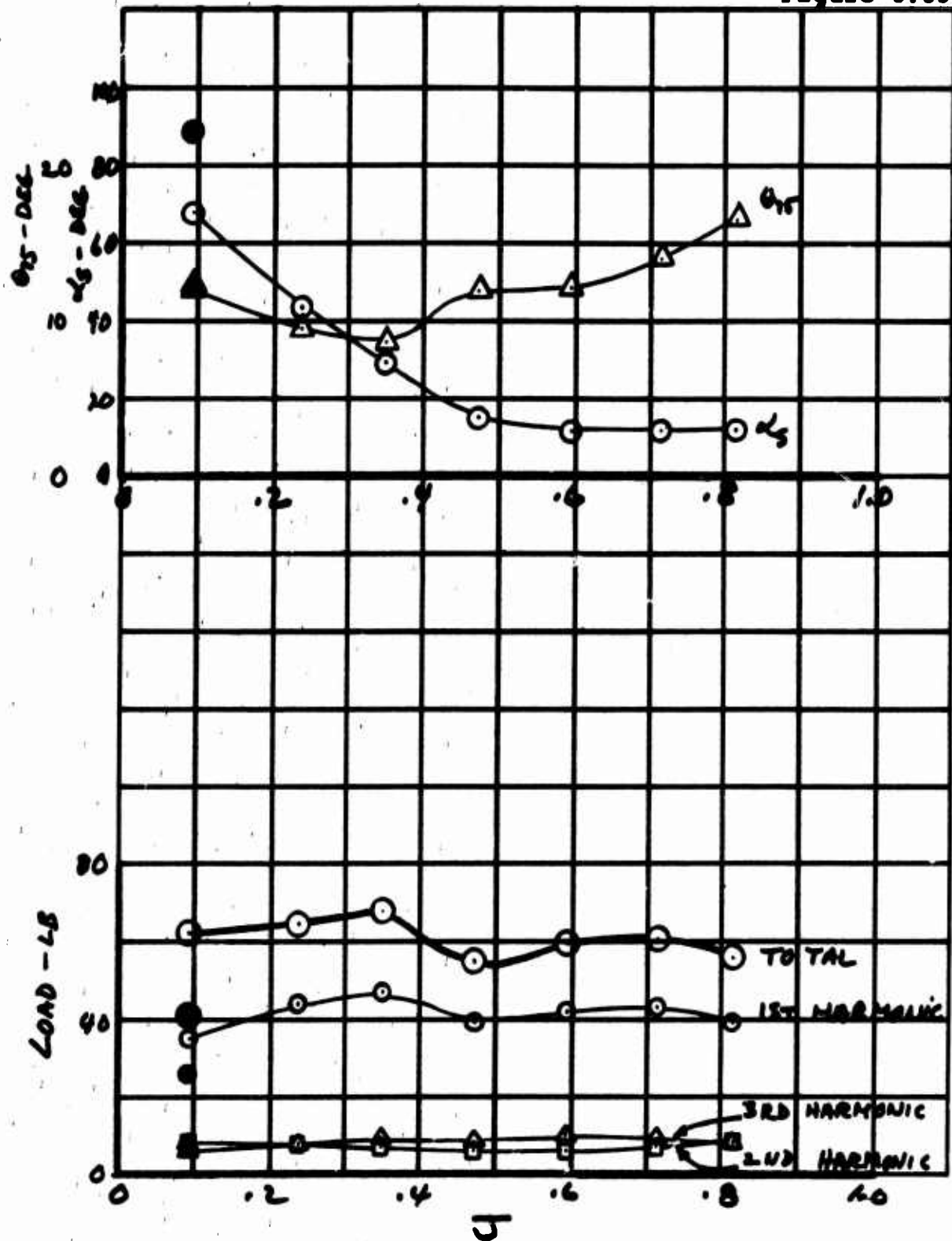
ALTERNATING FLAP BENDING LOAD THROUGH TILT TRANSITION  
X/R = .22 RUN 87



BLADE ALTERNATING CHORD BENDING LOAD THROUGH TILT  
TRANSITION - .22R, RUN 87

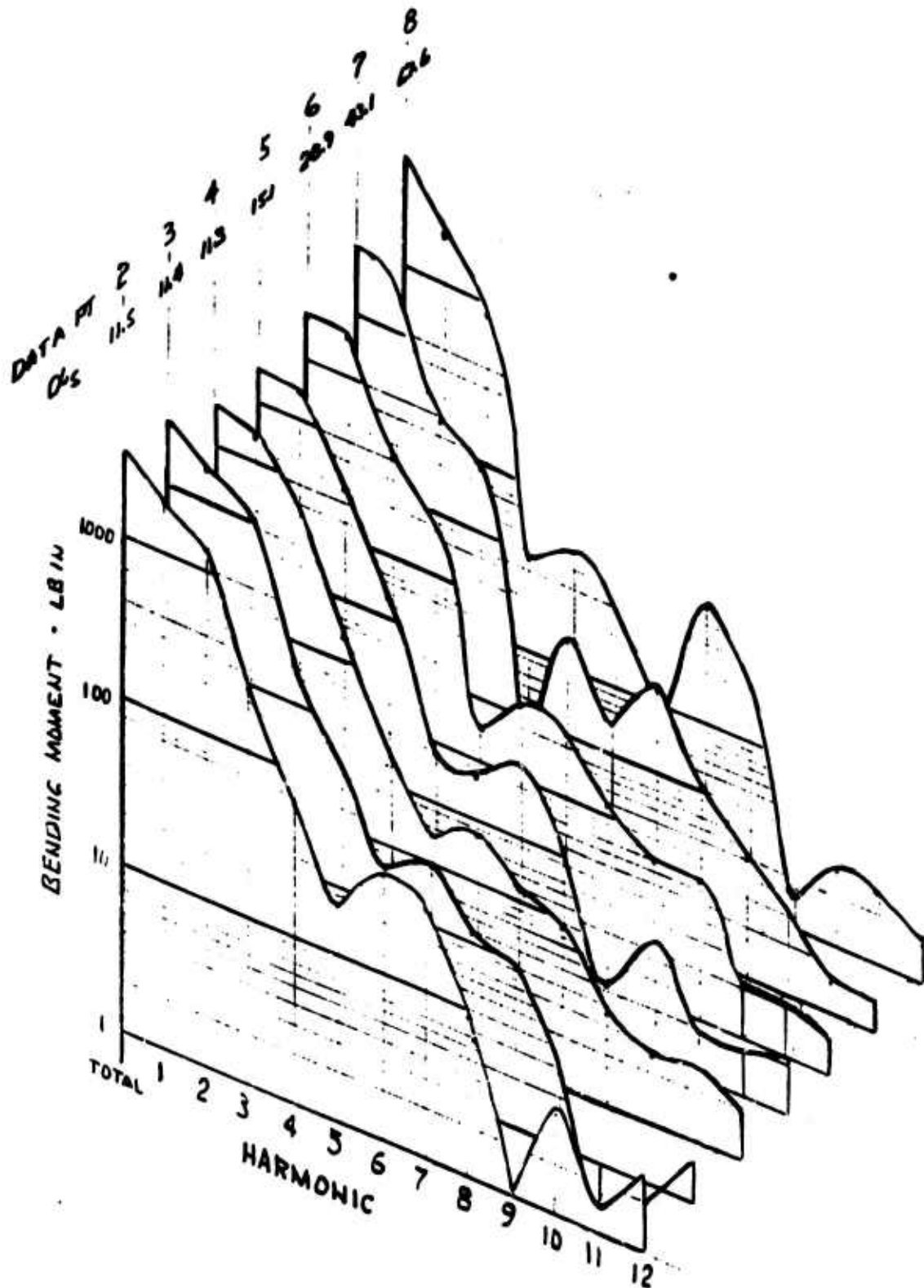


BLADE ALTERNATING TORSION LOAD THROUGH TILT TRANSITION -  
.22R, RUN 87

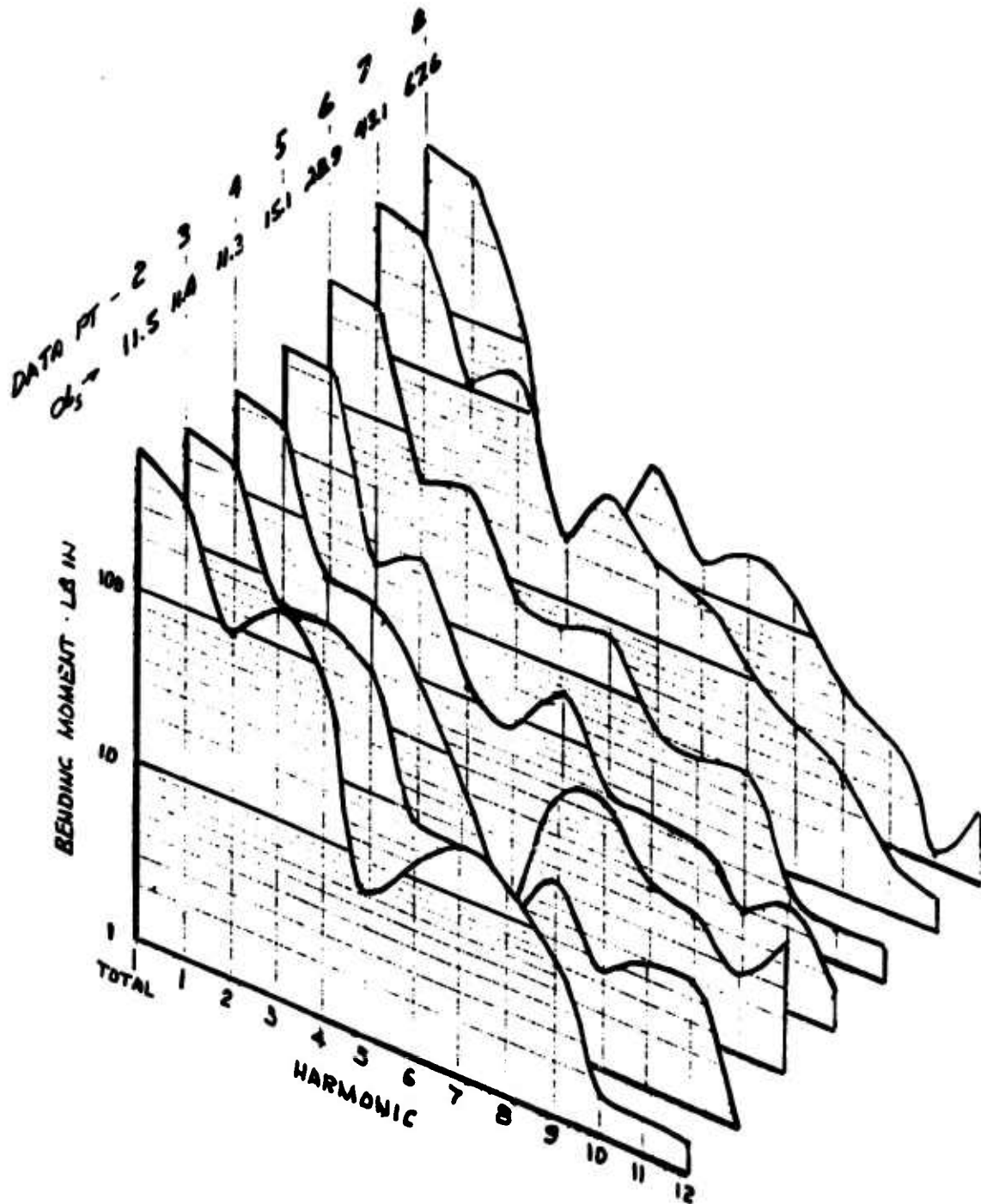


PITCH LINK ALTERNATING LOAD THROUGH TILT TRANSITION -  
.22R, RUN 87

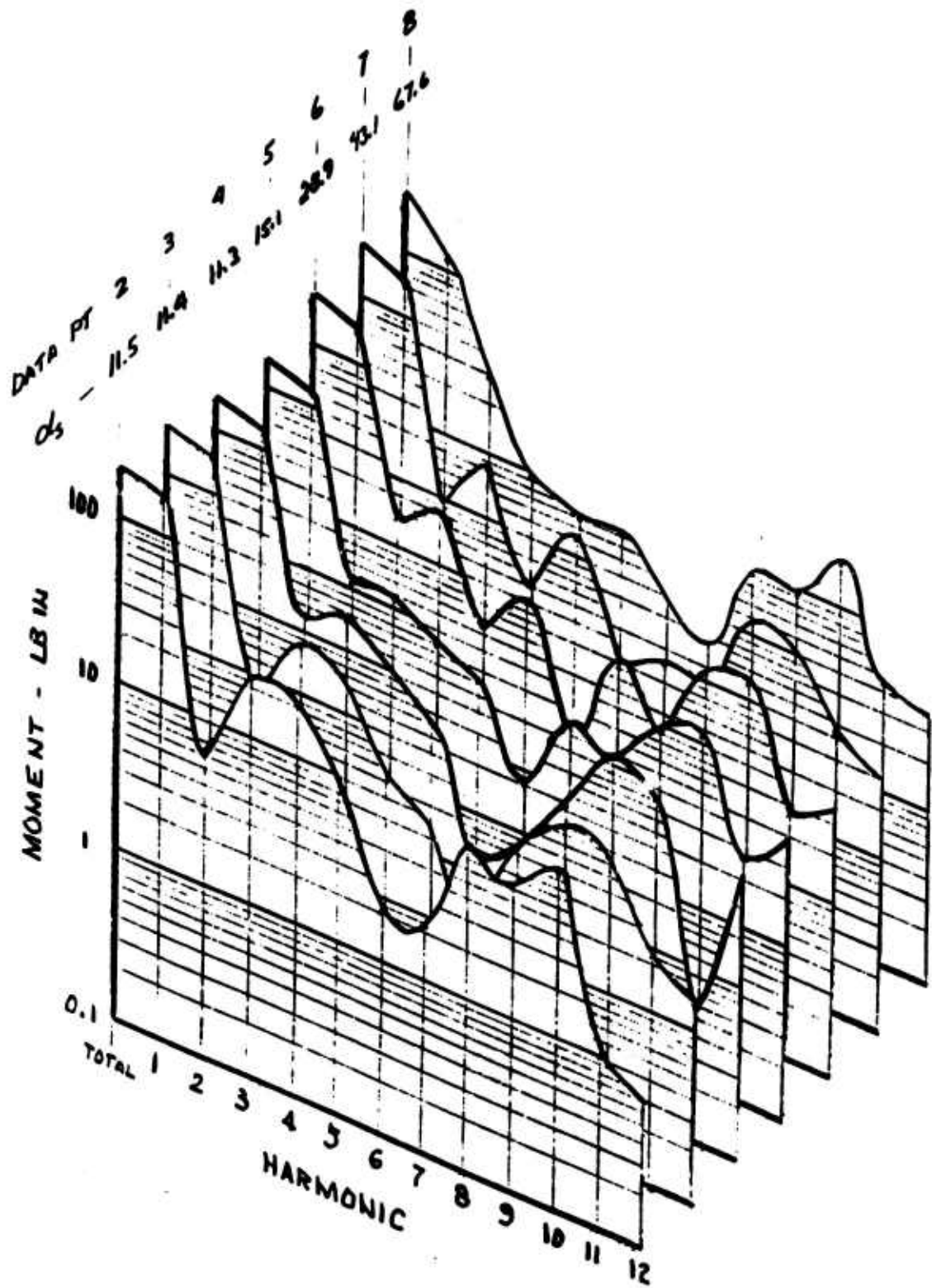




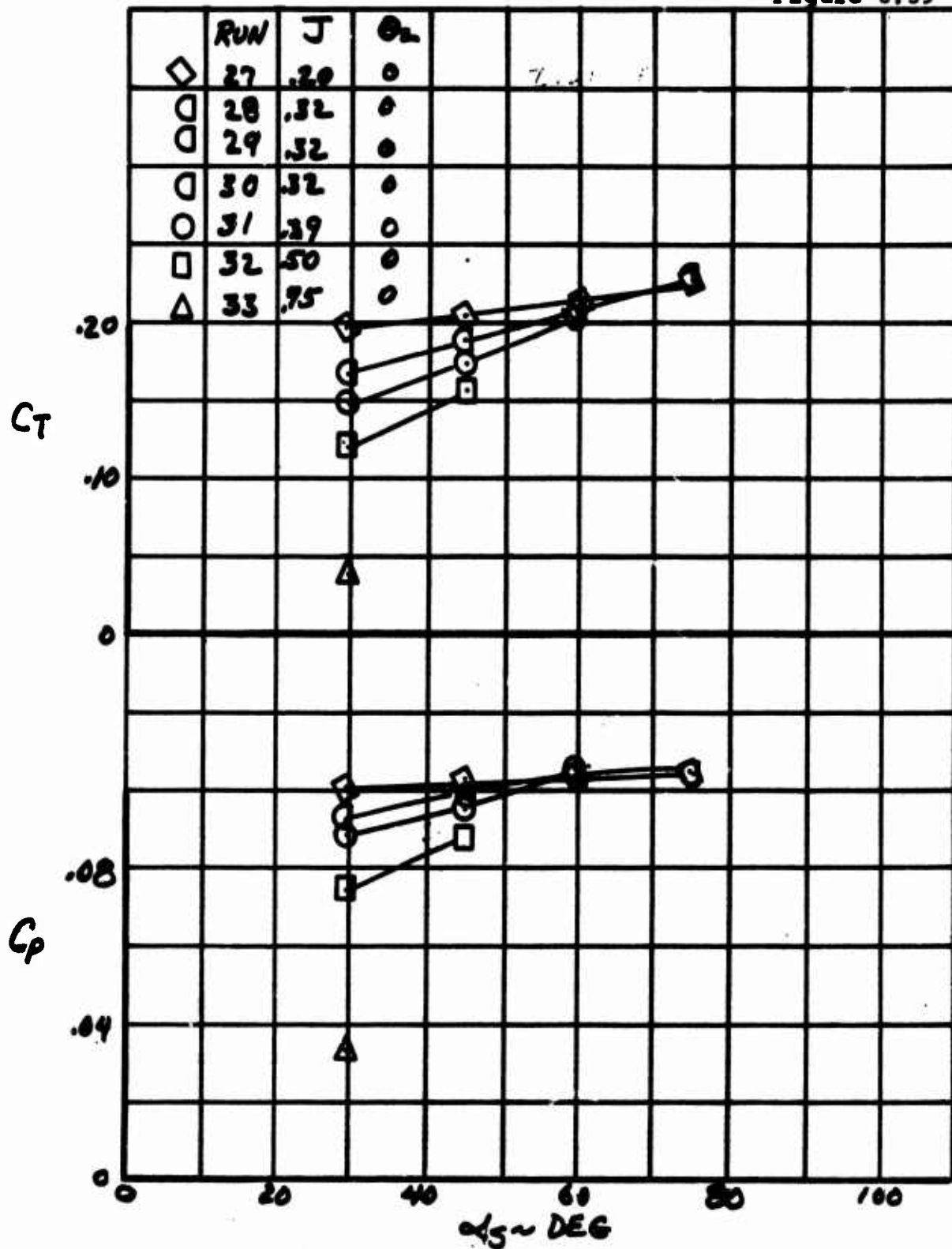
BLADE FLAP BENDING HARMONIC LOADS - .22R  
IN AQ RUN 87



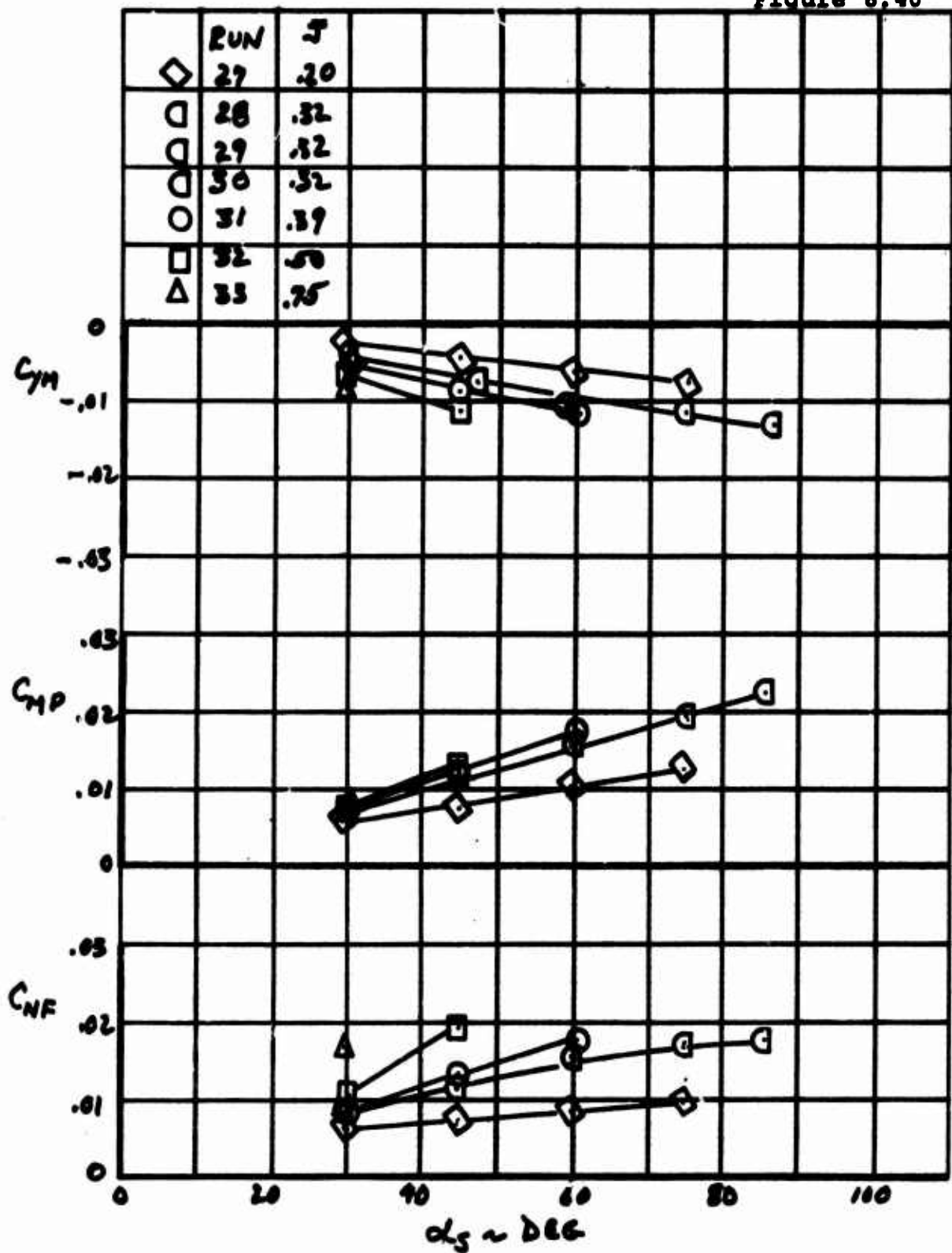
BLADE CHORD BENDING HARMONIC LOADS - .22R  
 IN Ag RUN 87



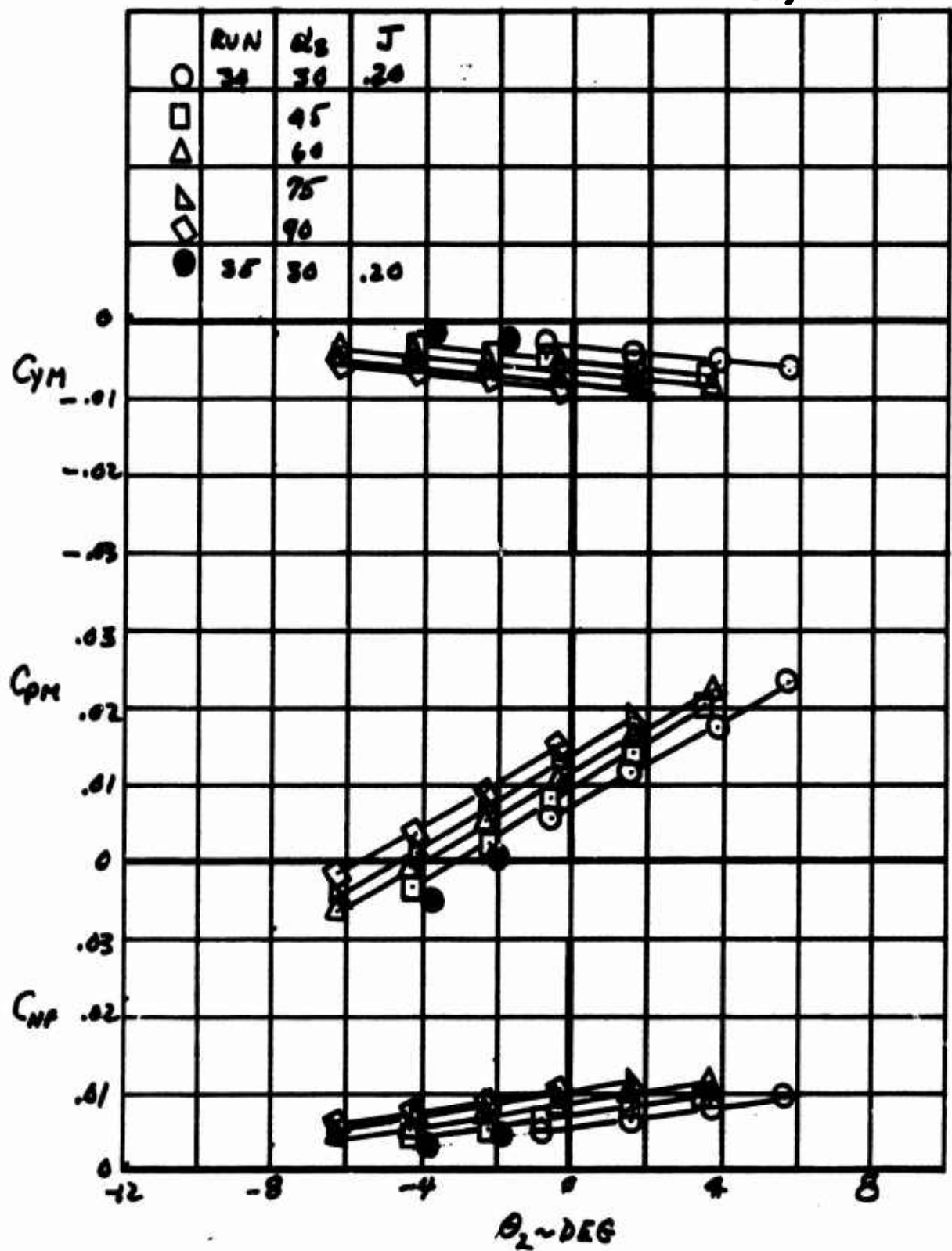
BLADE TORSION HARMONIC LOADS - .22R  
IN Aq RUN 87



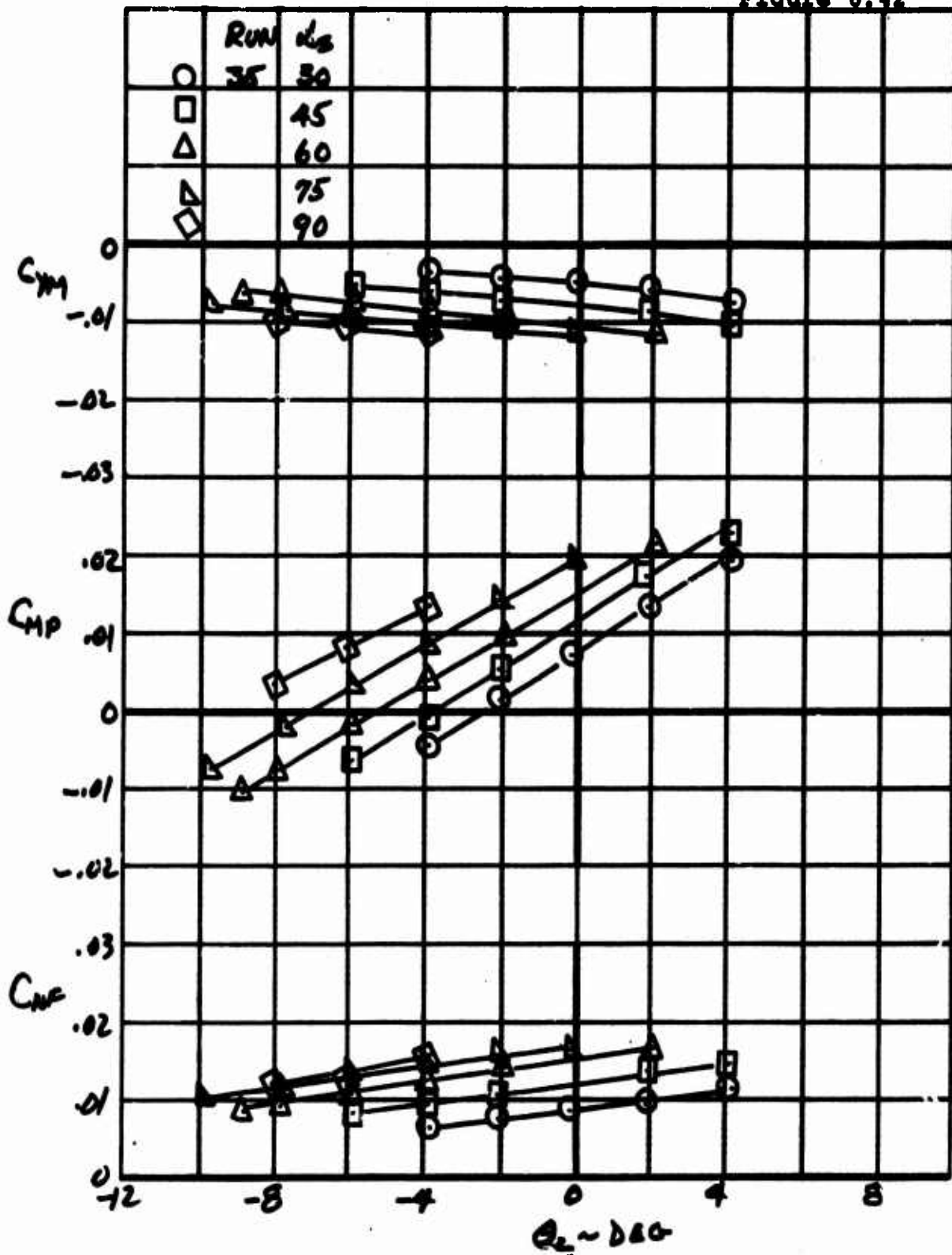
EFFECT OF  $J$  ON  $C_T$  AND  $C_P$  IN TRANSITION - ISOLATED PROPELLER



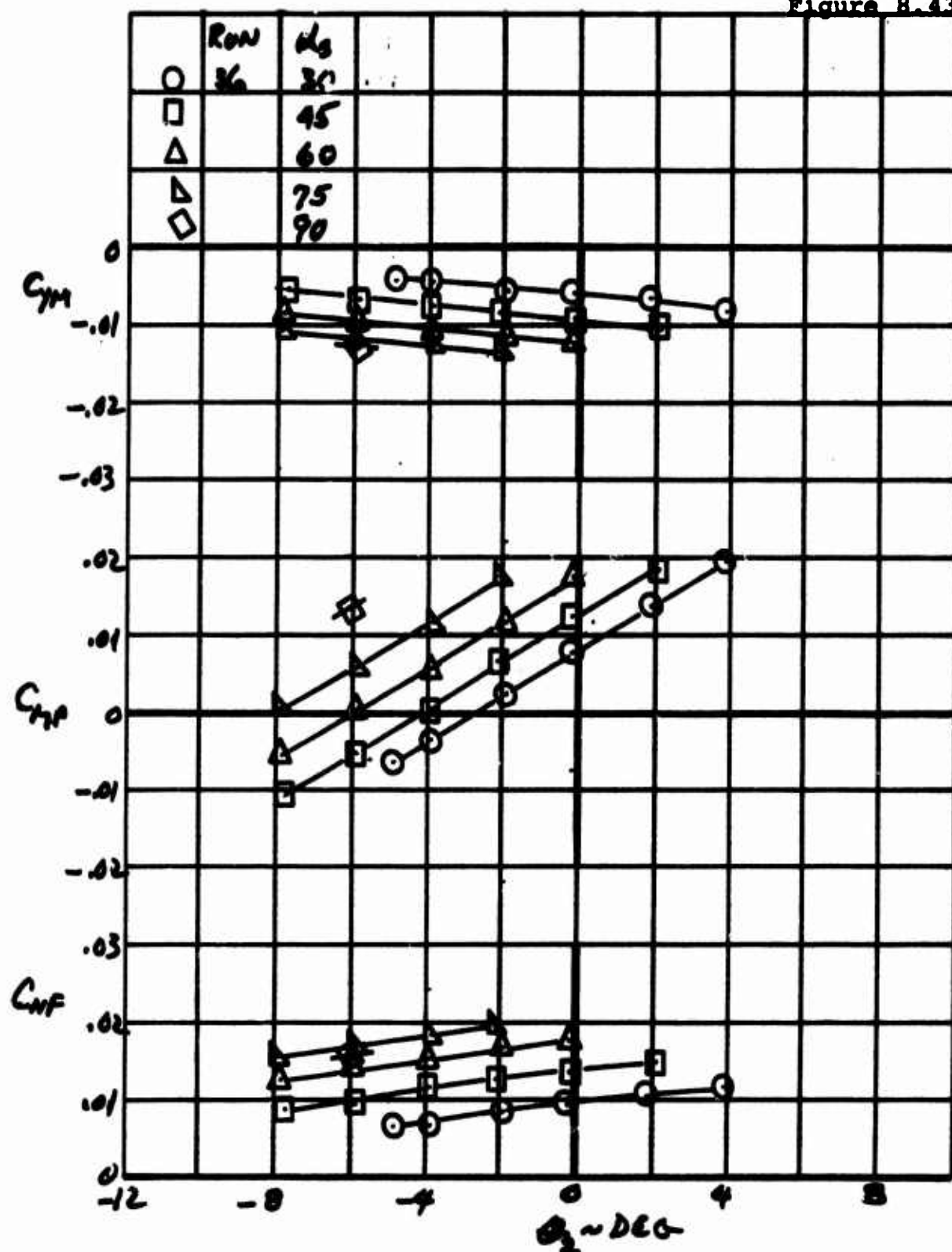
EFFECT OF J ON HUB FORCE AND MOMENT IN TRANSITION -  
ISOLATED PROPELLER



EFFECT OF CYCLIC PITCH ON HUB FORCES AND MOMENTS IN  
IN TRANSITION - ISOLATED PROPELLER,  $J = 0.20$

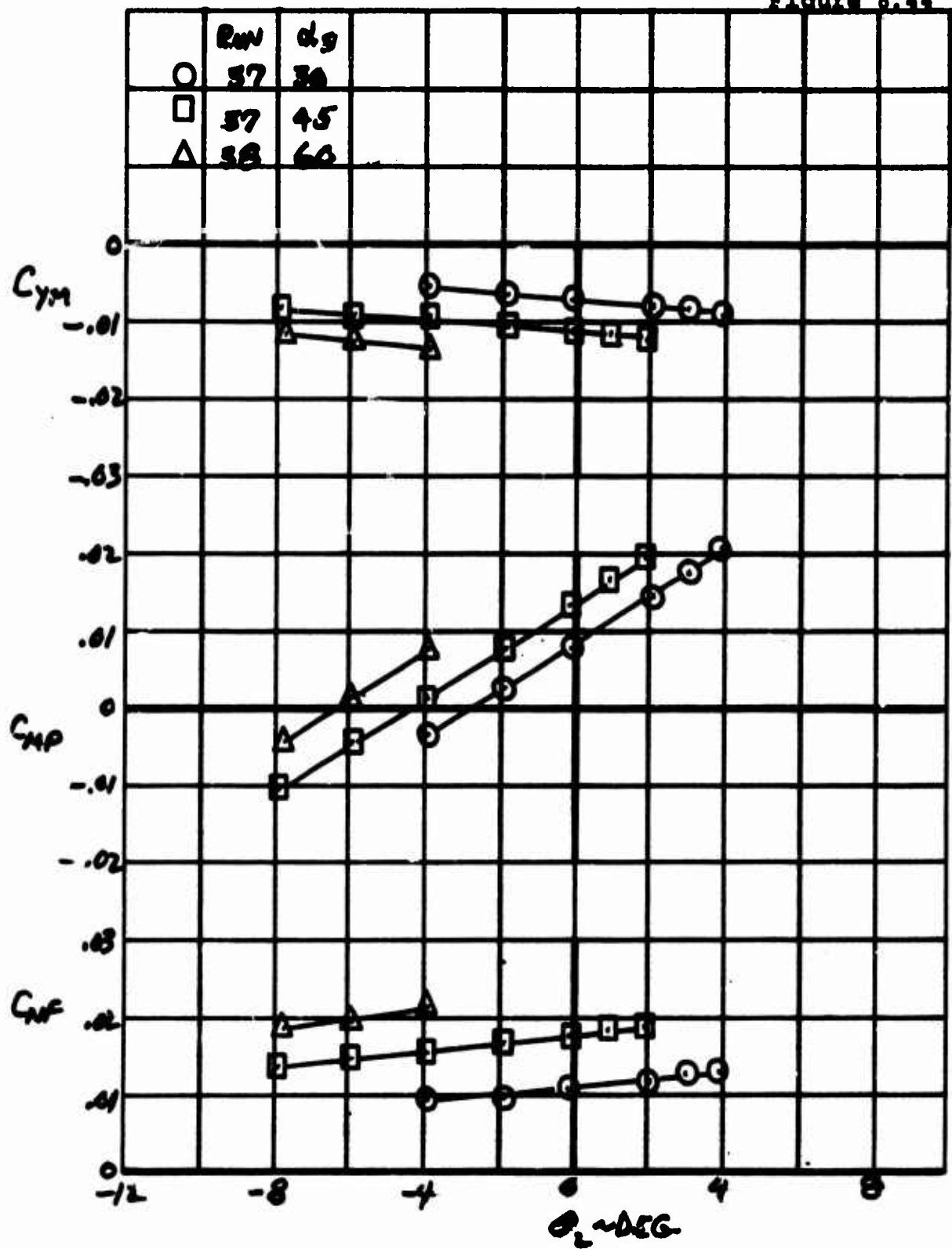


EFFECT OF CYCLIC PITCH ON HUB FORCES AND MOMENTS IN  
TRANSITION, ISOLATED PROPELLER,  $J = .32$

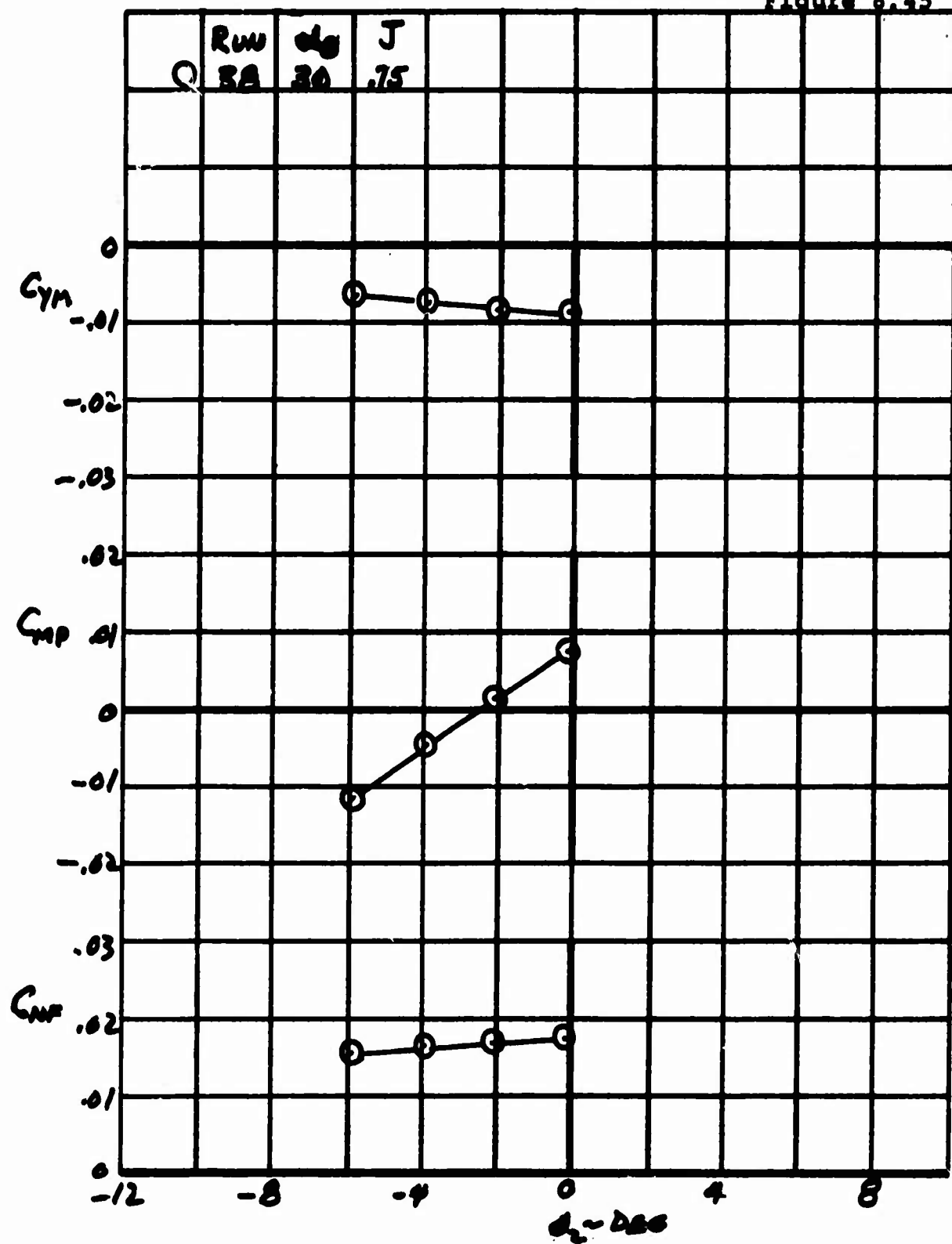


EFFECT OF CYCLIC PITCH ON HUB FORCES AND MOMENTS IN  
TRANSITION,  $J = .39$

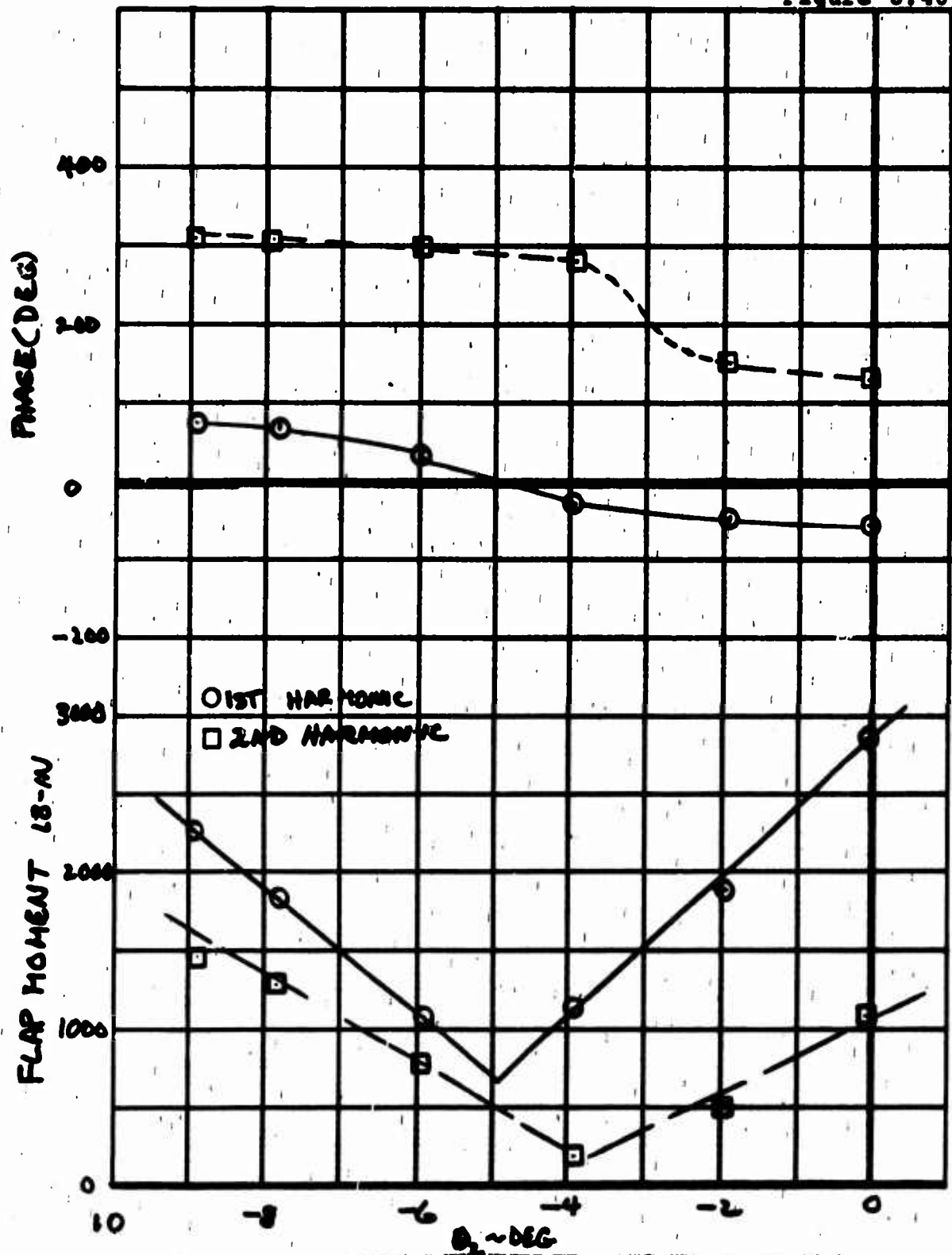




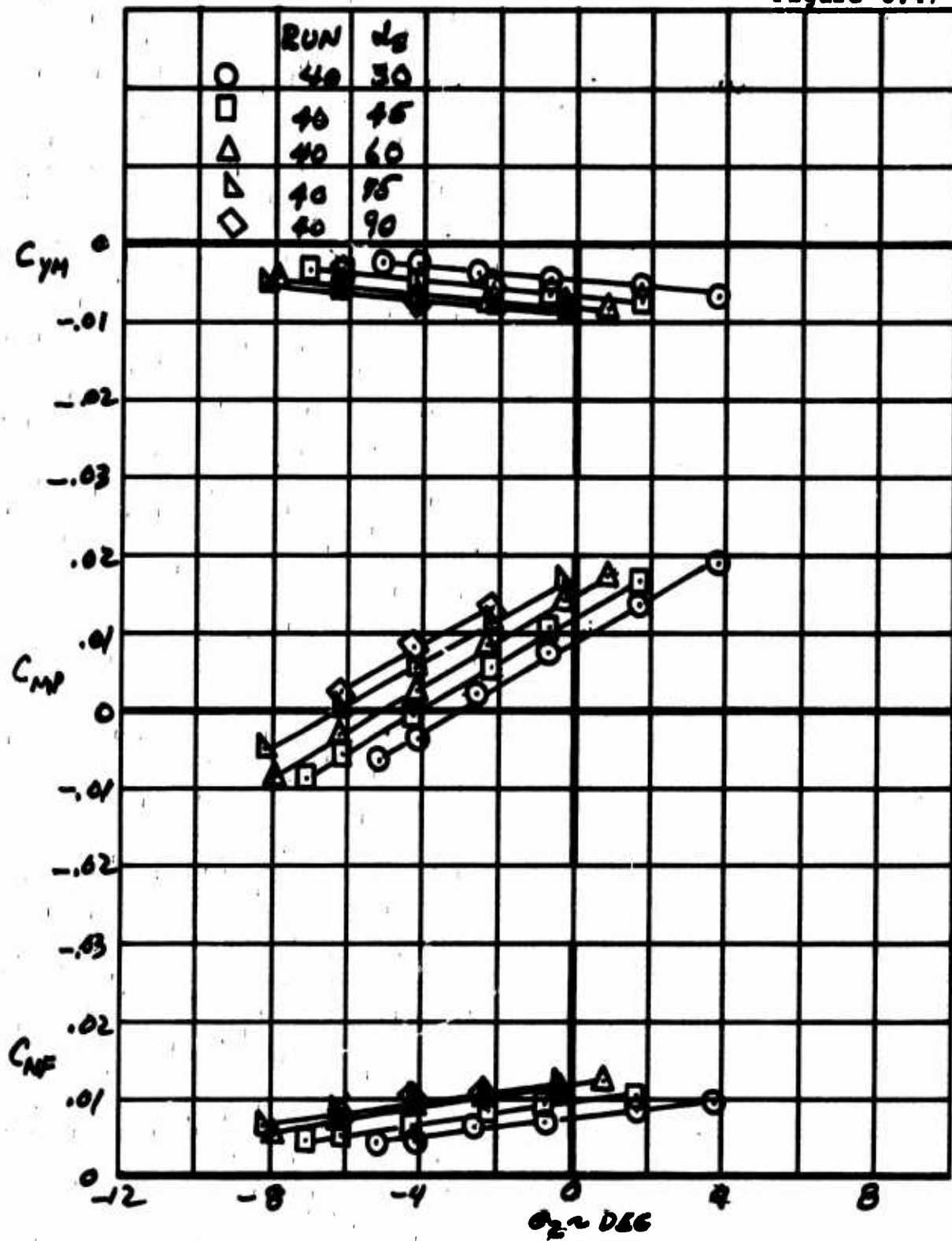
EFFECT OF CYCLIC PITCH ON HUB FORCES AND MOMENTS IN  
TRANSITION,  $J = .50$



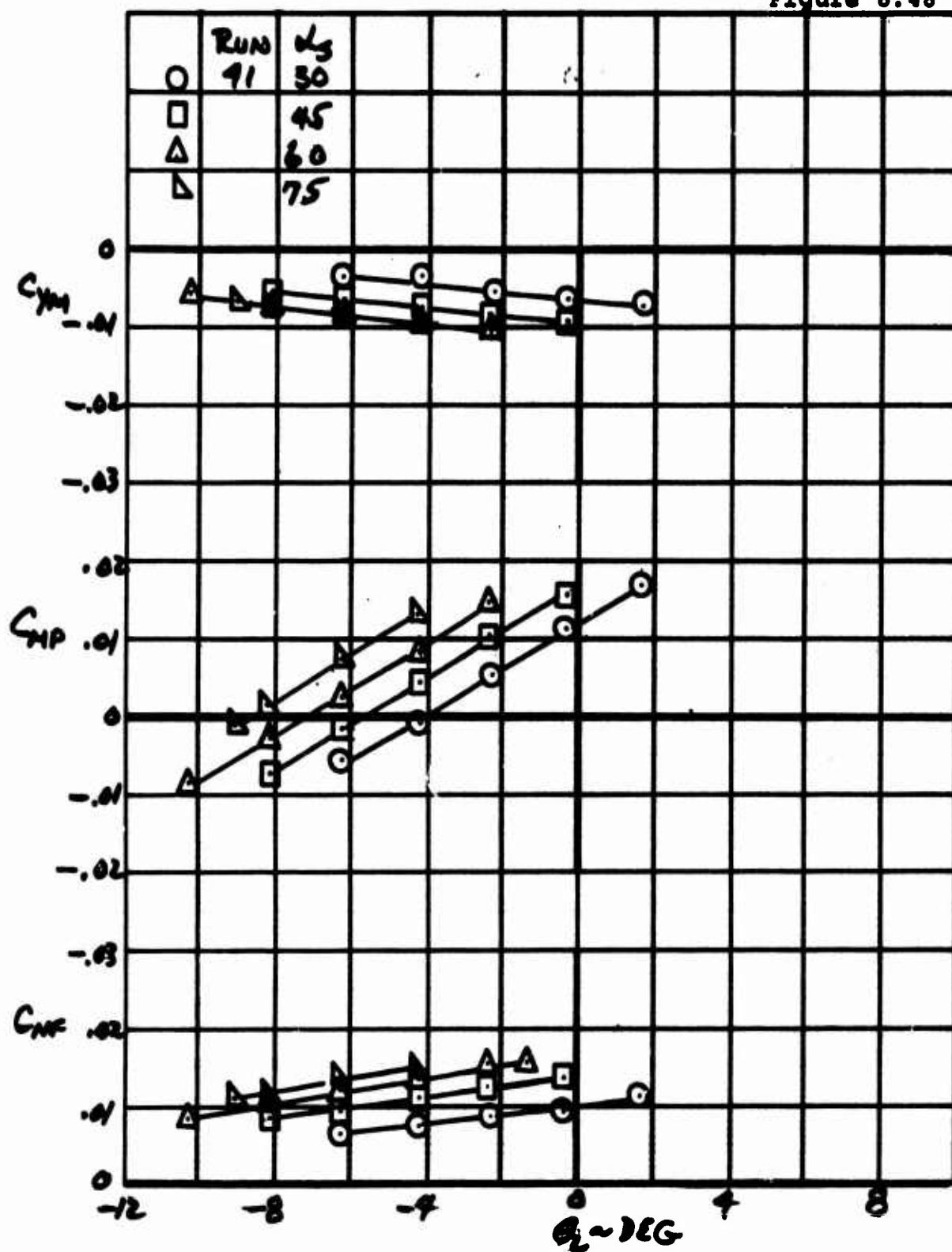
EFFECT OF CYCLIC PITCH ON HUB FORCES AND MOMENTS  
IN TRANSITION,  $J = .75$



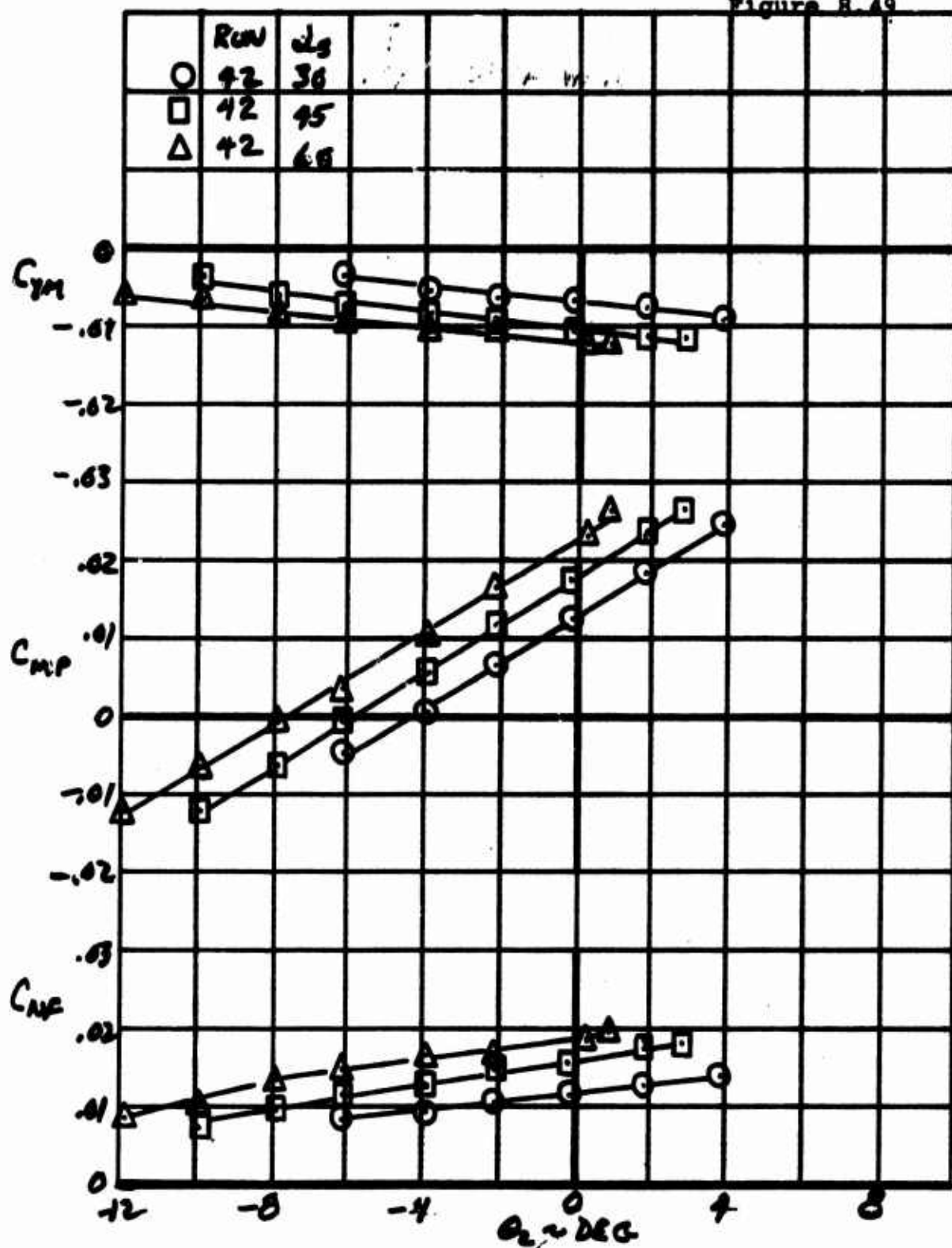
HARMONIC FLAP MOMENT AND PHASE VS  $\theta_2$   $X/R = .22$   
 $\alpha_s = 60^\circ$   $J = .32$   $\theta_{75} = 13.83^\circ$  RUN 35



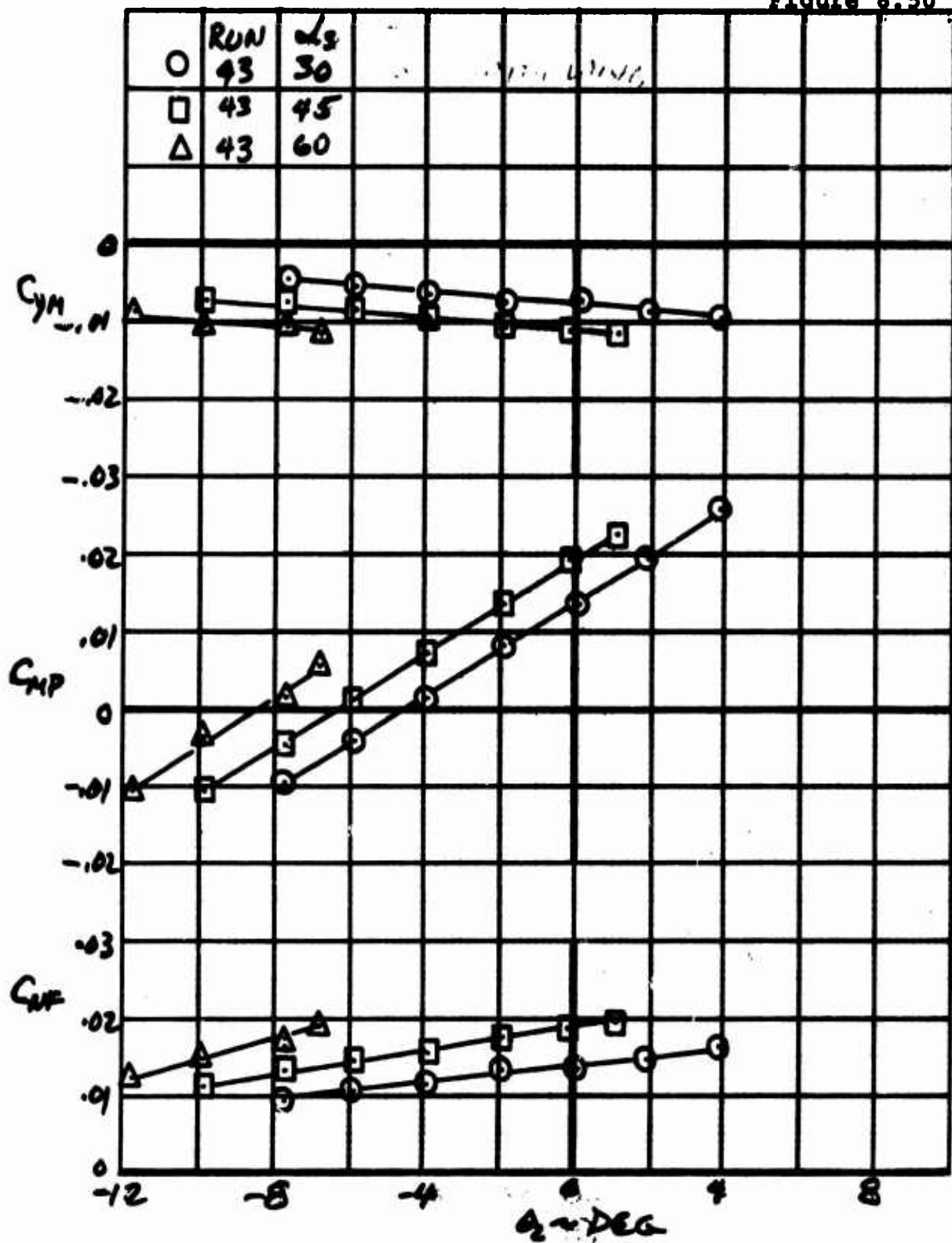
EFFECT OF CYCLIC PITCH ON HUB FORCES AND MOMENTS IN  
TRANSITION, INSTALLED PROPELLER,  $J = .20$



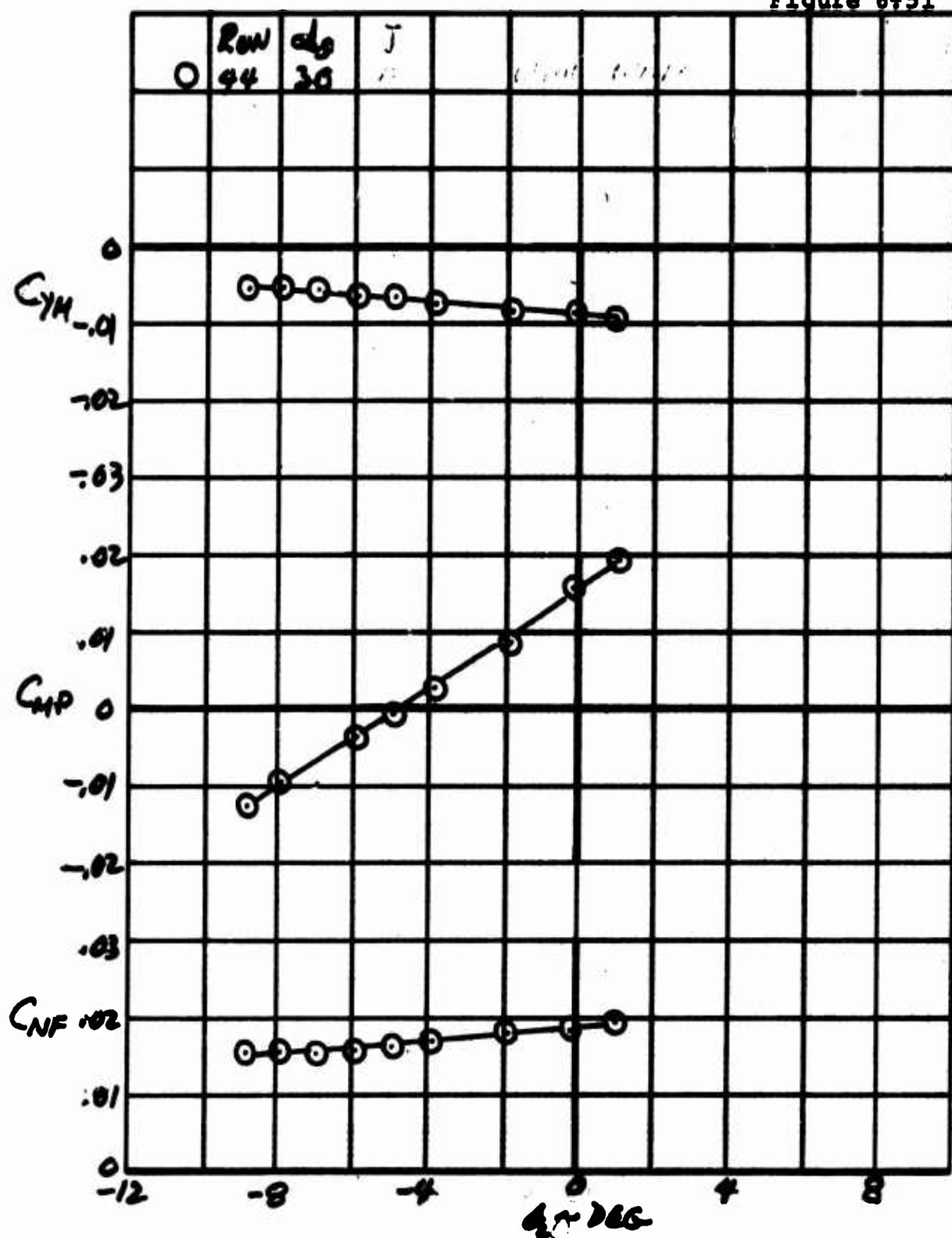
EFFECT OF CYCLIC PITCH ON HUB FORCES AND MOMENTS IN  
TRANSITION, INSTALLED PROPELLER,  $J = .32$



EFFECT OF CYCLIC PITCH ON HUB FORCES AND MOMENTS IN TRANSITION, INSTALLED PROPELLER,  $J = .39$

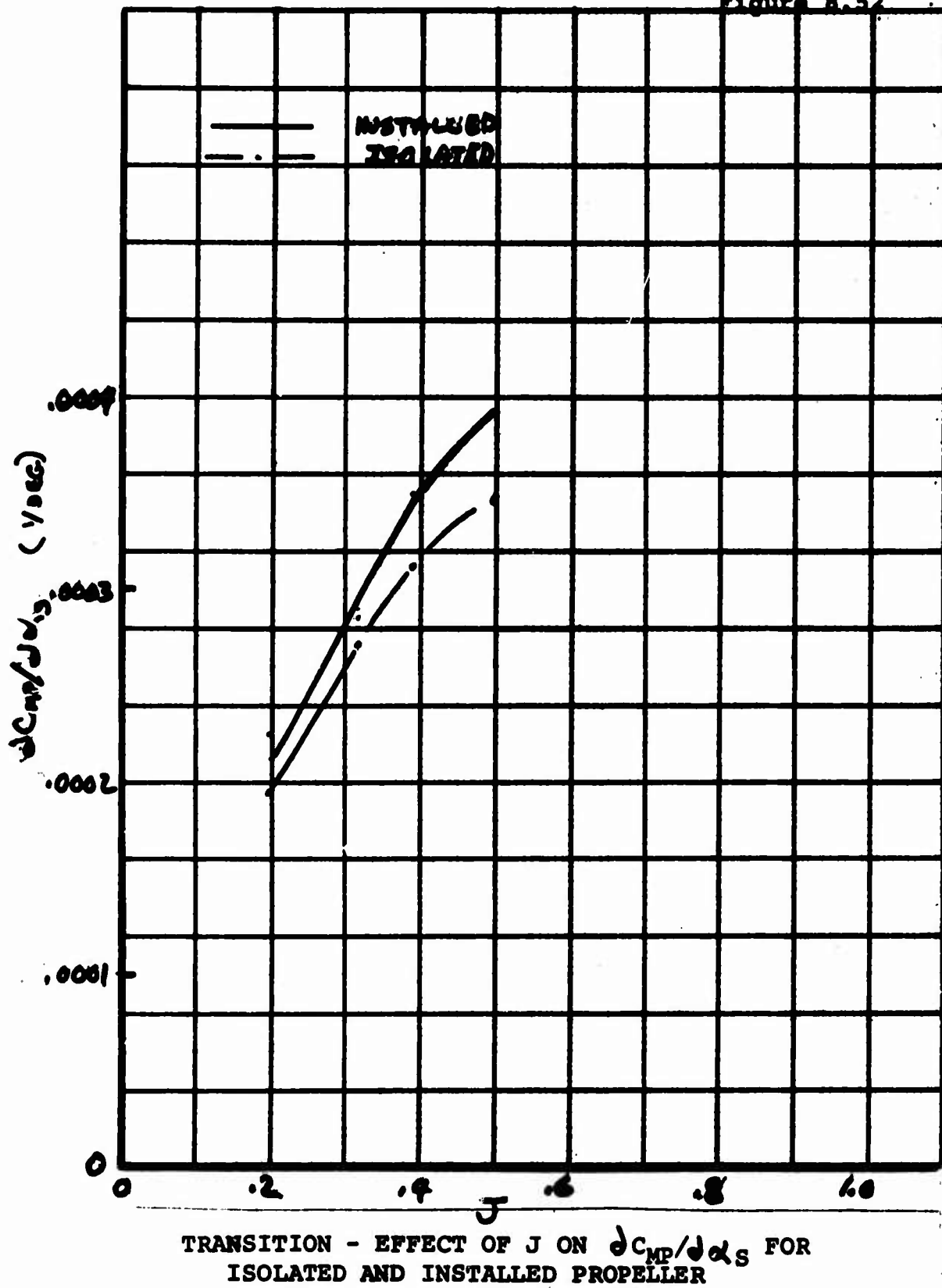


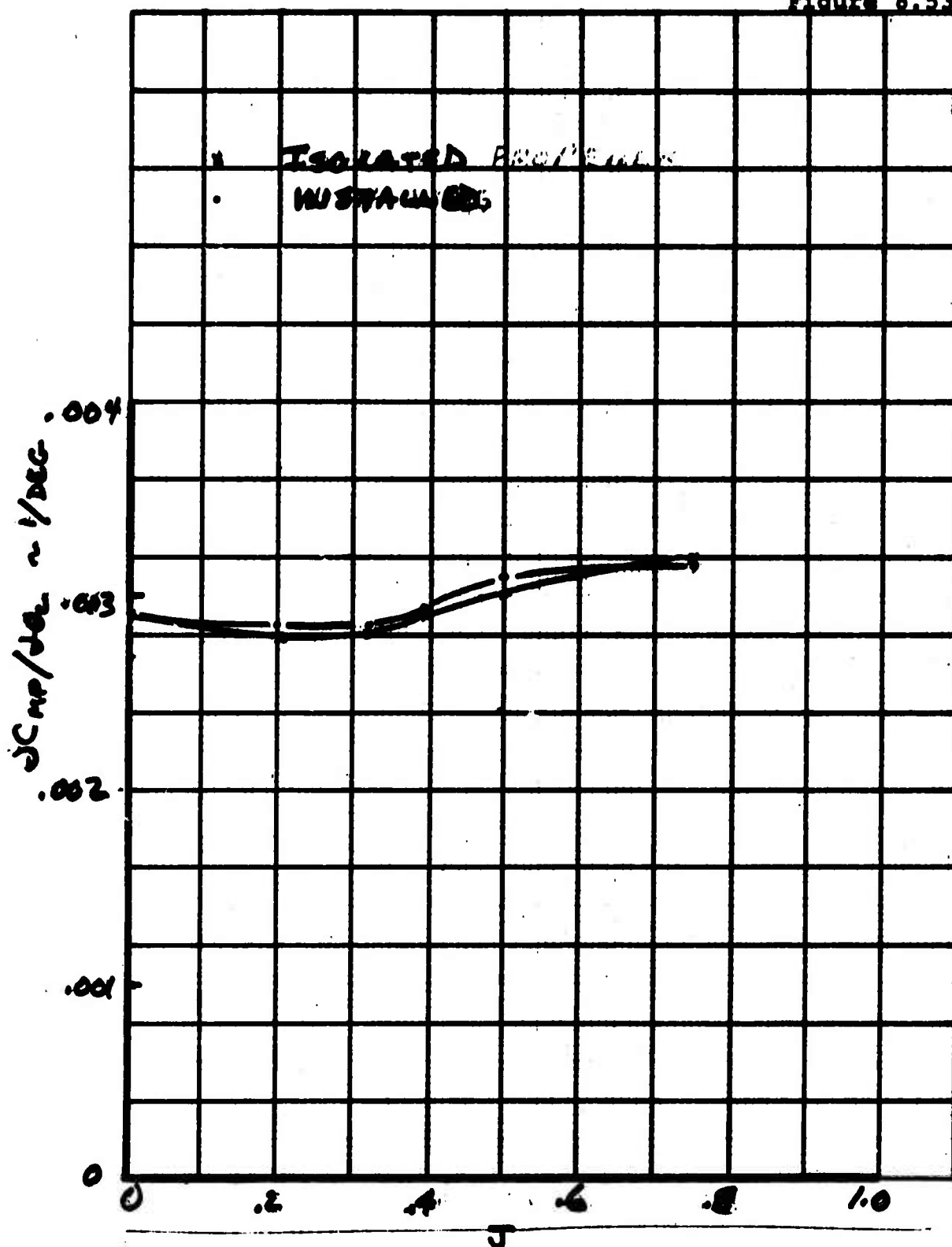
EFFECT OF CYCLIC PITCH ON HUB FORCES AND MOMENTS IN  
TRANSITION, INSTALLED PROPELLER, J = .30



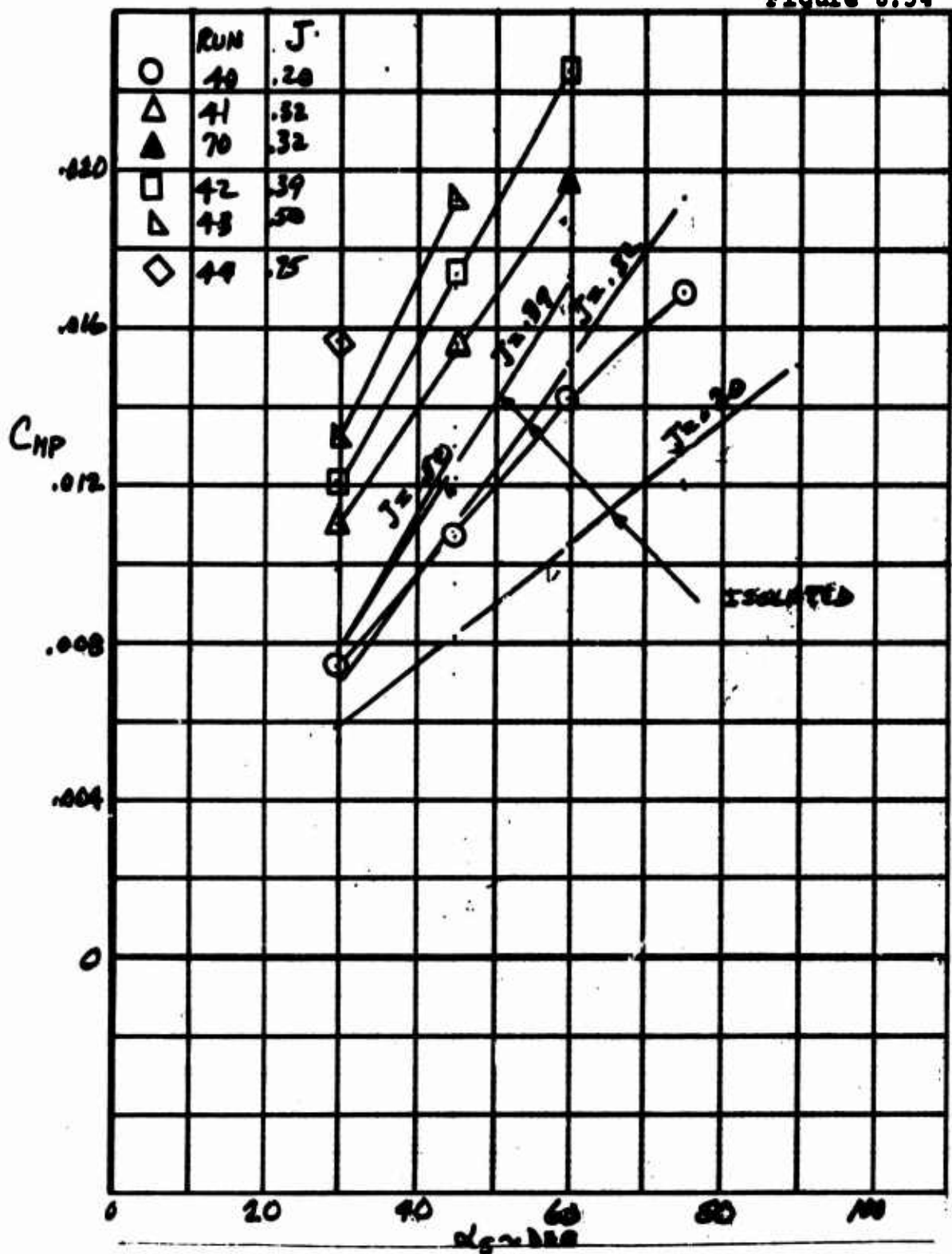
EFFECT OF CYCLIC PITCH ON HUB FORCES AND MOMENTS IN TRANSITION, INSTALLED PROPELLER,  $J = 0.75$





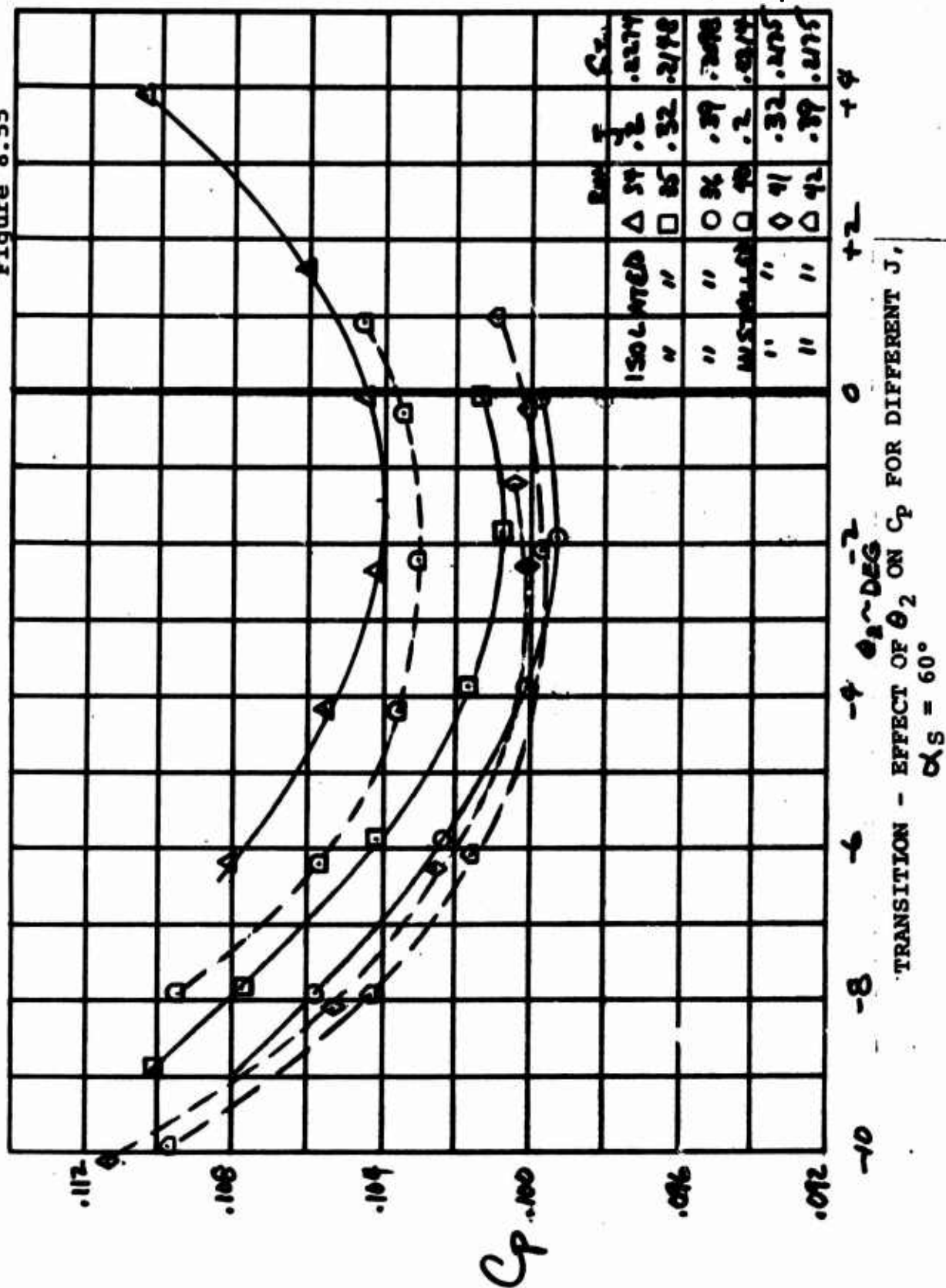


TRANSITION - EFFECT OF J ON  $\frac{dC_{mp}}{d\alpha}$  FOR  
ISOLATED AND INSTALLED PROPELLER



TRANSITION -  $C_{NP}$  VS  $\alpha_s$  FOR INSTALLED PROPELLER  
WITH COMPARISON TO ISOLATED PROPELLER

D170-10040-1  
Figure 8.55



## 9.0 CONCLUSIONS AND RECOMMENDATIONS

9.1 The mechanical and structural performance and reliability of the model throughout the test were very good. This dynamic model is considered to be an excellent tool for the investigation of cyclic pitch propeller phenomena.

9.2 The moments due to cyclic pitch agree well with previous data. Moments are linear with cyclic up to  $\pm 10^\circ$  with only a small fall-off in cyclic up to  $15^\circ$ . The maximum of thrust offset obtained was about 35% of blade radius.

9.3 Moment per degree of cyclic varies only slightly with advance ratio and shaft angle and is essentially unaffected by the presence of the wing. This again confirms previous testing.

9.4 Propeller hub moments in descent can be trimmed to zero with  $7^\circ$  of cyclic for  $90^\circ$  propeller incidence at 35 knots full scale speed.

9.5 Increase in power due to cyclic pitch for this high activity factor propeller is quite low. A 12% increase in power provides enough moment to give  $.6 \text{ radians/sec}^2$  on a typical tilt wing transport airplane.

9.6 Variation of isolated propeller pitching moments with shaft incidence was in general agreement with 1/12 scale model data.

9.7 The increase in propeller pitching moment vs shaft angle due to the presence of the wing in this test program was only about 50% which compares with a factor of 2 and more on the 1/12 scale model. This difference is at present unexplained and needs further investigation.

9.8 Blade loads in all regimes investigated were predominantly 1/rev with some 2/rev in some conditions and negligible loads from all higher harmonics.

9.9 Blade loads in hover are substantially linear with cyclic pitch.

9.10 The highest blade loads in transition occur at low speeds and high shaft angles.

9.11 Maximum Figure of Merit of the isolated propeller was about 82%. This is substantially higher than predicted. Figures of Merit in excess of 80% were achieved over a  $C_T$  range from .15 to .3.

9.12 The presence of the wing reduced Figure of Merit by approximately 4% which is a greater loss than predicted. Further examination and analysis of the hover performance recorded is required.

9.13 The cruise performance with the propeller was below predictions and, again, the adverse effect of the wing appears to reduce efficiency by about 5% which is greater than predicted.

9.14 Model testing of lightly loaded tilt rotor propellers has indicated possible large effects on cruise efficiency from such effects as spinner tares and live twist of the blades. Also, the model blades has exposed round root sections which would create high drag at the higher forward speeds tested. Further analysis of the data from this program and possibly additional testing is required before high confidence can be established in the cruise performance data shown herein.

#### Recommendations:

9.15 Comparisons should be made with the test results of this report to the results of other investigators to establish the areas of agreement and to identify any questions requiring further investigation.

9.16 Existing analytical methods should be used to calculate the hub and blade loads for the propeller in hover and in transition. These results would be compared with the results of the tests to evaluate the methodology and indicate areas where improvement is required.

9.17 Performance studies should be conducted to understand the high Figure of Merit and for the low cruise efficiency. In particular, supervelocity due to the spinner, live twist, and the aerodynamics at the blade root should be included in the calculations.

9.18 A test program to test at full scale Mach number for hover, transition and cruise should be conducted. For these tests, the propeller design should be further optimized for performance as regards geometry and twist distribution.

9.19 Additional testing of the Froude-scaled propeller should be conducted where the wing forces and moments are measured to resolve the question of wing interference effect.

**10. REFERENCES**

1. Test Report of Cyclic Pitch Propeller on AFAPL Thrust Rig - HSER 5592, Hamilton Standard, February 1970.
2. Isolated Cyclic Pitch Propeller: Results of Wind Tunnel Tests - D170-10037-1, Boeing Company, June 1970.
3. Miller, R. H., Rotor Blade Harmonic Loading, IAS Paper 62-82, January 1962.
4. Fry, B. L., Static Test of Monocyclic Control on a Full-Scale Boeing-Vertol 76 Rigid Propeller, The Boeing Company, R-339, Volume I, December 1963.
5. DeDecker, R. W., Investigation of an Isolated Monocyclic V/STOL Propeller Performance and Oscillatory Stress, USAAVLABS TR 65-80 February 1966.

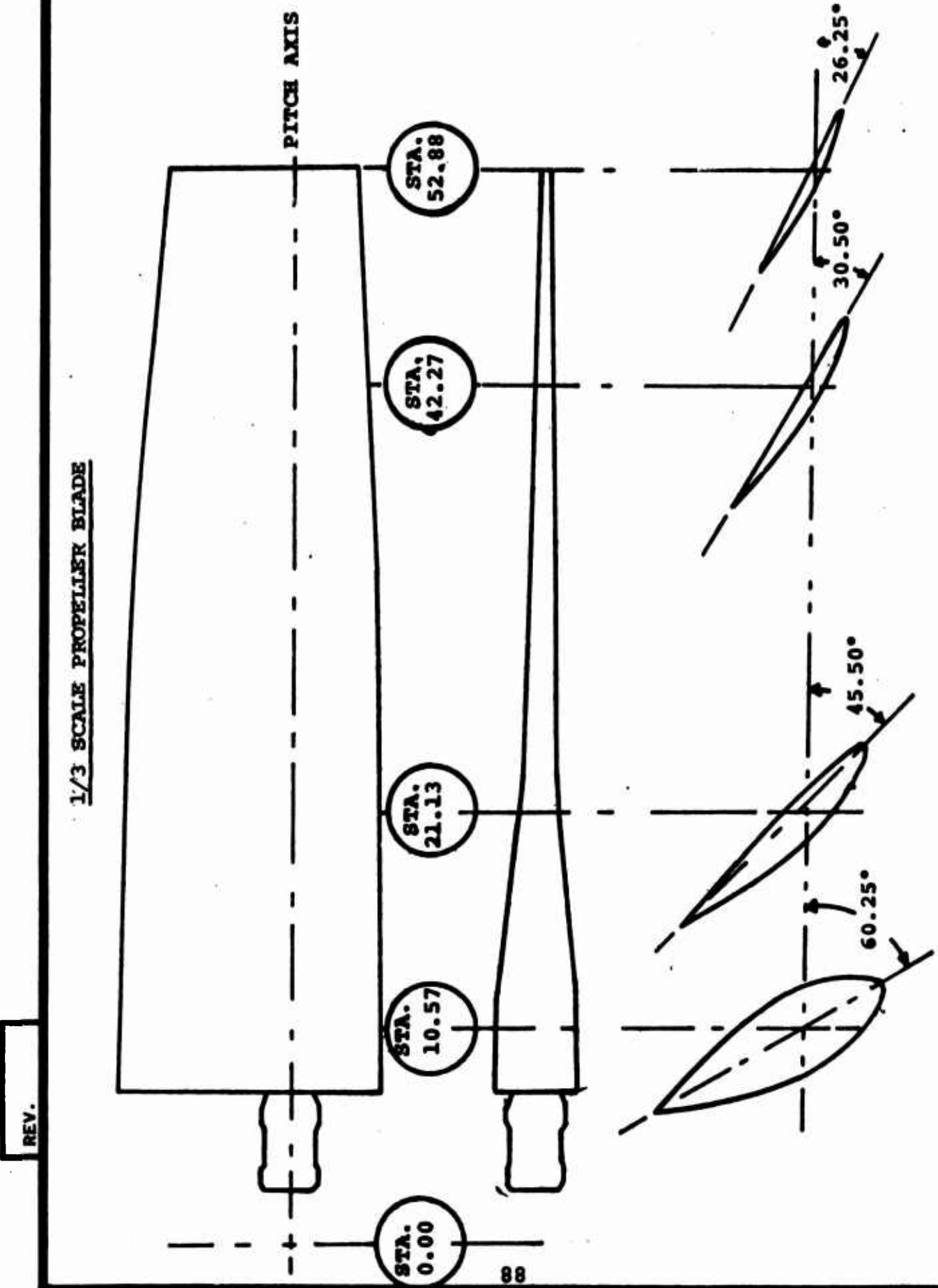


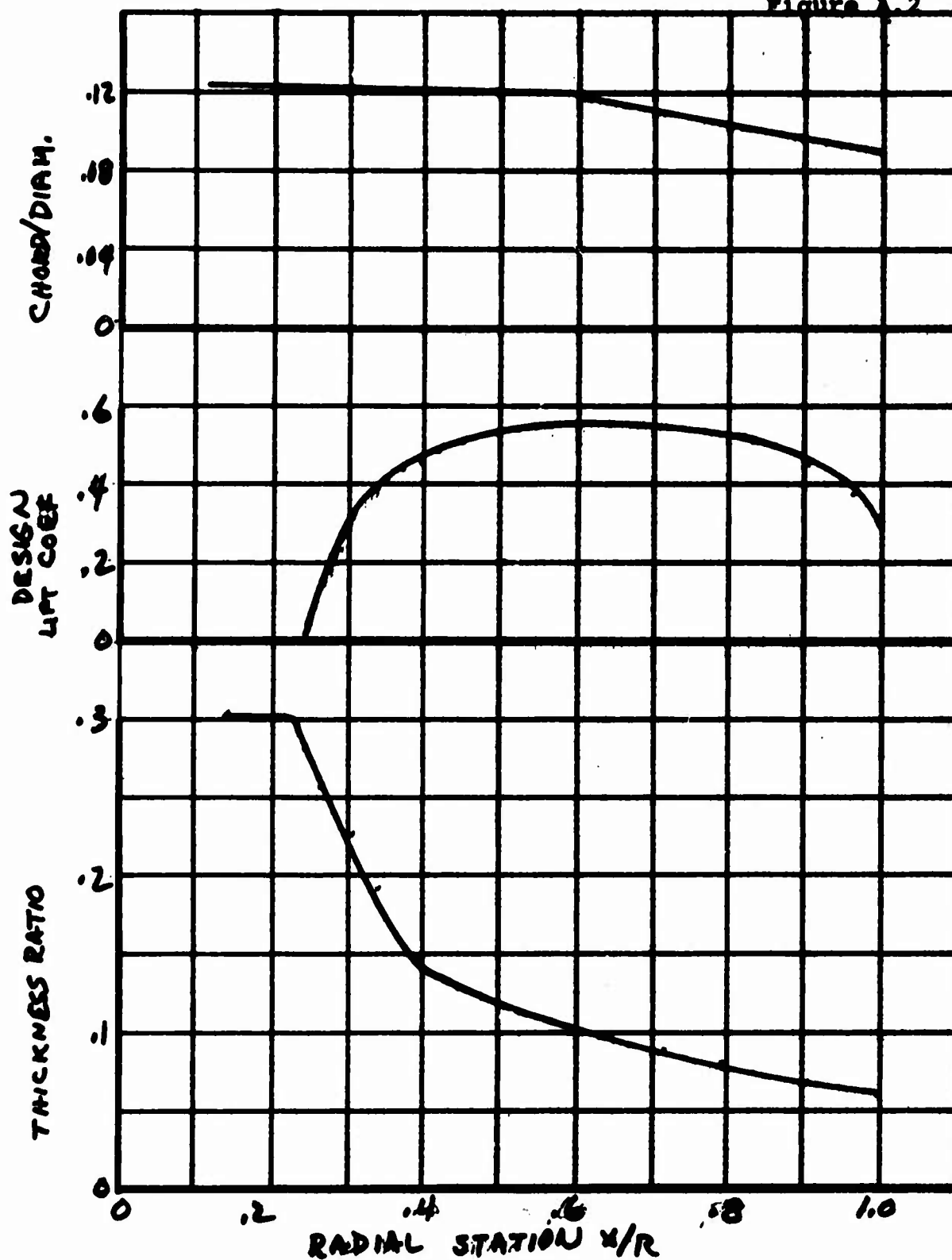
APPENDIX ABLADE DESIGN

The test propeller blade design is based on the full-scale properties of the 18D propeller. The 18D propeller is the outgrowth of a V/STOL transport study and is taken to be representative of a V/STOL propeller. The 18D design is shown in Figure A.1. The detailed properties of the 18D blade are given in Tables A.1 - A.3 and in Figures A.2. The airfoil for the blade is a modified NACA 64 series.

The design properties of the test blades are given in Table 4 and in Figures A.3 to A.13. The test blades differed in construction from the 18D blades in that the test blades had a glass box spar that provided essentially all the stiffness. The remainder of the blade was edge cut balsa to provide the contour. The blade was wrapped with crossply glass to provide a smooth surface. The proof of the design was in the simulation of the natural frequencies. The design natural frequencies are given in Figure A.14. The measured frequencies for the blades mounted in the hub with the hub firmly attached to ground are given in Table 5. As can be seen, the design meets the requirements.

The blades have a precone angle of  $1.5^\circ$  to relieve the steady bending moments.





BLADE AERODYNAMIC PROPERTIES

TABLE A.1

M-170 BLADE PROPERTIES - DESIGN 18D

(GEOMETRY)

R = 158.5 INCHES

PITCH AXIS - .35C

$x/R$	$e(x)$ (inch)	$q(x)$ (inch)	$s(x)$ (inch)
1.0	-4.28	-.13	-1.303
.91	-4.28	-.13	-1.303
.758	-1.92	+.658	-.239
.606	-.093	+.87	+.793
.455	-1.64	+1.051	+.010
.303	+.156	+.504	+.554
.2335	-.52	+.21	0.0
.1515	0.0	0.0	0.0
.056	0.0	0.0	0.0

$e(x)$  - chordwise distance of shear center from pitch axis (positive aft)

$q(x)$  - chordwise distance of mass center from pitch axis (positive aft)

$s(x)$  - chordwise distance of neutral axis from pitch axis (positive aft)

TABLE A.2

M-170 BLADE PROPERTIES - DESIGN 18D

R = 158.5 INCHES

PITCH AXIS = .35C

x/R	STIFFNESS			MASS		
	$EI_{\beta} \times 10^{-6}$ (lb in <sup>2</sup> )	$EI_{\zeta} \times 10^{-6}$ (lb in <sup>2</sup> )	$GJ \times 10^{-2}$ (lb in <sup>2</sup> )	$\Delta W / \Delta x$ lb/in	$\Delta I_{\theta} / \Delta x$ lb in <sup>2</sup> /in	$\Delta I_{\theta}^* / \Delta x$ lb in <sup>2</sup> /in
1.0	20.	1800.	51.5	.806	40.1	39.5
.91	20.3	2004.	51.5	.681	40.1	39.5
.758	45.7	2903.	114.1	.706	60.4	59.0
.606	140.	4211.	225.7	.953	79.8	76.2
.455	329.	5795.	477.6	1.311	108.5	100.4
.303	1200.	6231.	2295.	1.738	127.2	93.75
.2335	1425.	3795.	3024.	2.980	160.7	90.3
.2335	2746.	6589.	4146.	2.980	190.3	101.3
.18				4.62		
.1515	1150.	1150.	893.	3.589	76.4	43.4
.1515					23.0	0
.145			764.		19.75	
.139				5.72		
.132				2.12		
.12	1000.	1000.				
.115				5.32		
.115				1.36		
.098			1253.		32.45	
.084	4786.	4786.				
.078			1041.		27.0	
.073				1.14		
.064				3.20		
.056	4786.	4786.	1041.	3.20	27.0	0
.056				0		

TABLE A.3

M-170 BLADE PROPERTIES - DESIGN 18D

TWIST

R = 158.5 inches

$x/R$	$\theta_t$	$x/R$	$\theta_t$
.1419	36.86	.4353	13.27
.1514	35.57	.4542	12.40
.1703	33.15	.4921	10.74
.1893	30.93	.5299	9.19
.2082	28.88	.5678	7.70
.2271	27.00	.6057	6.30
.2334	26.41	.6435	4.93
.2461	25.27	.6814	3.62
.2650	23.66	.7192	2.38
.2839	22.18	.7571	1.22
.3028	20.80	.7950	.137
.3218	19.52	.8328	-.843
.3407	18.32	.8707	-1.71
.3596	17.19	.9085	-2.46
.3785	16.13	.9464	-3.08
.3975	15.13	.9653	-3.34
.4164	14.18	.9842	-3.58
.4227	13.87	1.0000	-3.75

$\theta_t$  is positive with leading edge up

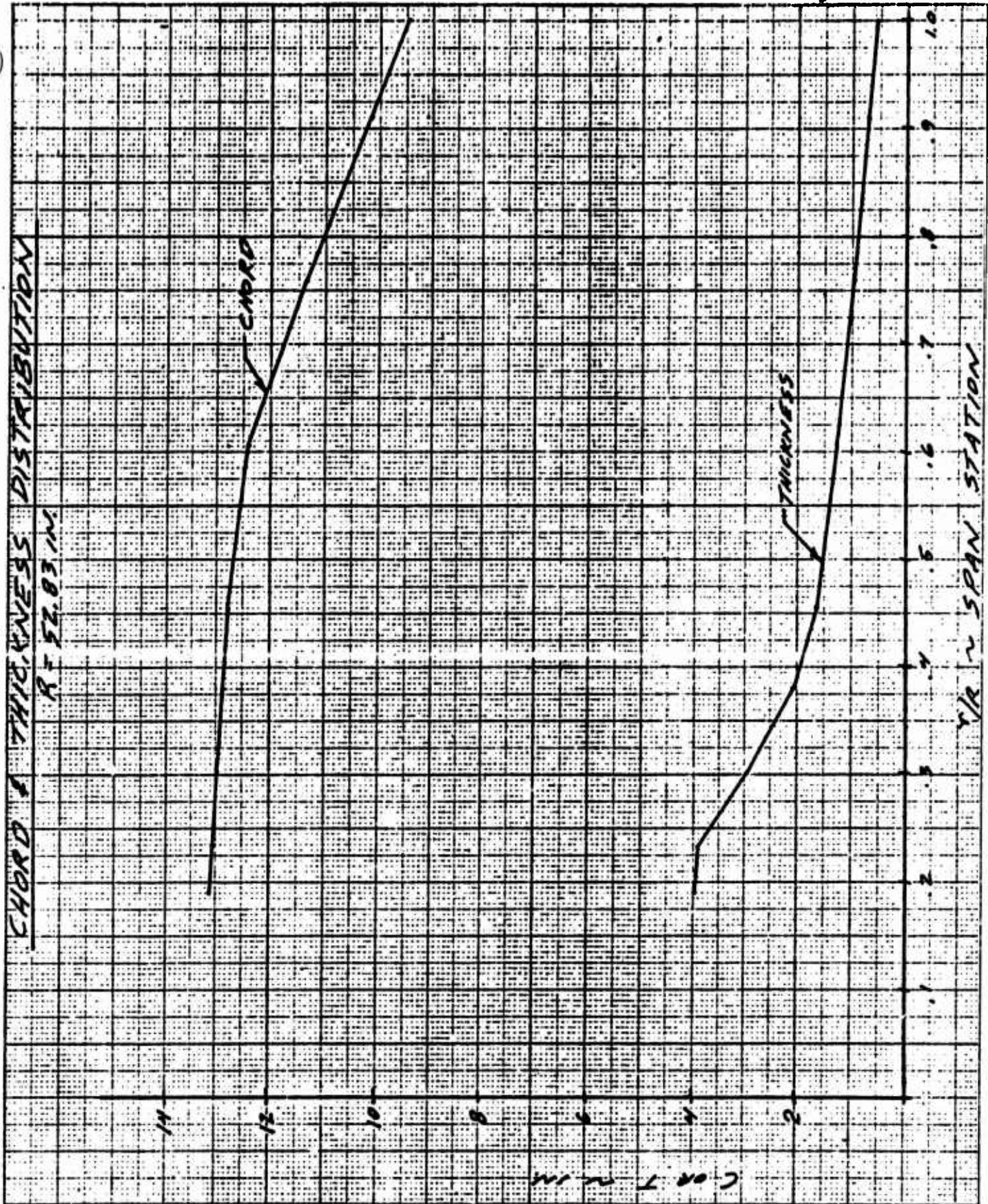
MODEL 170, REV. 1002, 1/3 SCALE V/STOL

R = 52.83 IN.

P.A. = .35 CHORD

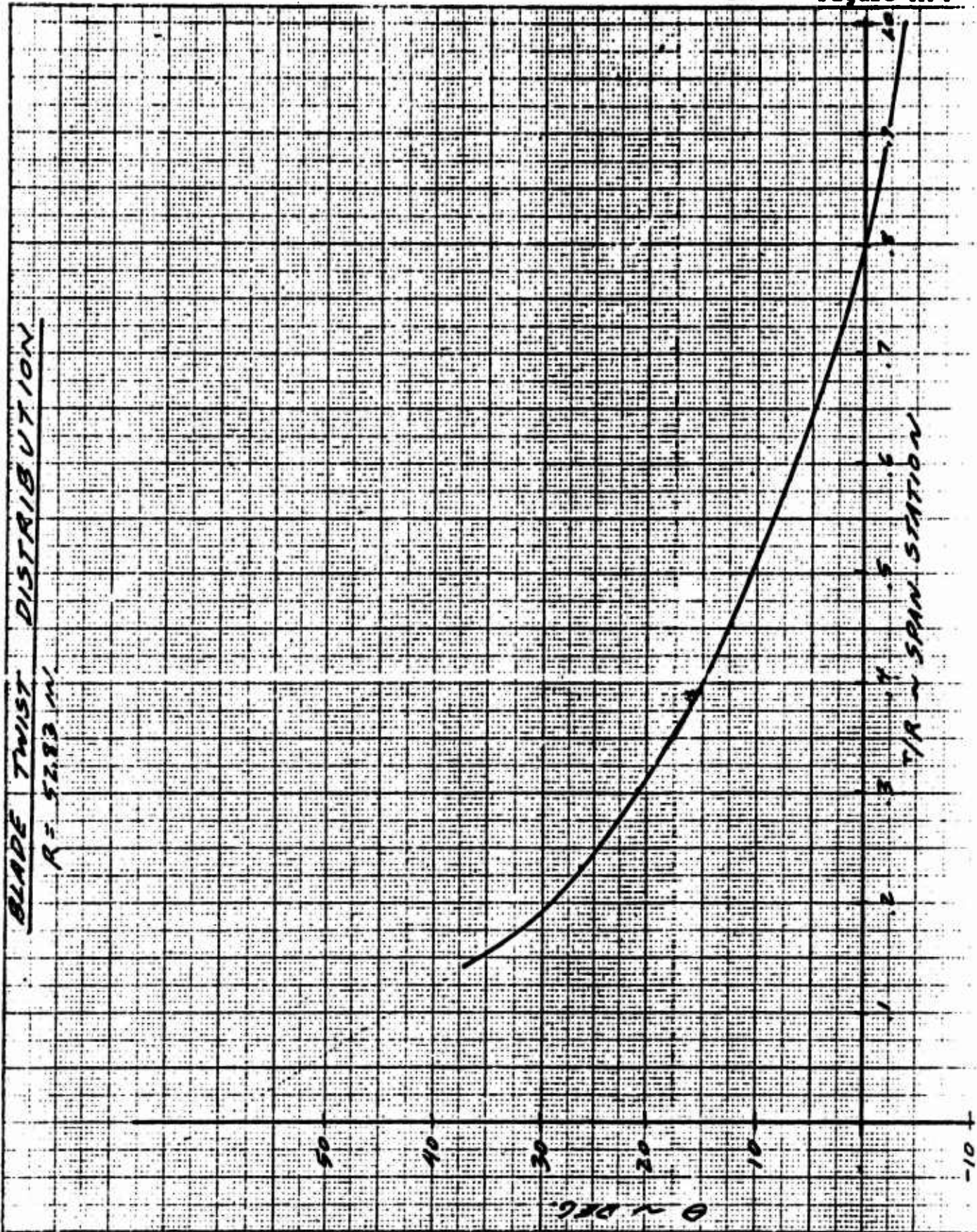
\* REF CHORD @.75R  
= 11.36

ITEM	~ PREDICTED ~			
	UNITS	BLADE ONLY	ABOUT Q ROT.	ABOUT END OF R.E. TIT. (STA 12.35)
FROM STA. TO BASE STA.	IN.	52.83	52.83	52.83
	IN.	2.07	0.0	12.35
WEIGHT	LB	15.546	15.55	6.153
SPANWISE C.G. FROM Q OF ROTATION T	IN.	15.14	15.14	26.59
	% R	.287	.287	.503
CHORDWISE C.G. FROM L.E. OF REF. CHORD *	IN.	3.984	3.98	3.961
	% C	.351	.351	.341
INERTIA ABOUT BASE STA	LB-IN <sup>2</sup>	4855.1	5763.	2027.7
DYNAMIC C.G. (FROM L.E. OF REF. CHORD)	% C	.343	.343	.339
PITCHING INERTIA ABOUT PITCH AXIS	LB-IN <sup>2</sup>			
TWIST FROM Q OF ROTATION TO TIP	DEG		-8.0	

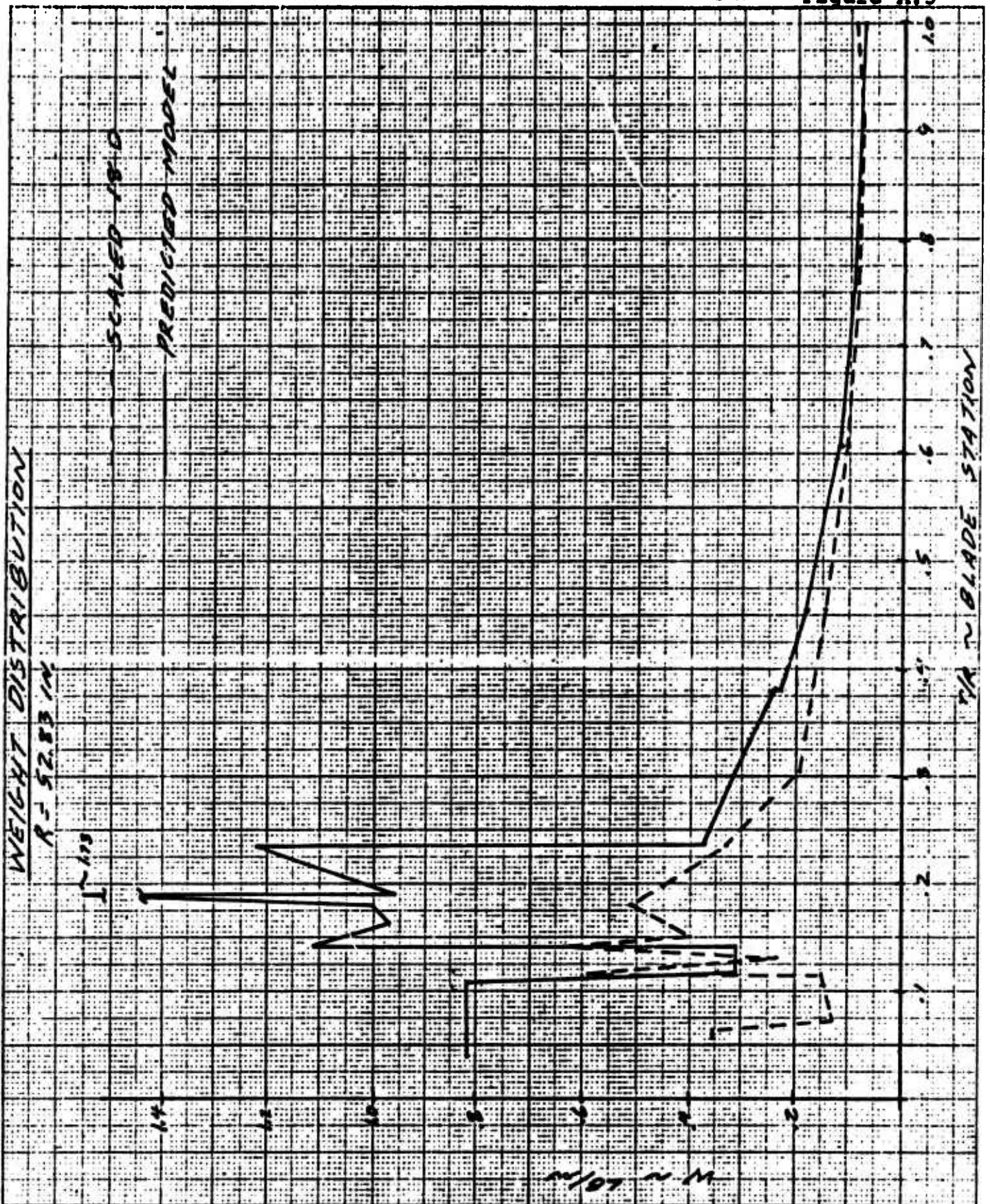


CALC	H.F. SIKORA	REVISED	DATE	MODEL 170 ~ 1/3 SCALE ROTOR REV. 1002
CHECK				
APPR				





DESIGNED BY	H.F. SLAGOX	11/25/70	REVISED	DATE	MODEL 170 ~ 1/2 SCALE ROTOR REV. 1002
CHECKED BY					
APPROVED BY					

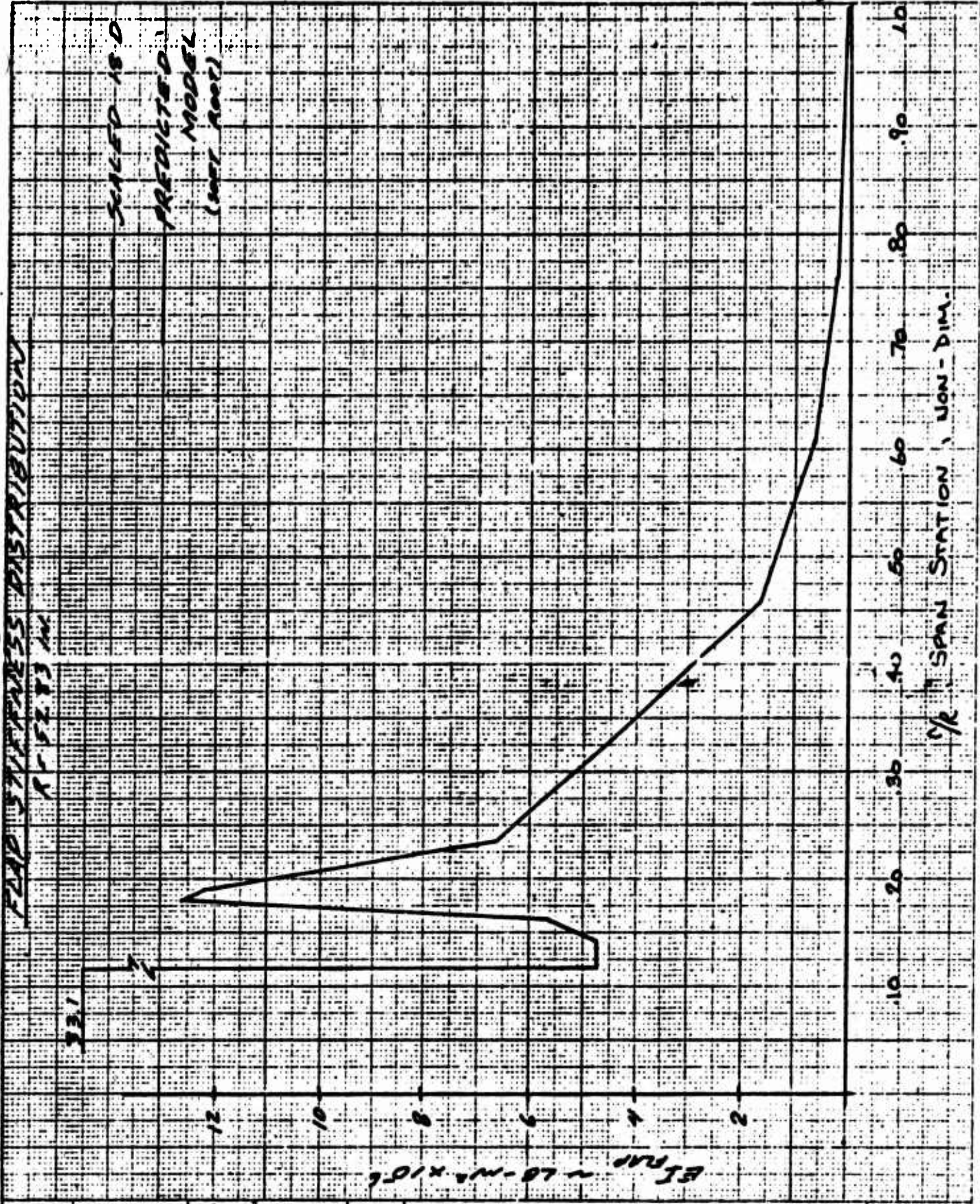


CALC	W.F. S/LCOX	8/1/70	REVISED	DATE
CHECK				
APPN				

MODEL 170-1/3 SCALE ROTOR  
REV. 1002





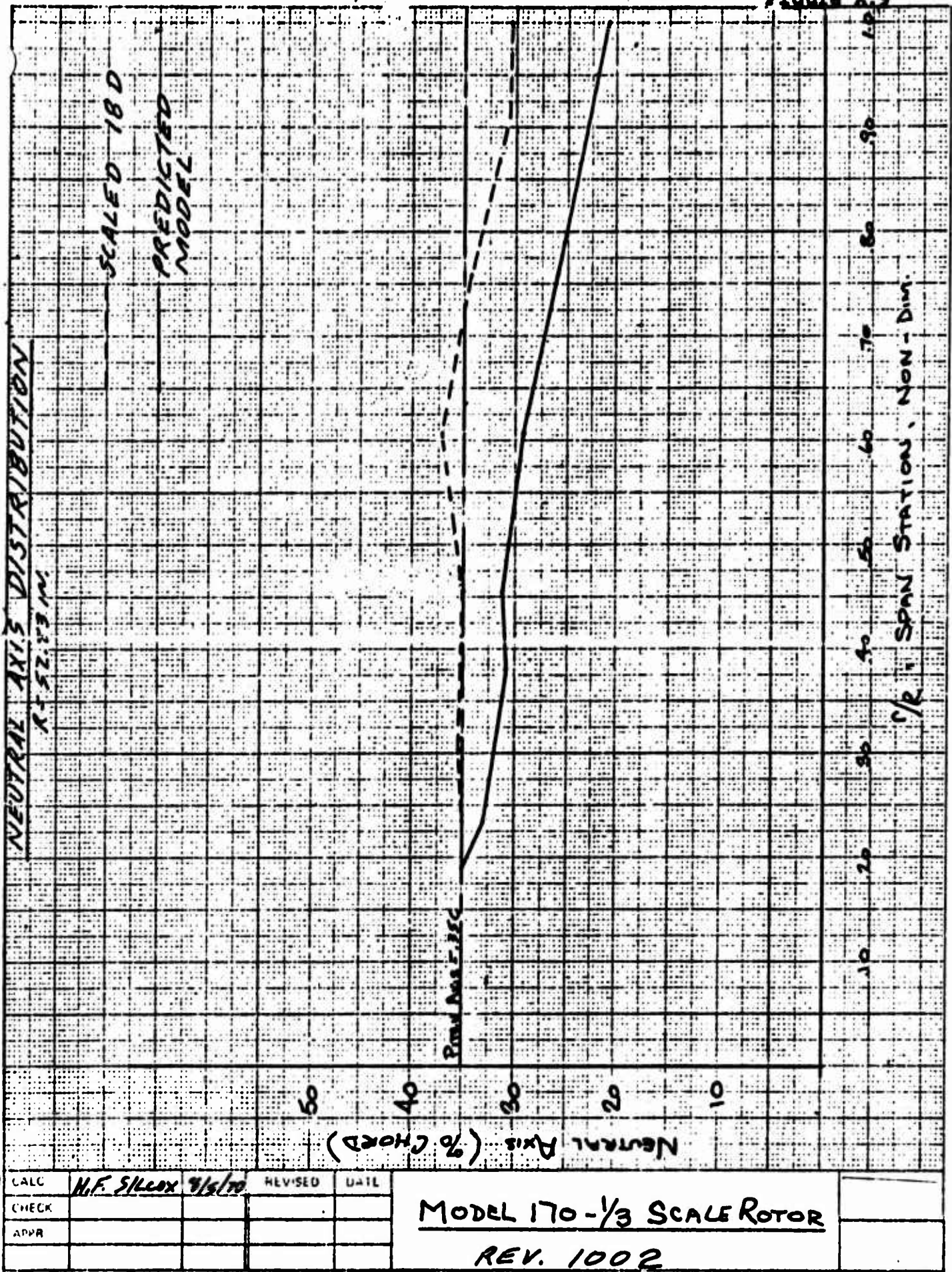


CALC	H.F. SILCOX 8/6/70	REVISED	DATE
CHECK			
APPR			

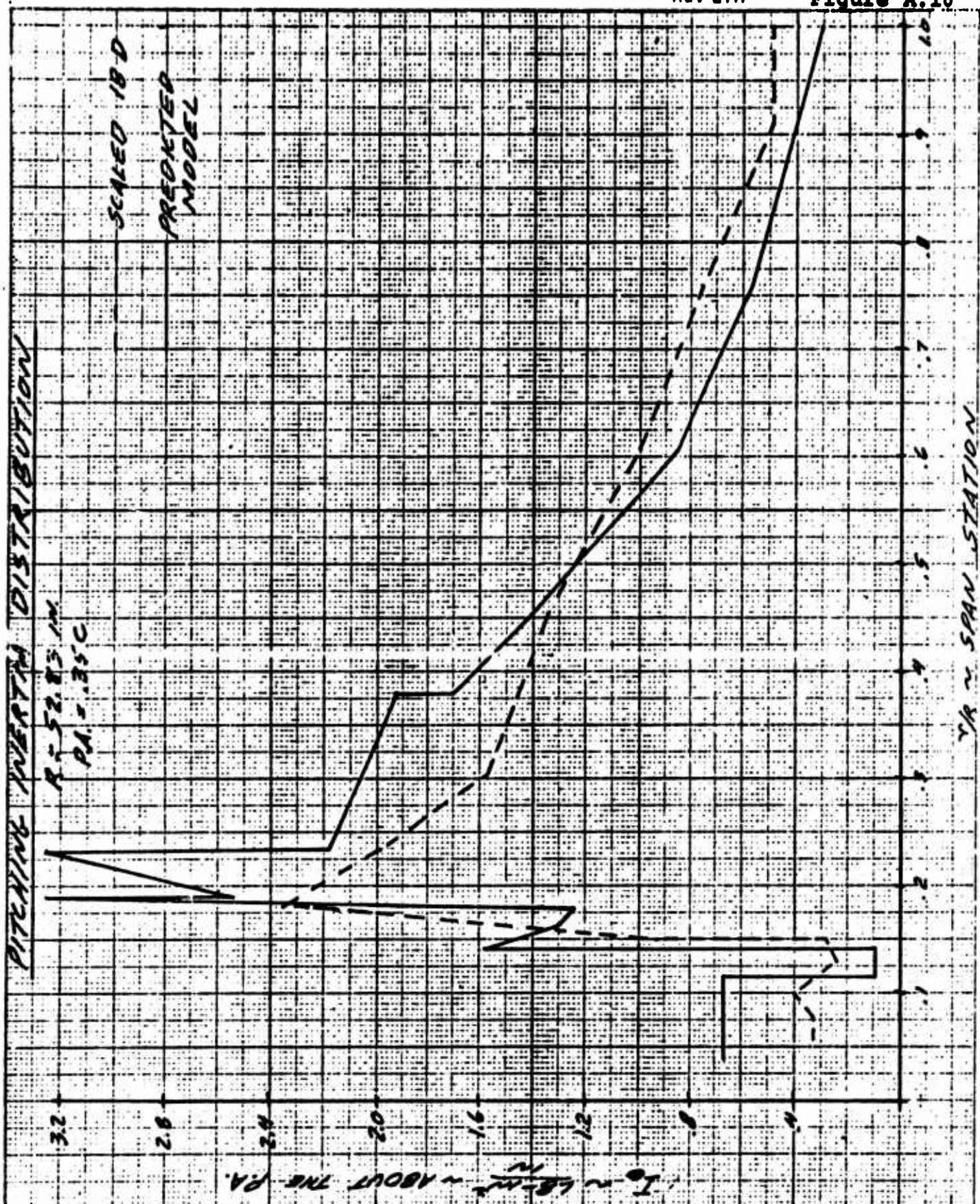
MODEL 170-1/3 SCALE ROTOR  
REV. 1002









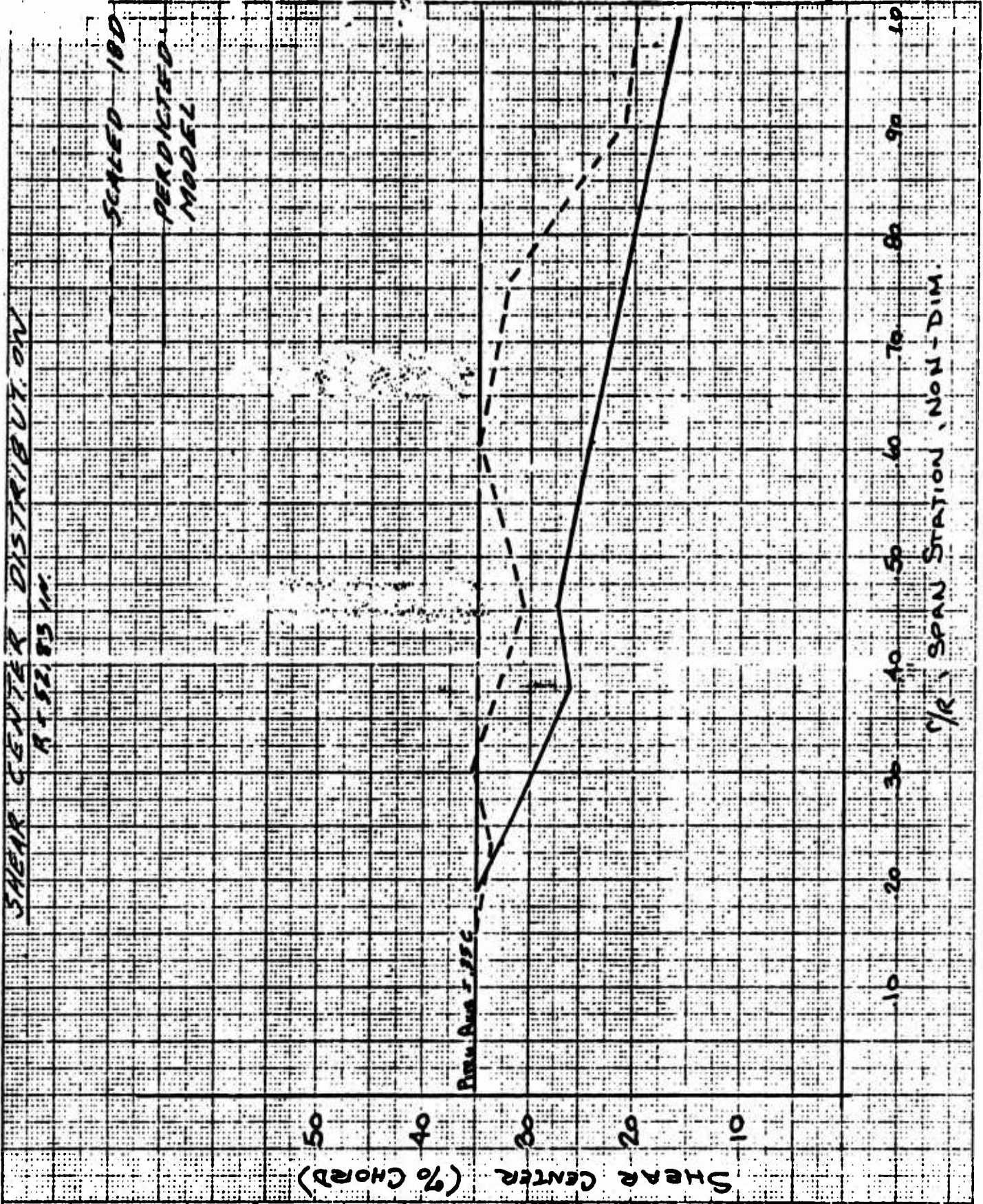


Calc	H.F. SILLER	8/5/70	REVISED	DATE
CHECK				
APPR				

MODEL 170 ~ 1/3 SCALE ROTOR

REV. 1002

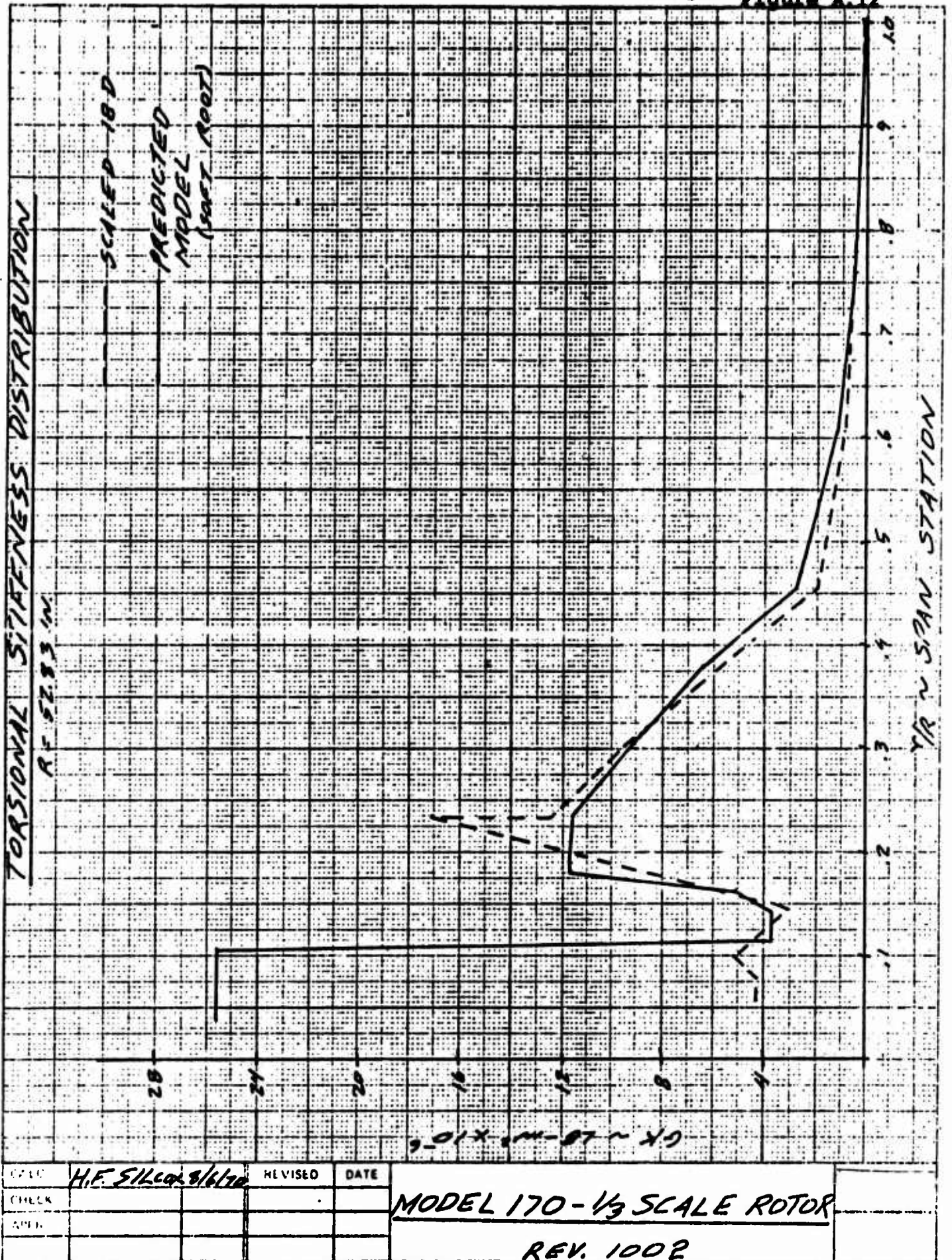
NOT REPRODUCIBLE



CALC			REVISED	DATE
CHECK				
APPR				

MODEL 170-1/3 SCALE ROTOR  
REV. 100 2







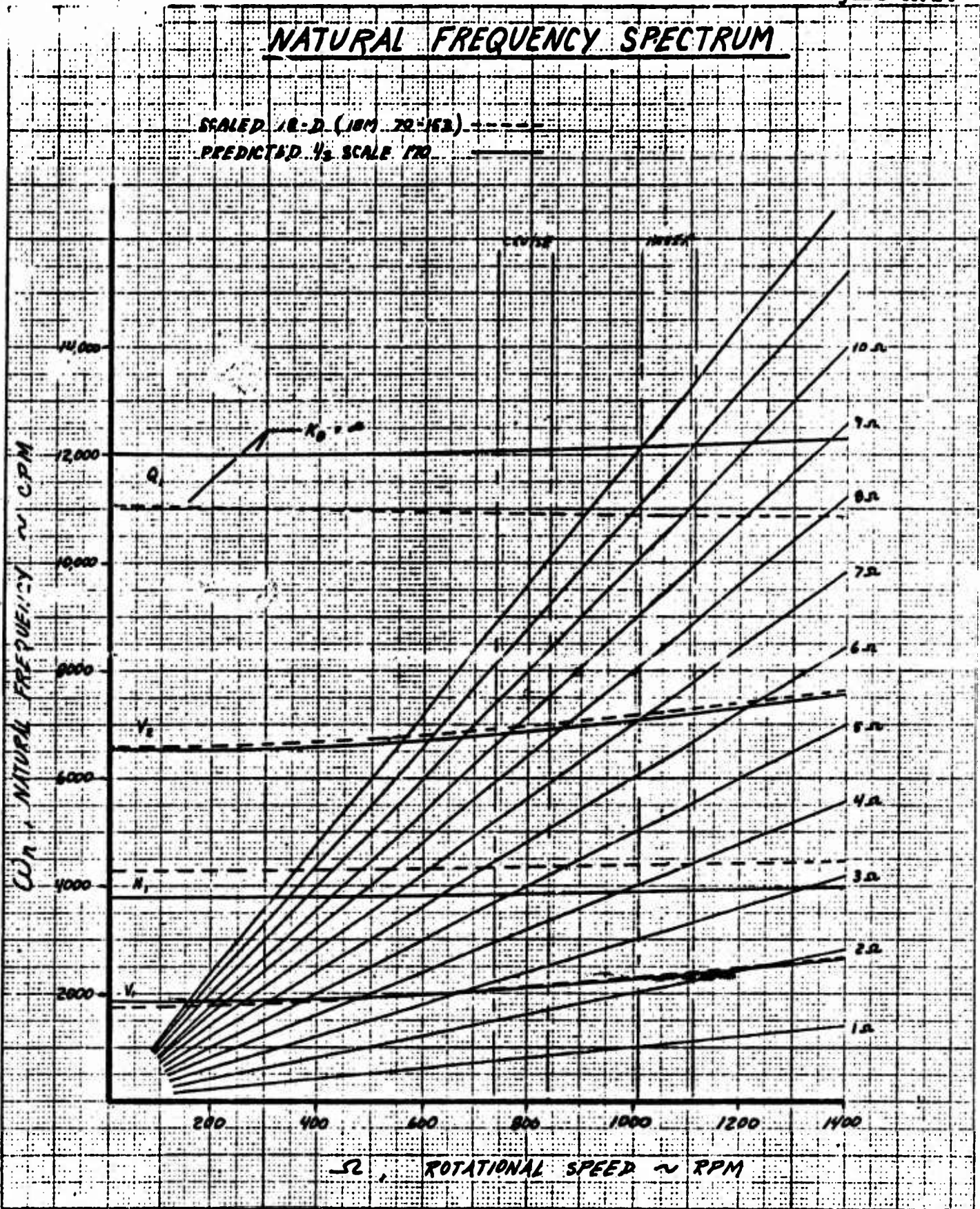
MODEL 170 - 1/3 SCALE

ACTUAL NATURAL FREQUENCIES

BLADE # MODE	PREDICTED (L-21)	71	72	73*	76	77
	CPM	CPM	CPM	CPM	CPM	CPM
(w <sub>1</sub> ) <sub>v</sub>	1840	1940	1940	1908		1980
(w <sub>2</sub> ) <sub>v</sub>	6518	6788	6811	6560		6700
(w <sub>3</sub> ) <sub>v</sub>						
(w <sub>1</sub> ) <sub>H</sub>	3778	4205	4366	4360		
(w <sub>2</sub> ) <sub>H</sub>						
(w <sub>1</sub> ) <sub>Q</sub>	12,000	11,800	11,900	11,400		

\* STAND BY BLADE DUE TO THICKNESS .12" GREATER THEN DESIGN.  
71, 72, & 73 RECORDED WITH HUB MOUNTED ON ROCKFORD PLATE.  
77 RECORDED ON DRTS.





CALC	R. DIRUSO	9/1/70	REVISED	DATE	<u>MODEL 170 - 1/3 SCALE</u>
CHECK					
APPR					

**APPENDIX B****B.1 MODEL INSTRUMENTATION AND DATA ACQUISITION SYSTEM****B.1.1 Model Instrumentation**

A tabulation of each item being recorded or monitored from the model is presented on Table B.1. This chart shows the following:

- a) The engineering units for each item
- b) The filter frequency cutoff for each data channel
- c) The anticipated range of data for each channel
- d) The allowable data range based on model capability
- e) The recording or display instrument for each channel of data.

**B.1.2 Five Component Balance**

The balance attaches to the aft end of the propeller stack and measures model thrust, normal force, side force, pitching moment, and yawing moment.

**B.1.3 Torque Shaft**

Torque measurements are obtained from strain gages located on the flexible coupling which prevents forces or moments, other than torque, from passing through the drive shaft.

**B.1.4 Propeller Rotational Speed and Aximuth Locator**

The propeller rpm is obtained from a 60-tooth gear located on the drive shaft and a magnetic proximity pickup which feeds a counter in the 1800 computer. The azimuth location of each propeller blade is determined from a second proximity pickup and a striker on the drive shaft. (See Figure B.2) which shows the azimuth location of the blades.

### B.1.5 Shaft Angle

The shaft angle relative to the sting was obtained from a rotary potentiometer that measures the angle between the propeller shaft and the sting which supports the model. The angular deflection of the sting due to center of gravity change and aerodynamic loading was measured by a pendulum potentiometer mounted at the end of the sting. The pendulum and rotary potentiometer readings were combined to provide the shaft angle relative to the remote wind axis.

### B.1.6 Control System

Remote control of cyclic pitch and collective pitch was provided by three hydraulic actuators controlled by an analog feedback system. This system provides step input of cyclic or collective pitch of 5° with rates up to 50 degrees/second. In addition sinusoidal inputs of cyclic pitch can be generated up to 60 CPS.

### B.1.7 Blade and Pitch Link

Two of the blades were strain gaged for flapwise, chordwise, and torsional bending moments. In addition to the blade strain gages, one pitch link was strain gaged.

### B.1.8 Data Acquisition System

The flow diagram of the wind tunnel data system used in this test is shown in Figure B.3. This data system can accept up to 120 channels from a model and the tunnel itself. These signals are routed as illustrated to an IBM 1800 computer for processing and data storage. The computed results are tabulated by a line printer. Final data is stored on magnetic tape.

A digital display of any nine channels is also available during testing for monitoring purposes. Dynamic data was continuously displayed on oscillographs. This provided assistance in preventing balance or structural limits from being exceeded.

For on-line data sampling rates of 6500 samples per channel/sec. was available. The sampling process is accomplished with channel switching devices called multiplexers (MPX). The channel band width was 2024 counts which was set in most instances to give the design allowables from Table B.1. The sample rate for the dynamic data was 2000 samples per channel per sec. Additional data reduction (harmonics analysis) of the dynamic data was conducted off-line on the IBM 360 series computer.

A

DATA CHANNEL IDENTIFICATION, DISPLAY AND RECORDING

FORM 46285 (12/65)

ITEM	UNITS	CPS RECORDING FREQUENCY	ANTICIPATED RANGE	ALLOWABLE*	DYNAMIC DATA DIGITAL TAPE	DYNAMIC DATA OSCILLOGRAPH	DYNAMIC DATA OSCILSCOPE	STEADY STATE COMPUTER	CONSOLE DISPLAY	AMPLITUDE METER DISPLAY	ON-LINE DYNAMIC DATA	AMP. METER PRINT-OUT
BALANCE												
Normal Force	Lb	1000	1000	2000+ 900	X	X	X	X X X X X X		X X X X X	X X X X X	
Axial Force	Lb	1000	300	1200+ 400	X							
Side Force	Lb	1000	300	1200+ 400	X							
Pitching Moment	Ft-Lb	1000	900	2000+ 700	X	X	X			X X X X X	X X X X X	
Rolling Moment	Ft-Lb	1000	500	2000+ 700	X							
Torque	Ft-Lb	1000	900	2000+ 700	X							
BLADES												
Flap Bending Moments												
Stat. 8.2 In	In-Lb	1000	3200+2550	3300+7000	X		X X			X X X	X X X	X X X
24.5 In	In-Lb	1000	2000+1000	2000+2600	X		X X			X X X	X X X	X X X
11.5 In*	In-Lb	1000	3200+2550	3300+6200	X							
Chord Bending Moments												
Stat. 8.2 In.	In-Lb	1000	1890+1800	1750+7000	X		X X X			X X X	X X X	X X X
24.5 In.	In-Lb	1000	1000+1000	1750+4500	X							
11.5 In*	In-Lb	1000		1750+7000	X							
Blade Torsion												
Stat. 8.2 In.	In-Lb	1000	150+ 160	1400+2270	X							X

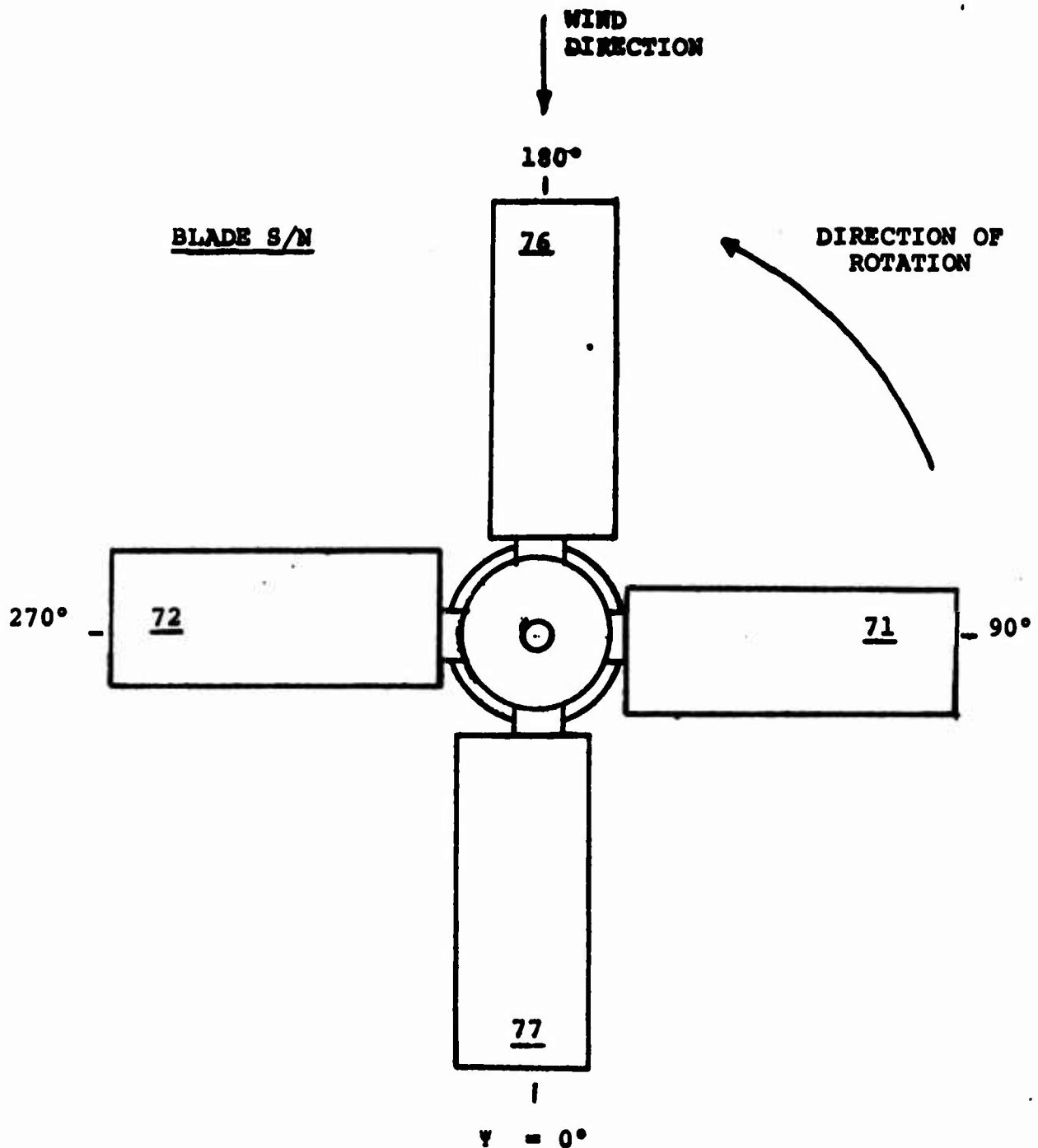


B

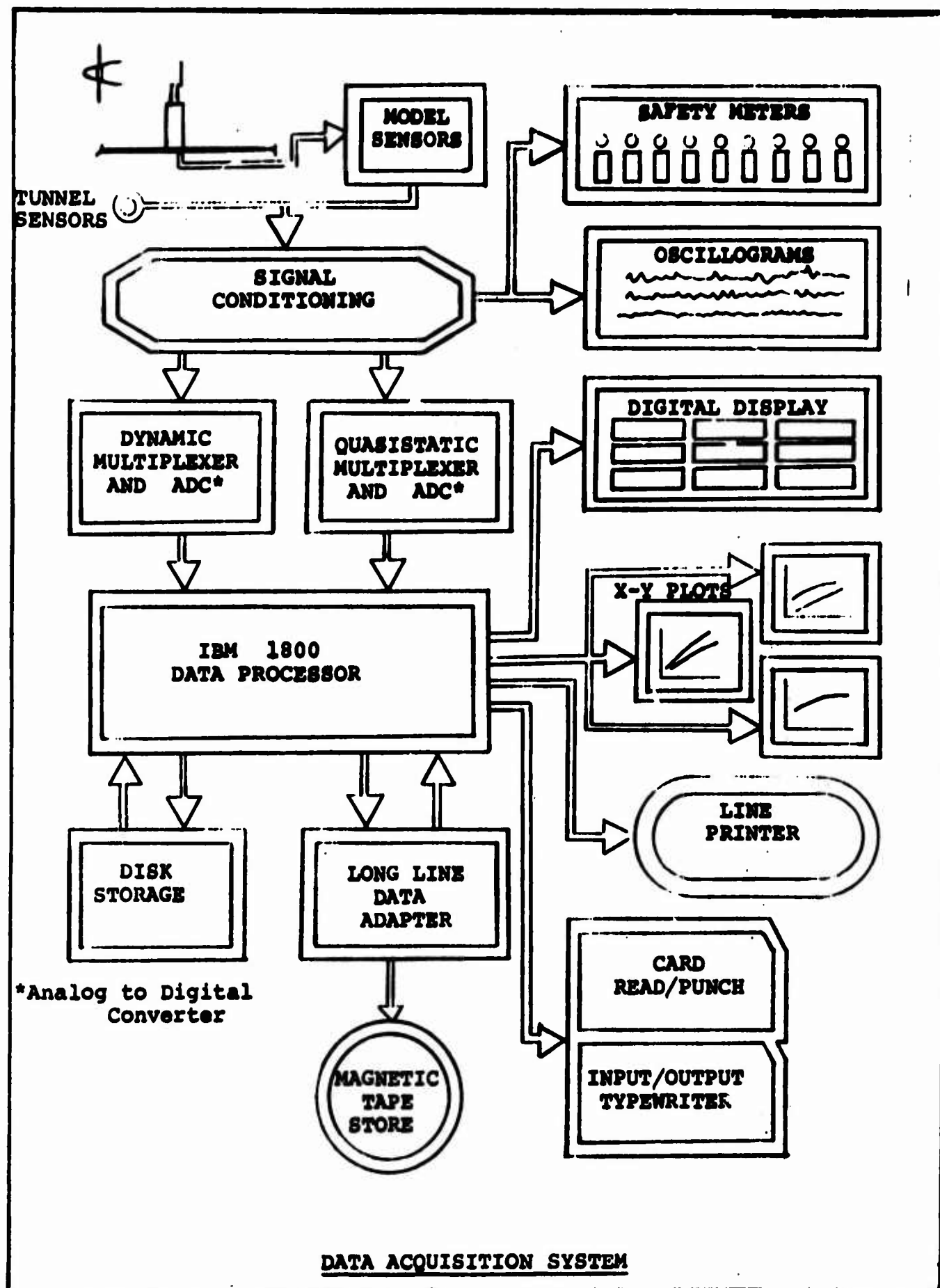
Blade Torsion Stat. 8.2 In	In-Lb	1000	150+ 160	1400+2270	X		X		X		X		X		X
HUB AND CONTROLS															
Pitch Link	Lb	1000		2100+ 650	X		X								
Collective Pitch	Deg	1000													
Longitudinal Cyclic	Deg	1000													
Lateral Cyclic	Deg	1000													
Shaft Angle	Deg	D.C.		0											
Delta Shaft Angle	Deg	D.C.		0 to 99°											
Rotor RPM	RPM	500		+ 2 Deg	X										
Rotor 1/Rev	RPM	500		1100	X										
TEMPERATURES															
Thrust Bearing	Deg F	D.C.													
Gearbox Output				160											
Shaft				160											
Motor Upper				160											
Bearing				160											
Motor Upper				220											
Bearing				220											
Stator Winding				220											
Stator Winding				220											
Stator Winding				220											
Motor Lower				145											
Bearing															
Gearbox Case				160											
Lower Slipring				160											
Bearing				160											
Pitch Bearing				160											
Housings				160											
Stationary				160											
Swashplate				160											
Upper Stack				250											
Bearing															
Motor Rotor															

\*BALANCE ALLOWABLES ARE REFERED TO THE BALANCE CENTERLINE

AZIMUTH LOCATION OF BLADES REFERENCED  
TO THE 1/REV INDICATOR



- NOTES:
- (1) For Runs 1 - 11, Blade S/N 77 was prime instrumented blade.
  - (2) For Runs 12 - 87, Blade S/N 76 was prime instrumented blade.
  - (3) Instrumented pitch link was on Blade S/N 77.



Data Reduction

At each test point, measurements were taken for computing and printing out on-line the quasistatic data listed below:

Density, $\rho$	slugs/ft <sup>3</sup>
Dynamic pressure, $q$	lb/ft <sup>2</sup>
Propeller RPM	
Shaft Angle, $\alpha_s$	degrees
Shaft torque (includes friction on cyclic pitch hub)	ft. lbs.
Thrust, $T$	lbs.
Normal force	lbs.
Side force	lbs.
Pitching moment (about hub centerline, See Figure 5.1)	ft.lbs.
Yawing moment (about hub centerline, See Figure 5.1)	ft.lbs.

Propeller forces and moments measured from the internal balance were reduced to coefficient form in propeller terminology. The propeller-type coefficients computed and printed out on-line were as follows:

$$\text{Advance ratio, } J = \frac{V}{nD}$$

$$\text{Thrust coefficient, } C_T = \frac{T}{\rho n^2 D^4} = C_T$$

$$\text{Prop pitching moment coefficient, } C_{M_P} = \frac{\text{Pitching Moment} = \text{CPM}}{\rho n^2 D^5}$$

$$\text{Shaft power coefficient, } C_P = \frac{\text{Shaft power}}{\rho n^3 D^5} = C_P$$

$$\text{Prop normal force coefficient, } C_{NF} = \frac{\text{Normal force}}{\rho n^2 D^4} = C_{NF}$$

$$\text{Prop side force coefficient, } C_{SF} = \frac{\text{Side force}}{\rho n^2 D^4} = C_{SF}$$

$$\text{Prop yawing moment coefficient, } C_{YM} = \frac{\text{Yawing moment}}{\rho n^2 D^5} = C_{YM}$$

#### Spinner and Hub Aerodynamic Tares

The spinner and hub aerodynamic tares were normalized as follows:

Thrust	TRB/q
Normal Force	NFRF/q
Side Force	SFRF/q
Pitching Moment	PMRB/q
Yawing Moment	YMRB/q
Torque	QRB/q

These data were curvefitted as a function of shaft angle (°SC) and then at a particular shaft angle applied to the data with blades on as a function of tunnel dynamic pressure. (See Appendix E).

On-line Computer Output

F.B.	Flapwise bending moment, in-lb.
C.B.	Chordwise bending moment, in-lb.
B.W.	Blade torsional moment, in-lb.
RPM	Propeller speed(revolutions per minute) (n revolutions per second)
$\Omega R$	Propeller tip speed, fps
J	Propeller advance ratio
VT	Tunnel velocity, fps
$\alpha_s$	Shaft angle of attack, deg.
$\alpha_{sc}$	Corrected shaft angle of attack, deg.
M(1) (90)	Advancing blade tip mach number
M(2) (270)	Retreating blade tip mach number
PT	Total pressure, lb/ft <sup>2</sup>
PS	Static pressure, lb/ft <sup>2</sup>
TS	Static temperature, deg. F
RHOT	Tunnel air density slugs/ft <sup>3</sup>
QT	Tunnel dynamic pressure, psf
VS	Velocity of sound fps
MT	Tunnel Mach number
AIRVC	Corrected tunnel velocity, fps
RN/FT	Reynolds Number per foot 1/ft
VMBGP	Velocity of moving belt ground plane .fps
QS	Slipstream dynamic pressure, psf
T/A	Disk loading, psf
NFRB	Reference body normal force, lb
PMRB	Reference body pitching moment, lb
TRB	Reference body thrust, lb
SFRF	Reference body side force, lb
YMRF	Reference body yawing moment, ft-lb
QRF	Reference body torque, ft-lb
CNF	(3600)NFRG/ (RPM) <sup>2</sup> (2R) <sup>4</sup>
CPM	(3600)PMRB/ (RPM) <sup>2</sup> (2R) <sup>5</sup>
CT	(3600)TRB/ (RPM) <sup>2</sup> (2R) <sup>4</sup>
CSF	(3600)SFRB/ (RPM) <sup>2</sup> (2R) <sup>4</sup>
CYM	(3600)YMRB/ (RPM) <sup>2</sup> (2R) <sup>5</sup>
CP	(7200 )QRB/ (RPM) <sup>2</sup> (2R) <sup>5</sup>
CTS	(TRB/A)/QS
FM	Figure of merit
EC	Cruise efficiency
REF	$[(NFRB)^2 + (SFRB)^2]^{1/2}$ ;PHIF-Angular location of resolved vector

D150-10040-1

On-line Computer Output (Cont.)

REN  $[(YMRB)^2 + (PMRB)^2]^{1/2}$  , PHIM-Angular  
location of resolved vector  
TO Thrust offset

Input Constants

Propeller Diameter	8.76 Ft.
Propeller Disk Area	60.24 ft <sup>2</sup>
Shaft Length (Pivot Point to Hub $\varnothing$ )	93.3 in.
Tunnel Test Section Cross Sectional Area	*99,999 Ft <sup>2</sup>

\*Do not apply tunnel wall corrections.

APPENDIX CTEST PROCEDURE**C.1 PRE-TEST FUNCTIONAL CHECKOUT AND CALIBRATION****C.1.1 Functional Checkout**

After the model and DRTS were mated and assembled, the following work items were accomplished to insure minimum downtime during the test period.

- a) Calibrate the Balance
  - 1) Without pressurizing the hydraulic lines that "cross" the balance.
  - 2) With the hydraulic lines pressurized to maximum required pressure.
- b) Experimentally verification of the cyclic and collective pitch envelope.
- c) Determination of the effect on balance sensitivity and loads due to step and oscillatory inputs to collective and cyclic pitch.
- d) Calibration of the instrumented pitch link.
- e) After all wire packs were installed and mechanical build-up was complete, a run was conducted at 1100 rpm to evaluate the total dynamic system, including dynamic balancing and evaluation of DRTS and model temperatures.
- f) A check was made for proper operation of the total integrated control system for collective and cyclic pitch.
- g) The blades and fairings were installed to insure proper fit and the strain gages on blades S/N 77 and 76 were calibrated.
- h) Calibrations of the cyclic and collective pitch were conducted. The longitudinal cyclic pitch was input at 170 degrees azimuth.



### C.1.2 Calibration

This section provides calibration data relating to the balance, blades, pitch link and swashplate controls.

#### a) Balance

The balance interaction matrix, as defined during the test is presented in Table C.1.

#### b) Blades

The initial calibration results of blade flap, chord and torsional moment are presented as Figures C.1 to C.3. The scatter in the torsional moment calibration is attributed to the gage being located inboard of the pitch bearing.

#### c) Pitch Link

The results of the pitch link calibration are shown in Figure C.4. The shift in the slope of this data is attributed to the load being applied to the blade outboard of the pitch bearings and the pitch link being inboard of these bearings. The calibration results are repeatable and since the slope of the curve is the same for increasing and decreasing loads, the resulting data is believed to be valid.

#### d) Swashplate Control System

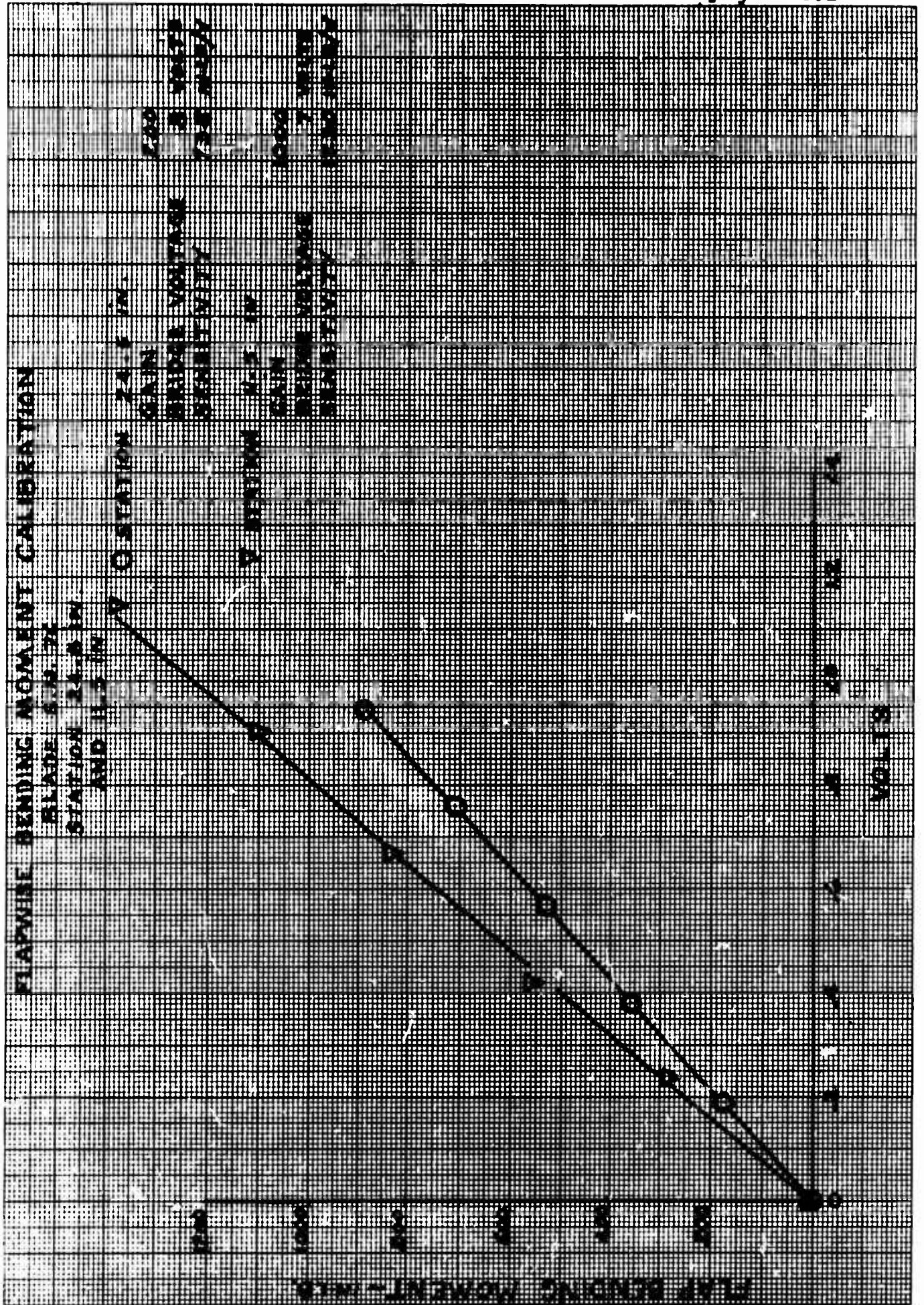
The calibration results of collective and longitudinal cyclic pitch are shown in Figures C.5 to C.6. This data is presented as actual pitch settings, from inclinometer readings, versus the control system and computer readout. At the higher values of collective pitch settings and at the higher value of cyclic there is about .5 degrees error in longitudinal cyclic setting. These errors are due to the non-linearity in the kinematics of the swashplate and hub controls.

TABLE C.1

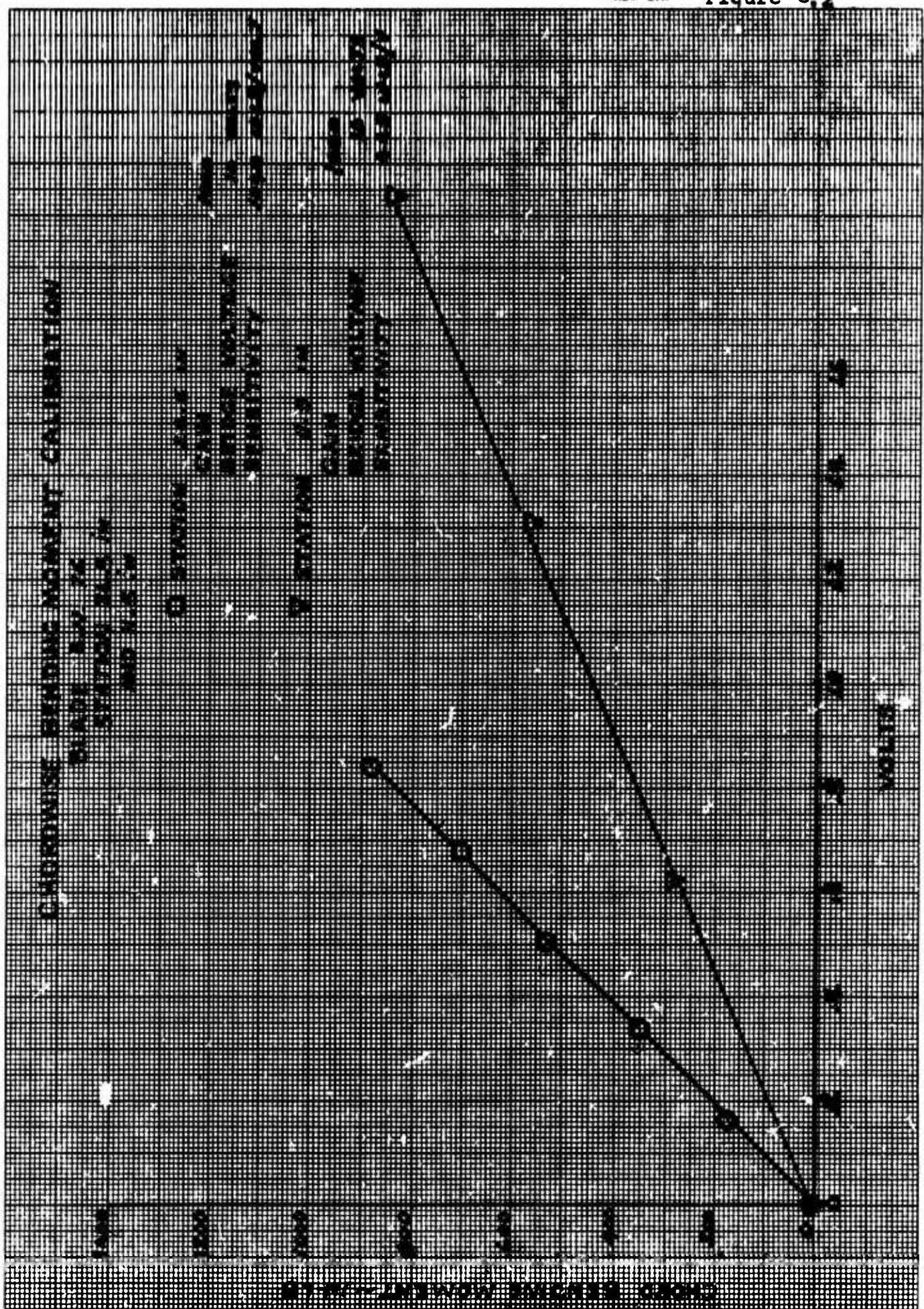
D170-100400-1

BALANCE "C" MATRIX BV 5007 RUNS 1 to 92

	NF	FM	AF	SF	YM	RM
N	C100 1.000	C127 -.028	C154 -.00342	C181 .00523	C208 0	C235 .00533
P	C101 0	C128 1.000	C155 -.0498	C182 -.0044	C209 0	C236 .00966
A	C102 -.0660	C129 2.48	C156 1.000	C183 -.0204	C210 0	C237 -.0123
S	C103 -.03437	C130 0	C157 -.0207	C184 1.000	C211 0	C238 2.465
Y	C104 0	C131 0	C158 0	C185 0	C212 1.000	C239 0
R	C105 -.00875	C132 -.003	C159 0	C186 -.04835	C213 0	C240 1.000
N <sup>2</sup>	C106 0	C133 -.00000906	C160 -.00000314	C187 0	C214 0	C241 0
P <sup>2</sup>	C107 .0000122	C134 0	C161 0	C188 0	C215 0	C242 0
A <sup>2</sup>	C108 .0000535	C135 0	C162 0	C189 0	C216 0	C243 0
S <sup>2</sup>	C109 0	C136 0	C163 0	C190 0	C217 0	C244 0
Y <sup>2</sup>	C110 0	C137 0	C164 0	C191 0	C218 0	C245 0
R <sup>2</sup>	C111 .00000944	C138 0	C165 0	C192 0	C219 0	C246 0
N.P	C112 0	C139 0	C166 0	C193 0	C220 0	C247 0
N.A	C113 0	C140 0	C167 0	C194 0	C221 0	C248 0
N.S	C114 0	C141 0	C168 0	C195 0	C222 0	C249 0
N.Y	C115 0	C142 0	C169 0	C196 0	C223 0	C250 0
N.R	C116 0	C143 0	C170 0	C197 0	C224 0	C251 0
P.A	C117 .0000600	C144 0	C171 0	C198 0	C225 0	C252 0
P.S	C118 0	C145 0	C172 0	C199 0	C226 0	C253 0
P.Y	C119 0	C146 0	C173 0	C200 0	C227 0	C254 0
P.R	C120 0	C147 0	C174 0	C201 0	C228 0	C255 0
A.S	C121 0	C148 0	C175 0	C202 0	C229 0	C256 0
A.Y	C122 0	C149 0	C176 0	C203 0	C230 0	C257 0
A.R	C123 0	C150 0	C177 0	C204 0	C231 0	C258 0
S.Y	C124 0	C151 0	C178 0	C205 0	C232 0	C259 0
S.R	C125 0	C152 0	C179 0	C206 0	C233 0	C260 0
Y.R	C126 0	C153 0	C180 0	C207 0	C234 0	C261 0





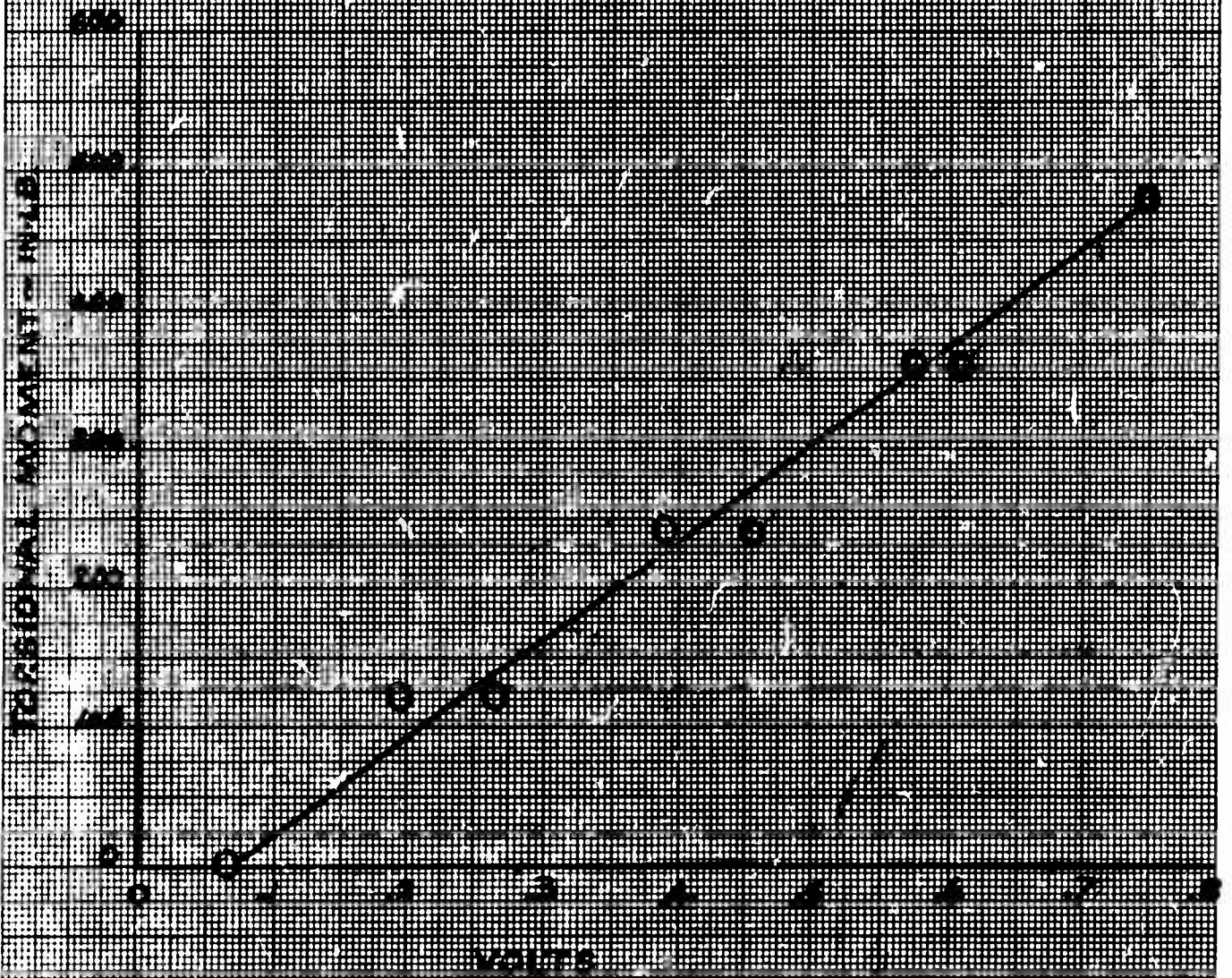


NUMBER  
REV LTR

D170-10040-1  
Figure C.3

TORQUE-MOMENT CALIBRATION  
BLADE 3.51 74  
STATION 2.10 IN

DATE: 10/1/74  
BY: J. J. J. J.  
CHECKED: J. J. J. J.  
SENSITIVITY: 1000

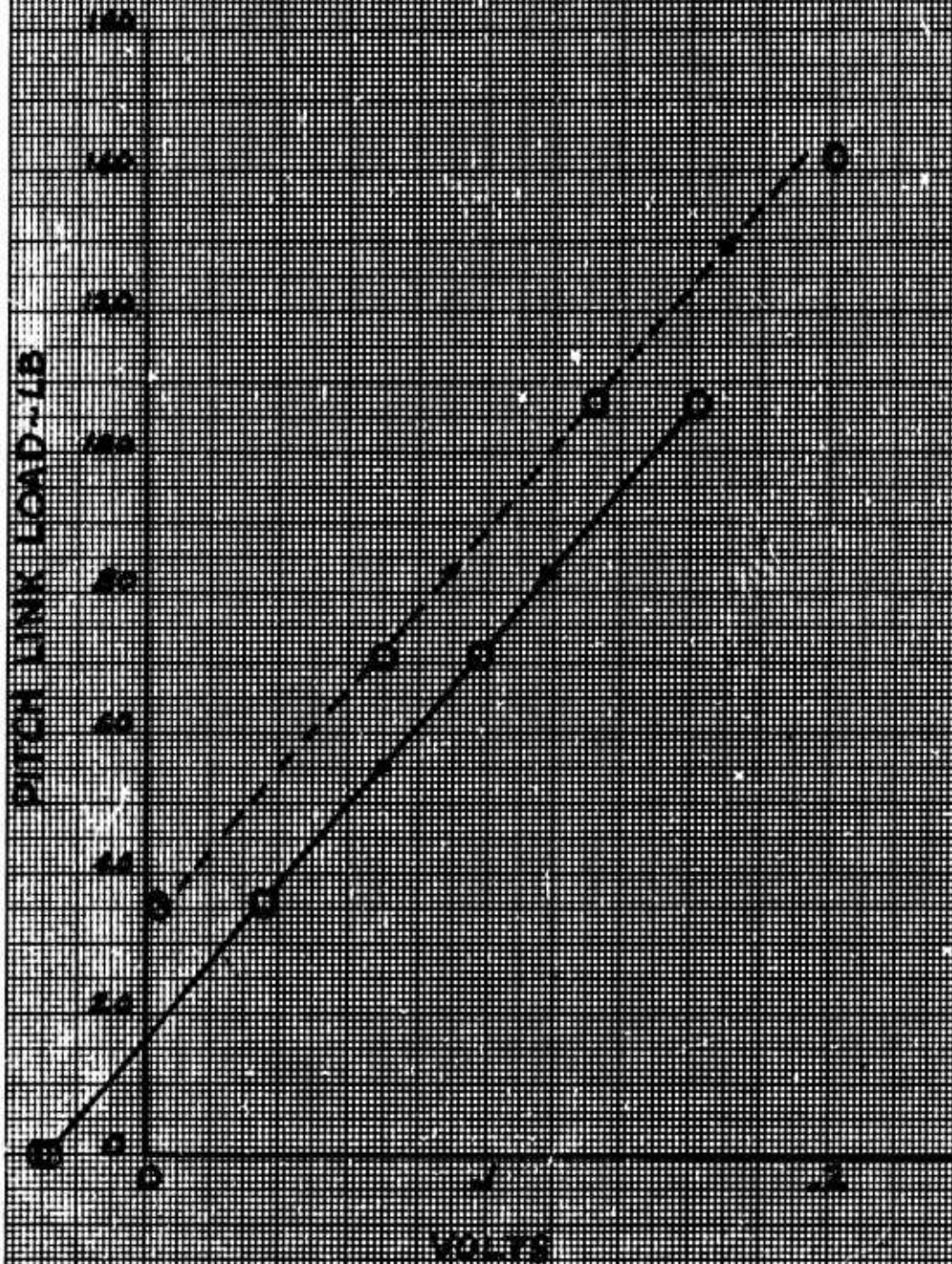




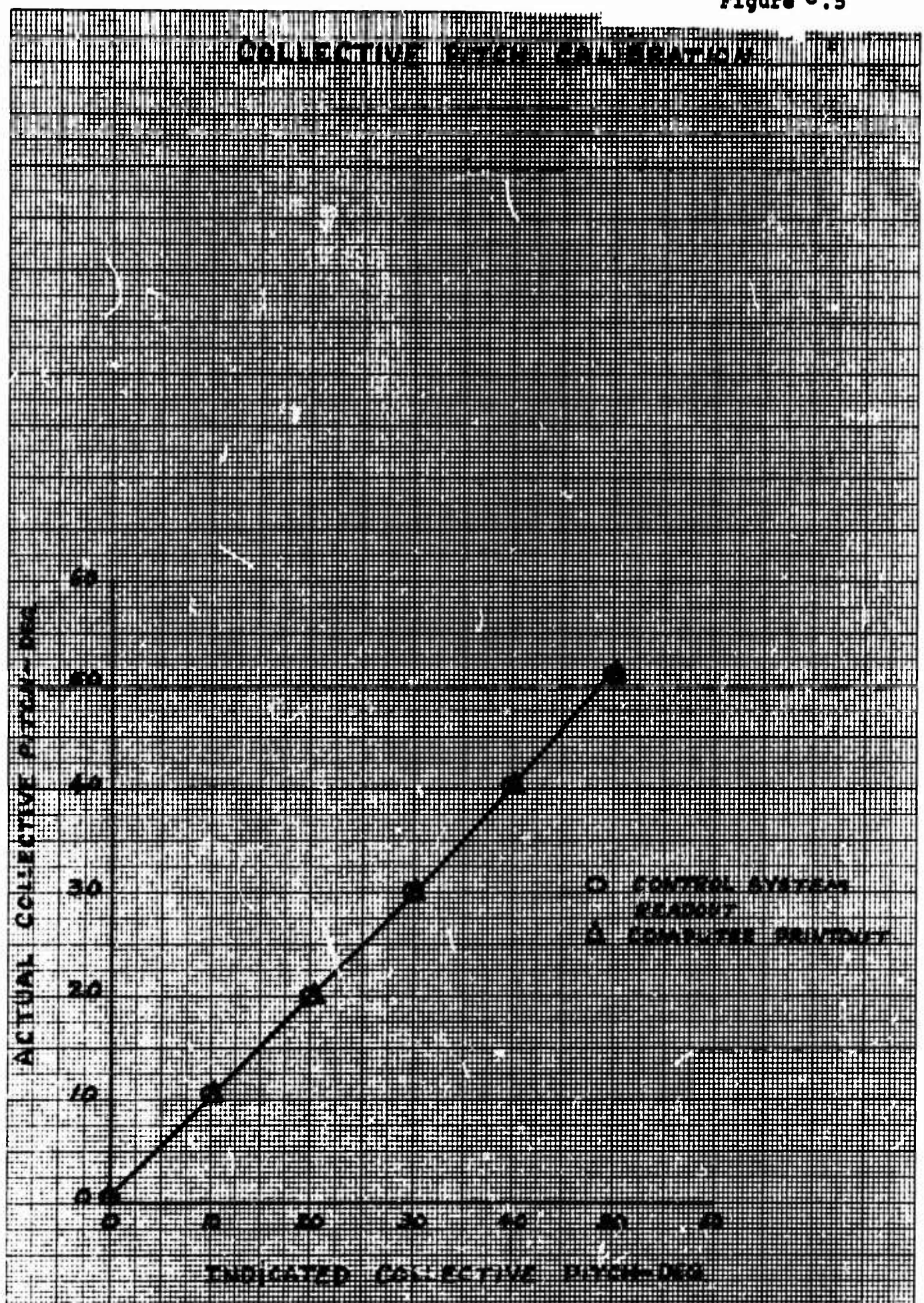
# PITCH LINK CALIBRATION

FOR BLADE A-1-70

GAIN 1000  
BRIDGE VOLTAGE 15 V  
SENSITIVITY 250 LB



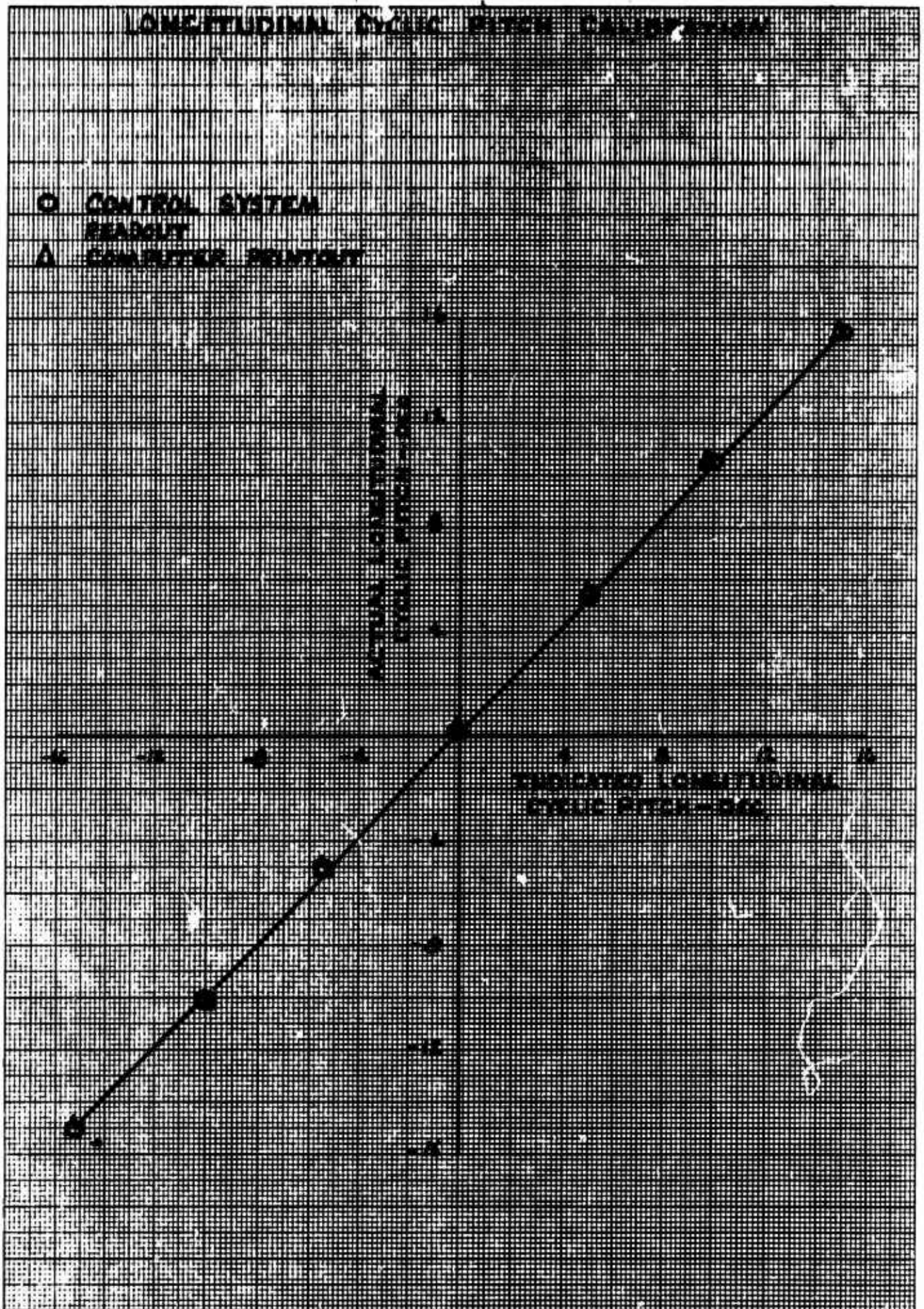




EUGENE DIETZGEN CO.  
MADE IN U. S. A.

NO. 340R-MP DIETZGEN GRAPH PAPER  
MILLIMETER







## C.2 OPERATING PROCEDURE AND SYSTEM REQUIREMENTS

### C.2.1 Operating Procedures

#### C.2.1.1 Testing

The procedures for a typical test run in forward flight were as follows:

- a) Record the wind-off zeros at 90° shaft angle. Record the weight tares at the shaft angles specified by Data Engineering and record a wind off data point. Set the desired collective pitch and cyclic pitch. Set rotor speed to some nominal value (200 to 400 rpm). Start the tunnel and bring both the rotor speed and tunnel speed to the desired values by making incremental changes to both simultaneously, making sure that conditions are not encountered which result in large blade loads. When stabilized conditions were reached, incremental changes to shaft angle were made recording data at each shaft angle until a load limit was approached or until the desired data had been collected. Then the shaft angle was returned to the initial point and the next run started. When shutting the system down, the shaft angle and collective pitch were set for about zero thrust, then the tunnel speed was decreased followed by decreasing the rotor speed in such a way that a slightly positive thrust was maintained. After shutdown, a wind-off data point was taken and compared with the pre-run point. Similar procedures were followed for rotor rpm, advance ratio, collective or cyclic pitch sweeps.
- b) For hover testing the test section roof, floor and walls were removed. Hover testing procedures involved recording wind-off zeros at zero shaft angle, weight tares as a function of shaft angle, a wind off data point, then setting the desired collective and cyclic pitch. The rotor was then started and data recorded at incremental values of rotor speed until a load limit was reached or the required data had been collected. The rotor speed was then decreased and a new collective pitch set and the rotor speed sweep repeated. After shutdown, a wind off data point was recorded and compared with pre-run

D170-10040-1

values. This same procedure was used for conducting collective or cyclic pitch sweeps at constant rotor speed.

← CENTERLINE

#### C.2.1.2 Aerodynamic Hub Tares (See Appendix E)

Aerodynamic hub tares were determined by removing the blades and recording data over the shaft angle range at a nominal  $q$  and rotor speed. This data was divided by  $q$  and stored for use in correcting the data from blades on testing. The tunnel walls and roof were removed for the hub tare runs.

#### C.2.1.3 Blade Balancing and Tracking

The rotor system was dynamically balanced by monitoring the unbalance from the balance pitching moment flexure and compensating for the unbalance by adding weights to the hub. The blades were tracked by use of a strobe light and corrections made by adjusting the length of individual pitch links at a nominal rotor speed for various collective pitch settings.

#### C.2.1.4 Emergency Shutdown Procedures (No emergencies encountered)

There are numerous reasons why an emergency shutdown could be required. The more obvious ones are listed below along with the shutdown procedures:

##### a) Structural Failure of Critical Model Component

- 1) Activate emergency shutdown of tunnel at most rapid deceleration rate.
- 2) Activate emergency shutdown of model at most rapid deceleration rate.

##### b) Loss of Lubrication of Model

- 1) Activate emergency shutdown of tunnel at most rapid deceleration rate.
- 2) Tilt rotor shaft forward and decrease rotor speed to maintain near zero rotor thrust.

D170-10040-1

c) Loss of Power to Tunnel Fan

- 1) Tilt rotor shaft forward and decrease rotor speed to maintain slightly positive rotor thrust.

d) Loss of Power to Model Rotor

- 1) Activate emergency shutdown of tunnel at most rapid deceleration rate and tilt rotor shaft forward.

e) Loss of Power to Model Rotor and Tunnel Fan

- 1) Tilt rotor shaft forward.

C.2.2 DRTS Systems Requirements

The following items give the test stand systems requirements for operation, and the pre-run checkout:

- a) Pressure gage for brake at 1200 to 1600 psi.
- b) Sump pump running.
- c) Upper bearing lube pump on pressure at 25 psi at pump.
- d) Gearbox pump running, flow set at 4-1/2 gals/min.
- e) Observe sight tube to check proper oil flow.
- f) Check coolant water is running with main valve set at 60 psi.
- g) Motor operates at 2 volts/cycle.
- h) Hydraulic pressure for swashplate control system set at 1500 psi.

D170-10040-1

APPENDIX D

DETAILED RUN LOG

COPY EXTENDING BEYOND RIGHT  
MARGIN LINE - MORE THAN 1  
CHARACTER WILL BE RETURNED  
TO RECOMPILER

NUMBER D170-10040-1  
REV LTR Table D.1

PREP.	CHK.	APPR	REVISED	DATE	CONFIGURATION	TYPE OF RUN	WT. TARE RUN	$\theta_{1/3}$ DEG	$B_1$ DEG	$\alpha_3$ DEG	RPM	DATE / TIME
					1 PHS	Func Check	1	0	0	90	%	11-12-70
					2 PHS	Motor	1	5	1	90	%	- - -
					3 PHS	-	1	0	0	90	850	- - -
					4 PHS	-	1	0	0	90	1050	- - -
					5 PNS	-	1	14	10	90	850	- - -
					6 PHS	-	1	0	0	90	1050	11-13-70
					7 PHS	-	1	14	1	90	%	- - -
					8 PHS	-	1	-4	0	90	1050	- - -
					9 PNS	-	1	0	0	90	1050	- - -
					10 PHS	-	1	5	3	90	1050	- - -
3)					$\theta_{1/3} = 9, 4, 8, 12, 16, 20^\circ$							
4)					$\theta_{1/3} = 0, 4, 8, 12, 16, 20^\circ$							
5)					$B_1 = 0, 1, 2, 3, 4, 5, 6, 7, 8, 9, 10, 11, 12, 13, 14, 15, 16, 17, 18, 19, 20^\circ$							
6)					$\theta_{1/3} = 8, 10, 12, 14, 16, 18, 20^\circ$							
7)					$B_1 = 0, 2, 4, 6, 8, 10, 12, 14, 16, 18, 20^\circ$							
8)					$B_1 = 0, 2, 4, 6, 8, 10, 12, 14, 16, 18, 20^\circ$							
9)					$B_1 = 0, 2, 4, 6, 8, 10, 12, 14, 16, 18, 20^\circ$							
10)					$B_1 = 2, 4, 6, 8, 10, 12, 14, 16, 18, 20^\circ$							

1/3 SCALE V/STOL PROP  
DATS

BVWT  
066  
VR070R-1

PREP.		REVISD		DATE		1/3 SCALE V/STOL PROP										BVWT	
CHK.						DRTS										066	
APPR																VR070R-1	

RUN NO.	CONFIGURATION	TYPE OF RUN	WT. OF TARE RUN	$\Theta_s$ DEG	B, DEG	$d_s$ DEG	RPM	DATE / TIME
11	PHS	1	1	16	0	90	0	11-13-70
12	PHS	12	12	12	0	90	100	11-17-70
13	PHS	12	12	14	6	90	100	- - -
14	PHS	12	12	14	7	90	100	- - -
15	PHS	12	12	5	6	90	100	- - -
16	PHS	12	12	20	8	90	100	- - -
17	PHS	12	12	12	10	90	850	- - -
18	PHS	12	12	14	13	90	850	- - -
19	PHSWFL	12	12	0	0	90	100	11-18-70
20	PHSWFL	12	12	14	6	90	100	- - -

12) THRUST OFFSET CALCULATION COMPLETED ON COMPUTER PRINTOUT  
SINK CONVENTION FOR B, FOR RUNS 1-12 LEADING EDGE DOWN ON ADVANCING  
BLADE IS POSITIVE. AFTER RUN 12 LEADING EDGE UP ON ADVANCING BLADE  
IS POSITIVE  
PRIME INSTRUMENTED BLADE IS NOW 5 IN. 76 WITH 12, 13, 14 AND 20 AT  
STATION 12.5 IN.  
Bys = 0.10, 0.14, 0.15, 0.16, 0.20  
AFTER RUN 14 CRACKS IN BL. 12, 13, 14, 15, 16, 17, 18, 19, 20  
170 B, 2 0.13, 0.0, 0.0, 0.  
180 B, 2 0.14, 0.14, 0.14, 0.14, 0.  
190 B, 2 0.13, 0.13, 0.13, 0.13, 0.  
200 B, 2 0.13, 0.13, 0.13, 0.13, 0.  
210 B, 2 0.13, 0.13, 0.13, 0.13, 0.  
220 B, 2 0.13, 0.13, 0.13, 0.13, 0.  
230 B, 2 0.13, 0.13, 0.13, 0.13, 0.  
240 B, 2 0.13, 0.13, 0.13, 0.13, 0.  
250 B, 2 0.13, 0.13, 0.13, 0.13, 0.  
260 B, 2 0.13, 0.13, 0.13, 0.13, 0.  
270 B, 2 0.13, 0.13, 0.13, 0.13, 0.  
280 B, 2 0.13, 0.13, 0.13, 0.13, 0.  
290 B, 2 0.13, 0.13, 0.13, 0.13, 0.  
300 B, 2 0.13, 0.13, 0.13, 0.13, 0.



PREP.	CHK.	APPR.	REVISD	DATE	RUN NO.	CONFIGURATION	TYPE OF TARE RUN	WT. RUN	Q <sub>16</sub> DEG	B <sub>1</sub> DEG	Q <sub>16</sub> DEG	RPM	J	d <sub>r</sub>	d <sub>s</sub>	DATE / TIME
					21	PHSWFL	UNDER	12	0	0	90	1100	0	EXT.	EXT.	11-18-70
					22	PHSWFL	-	12	14	6.6	90	1100	0	-	-	-
					23	PHSWFL	-	12	10	6.6	90	1100	0	-	-	-
					24	PHSWFL	-	12	20	6.6	90	1100	0	-	-	-
					25	PHSWFL	-	12	14	2	90	1100	0	-	-	-
					26	PHS	-	12	14	0	90	1100	0	0	0	-
					27	PHS	TRAMP	12	14	0	90	1100	.20	0	0	-
					28	PHS	-	12	14	0	90	1100	.32	0	0	-
					29	PHS	-	12	14	0	90	1100	.32	0	0	-
					30	PHS	-	12	14	0	90	1100	.32	0	0	11-19-70
<div>1/3 SCALE V/STOL PROP DRTS</div>					21)	Q <sub>16</sub> = 0.8, 10, 12, 15, 16, 18, 20										
					22)	B <sub>1</sub> = 0.13, 1.6, 2										
					23)	B <sub>1</sub> = 0.13, 1.6, 0										
					24)	B <sub>1</sub> = 0.13, 1.6, 0										
					25)	TEST SECTION WALLS, FLOOR AND ROOF EX-MODEL FIRST POINT BY 165 IN.										
<div>REACHED THE ALLOWABLE PER MOMENT FOR 5147. 11-18-70</div>					30)											
<div>BVWT 066 VR070R-1</div>																

PREP	CHK.	APPR	REVISD	DATE	RUN NO.	CONFIGURATION	TYPE OF RUN	WT. TARE RUN	$\Theta_{HS}$	B.	$\alpha_s$	RPM	J	$\delta_F$	$\delta_s$	DATE / TIME
					31	PHS	TRANS	12	8/14	0	30/75	1100	.39			11-19-70
					32	PHS	"	12	10/14	0	30/75	1100	.50			"
					33	PHS	"	12	14	0	30	1100	.75			"
					34	PHS	"	12	14	6-7	30/75	1100	.20			"
					35	PHS	"	12	14	5-10	30/75	1100	.35			"
					36	PHS	"	12	14	5-10	30	1100	.39			"
					37	PHS	"	12	14	5-10	30	1100	.50			"
					38	PHS	"	12	14	5-10	30	1100	.55			"
					39	PHS	"	12	14	5-10	40	1100	.35			"
					40	PHS WFL	"	12	14	5-10	30	1100	.20 EXT.			11-20-70
30) REACHED KM. MOMENT ALLOWABLE FOR STATION ME IN																
34) $\alpha_s$ 30 30 30 30 30 30 30 30 30 30 30 30 30 30 30 30 30																
35) $\alpha_s$ 30 30 30 30 30 30 30 30 30 30 30 30 30 30 30 30 30																
36) $\alpha_s$ 30 30 30 30 30 30 30 30 30 30 30 30 30 30 30 30 30																
37) $\alpha_s$ 30 30 30 30 30 30 30 30 30 30 30 30 30 30 30 30 30																
38) $\alpha_s$ 30 30 30 30 30 30 30 30 30 30 30 30 30 30 30 30 30																
39) $\alpha_s$ 30 30 30 30 30 30 30 30 30 30 30 30 30 30 30 30 30																
40) $\alpha_s$ 30 30 30 30 30 30 30 30 30 30 30 30 30 30 30 30 30																
30) REACHED KM. MOMENT ALLOWABLE FOR STATION ME IN																
34) $\alpha_s$ 30 30 30 30 30 30 30 30 30 30 30 30 30 30 30 30 30																
35) $\alpha_s$ 30 30 30 30 30 30 30 30 30 30 30 30 30 30 30 30 30																
36) $\alpha_s$ 30 30 30 30 30 30 30 30 30 30 30 30 30 30 30 30 30																
37) $\alpha_s$ 30 30 30 30 30 30 30 30 30 30 30 30 30 30 30 30 30																
38) $\alpha_s$ 30 30 30 30 30 30 30 30 30 30 30 30 30 30 30 30 30																
39) $\alpha_s$ 30 30 30 30 30 30 30 30 30 30 30 30 30 30 30 30 30																
40) $\alpha_s$ 30 30 30 30 30 30 30 30 30 30 30 30 30 30 30 30 30																
30) REACHED KM. MOMENT ALLOWABLE FOR STATION ME IN																
34) $\alpha_s$ 30 30 30 30 30 30 30 30 30 30 30 30 30 30 30 30 30																
35) $\alpha_s$ 30 30 30 30 30 30 30 30 30 30 30 30 30 30 30 30 30																
36) $\alpha_s$ 30 30 30 30 30 30 30 30 30 30 30 30 30 30 30 30 30																
37) $\alpha_s$ 30 30 30 30 30 30 30 30 30 30 30 30 30 30 30 30 30																
38) $\alpha_s$ 30 30 30 30 30 30 30 30 30 30 30 30 30 30 30 30 30																
39) $\alpha_s$ 30 30 30 30 30 30 30 30 30 30 30 30 30 30 30 30 30																
40) $\alpha_s$ 30 30 30 30 30 30 30 30 30 30 30 30 30 30 30 30 30																
30) REACHED KM. MOMENT ALLOWABLE FOR STATION ME IN																
34) $\alpha_s$ 30 30 30 30 30 30 30 30 30 30 30 30 30 30 30 30 30																
35) $\alpha_s$ 30 30 30 30 30 30 30 30 30 30 30 30 30 30 30 30 30																
36) $\alpha_s$ 30 30 30 30 30 30 30 30 30 30 30 30 30 30 30 30 30																
37) $\alpha_s$ 30 30 30 30 30 30 30 30 30 30 30 30 30 30 30 30 30																
38) $\alpha_s$ 30 30 30 30 30 30 30 30 30 30 30 30 30 30 30 30 30																
39) $\alpha_s$ 30 30 30 30 30 30 30 30 30 30 30 30 30 30 30 30 30																
40) $\alpha_s$ 30 30 30 30 30 30 30 30 30 30 30 30 30 30 30 30 30																
30) REACHED KM. MOMENT ALLOWABLE FOR STATION ME IN																
34) $\alpha_s$ 30 30 30 30 30 30 30 30 30 30 30 30 30 30 30 30 30																
35) $\alpha_s$ 30 30 30 30 30 30 30 30 30 30 30 30 30 30 30 30 30																
36) $\alpha_s$ 30 30 30 30 30 30 30 30 30 30 30 30 30 30 30 30 30																
37) $\alpha_s$ 30 30 30 30 30 30 30 30 30 30 30 30 30 30 30 30 30																
38) $\alpha_s$ 30 30 30 30 30 30 30 30 30 30 30 30 30 30 30 30 30																
39) $\alpha_s$ 30 30 30 30 30 30 30 30 30 30 30 30 30 30 30 30 30																
40) $\alpha_s$ 30 30 30 30 30 30 30 30 30 30 30 30 30 30 30 30 30																
30) REACHED KM. MOMENT ALLOWABLE FOR STATION ME IN																
34) $\alpha_s$ 30 30 30 30 30 30 30 30 30 30 30 30 30 30 30 30 30																
35) $\alpha_s$ 30 30 30 30 30 30 30 30 30 30 30 30 30 30 30 30 30																
36) $\alpha_s$ 30 30 30 30 30 30 30 30 30 30 30 30 30 30 30 30 30																
37) $\alpha_s$ 30 30 30 30 30 30 30 30 30 30 30 30 30 30 30 30 30																
38) $\alpha_s$ 30 30 30 30 30 30 30 30 30 30 30 30 30 30 30 30 30																
39) $\alpha_s$ 30 30 30 30 30 30 30 30 30 30 30 30 30 30 30 30 30																
40) $\alpha_s$ 30 30 30 30 30 30 30 30 30 30 30 30 30 30 30 30 30																
30) REACHED KM. MOMENT ALLOWABLE FOR STATION ME IN																
34) $\alpha_s$ 30 30 30 30 30 30 30 30 30 30 30 30 30 30 30 30 30																
35) $\alpha_s$ 30 30 30 30 30 30 30 30 30 30 30 30 30 30 30 30 30																
36) $\alpha_s$ 30 30 30 30 30 30 30 30 30 30 30 30 30 30 30 30 30																
37) $\alpha_s$ 30 30 30 30 30 30 30 30 30 30 30 30 30 30 30 30 30																
38) $\alpha_s$ 30 30 30 30 30 30 30 30 30 30 30 30 30 30 30 30 30																
39) $\alpha_s$ 30 30 30 30 30 30 30 30 30 30 30 30 30 30 30 30 30																
40) $\alpha_s$ 30 30 30 30 30 30 30 30 30 30 30 30 30 30 30 30 30																
30) REACHED KM. MOMENT ALLOWABLE FOR STATION ME IN																
34) $\alpha_s$ 30 30 30 30 30 30 30 30 30 30 30 30 30 30 30 30 30																
35) $\alpha_s$ 30 30 30 30 30 30 30 30 30 30 30 30 30 30 30 30 30																
36) $\alpha_s$ 30 30 30 30 30 30 30 30 30 30 30 30 30 30 30 30 30																
37) $\alpha_s$ 30 30 30 30 30 30 30 30 30 30 30 30 30 30 30 30 30																
38) $\alpha_s$ 30 30 30 30 30 30 30 30 30 30 30 30 30 30 30 30 30																
39) $\alpha_s$ 30 30 30 30 30 30 30 30 30 30 30 30 30 30 30 30 30																
40) $\alpha_s$ 30 30 30 30 30 30 30 30 30 30 30 30 30 30 30 30 30																
30) REACHED KM. MOMENT ALLOWABLE FOR STATION ME IN																
34) $\alpha_s$ 30 30 30 30 30 30 30 30 30 30 30 30 30 30 30 30 30																
35) $\alpha_s$ 30 30 30 30 30 30 30 30 30 30 30 30 30 30 30 30 30																
36) $\alpha_s$ 30 30 30 30 30 30 30 30 30 30 30 30 30 30 30 30 30																
37) $\alpha_s$ 30 30 30 30 30 30 30 30 30 30 30 30 30 30 30 30 30																
38) $\alpha_s$ 30 30 30 30 30 30 30 30 30 30 30 30 30 30 30 30 30																
39) $\alpha_s$ 30 30 30 30 30 30 30 30 30 30 30 30 30 30 30 30 30																
40) $\alpha_s$ 30 30 30 30 30 30 30 30 30 30 30 30 30 30 30 30 30																
30) REACHED KM. MOMENT ALLOWABLE FOR STATION ME IN																
34) $\alpha_s$ 30 30 30 30 30 30 30 30 30 30 30 30 30 30 30 30 30																
35) $\alpha_s$ 30 30 30 30 30 30 30 30 30 30 30 30 30 30 30 30 30																
36) $\alpha_s$ 30 30 30 30 30 30 30 30 30 30 30 30 30 30 30 30 30																
37) $\alpha_s$ 30 30 30 30 30 30 30 30 30 30 30 30 30 30 30 30 30																
38) $\alpha_s$ 30 30 30 30 30 30 30 30 30 30 30 30 30 30 30 30 30																
39) $\alpha_s$ 30 30 30 30 30 30 30 30 30 30 30 30 30 30 30 30 30																
40) $\alpha_s$ 30 30 30 30 30 30 30 30 30 30 30 30 30 30 30 30 30																
30) REACHED KM. MOMENT ALLOWABLE FOR STATION ME IN																
34) $\alpha_s$ 30 30 30 30 30 30 30 30 30 30 30 30 30 30 30 30 30																
35) $\alpha_s$ 30 30 30 30 30 30 30 30 30 30 30 30 30 30 30 30 30																
36) $\alpha_s$ 30 30 30 30 30 30 30 30 30 30 30 30 30 30 30 30 30																
37) $\alpha_s$ 30 30 30 30 30 30 30 30 30 30 30 30 30 30 30 30 30																
38) $\alpha_s$ 30 30 30 30 30 30 30 30 30 30 30 30 30 30 30 30 30																
39) $\alpha_s$ 30 30 30 30 30 30 30 30 30 30 30 30 30 30 30 30 30																
40) $\alpha_s$ 30 30 30 30 30 30 30 30 30 30 30 30 30 30 30 30 30																
30) REACHED KM. MOMENT ALLOWABLE FOR STATION ME IN																
34) $\alpha_s$ 30 30 30 30 30 30 30 30 30 30 30 30 30 30 30 30 30																
35) $\alpha_s$ 30 30 30 30 30 30 30 30 30 30 30 30 30 30 30 30 30																
36) $\alpha_s$ 30 30 30 30 30 30 30 30 30 30 30 30 30 30 30 30 30																
37) $\alpha_s$ 30 30 30 30 30 30 30 30 30 30 30 30 30 30 30 30 30																
38) $\alpha_s$ 30 30 30 30 30 30 30 30 30 30 30 30 30 30 30 30 30																
39) $\alpha_s$ 30 30 30 30 30 30 30 30 30 30 30 30 30 30 30 30 30																
40) $\alpha_s$ 30 30 30 30 30 30 30 30 30 30 30 30 30 30 30 30 30																
30) REACHED KM. MOMENT ALLOWABLE FOR STATION ME IN																
34) $\alpha_s$ 30 30 30 30 30 30 30 30 30 30 30 30 30 30 30 30 30																
35) $\alpha_s$ 30 30 30 30 30 30 30 30 30 30 30 30 30 30 30 30 30																
36) $\alpha_s$ 30 30 30 30 30 30 30 30 30 30 30 30 30 30 30 30 30																
37) $\alpha_s$ 30 30 30 30 30 30 30 30 30 30 30 30 30 30 30 30 30																
38) $\alpha_s$ 30 30 30 30 30 30 30 30 30 30 30 30 30 30 30 30 30																
39) $\alpha_s$ 30 30 30 30 30 30 30 30 30 30 30 30 30 30 30 30 30																
40) $\alpha_s$ 30 30 30 30 30 30 30 30 30 30 30 30 30 30 30 30 30																
30) REACHED KM. MOMENT ALLOWABLE FOR STATION ME IN																
34) $\alpha_s$ 30 30 30 30 30 30 30 30 30 30 30 30 30 30 30 30 30																
35) $\alpha_s$ 30 30 30 30 30 30 30 30 30 30 30 30 30 30 30 30 30																
36) $\alpha_s$ 30 30 30 30 30 30 30 30 30 30 30 30 30 30 30 30 30																
37) $\alpha_s$ 30 30 30 30 30 30 30 30 30 30 30 30 30 30 30 30 30																
38) $\alpha_s$ 30 30 30 30 30 30 30 30 30 30 30 30 30 30 30 30 30																
39) $\alpha_s$ 30 30 30 30 30 30 30 30 30 30 30 30 30 30 30 30 30																
40) $\alpha_s$ 30 30 30 30 30 30 30 30 30 30 30 30 30 30 30 30 30																
30) REACHED KM. MOMENT ALLOWABLE FOR STATION ME IN																
34) $\alpha_s$ 30 30 30 30 30 30 30 30 30 30 30 30 30 30 30 30 30																
35) $\alpha_s$ 30 30 30 30 30 30 30 30 30 30 30 30 30 30 30 30 30																
36) $\alpha_s$ 30 30 30 30 30 30 30 30 30 30 30 30 30 30 30 30 30																
37) $\alpha_s$ 30 30 30 30 30 30 30 30 30 30 30 30 30 30 30 30 30																
38) $\alpha_s$ 30 30 30 30 30 30 30 30 30 30 30 30 30 30 30 30 30																
39) $\alpha_s$ 30 30 30 30 30 30 30 30 30 30 30 30 30 30 30 30 30																
40) $\alpha_s$ 30 30 30 30 30 30 30 30 30 30 30 30 30 30 30 30 30																
30) REACHED KM. MOMENT ALLOWABLE FOR STATION ME IN																
34) $\alpha_s$ 30 30 30 30 30 30 30 30 30 30 30 30 30 30 30 30 30																
35) $\alpha_s$ 30 30 30 30 30 30 30 30 30 30 30 30 30 30 30 30 30																
36) $\alpha_s$ 30 30 30 30 30 30 30 30 30 30 30 30 30 30 30 30 30																
37) $\alpha_s$ 30 30 30 30 30 30 30 30 30 30 30 30 30 30 30 30 30																
38) $\alpha_s$ 30 30 30 30 30 30 30 30 30 30 30 30 30 30 30 30 30																
39) $\alpha_s$ 30 30 30 30 30 30 30 30 30 30 30 30 30 30 30 30 30																
40) $\alpha_s$ 30 30 30 30 30 30 30 30 30 30 30 30 30 30 30 30 30																
30) REACHED KM. MOMENT ALLOWABLE FOR STATION ME IN																
34) $\alpha_s$ 30 30 30 30 30 30 30 30 30 30 30 30 30 30 30 30 30																
35) $\alpha_s$ 30 30 30 30 30 30 30 30 30 30 30 30 30 30 30 30 30																
36) $\alpha_s$ 30 30 30 30 30 30 30 30 30 30 30 30 30 30 30 30 30																
37) $\alpha_s$ 30 30 30 30 30 30 30 30 30 30 30 30 30 30 30 30 30																
38) $\alpha_s$ 30 30 30 30 30 30 30 30 30 30 30 30 30 30 30 30 30																
39) $\alpha_s$ 30 30 30 30 30 30 30 30 30 30 30 30 30 30 30 30 30																
40) $\alpha_s$ 30 30 30 30 30 30 30 30 30 30 30 30 30 30 30 30 30																
30) REACHED KM. MOMENT ALLOWABLE FOR STATION ME IN																
34) $\alpha_s$ 30 30 30 30 30 30 30 30 30 30 30 30 30 30 30 30 30																
35) $\alpha_s$ 30 30 30 30 30 30 30 30 30 30 30 30 30 30 30 30 30																
36) $\alpha_s$ 30 30 30 30 30 30 30 30 30 30 30 30 30 30 30 30 30																
37) $\alpha_s$ 30 30 30 30 30 30 30 30 30 30 30 30 30 30 30 30 30																
38) $\alpha_s$ 30 30 30 30 30 30 30 30 30 30 30 30 30 30 30 30 30																
39) $\alpha_s$ 30 30 30 30 30 30 30 30 30 30 30 30 30 30 30 30 30																
40) $\alpha_s$ 30 30 30 30 30 30 30 30 30 30 30 30 30 30 30 30 30																
30) REACHED KM. MOMENT ALLOWABLE FOR STATION ME IN																
34) $\alpha_s$ 30 30 30 30 30 30 30 30 30 30 30 30 30 30 30 30 30																
35) $\alpha_s$ 30 30 30 30 30 30 30 30 30 30 30 30 30 30 30 30 30																
36) $\alpha_s$ 30 30 30 30 30 30 30 30 30 30 30 30 30 30 30 30 30																
37) $\alpha_s$ 30 30 30 30 30 30 30 30 30 30 30 30 30 30 30 30 30																
38) $\alpha_s$ 30 30 30 30 30 30 30 30 30 30 30 30 30 30 30 30 30																
39) $\alpha_s$ 30 30 30 30 30 30 30 30 30 30 30 30 30 30 30 30 30																
40) $\alpha_s$ 30 30 30 30 30 30 30 30 30 30 30 30 30 30 30 30 30																
30) REACHED KM. MOMENT ALLOWABLE FOR STATION ME IN																
34) $\alpha_s$ 30 30 30 30 30 30 30 30 30 30 30 30 30 30 30 30 30																
35) $\alpha_s$ 30 30 30 30 30 30 30 30 30 30 30 30 30 30 30 30 30																
36) $\alpha_s$ 30 30 30 30 30 30 30 30 30 30 30 30 30 30 30 30 30																
37) $\alpha_s$ 30 30 30 30 30 30 30 30 30 30 30 30 30 30 30 30 30																
38) $\alpha_s$ 30 30 30 30 30 30 30 30 30 30 30 30 30 30 30 30 30																
39) $\alpha_s$ 30 30 30 30 30 30 30 30 30 30 30 30 30 30 30 30 30																
40) $\alpha_s$ 30 30 30 30 30 30 30 30 30 30 30 30 30 30 30 30 30																
30) REACHED KM. MOMENT ALLOWABLE FOR STATION ME IN																
34) $\alpha_s$ 30 30 30 30 30 30 30 30 30 30 30 30 30 30 30 30 30																
35) <																



FORM 48510 (2/70)

PREP.	CHK.	APPR	REVISD	DATE	RUN NO.	CONFIGURATION	TYPE OF TARE RUN	WT. TARE RUN	$\Theta_{75}$ DEG	B <sub>1</sub> DEG	$\alpha_s$ DEG	RPM	J	$\int_F$	$\int_s$	DATE / TIME
					51	PHSW	CRASH	12	40 45	0	0	788	2.10	0	0	11-20-70
					52	PHSW	-	12	43 44	0	0	788	2.35	0	0	- - -
					53	PHSW	-	12	45 47	0	0	788	2.40	0	0	- - -
					54	PHSW	-	12	47 48	0	5	788	2.4	0	0	- - -
					55	PHSW	-	12	49 49	0	10	788	2.4	0	0	- - -
					56	PHSW	-	12	50 50	0	15	788	2.4	0	0	- - -
					57	PHSW	-	12	12	0	0	1100	0	0	0	- - -
					58	PHS	-	12	11 12	0	0	788	.60	-	-	11-23-70
					59	PHS	-	12	15 16	0	0	788	.75	-	-	- - -
					60	PHS	-	12	21 24	0	0	788	1.00	-	-	- - -
537 MODEL MOTOR AMPERAGE LIMIT REACHED																
54) 1   .6   7.8   7.8   7.8   7.8   7.8   7.8   7.8   7.8   7.8   7.8   7.8   7.8   7.8   7.8   7.8																
55) 1   .6   7.8   7.8   7.8   7.8   7.8   7.8   7.8   7.8   7.8   7.8   7.8   7.8   7.8   7.8   7.8																
56) 1   .6   7.8   7.8   7.8   7.8   7.8   7.8   7.8   7.8   7.8   7.8   7.8   7.8   7.8   7.8   7.8																

FORM 49610 (8/70)

PREP.	CHK.	APPR	REVISD	DATE	RUN NO.	CONFIGURATION	TYPE OF RUN	WT. TARE RUN	$Q_{75}$	$B_1$	$d_s$	RPM	J	$\delta_r$	$\delta_s$	DATE / TIME
					61	PHS	CONST	12	27 34	0	0	799	1.35	-	-	11-23-70
					62	PHS	-	12	34 42	0	0	788	1.70	-	-	-
					63	PHS	-	12	42 49	0	0	788	2.10	-	-	-
					64	PHS	-	12	49 55	0	0	788	2.35	-	-	-
					65	PHS	-	12	55 62	0	0	788	2.40	-	-	-
					66	PHS	-	12	62 69	0	5	788	2.4	-	-	-
					67	PHS	-	12	VAR	0	5	788	2.4	-	-	-
					68	PHS	-	12	69 75	0	0	788	2.4	-	-	-
					69	PHS	-	12	75 82	0	0	788	2.4	-	-	-
					70	PHSWFL	TRAC	12	14	2 30	30	1100	3.2	EXT.	EXT.	-
1/3 SCALE V/STOL PROP DRTS					66)	$Q_{75}$   15   20   25   31   38   45   55										
						Y   1.6   1.75   1.9   2.1   2.3   2.5   2.7										
					67)	CONSTANT $C_p = 0.20$										
					68)	$Q_{75}$   15   20   25   31   38   45   55										
1/3 SCALE V/STOL PROP DRTS						Y   1.6   1.75   1.9   2.1   2.3   2.5   2.7										
					69)	CONSTANT $C_p = 0.20$										
						DATA POINT RE. 7 AND 8 Y/A SATURATED $C_p$ INVALID										
					70)	$Q_{75}$   15   20   25   31   38   45   55										
1/3 SCALE V/STOL PROP DRTS						Y   1.6   1.75   1.9   2.1   2.3   2.5   2.7										
					71)	CONSTANT $C_p = 0.20$										
						DATA POINT RE. 7 AND 8 Y/A SATURATED $C_p$ INVALID										
					72)	$Q_{75}$   15   20   25   31   38   45   55										
1/3 SCALE V/STOL PROP DRTS						Y   1.6   1.75   1.9   2.1   2.3   2.5   2.7										
					73)	CONSTANT $C_p = 0.20$										
						DATA POINT RE. 7 AND 8 Y/A SATURATED $C_p$ INVALID										
					74)	$Q_{75}$   15   20   25   31   38   45   55										
1/3 SCALE V/STOL PROP DRTS						Y   1.6   1.75   1.9   2.1   2.3   2.5   2.7										
					75)	CONSTANT $C_p = 0.20$										
						DATA POINT RE. 7 AND 8 Y/A SATURATED $C_p$ INVALID										
					76)	$Q_{75}$   15   20   25   31   38   45   55										
1/3 SCALE V/STOL PROP DRTS						Y   1.6   1.75   1.9   2.1   2.3   2.5   2.7										
					77)	CONSTANT $C_p = 0.20$										
						DATA POINT RE. 7 AND 8 Y/A SATURATED $C_p$ INVALID										
					78)	$Q_{75}$   15   20   25   31   38   45   55										
1/3 SCALE V/STOL PROP DRTS						Y   1.6   1.75   1.9   2.1   2.3   2.5   2.7										
					79)	CONSTANT $C_p = 0.20$										
						DATA POINT RE. 7 AND 8 Y/A SATURATED $C_p$ INVALID										
					79)	$Q_{75}$   15   20   25   31   38   45   55										
1/3 SCALE V/STOL PROP DRTS						Y   1.6   1.75   1.9   2.1   2.3   2.5   2.7										
					80)	CONSTANT $C_p = 0.20$										
						DATA POINT RE. 7 AND 8 Y/A SATURATED $C_p$ INVALID										
					80)	$Q_{75}$   15   20   25   31   38   45   55										
1/3 SCALE V/STOL PROP DRTS						Y   1.6   1.75   1.9   2.1   2.3   2.5   2.7										
					81)	CONSTANT $C_p = 0.20$										
						DATA POINT RE. 7 AND 8 Y/A SATURATED $C_p$ INVALID										
					81)	$Q_{75}$   15   20   25   31   38   45   55										
1/3 SCALE V/STOL PROP DRTS						Y   1.6   1.75   1.9   2.1   2.3   2.5   2.7										
					82)	CONSTANT $C_p = 0.20$										
						DATA POINT RE. 7 AND 8 Y/A SATURATED $C_p$ INVALID										
					82)	$Q_{75}$   15   20   25   31   38   45   55										
1/3 SCALE V/STOL PROP DRTS						Y   1.6   1.75   1.9   2.1   2.3   2.5   2.7										
					83)	CONSTANT $C_p = 0.20$										
						DATA POINT RE. 7 AND 8 Y/A SATURATED $C_p$ INVALID										
					83)	$Q_{75}$   15   20   25   31   38   45   55										
1/3 SCALE V/STOL PROP DRTS						Y   1.6   1.75   1.9   2.1   2.3   2.5   2.7										
					84)	CONSTANT $C_p = 0.20$										
						DATA POINT RE. 7 AND 8 Y/A SATURATED $C_p$ INVALID										
					84)	$Q_{75}$   15   20   25   31   38   45   55										
1/3 SCALE V/STOL PROP DRTS						Y   1.6   1.75   1.9   2.1   2.3   2.5   2.7										
					85)	CONSTANT $C_p = 0.20$										
						DATA POINT RE. 7 AND 8 Y/A SATURATED $C_p$ INVALID										
					85)	$Q_{75}$   15   20   25   31   38   45   55										
1/3 SCALE V/STOL PROP DRTS						Y   1.6   1.75   1.9   2.1   2.3   2.5   2.7										
					86)	CONSTANT $C_p = 0.20$										
						DATA POINT RE. 7 AND 8 Y/A SATURATED $C_p$ INVALID										
					86)	$Q_{75}$   15   20   25   31   38   45   55										
1/3 SCALE V/STOL PROP DRTS						Y   1.6   1.75   1.9   2.1   2.3   2.5   2.7										
					87)	CONSTANT $C_p = 0.20$										
						DATA POINT RE. 7 AND 8 Y/A SATURATED $C_p$ INVALID										
					87)	$Q_{75}$   15   20   25   31   38   45   55										
1/3 SCALE V/STOL PROP DRTS						Y   1.6   1.75   1.9   2.1   2.3   2.5   2.7										
					88)	CONSTANT $C_p = 0.20$										
						DATA POINT RE. 7 AND 8 Y/A SATURATED $C_p$ INVALID										
					88)	$Q_{75}$   15   20   25   31   38   45   55										
1/3 SCALE V/STOL PROP DRTS						Y   1.6   1.75   1.9   2.1   2.3   2.5   2.7										
					89)	CONSTANT $C_p = 0.20$										
						DATA POINT RE. 7 AND 8 Y/A SATURATED $C_p$ INVALID										
					89)	$Q_{75}$   15   20   25   31   38   45   55										
1/3 SCALE V/STOL PROP DRTS						Y   1.6   1.75   1.9   2.1   2.3   2.5   2.7										
					90)	CONSTANT $C_p = 0.20$										
						DATA POINT RE. 7 AND 8 Y/A SATURATED $C_p$ INVALID										
					90)	$Q_{75}$   15   20   25   31   38   45   55										
1/3 SCALE V/STOL PROP DRTS						Y   1.6   1.75   1.9   2.1   2.3   2.5   2.7										
					91)	CONSTANT $C_p = 0.20$										
						DATA POINT RE. 7 AND 8 Y/A SATURATED $C_p$ INVALID										
					91)	$Q_{75}$   15   20   25   31   38   45   55										
1/3 SCALE V/STOL PROP DRTS						Y   1.6   1.75   1.9   2.1   2.3   2.5   2.7										
					92)	CONSTANT $C_p = 0.20$										
						DATA POINT RE. 7 AND 8 Y/A SATURATED $C_p$ INVALID										
					92)	$Q_{75}$   15   20   25   31   38   45   55										
1/3 SCALE V/STOL PROP DRTS						Y   1.6   1.75   1.9   2.1   2.3   2.5   2.7										
					93)	CONSTANT $C_p = 0.20$										
						DATA POINT RE. 7 AND 8 Y/A SATURATED $C_p$ INVALID										
					93)	$Q_{75}$   15   20   25   31   38   45   55										
1/3 SCALE V/STOL PROP DRTS						Y   1.6   1.75   1.9   2.1   2.3   2.5   2.7										
					94)	CONSTANT $C_p = 0.20$										
						DATA POINT RE. 7 AND 8 Y/A SATURATED $C_p$ INVALID										
					94)	$Q_{75}$   15   20   25   31   38   45   55										
1/3 SCALE V/STOL PROP DRTS						Y   1.6   1.75   1.9   2.1   2.3   2.5   2.7										
					95)	CONSTANT $C_p = 0.20$										
						DATA POINT RE. 7 AND 8 Y/A SATURATED $C_p$ INVALID										
					95)	$Q_{75}$   15   20   25   31   38   45   55										
1/3 SCALE V/STOL PROP DRTS						Y   1.6   1.75   1.9   2.1   2.3   2.5   2.7										
					96)	CONSTANT $C_p = 0.20$										
						DATA POINT RE. 7 AND 8 Y/A SATURATED $C_p$ INVALID										
					96)	$Q_{75}$   15   20   25   31   38   45   55										
1/3 SCALE V/STOL PROP DRTS						Y   1.6   1.75   1.9   2.1   2.3   2.5   2.7										
					97)	CONSTANT $C_p = 0.20$										
						DATA POINT RE. 7 AND 8 Y/A SATURATED $C_p$ INVALID										
					97)	$Q_{75}$   15   20   25   31   38   45   55										
1/3 SCALE V/STOL PROP DRTS						Y   1.6   1.75   1.9   2.1   2.3   2.5   2.7										
					98)	CONSTANT $C_p = 0.20$										
						DATA POINT RE. 7 AND 8 Y/A SATURATED $C_p$ INVALID										
					98)	$Q_{75}$   15   20   25   31   38   45   55										
1/3 SCALE V/STOL PROP DRTS						Y   1.6   1.75   1.9   2.1   2.3   2.5   2.7										
					99)	CONSTANT $C_p = 0.20$										
						DATA POINT RE. 7 AND 8 Y/A SATURATED $C_p$ INVALID										
					99)	$Q_{75}$   15   20   25   31   38   45   55										
1/3 SCALE V/STOL PROP DRTS						Y   1.6   1.75   1.9   2.1   2.3   2.5   2.7										
					100)	CONSTANT $C_p = 0.20$										
						DATA POINT RE. 7 AND 8 Y/A SATURATED $C_p$ INVALID										
					100)	$Q_{75}$   15   20   25   31   38   45   55										
1/3 SCALE V/STOL PROP DRTS						Y   1.6   1.75   1.9   2.1   2.3   2.5   2.7										
					101)	CONSTANT $C_p = 0.20$										
						DATA POINT RE. 7 AND 8 Y/A SATURATED $C_p$ INVALID										
					101)	$Q_{75}$   15   20   25   31   38   45   55										
1/3 SCALE V/STOL PROP DRTS						Y   1.6   1.75   1.9   2.1   2.3   2.5   2.7										
					102)	CONSTANT $C_p = 0.20$										
						DATA POINT RE. 7 AND 8 Y/A SATURATED $C_p$ INVALID										
					102)	$Q_{75}$   15   20   25   31   38   45   55										
1/3 SCALE V/STOL PROP DRTS						Y   1.6   1.75   1.9   2.1   2.3   2.5   2.7										
					103)	CONSTANT $C_p = 0.20$										
						DATA POINT RE. 7 AND 8 Y/A SATURATED $C_p$ INVALID										
					103)	$Q_{75}$   15   20   25   31   38   45   55										
1/3 SCALE V/STOL PROP DRTS						Y   1.6   1.75   1.9   2.1   2.3   2.5   2.7										
					104)	CONSTANT $C_p = 0.20$										
						DATA POINT RE. 7 AND 8 Y/A SATURATED $C_p$ INVALID										
					104)	$Q_{75}$   15   20   25   31   38   45   55										
1/3 SCALE V/STOL PROP DRTS						Y   1.6   1.75   1.9   2.1   2.3   2.5   2.7										
					105)	CONSTANT $C_p = 0.20$										
						DATA POINT RE. 7 AND 8 Y/A SATURATED $C_p$ INVALID										
					105)	$Q_{75}$   15   20   25   31   38   45   55										
1/3 SCALE V/STOL PROP DRTS						Y   1.6   1.75   1.9   2.1   2.3   2.5   2.7										
					106)	CONSTANT $C_p = 0.20$										
						DATA POINT RE. 7 AND 8 Y/A SATURATED $C_p$ INVALID										
					106)	$Q_{75}$   15   20   25   31   38   45   55										
1/3 SCALE V/STOL PROP DRTS						Y   1.6   1.75   1.9   2.1   2.3   2.5   2.7										
					107)	CONSTANT $C_p = 0.20$										
						DATA POINT RE. 7 AND 8 Y/A SATURATED $C_p$ INVALID										
					107)	$Q_{75}$   15   20   25   31   38   45   55										
1/3 SCALE V/STOL PROP DRTS						Y   1.6   1.75   1.9   2.1   2.3   2.5   2.7										
					108)	CONSTANT $C_p = 0.20$										
						DATA POINT RE. 7 AND 8 Y/A SATURATED $C_p$ INVALID										
					108)	$Q_{75}$   15   20   25   31   38   45   55										
1/3 SCALE V/STOL PROP DRTS						Y   1.6   1.75   1.9   2.1   2.3   2.5   2.7										
					109)	CONSTANT $C_p = 0.20$										
						DATA POINT RE. 7 AND 8 Y/A SATURATED $C_p$ INVALID										
					109)	$Q_{75}$   15   20   25   31   38   45   55										
1/3 SCALE V/STOL PROP DRTS						Y   1.6   1.75   1.9   2.1   2.3   2.5   2.7										
					110)	CONSTANT $C_p = 0.20$										
						DATA POINT RE. 7 AND 8 Y/A SATURATED $C_p$ INVALID										
					110)	$Q_{75}$   15   20   25   31   38   45   55										
1/3 SCALE V/STOL PROP DRTS						Y   1.6   1.75   1.9   2.1   2.3   2.5   2.7										
					111)	CONSTANT $C_p = 0.20$										
						DATA POINT RE. 7 AND 8 Y/A SATURATED $C_p$ INVALID										
					111)	$Q_{75}$   15   20   25   31   38   45   55										
1/3 SCALE V/STOL PROP DRTS						Y   1.6   1.75   1.9   2.1   2.3   2.5   2.7										
					112)	CONSTANT $C_p = 0.20$										
						DATA POINT RE. 7 AND 8 Y/A SATURATED $C_p$ INVALID										
					112)	$Q_{75}$   15   20   25   31   38   45   55										
1/3 SCALE V/STOL PROP DRTS						Y   1.6   1.75   1.9   2.1   2.3   2.5   2.7										
					113)	CONSTANT $C_p = 0.20$										
						DATA POINT RE. 7 AND 8 Y/A SATURATED $C_p$ INVALID										
					113)	$Q_{75}$   15   20   25   31   38   45   55										
1/3 SCALE V/STOL PROP DRTS						Y   1.6   1.75   1.9   2.1   2.3   2.5   2.7										
					114)	CONSTANT $C_p = 0.20$										
						DATA POINT RE. 7 AND 8 Y/A SATURATED $C_p$ INVALID										
					114)	$Q_{75}$   15   20   25   31   38   45   55										
1/3 SCALE V/STOL PROP DRTS						Y   1.6   1.75   1.9   2.1   2.3   2.5   2.7										
					115)	CONSTANT $C_p = 0.20$										
						DATA POINT RE. 7 AND 8 Y/A SATURATED $C_p$ INVALID										
					115)	$Q_{75}$   15   20   25   31   38   45   55										
1/3 SCALE V/STOL PROP DRTS						Y   1.6   1.75   1.9   2.1   2.3   2.5   2.7										
					116)	CONSTANT $C_p = 0.20$										
						DATA POINT RE. 7 AND 8 Y/A SATURATED $C_p$ INVALID										
					116)	$Q_{75}$   15   20   25   31   38   45   55										
1/3 SCALE V/STOL PROP DRTS						Y   1.6   1.75   1.9   2.1   2.3   2.5   2.7										
					117)	CONSTANT $C_p = 0.20$										
						DATA POINT RE. 7 AND 8 Y/A SATURATED $C_p$ INVALID										
					117)	$Q_{75}$   15   20   25   31   38   45   55										
1/3 SCALE V/STOL PROP DRTS						Y   1.6   1.75   1.9   2.1   2.3   2.5   2.7										
					118)	CONSTANT $C_p = 0.20$										
						DATA POINT RE. 7 AND 8 Y/A SATURATED $C_p$ INVALID										
					118)	$Q_{75}$   15   20   25   31   38   45   55										
1/3 SCALE V/STOL PROP DRTS						Y   1.6   1.75   1.9   2.1   2.3   2.5   2.7										
					119)	CONSTANT $C_p = 0.20$										
						DATA POINT RE. 7 AND 8 Y/A SATURATED $C_p$ INVALID										
					119)	$Q_{75}$   15   20   25   31   38   45   55										
1/3 SCALE V/STOL PROP DRTS						Y   1.6   1.75   1.9   2.1   2.3   2.5   2.7										
					120)	CONSTANT $C_p = 0.20$										
						DATA POINT RE. 7 AND 8 Y/A SATURATED $C_p$ INVALID										
					120)	$Q_{75}$   15   20   25   31   38   45   55										
1/3 SCALE V/STOL PROP DRTS						Y   1.6   1.75   1.9   2.1   2.3   2.5   2.7										
					121)	CONSTANT $C_p = 0.20$										
						DATA POINT RE. 7 AND 8 Y/A SATURATED $C_p$ INVALID										
					121)	$Q_{75}$   15   20   25   31   38   45   55										
1/3 SCALE V/STOL PROP DRTS						Y   1.6   1.75   1.9   2.1   2.3   2.5   2.7										
					122)	CONSTANT $C_p = 0.20$										
						DATA POINT RE. 7 AND 8 Y/A SATURATED $C_p$ INVALID										
					122)	$Q_{75}$   15   20   25   31   38   45   55										
1/3 SCALE V/STOL PROP DRTS						Y   1.6   1.75   1.9   2.1   2.3   2.5   2.7										
					123)	CONSTANT $C_p = 0.20$										
						DATA POINT RE. 7 AND 8 Y/A SATURATED $C_p$ INVALID										
					123)	$Q_{75}$   15   20   25   31   38   45   55										
1/3 SCALE V/STOL PROP DRTS						Y   1.6   1.75   1.9   2.1   2.3   2.5   2.7										
					124)											



[illegible]



**D170-10040-1**  
**Table D.1**

**FORM 49610 (3/70)**

APPENDIX ESPINNER AND HUB TARES

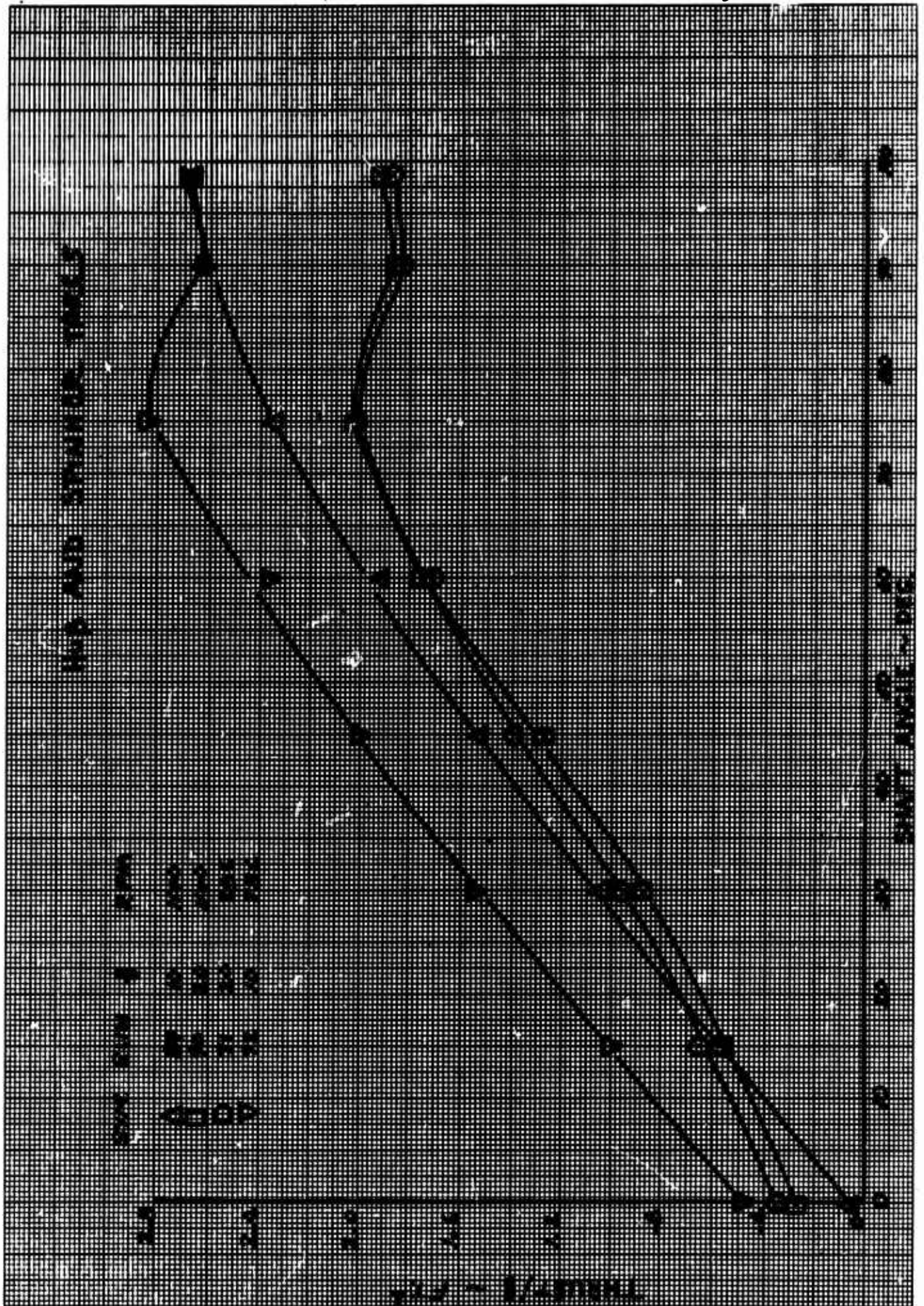
Six component forces and moments were taken at two values of tunnel dynamic pressure and two values of hub RPM. (20 PSF at 1100 and 786 RPM; also 10 PSF at 1100 and 786 RPM). The hub tares were taken with the test section in the "open throat" configuration. Spinner and hub tares have been removed from the plotted data using the data from Run No. 90; i.e., dynamic pressure of 20 PSF and 1100 RPM. The tabulated data are presented both with and without hub tares removed.

The blades were removed and the blade retention socket taped for the spinner and hub tare runs. The tares were obtained by setting the hub RPM and tunnel dynamic pressure then taking data over a range of propeller angles from 0 to 99 degrees. Each component of the spinner and hub tare data were divided by tunnel dynamic pressure. This data was then curve-fitted as a function of shaft angle and applied to each data point, with blades on, as a function of tunnel dynamic pressure and propeller shaft angles.

The spinner and hub tare data are presented in Figures E.1 through E.5 in two ways. First, to show the results of using tunnel dynamic pressure as a normalizing factor and second, to show the magnitude of the tares in propeller coefficient notation. The two components showing the largest spinner and hub tares (See Figure E.6) in propeller coefficient notation) are normal force and side force. It is postulated that the side force tare and yawing moment tares are produced by the rotating cylinder effect on the spinner. This is to some degree justified by Figure E.2 which shows that side force can be normalized by tunnel dynamic pressure if RPM is held constant.

The variation of thrust tare with shaft angle is not understood; however, a correlation with a  $1/l^2$  scale isolated propeller shows a similar trend. See Figure E.7.

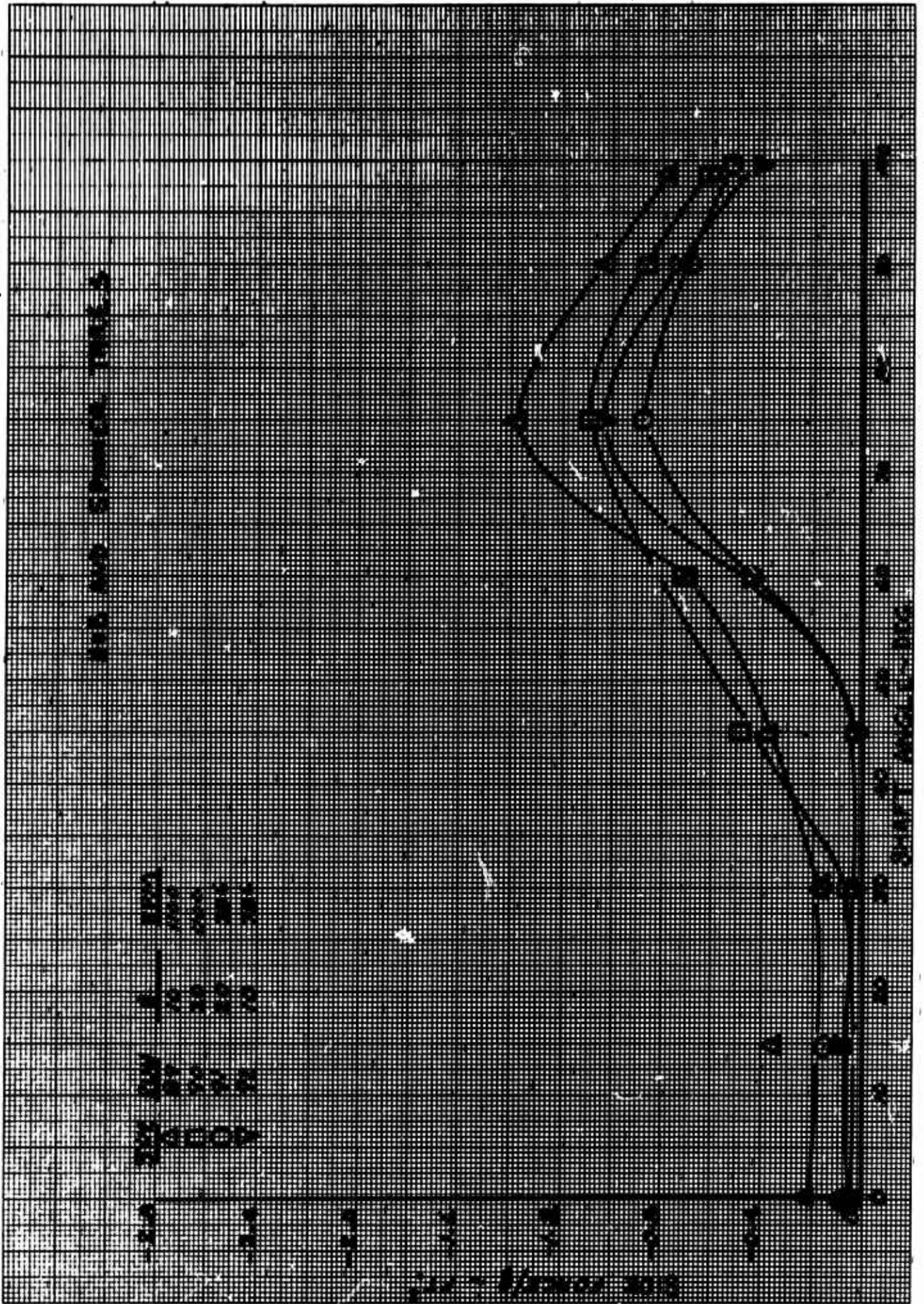






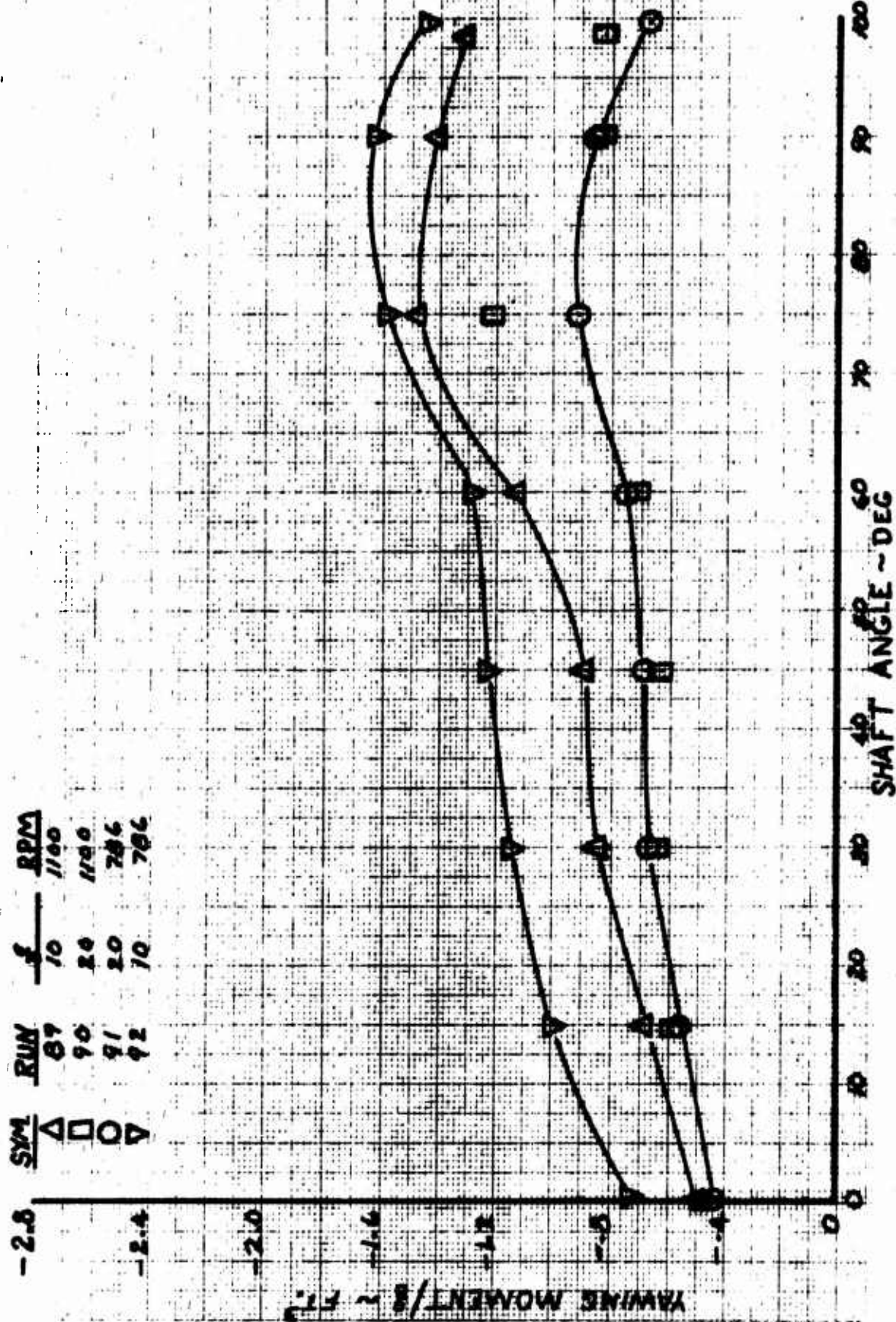
EUGENE DIETZGEN CO.  
MADE IN U. S. A.

NO. 3408-MP DIETZGEN GRAPH PAPER  
MILLIMETER

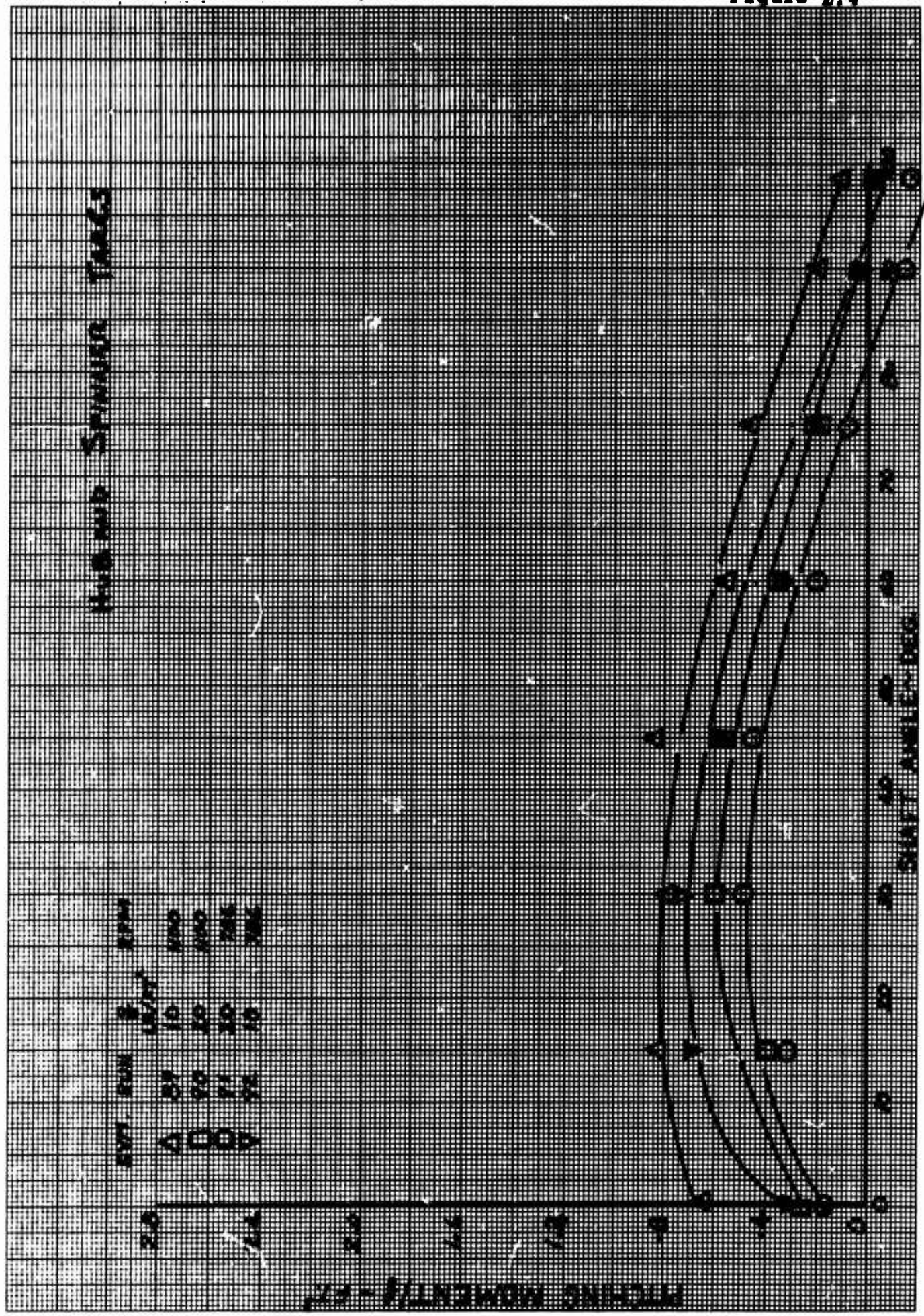


HUB AND SPINNER TARES

SYM	RUN	f	RPM
Δ	89	10	1100
□	90	20	1100
○	91	20	706
▽	92	10	706









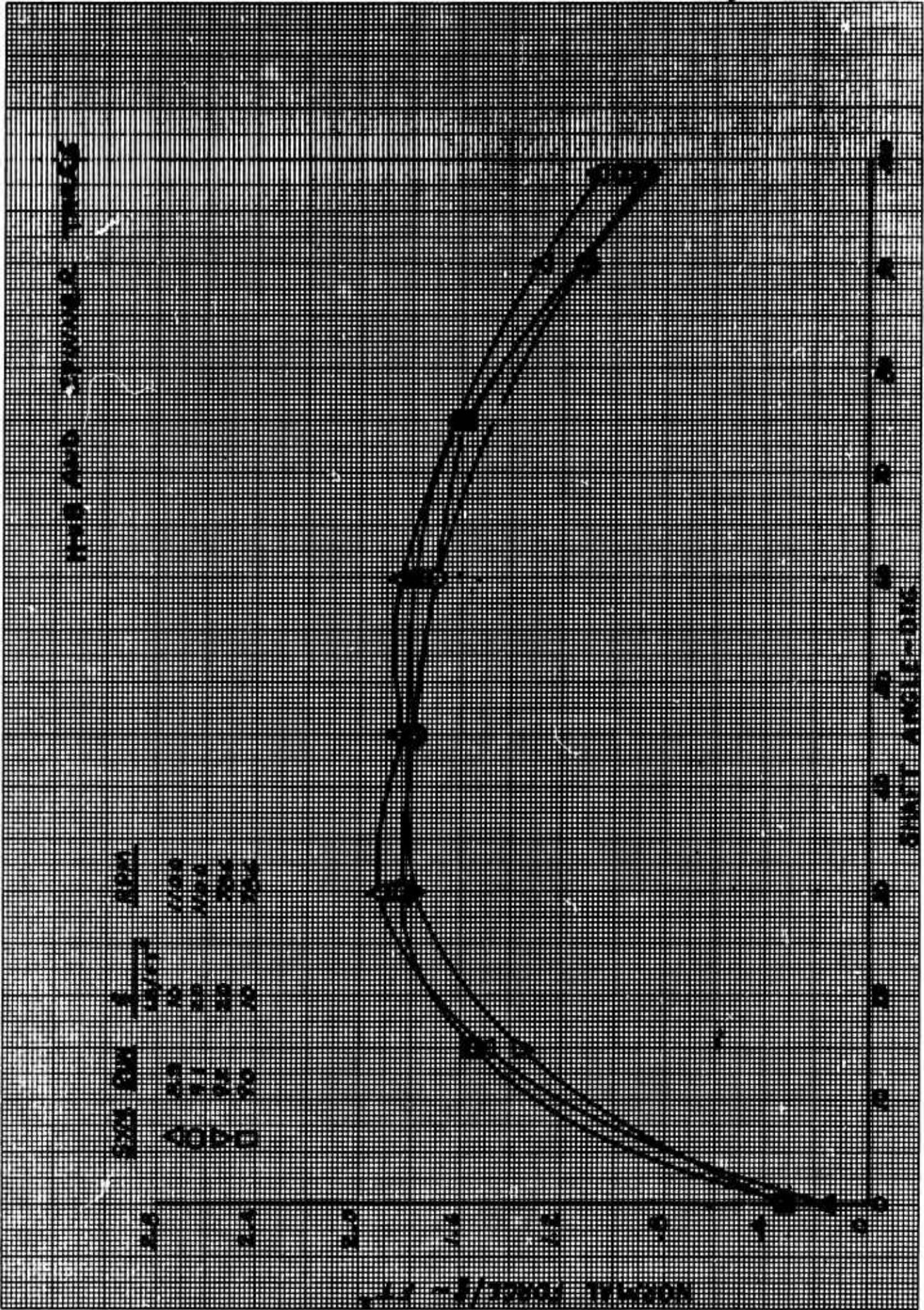
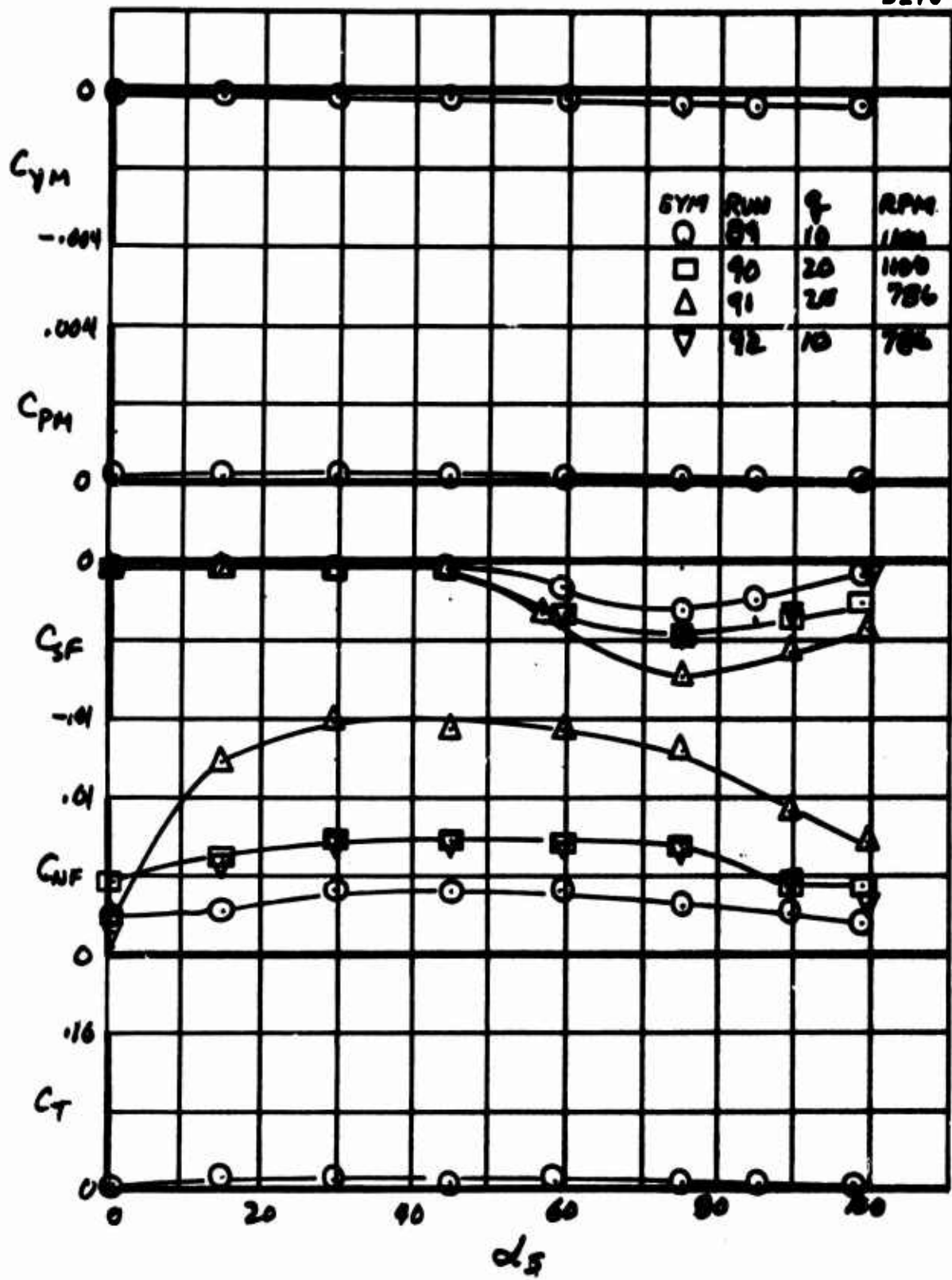


Figure E.6  
D170-10040-1



PROPELLER HUB AND SPINNER TARES



